KANSAS GEOLOGICAL SURVEY
OPEN-FILE REPORT 91-53

Geochemical Characterization of Black Shale Types
in the Midcontinent Pennsylvanian

by

Richard B. Schultz

KANSAS GEOLOGICAL SURVEY
1930 Constant Avenue
University of Kansas
Lawrence, KS 66047

Geochemical Characterization of Black Shale Types in the Midcontinent Pennsylvanian

A dissertation submitted to the

Division of Graduate Studies and Research
of the University of Cincinnati

in partial fulfillment of the
requirements for the degree of

DOCTOR OF PHILOSOPHY

in the Department of Geology
of the College of Arts and Sciences

1991

by

Richard B. Schultz

B. S., Illinois State University, 1985

M. S., The Wichita State University, 1988

UNIVERSITY OF CINCINNATI

June 3 1991

I hereby recommend that the thesis prepared under my supervision by Richard B. Schultz

entitled Geochemical Characterization of Black Shale Types in the Midcontinent Pennsylvanian

be accepted as fulfilling this part of the requirements for the degree of Doctor of Philosophy

Approved by:

Abstract

Various geochemical parameters including type and abundance of organic matter (TOC), sulfide-sulfur quantities, fluctuations in bottom-water anoxicity (DOP), metal content differences, and sulfur isotope variations have been assessed in order to characterize Midcontinent Pennsylvanian black shales. Based on these geochemical parameters, the deposits can be grouped into three types: Mecca-type, Heebner-type, and Shanghai-type.

Mecca-type black shales are characterized by at least 20% TOC (mostly terrestrial-type), high metal content (especially V, Cr, Ni, Mo, U, and Sn), erratic and heavy ^{34}S values, high DOP, and an association with underlying coals and siliciclastics.

Heebner-type black shales are characterized by less than 20% TOC (mostly marine-type, although somewhat mixed), moderate metal content, light, consistent $\delta^{34}S$ values, moderate DOP, and an association with phosphatic nodules and laminae. A sedimentary association with siliciclastics (Missourian) and carbonates (Virgilian) is evident.

Shanghai-type deposits are characterized by less than 15% TOC (mostly mixed terrestrial and marine types), low metal contents, erratic and heavy $\delta^{34}S$ values, low DOP, and a mostly phosphatic fauna.

Multivariate statistical analyses performed on geochemical data indicate that a 94% probability exists that Pennsylvanian black shales of Midcontinent North America can be classified into one of these groupings.

Metal constituents in the Mecca-type shales and metalliferous Heebner-type shales developed in response to repeated contact of black shales and organic matter with various types of fluids: brackish seawater, connate water, basinal brines, and modern groundwater. It is probable that a redox interface existed so that metals present in fluids were attracted to the nearshore organic materials in Mecca-type (Desmoinesian) shales. Favorable conditions for the emplacement of metals in the shales includes a semieuxinic to euxinic basinal setting, DOP between 7.0 and 1.00, the presence of available metals, an abundance of organic material to absorb the metals, and a predominance of quiescence to fixate metals.

A model for time-dependent changes of Midcontinent Pennsylvanian black shales is offered that shows a progressive ventilation for deposition of the black shales from the Desmoinesian through the Virgilian in the Midcontinent so that metal supplies, DOP, and TOC contents decrease with time as a result of decreased sediment supply or a fluctuation in sediment source.

Geochemical Characterization of Black Shale Types in the Midcontinent Pennsylvanian

List of Figures

List of Tables

Chapter 1. Introduction

The study of black shales has been difficult and usually without useful results until recently. Technological advancements have opened new doors regarding the study of fine grained rocks. Papers by Zangerl and Richardson (1963), Vine and Tourtelot (1970), and Heckel (1977) stand out as pioneering works on these beds. Early work was hampered because outcrops can yield only limited data about the origin of black shales. Generally, theories of their origin were limited to the simple explanation that black shales were formed under reducing conditions. Recently, geochemistry has played an increasingly important role in the characterization of both organic material and inorganic constituents, widening the scope of inferences drawn about the genesis of black shales.

Importance of Black Shales

Black shale is a dark-colored mudrock containing organic matter that may be associated with hydrocarbons (Huyck, 1991). Some emphasis is currently being placed on using chemical parameters to define "black shale" and "metalliferous black shale", under the aegis of IGCP (International Geological Correlation Project) Working Group 254 (Huyck, 1991). Their working definition for black shale is "a dark-colored, laminated, fine-grained, clastic sediment that

contains 50% or more particles sized less than 0.062 mm equivalent spherical diameter (i.e., silt or clay) and greater than 0.5% organic carbon." A "metalliferous black shale" is provisionally defined as "a black shale that is enriched in any given metal by 2X (except for beryllium, cobalt, and uranium where 1X is sufficient) relative to the United States Geological Survey Geochemical Standard SDO-1 (Ohio Devonian Shale)". Note that in this definition an anomalously high concentration of any one element is sufficient to place the shale into the metalliferous category. Leventhal (in Huyck, 1991) has offered an alternative definition of "metalliferous black shale" based on the total metal content:

$$[(V + Cr + Co + Ni + Cu + Zn + Mo + Ag + Cd + Pb + U) + (As\ Se + Sb + Ti) + (Ba + Mn + REE + Zr) / 5] > 1000$$

where all concentrations are given in ppm. In practice, these two definitions yield similar assignments, but are philosophically different.

Black shales can be repositories for valuable metal constituents and represent a record of past anoxic water conditions. These metalliferous, carbon-rich rocks also record geochemical interactions of carbon, iron, sulfur, oxygen, and phosphorous. Thus, although not generally considered as commercial ores, with the exception of some

small operations in China, metalliferous black shales have considerable importance in understanding processes of metal enrichment in sedimentary rocks. Black shales are important to the natural resource economy because, after coal, they provide the most accessible reservoir of organic constituents in the crust (Tourtelot, 1979). Additionally, black shales are important as the host strata of some syngenetic metal deposits (Tourtelot, 1979). Examples of this include the Kupferschiefer of Permian age in central Europe and the Nonesuch Shale of Proterozoic age in Michigan, U.S.A.

History of Research

Significant early work on black shales addressed the importance of anoxic-water conditions in their formation (Pettijohn, 1949), association with a distinctive biofacies, (e.g. Bulman, 1955), and the conclusion that, under modern conditions, these anoxic-water sediments are formed in basins restricted from free exchange with the open ocean, leading to stagnation in the bottom part of the water column (Strom, 1939). Such situations are rare in modern oceans, but the Lower Paleozoic and Mesozoic rock records are indicative of more widespread anoxia when global climates were warmer and more equable.

The chemistry of black shales has recently attracted attention. Vine and Tourtelot (1970) analyzed about 800

black shale samples using wet chemical and spectrographic techniques in their classic study. They were the first to try to define a normal range for metal contents of black shales and to develop criteria for recognizing black shales enriched in metals. Considerable progress has been made in understanding the chemistry of black shales by going beyond bulk chemical analyses to a determination of the speciation of the elements. Particularly germane to the study of the behavior of metals is the determination of the oxidation state of sulfur, because many heavy metals are immobilized in the presence of sulfide (Canfield et al., 1986). Raiswell and Berner (1985) combined the determination of S species with similar Fe measurements into a parameter they term DOP (degree of pyritization), originally defined by Berner, 1970:

$$DOP = \text{Pyritic Iron } (Fe_{py}) \; / \; (Fe_{py} + \text{HCl-soluble Iron } (Fe_{HCl}))$$

that, combined with C/S ratios, can be used to quantify the degree of anoxia.

However defined, any metalliferous black shale being studied needs to be characterized in terms of chemical and physical parameters useful in determining its paleoenvironment. Where present, study of body fossils can be particularly useful, but they are often difficult to find in shales, with the possible exception of graptolites and phosphatic brachiopods in Midcontinent Pennsylvanian depos-

its. Trace fossils are also revealing and are more widely distributed in black shales than are shelly fossils. The degree of bioturbation imposed on the sediment by animals is a useful measure of the amount of oxygen in the bottom water at the time of deposition (Byers, 1977). However, many Phanerozoic sections, and all Precambrian sections, lack even these guides to environmental conditions. Therefore, chemical indicators have been widely pursued.

Perhaps the most widely used chemical indicator is the content of organic carbon, which is incorporated into the IGCP definition. However, the organic carbon content is influenced by a number of factors, including the rate of production of biomass in the surface water as well as the amount of oxygen present in the bottom water (Pedersen and Calvert, 1990). A method to isolate the effects of bottom-water oxygenation, and, in a sense, circumvent surface-water effects, while quantifying the degree of anoxicity in marine environments, has been proposed by Raiswell and Berner (1985). Two parameters are useful: the first is the ratio of organic carbon to sulfide sulfur, mostly pyritic sulfur. If organic carbon (C_{org}) is plotted against sulfide sulfur (S_{py}) for modern environments, three types of patterns emerge. Normal marine environments provide a straightline correlation passing through the origin, a reflection of the fact that, in these environments, the amount of sulfur converted from sulfate to sulfide by the bacteria is con-

trolled by the amount of carbon they have to use as a food source. In freshwater environments, where sulfate is sparse, the amount of sulfate rather than the amount of organic matter is rate-limiting and a distribution of points close to the C_{org} axis, but passing through the origin, is seen. Under euxinic conditions, that is in a marine basin where oxygen has been completely removed from the water column, free H_2S forms in the water, suppressing all benthonic life forms, and bacterial sulfate reduction commences in the water column. The result is a plot of C versus S with a poor correlation and a positive intercept on the S axis (Leventhal, 1983) (Figure 1).

Environments apparently can vary in the degree to which euxinic (anoxic, H_2S-containing, and usually relatively deep water) conditions are developed. Using the parameter DOP, coupled with C/S ratios, a scale can be established separating marine basins into noneuxinic, semieuxinic, and fully euxinic categories. Raiswell et al. (1988) established a range of values for DOP using paleoecological and sedimentological characteristics. They defined aerobic (noneuxinic) conditions as sediments deposited in fully oxygenated bottom-water (DOP < 0.45), restricted marine (semieuxinic) conditions where sediments are deposited in waters with low-oxygen concentrations (0.45 < DOP < 0.75), and inhospitable (fully euxinic) conditions where sediments are deposited in

Figure 1. Plot of %TOC (total organic carbon) versus $\%S_{py}$ (pyritic sulfur) in this study. Note the presence of carbon-limited diagenetic pyrite indicated by arrow and full range of values for samples in this study. Black Sea data from Leventhal (1983).

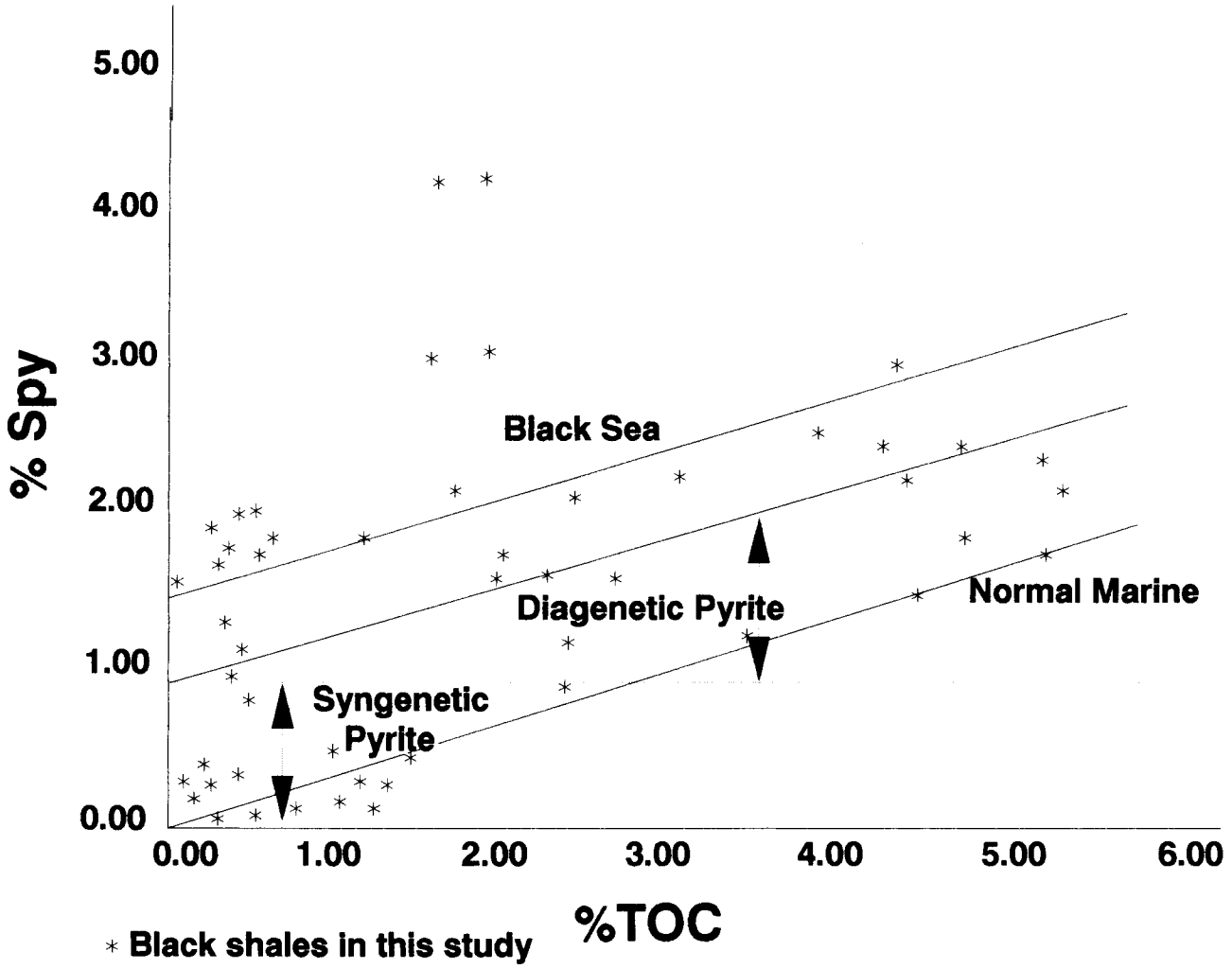
5.00
4.00
3.00
2.00
1.00
0.00
% Spy
Black Sea
Diagenetic Pyrite
Normal Marine
Syngenetic
Pyrite
0.00
1.00
2.00
3.00
4.00
5.00
6.00
%TOC
* Black shales in this study

a setting with little or no oxygen present and the continual or intermittent presence of H_2S (DOP > 0.75). In this study of Midcontinent black shales, DOP is especially important in deciphering fluctuations in the degree of anoxicity during the Pennsylvanian (Figure 2).

Several well-studied black shale units stand out as being particularly metalliferous, mostly enriched in U, V, Mo, Pb, Cu, Ni, and Zn (Schultz, 1991). Among these are the Alum Shale of Scandinavia, New Albany Shale of Indiana, U.S.A., Mecca Quarry Shale of Indiana and Illinois, U.S.A., and several Chinese Cambrian black shale units. The geochemical characteristics of Midcontinent North American Pennsylvanian black shales in this study are compared to these metalliferous black shales.

Objectives of Research

Similar to other recent investigations of Midcontinent Pennsylvanian black shales, this study reports geochemical results of the Midcontinent Pennsylvanian units. However, data for separate species (C, Fe, and S) as well as for the whole-rock (i.e., XRF) are reported and are used to infer that the character of black shale units changed during Middle to Late Pennsylvanian time in Midcontinent North America (Schultz and Coveney, in press). The focus of this study is on the Midcontinent Pennsylvanian black shale

Figure 2. Variations in DOP with depositional environment as defined by Raiswell et al. (1988).

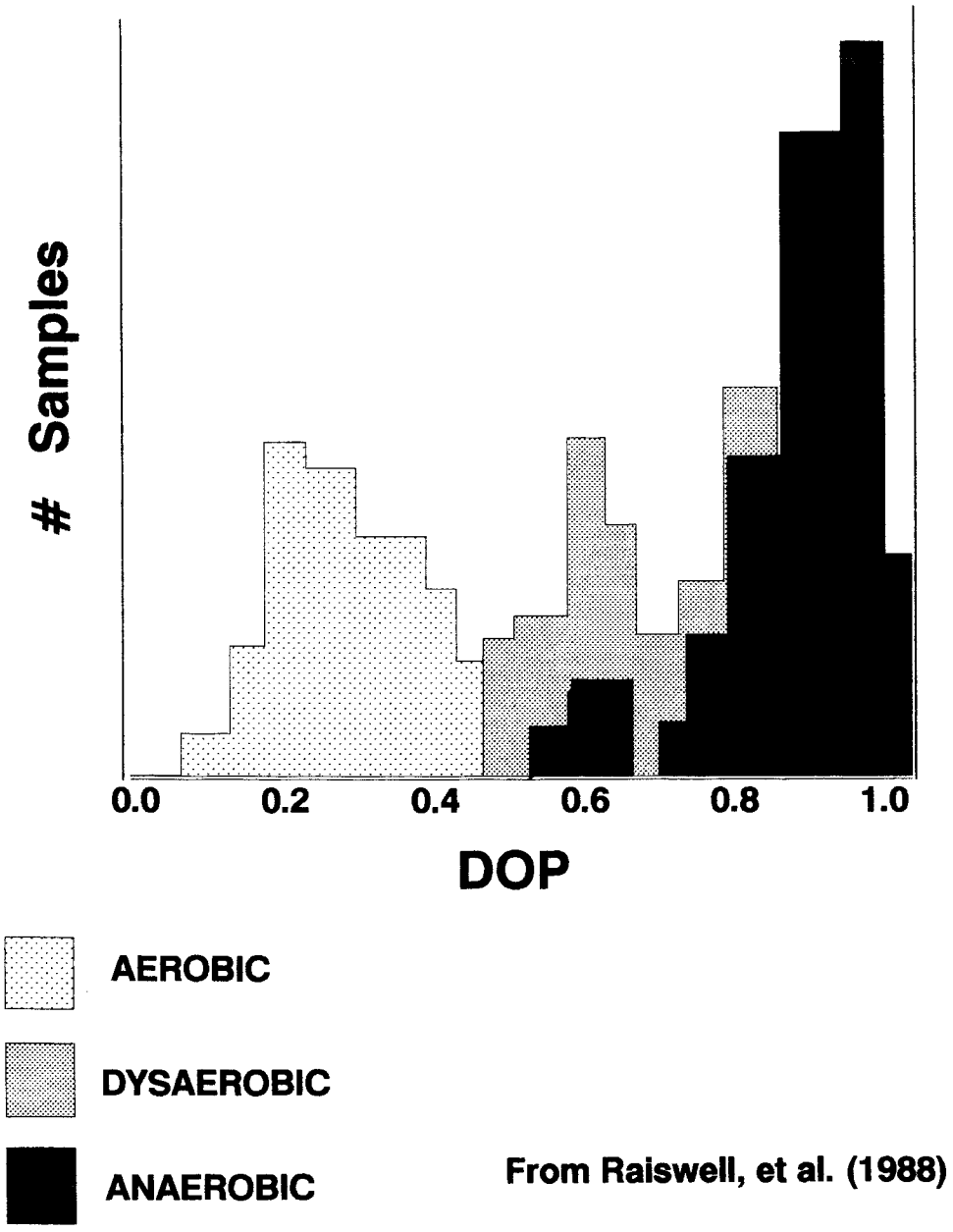

From Raiswell, et al. (1988)

units with comparisons to the Mecca Quarry Shale, and environmental and geochemical comparisons to the Alum Shale, New Albany Shale, and Chinese Cambrian black shale units. The objective of this research is three-fold: (1) to investigate geochemically different types of Midcontinent Pennsylvanian black shales; (2) to categorize these black shales into types so that other Pennsylvanian black shales from other localities may be placed into the categories; and (3) to speculate on a source for the metals in the more metalliferous black shale units.

Chapter 2. Importance of TOC-S-Fe Relationships: Pyrite Formation

Understanding biologically mediated, early diagenetic processes in marine settings is a goal of many earth scientists. Berner (1970, 1984), Sweeney (1972), Goldhaber and Kaplan (1974), and Leventhal and Taylor (1990) are just a few of the many workers who have observed relationships among organic carbon, sulfur, and iron leading to pyrite formation. Overall reactions that occur in this process include:

$$HS^- + Fe^{+2} \longleftrightarrow FeS + H^+$$
$$FeS + S \longleftrightarrow FeS_2$$

and are dominantly controlled by the quantity of available organic carbon and sulfate metabolizers, H_2S concentration, amount of iron present, and reactivity of iron (Berner, 1970; Canfield, 1988). Therefore, sulfidization tends to decrease with depth as a result of SO_4^{2-} depletion, lack of metabolizable organics, or depletion of reactive iron (Berner, 1970, 1974; Goldhaber and Kaplan, 1974; Leventhal and Taylor, 1990).

The mineral pyrite, FeS_2, is an abundant and widespread authigenic constituent of sediments where it is associated with organic matter (Berner, 1970). Pyrite is stable only

in the absence of oxygen and in the presence of dissolved sulfide (Garrels and Christ, 1965). In modern sediments, the accumulation of organic matter metabolized by bacteria results in the removal of oxygen from associated waters and the subsequent replenishment by dissolved sulfide. Thus, pyrite is present with organic matter and is indicative of anaerobic, sulfidic diagenesis.

The fundamental stages in the process of sedimentary pyrite formation include: bacterial sulfate reduction, reaction of H_2S with iron minerals, and the transformation of black iron monosulfides to pyrite (Berner, 1970). Principal sources of H_2S for pyrite formation are the bacterial reduction of dissolved sulfate (by Desulfovibro desulfuricans) (Leventhal, 1987) and the decomposition of organic sulfur compounds (Berner, 1970). Once H_2S is formed, it reacts with various iron-containing minerals to form iron sulfide. The final stage in pyrite formation is the transformation of iron monosulfide to pyrite. These processes can be summarized in the following reactions:

$$2CH_2O + SO_4^{--} \text{ ------> } 2HCO_3^- + H_2S$$

(Bacterial Sulfate Reduction)

$$3H_2S + 2FeO.OH \text{ ------> } 2\ FeS + S^0 + 4H_2O$$

(Raiswell et al., 1988)

Raiswell and Berner (1985, 1986), Leventhal (1983, 1987), and Raiswell et al. (1988) are just a few of the many

workers who have discussed the roles of TOC-S-Fe relationships in reconstructing depositional environment. C/S ratios are influenced by sedimentation rate, availability of metabolized organic matter, availability of reactive iron to fix sulfides into sediments, and the presence or absence of anaerobic conditions above the sediment-water interface (Dean and Arthur, 1989).

Leventhal (1983a, 1983b) has discussed the relationships of organic carbon and sulfur in order to make inferences about depositional environment in terms of the presence of oxygen (normal marine) or H_2S (euxinic) in overlying bottom water. These relations have been discussed in similar contexts by Berner and Raiswell (1983, 1984), Raiswell and Berner (1985), and Berner (1984) and are established by plotting total organic carbon (TOC), S_{py} (pyritic sulfur) and Fe_t (total iron) or Fe_{HCl} (acid-soluble reactive iron). Normal marine settings are indicated by a positive correlation between TOC and S_{py}, which passes through the origin (Berner, 1984). In contrast, euxinic sediments are typified by high S_{py} values and low TOC, so that an intercept on the S axis results (Leventhal, 1979). Occasionally, S versus TOC plots for euxinic sediments indicate flat (zero) slopes (Raiswell and Berner, 1985) or weak negative slopes (Williams, 1978).

Organic carbon versus sulfur plots have been used to imply depositional settings of modern and ancient rocks

(Leventhal, 1983, 1987; Berner and Raiswell, 1983; Raiswell and Berner, 1985, 1986). Total iron versus sulfur plots (Coveney et al., 1987) also have been used in much the same manner. Unfortunately, these plots (including TOC versus S_{py}) provide little information on reactive iron and its availability. Leventhal and Taylor (1990) point out that this type of plot is greatly influenced by reactive iron availability, a variable that can fluctuate between samples, basins, and source areas.

Differing behavior of TOC-S_{py} plots is caused chiefly by different factors that affect pyrite formation in normal marine and euxinic settings. In the situation of normal marine environments, H_2S necessary for the formation of pyrite is produced by bacterial sulfate reduction below the sediment-water interface (Raiswell and Berner, 1985). Additionally, burial of organic matter is important because it is necessary for in situ sulfate reduction and H_2S formation (Berner, 1971). Therefore, for most normal marine sediments possessing adequate detrital iron (from iron coatings on grains), the principal factor limiting pyrite formation is the amount of organic matter buried (Raiswell and Berner, 1985). Pyrite forms diagenetically resulting in a good correlation between pyrite content and organic matter.

Euxinic sediments possess H_2S above the sediment-water interface as well as within the sediment so that pyrite can

form before burial (syngenetically) in the water column and at the sediment-water interface (Raiswell and Berner, 1985). Consequently, as a result of the presence of H_2S, organic carbon is not required at the site of pyrite formation, which leads to a situation in which high pyrite sulfur can coexist with low organic carbon content. Thus, the limiting factor in pyrite formation in euxinic settings is not the amount of organic carbon buried as in normal marine conditions, but the quantity of detrital reactive iron present (Raiswell, 1982; Leventhal, 1983b; Berner, 1984; Fisher and Hudson, 1987). As a consequence, S is normally better correlated with Fe than with TOC in euxinic sediments.

A complication usually results in euxinic sediments when additional diagenetic pyrite is formed. The diagenetic pyrite is carbon-limited as opposed to the syngenetic pyrite which is iron-limited rather than carbon-limited. A TOC-S plot here results in a situation similar to that of normal marine conditions (positive slope), but with a positive intercept on the S axis (Leventhal, 1979) (Figure 3).

To discern accurately the influence of iron availability, reactive iron contents must be determined, leading to DOP values. DOP is defined as a paleoenvironmental indicator of bottom-water oxygenation conditions (Raiswell et al., 1988) and is calculated as follows:

$$DOP = Fe_{py} / (Fe_{py} + Fe_{HCl})$$

Figure 3. Idealized plots resulting from the formation of iron-limited syngenetic pyrite (A). Note uniform DOP with an increase in % TOC (B). Adapted from Raiswell and Berner (1985).

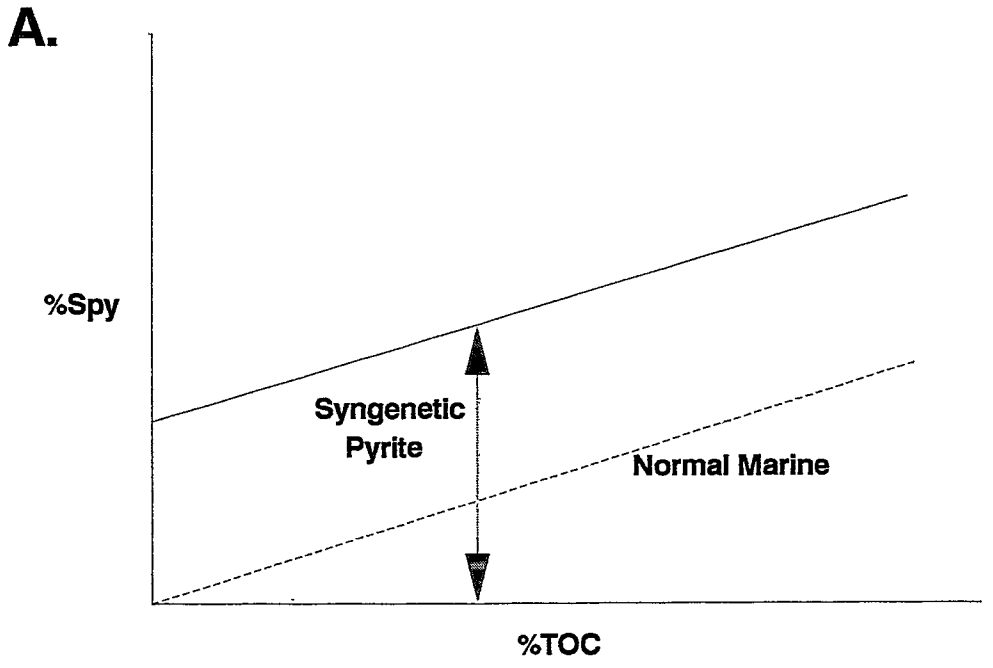
A.
%Spy
Syngenetic
Pyrite
Normal Marine
%TOC

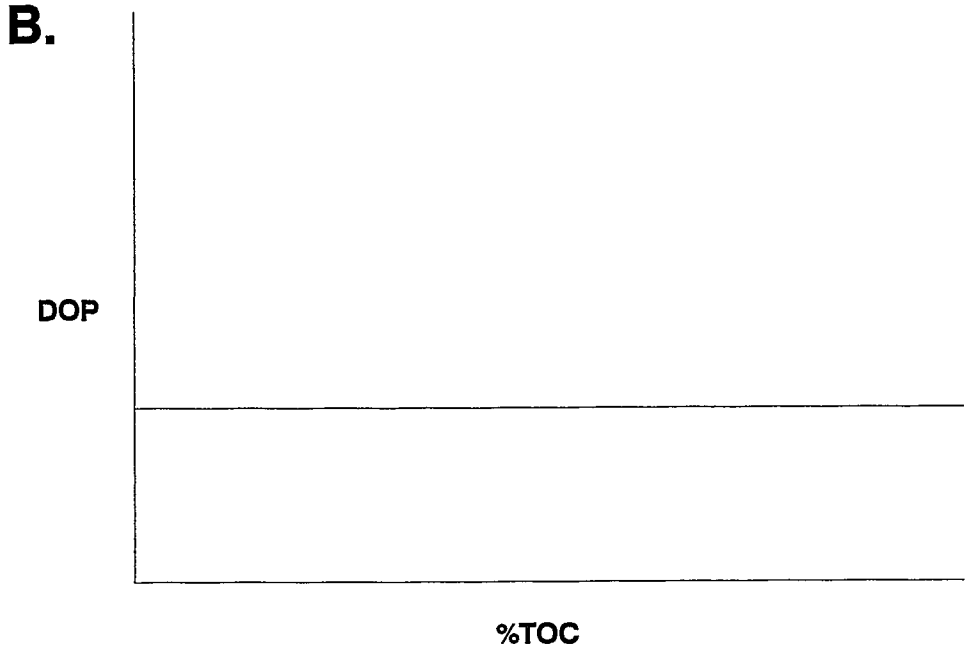
B.
DOP
%TOC

where Fe_{py} is pyritic iron and Fe_{HCl} is acid-soluble iron. DOP has the advantage of removing the effects of total iron on pyrite sulfur concentration (Raiswell and Berner, 1985). The use of the parameter eliminates the effects from sediment to sediment of total iron and places the emphasis on the reactivity of iron and H_2S production. Overall, if DOP is high, the higher the H_2S concentration, the greater the reactivity of iron minerals present, and the longer that H_2S remains in contact with the iron minerals (Raiswell and Berner, 1985).

DOP also can be related to the redox state of the overlying seawater and microenvironments in the top few centimeters of the sediment (Raiswell and Berner, 1985, 1986). Various terminology has been applied to the oxygenation levels within environments. Aerobic or normal marine (well-oxygenated) water columns generally produce DOP values less than 0.45. Dysaerobic or suboxic (low to no O_2 present, but no H_2S) water columns provide intermediate DOP values from 0.46 to 0.75. Bituminous, inhospitable conditions, anaerobic, or euxinic have been applied to water columns containing no O_2, but H_2S-containing, with DOP values greater than 0.75. These boundaries between aerobic, dysaerobic, and inhospitable conditions in the bottom-water have been applied according to work by Raiswell et al. (1988).

Reactive iron is essentially nonsilicate-bound iron (amorphous iron oxides, oxyhydroxides, and crystalline oxides), but may also include iron monosulfides (Canfield, 1989). DOP measures the completeness of reactive iron reacting with aqueous sulfides. In other words, a sample that possesses a DOP of 0.80 indicates that 20% of the remaining reactive iron could undergo sulfidization, providing sufficient sulfide material is present and the reaction has ample time to take place.

The importance of DOP is in its usefulness in the study of euxinic (and near-euxinic) sediments. In the euxinic scenario, C/S plots yield a positive slope with a positive intercept on the S axis. The nonzero intercept contrasts with the normal marine scenario. Percentage of organic carbon present plotted versus DOP yields a pronounced positive slope in the euxinic situation (as a result of pyrite forming syngenetically as well as diagenetically) compared with a flat (zero) slope on the TOC versus DOP in the normal marine situation. Thus, the two scenarios are separated only easily if DOP as well as C/S ratios are used, but are difficult to separate using only C/S plots (Raiswell and Berner, 1985).

In summary, three principal depositional settings characterize black shale development (Table 1). These in clude euxinic (inhospitable bottom-water oxygenation conditions), normal marine (oxygenated bottom waters), and fresh-

water (oxygen-rich). Eight parameters (both qualitative and quantitative) are used to separate the three principal environments of carbonaceous shale units: rate of sedimentation, ^{34}S values, TOC/S_{py} ratios, organic carbon character, DOP values, pyrite mode of formation, bottom-water oxygenation conditions, and circulatory processes.

Table 1. A general comparison of various depositional settings of black shales. Note the lack of modern analog for semi-euxinic depositional environment, thus pyrite formation and bottom-water oxygenation are unclear. Compiled from numerous sources.

General Comparison of Depositional Settings of Black Shales				
	Euxinic	**Semi-euxinic**	**Normal marine**	**Freshwater**
Example	Black Sea (modern) Upper Devonian of Appalachians (ancient)	Midcontinent Pennsylvanian (ancient)	anoxic sediments Holocene	lacustrine environments
S isotopes	light	intermediate	intermediate	heavy
C/S ratios	low (1-2)	low (1-2)	moderate (3)	high (8-10)
DOP value	high	low-moderate	moderate	low
Pyrite fm.	Addn. of C-limited diagenetic pyrite high reactive iron Fe-limited	?	syngenetic pyrite reactive iron C-limited	syngenetic pyrite low reactive iron S-limited
Bottom-water oxygenation	H2S-laden	?	No H2S O2-rich	No H2S Low O2
Organic C Control	preservation	combination preservation and production	mostly production	production

Chapter 3. Description of Analytical Methodology

Study methods for the research of Midcontinent Pennsylvanian black shales includes field work, core analysis, X-ray fluorescence (XRF), organic carbon measurement, sulfide-sulfur determination, acid-soluble iron determination, X-ray diffraction (XRD), sulfur isotope analyses, pyrolysis (Rock-Eval), instrumental neutron activation analysis (INAA), and statistical analysis (Figure 4). X-ray fluorescence (XRF, Rigaku Model 3070 made with pressed microcrystalline cellulose disks), organic carbon measurement (Perkin-Elmer Model 240 Elemental Analyzer), sulfide-sulfur determination (modified method of Canfield et al. (1986)), acid-soluble iron determination (Beckman Model DU-2 Spectrophotometer using 0-phenanthroline method), and X-ray diffraction (XRD, Siemens Model 500 X-ray Diffractometer with Cu tube) were conducted at the Department of Geology, University of Cincinnati. Statistical analyses were conducted with the aid of Mr. Roger Stuebing at the Department of Social Sciences, University of Cincinnati using the Statistical Package for the Social Sciences (SPSS). Representative samples were sent to XRAL Laboratories in Ann Arbor, Michigan for instrumental neutron activation analysis (INAA). Other INAA data were provided by Dr. Raymond M. Coveney, Jr., of the University of Missouri-Kansas City. Selected samples were sent to Dr. Edward M. Ripley of Indiana University in Bloomington,

Figure 4. Flowchart of analytical methodology for the study of the geochemistry of Midcontinent Pennsylvanian black shales.

FLOWCHART OF ANALYTICAL METHODOLOGY

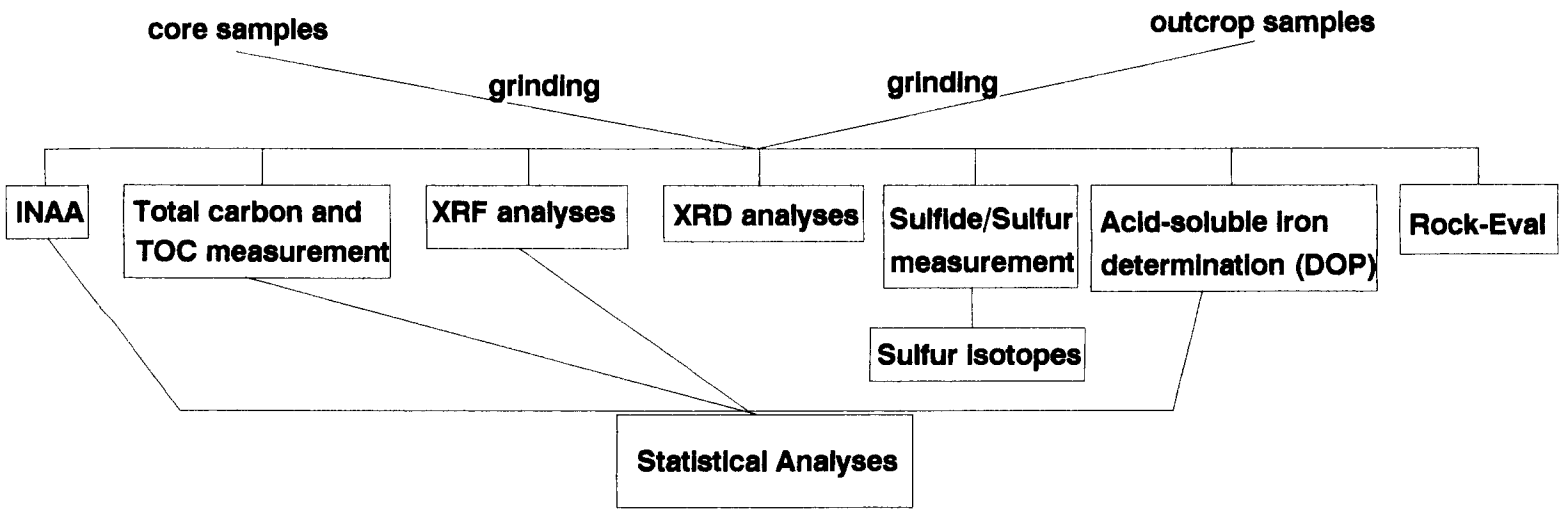

Indiana, for sulfur isotope analyses. Additionally, several representative samples were sent to Dr. Michael D. Lewan of Amoco Production Company Research Center in Tulsa, Oklahoma for pyrolysis (Rock-Eval).

Sample Collection

Rock samples comprising this study consisted of both outcrop and core samples. Most core samples were provided by the Kansas Geological Survey in Lawrence, Kansas. Two core samples were provided by Dr. Raymond M. Coveney, Jr., of the University of Missouri-Kansas City, and one core sample suite was provided by Dr. Daniel F. Merriam of The Wichita State University and Kansas Geological Survey. Outcrop samples of the Heebner- and Shanghai-type black shales were collected during the field seasons of 1988, 1989, and 1990. A total of 75 outcrop and core samples from 37 localities were utilized for this study (Figure 5). Additional samples were provided by the Indiana, Missouri, and Iowa Geological Surveys through the courtesy of Dr. R. M. Coveney, Jr. of the University of Missouri-Kansas City. In addition, published data of organic carbon measurements, DOP values, and sulfide-sulfur measurements also were used for comparison.

Figure 5. Study area of Heebner-type, Shanghai-type, and Mecca-type black shales in this study. Symbols generalized locations. Adapted from Schultz and Coveney (in press).

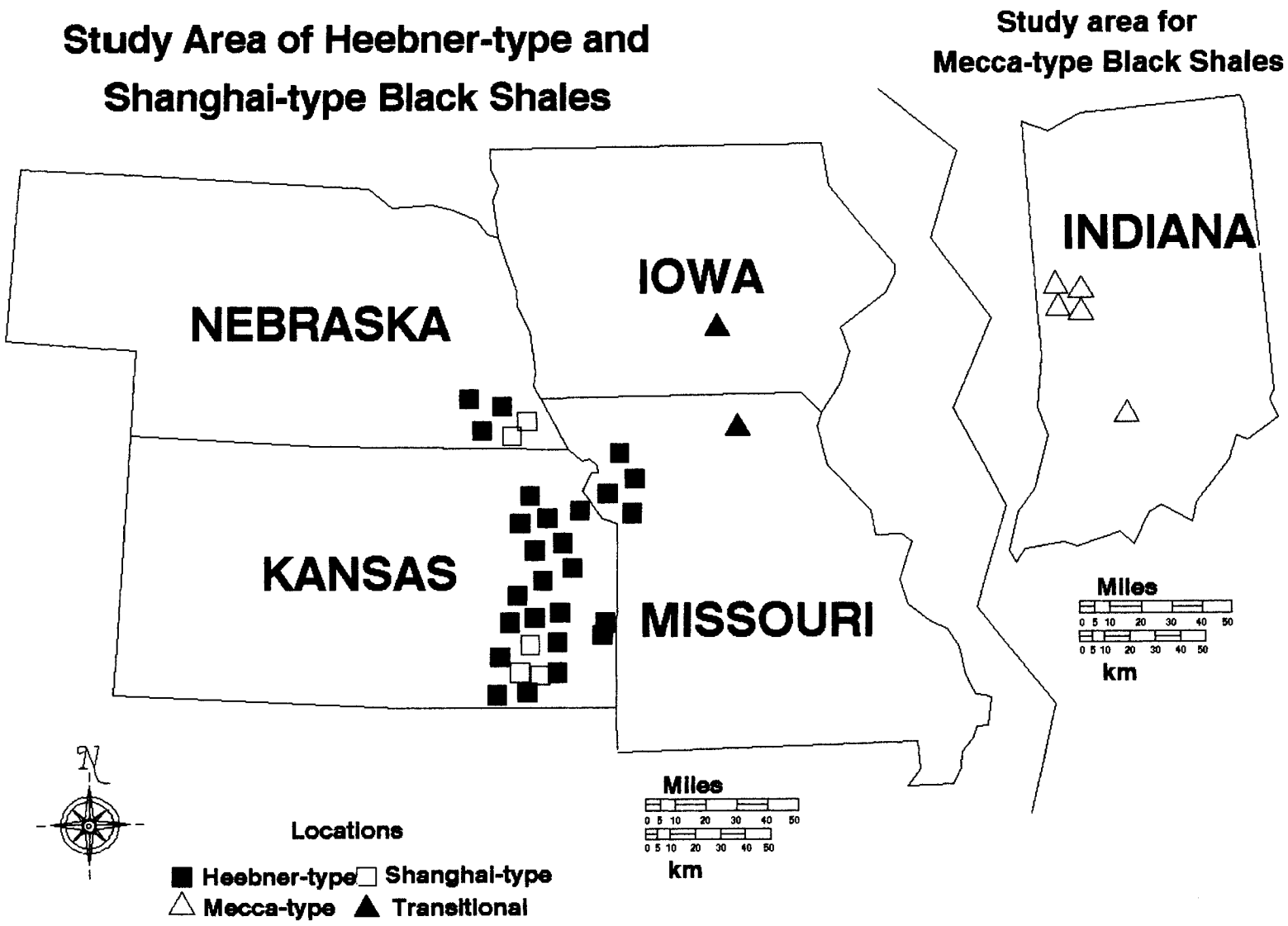
Study Area of Heebner-type and
Shanghai-type Black Shales
Study area for
Mecca-type Black Shales
NEBRASKA
IOWA
INDIANA
KANSAS
MISSOURI
Miles
0 5 10 20 30 40 50
0 5 10 20 30 40 50
km
N
Locations
Heebner-type
Shanghai-type
Mecca-type
Transitional
Miles
0 5 10 20 30 40 50
0 5 10 20 30 40 50
km

The sampling scheme for outcrop samples consisted of tracing individual units along strike in eastern Kansas, southeastern Nebraska, and west-central Missouri. The Mecca Quarry Shale samples were collected in several locations in west-central Indiana near the type section: the Mecca Quarry fossil dig of Zangerl and Richardson (1963) near Mecca, Indiana (Figure 5). Samples collected are representative of the least-weathered surfaces, nearest the watertable where repeated wetting and desiccation is at a minimum. Continuous channel samples (1-4 cm intervals) were collected in several locations to characterize fully the vertical succession of the units.

Representative Heebner-type and Shanghai-type black shale samples (both outcrop and core) from west-central Missouri, southeastern Nebraska, and eastern Kansas were powdered to -400 mesh in a shatterbox at the University of Cincinnati. In order to minimize oxidation of samples, crushing occurred as soon as possible following collection. It was determined by microscopy that two to three minutes per sample in a Spex Mill shatterbox with tungsten carbide mill reduced samples to uniform (< 400 μm) powders. Observations of the resulting powders under a standard petrographic microscope confirmed that the grain size was uniform between mineral types within the black shales. Following crushing, the powders were stored immediately in air-tight nalgene plastic containers for later analyses (colorimetric

iron determination, sulfide-sulfur measurements, organic carbon investigations, INAA, XRF, XRD, etc.). The selection of samples for various analytical measurements was based on location (both vertically within a given section and regionally), lithology (black shale, dark-gray shale, or gray shale), and black shale type (Heebner-type, Shanghai-type, or Mecca-type).

Whole-Rock X-ray Fluorescence (XRF) Analyses

A Rigaku 3070 X-ray wavelength dispersive spectrometer at the University of Cincinnati, Department of Geology was used for determining percentages of major oxides and elements within black shale samples. Standards used for calibration curves included both U.S. Geological Survey geochemical standards and N.I.S.T. standards (see Appendix B.). A total of 25 geochemical standards were used in the construction of calibration curves. Major oxides and elements analyzed for included: SiO_2, TiO_2, Al_2O_3, Fe_2O_3, MnO_2, CaO, Na_2O, K_2O, P_2O_5, and total sulfur (S). Both core and outcrop samples were crushed and pressed into thin pellets with microcrystalline cellulose serving as the base. A Spex X-press was used at 20 tons of pressure to press the pellets. The reasons for using a microcrystalline cellulose base include: ease of handling, durability, chemical stability,

and it provided a nonreactive, semi-nonporous medium. Pellets were analyzed at three repetitions each and plotted interactively on the calibration curves using a DEC computer system. Settings for the XRF unit were as follows: voltage - 50kV, current - 50 mA, P-10 gas - 50.

Total and Organic Carbon Measurement

Total and organic carbon measurements were conducted using a Perkin-Elmer 240 Elemental Analyzer at the Depart ment of Geology at the University of Cincinnati. The measurements were made by the detection of combustible products (i.e., CO_2 for carbon). Besides carbon, the Perkin-Elmer 240 Elemental Analyzer accurately determines nitrogen, hydrogen, and sulfur contents of whole rock samples by detecting their combustion products (N_2, H_2O, and SO_2). Only the carbon content was measured in this study.

The U. S. Geological Survey geochemical standard SDO-1 (Ohio Devonian Shale) was used as a reference standard in both total carbon and total organic carbon measurements. SDO-1 contains 10.48% total carbon and 10.13% total organic carbon (TOC) as measured by the U.S. Geological Survey.

Calculations to determine the weight percent total carbon in the SDO-1 standard consisted of taking the voltage difference (in mV) between the blank ladle and the standard sample in the ladle. A K value was determined by dividing

the voltage difference (in mV) by 0.1048 and the weight (in mg). The K value then is used to convert the voltage difference to a weight percent of total carbon present. Unknown samples were then run and compared to the standard SDO-1 in terms of intensity on a chart recorder attached to the system.

Following determinations for weight percent total carbon, powder samples were treated with concentrated HCl (12 N) to dissolve any carbonate (nonorganic) carbon present. Samples were filtered and residue allowed to dry overnight at 50°C in an oven. Procedures were followed as in the investigation for total weight percent carbon, but using 0.1013 total organic carbon in place of 0.1048 total carbon for the SDO-1 standard. A K value was determined by dividing the voltage difference (in mV) by 0.1013 and the weight (in mg) of the sample. The K value is used, as in the total carbon investigation, to convert the voltage difference to a weight percent total organic carbon (TOC) present. Unknown samples were run in an identical manner and compared to SDO-1 in terms of intensity on the chart recorder. All samples throughout the investigation were weighed on a microbalance to the nearest 0.0001 gm. Experimental error in this study was 0.5-1.0% based on duplicate runs, although Liu (1988) reported errors of only 0.1-0.5% with the same equipment and standard. Three repetitions of each sample were run to insure reproducible results. The

Perkin-Elmer 240 Elemental Analyzer was allowed to warm up for one to two weeks before stabilizing and sample blanks were run and new K values calculated each time the machinery was used.

Sulfide-Sulfur Measurement

Because sulfur is present in both modern sediments and ancient rocks in a variety of phases (e.g., pyrite, elemental sulfur, sulfate, and organic sulfur), a method of partitioning these sulfur phases was necessary in this study (Liu, 1988). The technique, designed specifically to determine reduced inorganic sulfide-sulfur, is essentially the same as that devised by Canfield et al. (1986), with minor modifications. Powder samples are used to convert sulfur compounds within the black shales to a silver sulfide precipitate, which can be used later for sulfur isotope analyses.

The technique used in this study utilized a chromium reduction system described by Canfield et al. (1986) and modified by Okita (1987) and Liu (1988). In this study, further modifications were necessary in order to accommodate the high content of pyrite in the Pennsylvanian black shales. Essentially, the procedure involved digesting approximately 0.1-1.0 gms of sample (crushed to -400 mesh) in two portions. Initially, boiling in 6 N HCl is accom-

plished to remove acid-soluble sulfates and carbonate material present. Secondly, the conversion of pyrite to H_2S is accomplished by adding a solution of $CrCl_3$ (a Jones Reductor) reduced over zinc and heating for 2 to 4 hours, or until reduction occurs. A nitrogen atmosphere is maintained throughout the process. H_2S is piped into a $AgNO_3$ trap where an Ag_2S precipitate is formed. The Ag_2S precipitate is weighed and used to calculate sulfide-sulfur content. Sample weight is recorded in gms and is acquired by taking the difference between the filter paper weight + sulfide weight and filter paper weight. The result (silver sulfide weight in gms) is multiplied by 12.9381% (the weight percent of sulfur present in Ag_2S) and divided by the original black shale sample weight. The final result is sulfide in weight percent.

It should be noted that this technique represents the most efficient and reproducible method to obtain inorganic sulfide-sulfur data. It was determined that, unlike the method of Liu (1988), who used powdered zinc, zinc shot was most effective in totally reducing the $CrCl_3$ solution. Zinc powder tended to float and flocculate, thus making transfer of the $CrCl_3$ solution into the sample chamber difficult. Thus, this method represents a combination of the Canfield et al. (1986), Okita (1987), and portions of the Liu (1988) methods. However, an innovation not used in any of these techniques includes a stopcock technique rather than syringe

methods. The glassware with stopcocks provided an efficient way of transferring fluids without the difficulty of syringes. $CrCl_3$ added to the sample must be reduced (evidenced by a blue color from the original green of the solution). To accomplish the $CrCl_3$ reduction, 60 ml of H_2O + 10 ml 6 N HCl was added to approximately fifty zinc pellets. The reaction progresses for approximately 15 minutes at which time the solution was drained and $CrCl_3$ (now green) is added to the zinc shot. An exothermic reaction continues for 15 to 20 minutes or until a blue color results. At that time, the solution is added to the sample chamber by opening the appropriate stopcock.

Additionally, it was determined that large amounts of total sulfur in shale samples tended to overwhelm the system. Through experimentation, it was determined that total sulfur contents for shale samples with greater than 3.0% total sulfur content, only 0.1 gm of sample could be used. From 2.5 to 3.0% total sulfur in samples, 0.25 to 0.50 gms of sample were used, and for sample containing less than 2.5% total sulfur, 0.50 to 1.0 gms of sample was used. The accuracy of this method was determined by using pure pyrite samples (weight percent of sulfur in pyrite is 53.34). Three samples were run resulting in an average weight percent of 51.21 or 96% return. Average error is approximately 0.5 to 1.0%. Liu (1988), using a similar but not identical setup, reported a 97% return and 0.1% error. The time for

complete conversion of pyrite varied from 1.5 hours for pyrite-poor samples to 4.5 hours for pyrite-rich samples.

Colorimetric Iron Determination (Acid-soluble iron determination) and Degree of Pyritization (DOP)

Colorimetry is based on the principle that iron is dissolved into solution and reduced (to the ferrous or Fe^{+2} state) by boiling with concentrated HCl and hydroxylamine. The solution is treated with 1,10 phenanthroline (indicator) solution. The orange-red solution obeys Beer's Law and a pH of 2.9-3.5 insures rapid (15 minutes) color development in the presence of excess phenanthroline (Taras, 1971; Liu, 1988). The purpose of colorimetric iron determination is to express ferrous, ferric, and total iron concentrations in a sample solution and calculate DOP (degree of pyritization), therefore inferring a quantitative expression of depositional setting.

The colorimetric iron determination was used in this study because it extracts the most reactive iron compounds and is readily reproducible (Liu, 1988). A Beckman DU-2 spectrophotometer was used to determine ferrous (acid-soluble), ferric, and total iron contents. Ferric iron was not measured directly during the process, but was calculated as the difference between total iron minus ferrous iron

present.

Reactive iron determination in the laboratory is critical to an accurate assessment of DOP. Reactive iron is often equated with acid-extractable iron, which is thought to represent the iron that has the potential to react with dissolved sulfides in order to form pyrite (Leventhal and Taylor, 1990). Experimentally, DOP has been determined using a number of different methods. Berner (1970) defined reactive iron as the iron that was solubilized from a 100 mg sample by a 1-minute concentrated HCl boil. More recently, however, Leventhal and Taylor (1990) have shown that a 24-hour room temperature treatment with 1 N HCl is as accurate and effective, yet with easier laboratory handling. Additionally, Canfield (1988) and Berner (1987) have presented results indicating reaction with reagents such as Na-dithionite in a citrate buffer, provide ample results. A comparison of the DOP of SDO-1 (Ohio Devonian Shale Standard) in this study with that of the U.S. Geological Survey in Denver, Colorado revealed virtually identical results. Leventhal and Taylor (1990) obtained values of 0.73-0.76 for DOP of SDO-1 using a 24 hour room temperature leaching method, whereas a value of 0.71 was obtained in this study using a one-minute boil in HCl procedure.

In this study, standard solutions for the colorimetric iron determination were prepared by using ferrous sulfate ($FeSO_4$). The standard solution was diluted into four con-

centrations (1 mg/l, 2 mg/l, 5 mg/l, and 10 mg/l) with deionized distilled water in order to construct a standard calibration curve. Solution aliquots were treated with hydroxylamine (100 g/l concentration) reducing ferric iron to the ferrous state. An ammonium acetate buffer was then added to the aliquots with phenanthroline (indicator) present to develop an orange color in the solution. Sample solutions were measured for iron in a Beckman DU-2 spectrophotometer (tungsten light source and 510 μ for iron) to obtain absorption values. Absorption versus concentration was plotted to produce a standard linear plot and subsequent shale samples were treated in an identical fashion as the standards.

X-ray Diffraction (XRD) and Clay Mineralogy

A brief examination of the clay mineralogy of the Midcontinent Pennsylvanian black shales is important in understanding the chemical make-up of the shale units. The preparation of the samples for analysis consisted of a single method of preparation for all samples; this includes samples from all three black shale types.

Samples were collected in the field and from cores (see section on sample collection). Samples were crushed into a fine powder with a mortar and pestle and placed in airtight Nalgene containers. Following crushing, each sample was run

as a randomly oriented pressed powder sample on the X-ray diffractometer. This method provides an indication of both the bulk mineralogy of the shale samples and the proportion of clay and nonclay minerals present. Diffraction traces were recorded from 2 degrees two-theta to 50 degrees two-theta, in order to access the range of minerals present. The equipment used for the X-ray diffraction analyses was a fully automated Siemens D-500 X-ray powder diffractometer with copper (K_{alpha} radiation) tube and a monochromator. Settings for the diffractometer were: voltage - 40 kV, current - 30 mA, and a scan time of 0.10 degrees per second. Nonclay minerals such as quartz, feldspars, carbonates, pyrite, as well as organic matter are normally present in coarser size fractions and can be separated from the clay minerals by extracting a fine particle size, leaving the coarser fraction as a residue (Moore and Reynolds, 1989).

Because many of the nonclay minerals can mask basal clay mineral peak intensities, it was necessary to separate the samples into size fractions. Approximately 10 gm of shale sample powder was placed in a 200 ml beaker filled with deionized water. Sample and water were poured into a stainless steel mixing cup and placed under a high speed stirrer for 2-3 minutes. Small amounts of 0.02 N sodium pyrophosphate were added to aid in the dispersion process. The sample was transferred back to the 200 ml beaker and allowed to stand until sand-sized particles (62 mu) were

sedimented. The clay-silt suspension was decanted and water was added to the 200 ml mark. The suspension was allowed to stand so that the < 2 mμ e.s.d. (equivalent spherical diameter) particles settled according to Stokes' Law. According to Moore and Reynolds (1989), particles less than 20 mu generally settle in a fluid obeying Stokes' Law. Samples in this study were separated into powder, 2 mμ, 1 mμ, and < 1 mμ size fractions according to the settling velocities determined using Stokes' Law.

Because of the difficulty of producing random powder mounts of clay minerals, a preferentially oriented sample is most appropriate in the analysis of clays (Moore and Reynolds, 1989). Only a qualitative assessment of clays was necessary for this study, therefore, the glass slide pipette method was selected for the oriented clay mineral aggregate. Approximately 5 ml of clay-water suspension was transferred to a glass slide by a pipette equipped with a rubber suction bulb. The suspension was allowed to dry at room temperature. Slides from all three size fractions were prepared and subsequently air dried. Slides were X-rayed according to normal operating procedures.

An ethylene glycol solvation method was employed on select samples to improve identification of clay minerals on the diffractometer trace. Slides, prepared in the various size fractions, were placed on a porcelain plate in a desiccator jar with ethylene glycol in the bottom of the jar.

The jar was closed and placed in an oven at 60°C for a minimum of 8 hours. After saturation was complete, the slides were X-rayed within one hour following removal from the oven.

Clay minerals are identified by the basal (001) peaks on the diffractograms, usually enhanced by oriented aggregates. Normal (hkl) peaks are not diagnostic because structures of most clays are similar in the X-Y directions (Moore and Reynolds, 1989). The atomic pattern apparently differs in the Z direction and therefore is most diagnostic. JCPDS (Joint Committee on Powder Diffraction Studies) powder diffraction cards are most useful for the identification of the nonclay minerals, and do not include oriented aggregates, therefore making the identification of clay mineral constituents difficult. In this study, powder sample diffractograms were interpreted using the JCPDS powder diffraction cards and oriented clay mineral aggregates were interpreted using data gathered from Moore and Reynolds (1989) (Table 2).

Measurement of polytypes was accomplished by using the random powder mounts. The polytype determinations were made using the .IDM program on the X-ray diffractometer setup on chlorite, illite, and kaolin groups. Polytypes were identified using Table 3 compiled from Moore and Reynolds (1989).

Table 2. Clay minerals and corresponding basal spacings and 2-theta angles.

Clay Mineral	Basal Spacings (00l)	2–theta	Glycolation effect
Illite	10 Å (002)	8.70	none
Chlorite	14.2 Å + series of basal spacings	6.27	none
Kaolinite	7.15 Å, 3.75 Å (002)	12.56	none
Smectite	15 Å (001)	6.00	shift to 5.2 degrees 2–theta (16.9 Å)

Table 3. Clay minerals, polytypes, and their associated peaks on the X-ray diffraction trace. Data compiled from Moore and Reynolds (1989).

Clay Mineral	Polytype	peaks
Chlorite	Ia	d=2.65
		d=2.39 strong
	Ib	d=2.69
		d=2.65
		d=2.51 strong
		d=2.15
	Ib	d=2.47
	IIb	d=2.66
		d=2.59 strong
		d=2.55 strong
		d=2.45 strong
		d=2.39 strong
		d=2.26 strong
Kaolin	Kaolinite	d=3.842
		d=3.12
		d=2.750
		d=2.340
		d=2.290
		d=2.184
		d=1.99
		d=1.839
		d=1.619
	Dickite	d=3.262
		d=3.097
		d=2.937
		d=2.795
		d=2.324
		d=2.211
		d=1.974
		d=1.860
	Nacrite	d=3.44
		d=3.09
		d=2.927
		d=2.41
		d=2.27
		d=2.09
		d=1.92
		d=1.67
		d=1.62
Micas	1Md and 1M	d=2.450 (131)
		d=2.405 (132)
		d=2.156 (133)
	1M	d=4.35 (111)
		d=4.12 (021)
		d=3.66 (112)
		d=3.07 (112)
		d=2.93 (113)
		d=2.69 (023)
	2M1	d=4.29 (111)
		d=4.09 (022)
		d=3.88 (113)
		d=3.72 (023)
		d=3.49 (114)
		d=3.20 (114)
		d=2.98 (025)
		d=2.86 (115)
		d=2.79 (116)

Pyrolysis (Rock-Eval) Analysis of Whole-Rock Samples

A standard method of source-rock evaluation (Rock-Eval) was used in the study of Midcontinent Pennsylvanian black shale samples. Rock-Eval utilizes a pyrolysis device where the sample (approximately 100 mg) is heated progressively to 550°C under an inert atmosphere (e.g., helium) using a temperature program or pyrogram (Peters, 1986). Allowing for time to cool the oven, most sample analyses require 20 to 30 minutes.

Hydrocarbons already present in the rock in a free state or adsorbed state are volatized at moderate temperatures so that the quantity of these hydrocarbons (REVOL = S_1) is measured by a flame ionization detector (FID) (Tissot and Welte, 1984). Subsequently, pyrolysis of kerogen results in the generation of hydrocarbons and hydrocarbon-like compounds (REGEN = S_2) and oxygen-containing volatiles (i.e., CO_2 (S_3) and water) (Tissot and Welte, 1984). Volatile compounds generated are split into two streams passing respectively through an FID which measures S_2 and a thermal conductivity meter measuring S_3 (Tissot and Welte, 1984). A temperature program (pyrogram) allows for good S_1 and S_2 peak separation on the FID (Peters, 1986). However, the measurement of S_3 is limited to a convenient temperature window in order to include the main stage of CO_2 generation from kerogen, and to avoid other CO_2 sources (i.e., carbon-

ate decomposition, especially of siderite) and was not measured during this analysis. An additional parameter measured is the maximum temperature of hydrocarbon generation during pyrolysis (T_{max}). This parameter is utilized mainly for evaluation of maturation stages (Claypool and Read, 1976).

The type of kerogen is characterized by the hydrogen index (REG-TOC = S_2/TOC in wgt. % / wgt. %). This index is independent of organic matter abundance and is strongly related to the elemental composition of kerogen (Tissot and Welte, 1984). Therefore, a semiquantitative evaluation of the genetic potential of a given rock can be achieved by pyrolysis. The S_1 quantity represents the fraction of original genetic potential effectively transformed into hydrocarbons. The S_2 quantity reflects the other fraction of the genetic potential or the residual potential which has not yet been used to generate hydrocarbons (Peters, 1986). Therefore, $S_1 + S_2$ is an expression that evaluates the genetic potential, which accounts for abundance and type of organic matter.

The pyrolysis method of Espitalie et al. (1977) utilizes the three parameters S_1, S_2, and S_3. However, other methods, such as that used in this study, measure only S_1 and S_2. Additionally, T_{max} is recorded at the maximum temperature of hydrocarbon generation during pyrolysis.

Barker (1974), Claypool and Read (1976), and Espitalie et al. (1977) have shown that two indices are of specific importance in characterizing the rank of evolution: $S_1/(S_1 + S_2)$ and the temperature T_{max} (Tissot and Welte, 1984). Barring migration, $S_1/(S_1 + S_2)$ represents the transformation ratio where the continual increase of this ratio with depth makes it a valuable index of maturation (Tissot and Welte, 1984). Additionally, these values may be used as a quantitative evaluation of the hydrocarbons generated.

T_{max} also increases with depth, but the numerical scale must be calibrated with depth because of the scale change with the rate of heating. T_{max} is among the most reliable parameters for characterizing thermal evolution (Tissot and Welte, 1984).

A classification scheme generally used for source-rock potential (Tissot and Welte, 1984) is:

for S_1: <2000 ppm: no oil source rock, potential for gas
2000-6000 ppm: moderate source rock
>6000 ppm: good source rock

In summary, Rock-Eval is a pyrolysis process used to rapidly evaluate the petroleum-generative potential and thermal maturity of whole-rock samples. Pyrolysis de-emphasizes organic-poor, clay-rich samples that show low-hydrogen indices and high T_{max} values. T_{max} is affected by maturation, organic matter type, contamination, and mineral types. Constant sample weights (100 mg) are used and organic-rich

samples may be diluted with carbonate material so that detector linearity by pyrolizing various weights of an organic-rich rock may be determined (Tissot and Welte, 1984).

Instrumental Neutron Activation Analyses (INAA): Rare Earth Elements

Rare earth elements (REE) are trace constituents in most geochemical environments. Only rarely are they individually present at more than a few parts per million, as in situations of extreme fractionation (Taylor and McLennan, 1988). In this study, instrumental neutron activation analysis (INAA) was used to determine quantities of REE present in black shale samples. The analyses were performed by XRAL Laboratories in Ann Arbor, Michigan. Detection limits were as follows:

La	0.500 ppm
Ce	3.000 ppm
Nd	5.000 ppm
Sm	0.100 ppm
Eu	0.200 ppm
Tb	0.500 ppm
Yb	0.200 ppm

One difficulty in the comparison of REE data is the "odd-even effect", in which even-numbered lanthanides are more abundant than those with odd-numbered atomic numbers.

Numerous types of normalizing procedures have been adopted to overcome the difficulties in data comparison. Currently, two methods are generally accepted and widely used in normalizing the data. The Coryell-Masuda method (Coryell et al., 1963) consists of forming a ratio of one pattern to another, usually a chondritic-abundance pattern. This removes the "odd-even effect" producing a smooth REE pattern and allows for comparisons between different patterns. It also openly displays enrichment or depletion of an element and behavior of neighboring elements (Taylor and McLennan, 1988). Chondrite normalizing parameters are not uniform from lab to lab, but usually the values from Evensen et al. (1978), are used in comparisons. Use of different normalizing factors is not normally a problem because various sets of chondrite-normalized values have similar interelement ratios, although patterns may be displaced 15 to 20% (Taylor and McLennan, 1988).

The second type of abundance pattern used for normalization is the NASC (North American Shale Composite) or PAAS (Post-Archean Australian Average Shale) methods. These patterns are generally taken to represent the upper continental crust after exposure to erosion and weathering. The preference for use of PAAS over NASC (composite) is based on the potential for inclusion of aberrant material in composite samples.

Europium (Eu) is generally fractionated from other REE and thus it is useful in quantifying element enrichment or depletion. Eu/Eu* is the ratio of Eu to a theoretical smoothing value for no anomaly and is calculated as:

$$Eu/Eu^* = Eu_N/(Sm_N * Gd_N)^{1/2}$$
where N = chondrite-normalized values

The clay mineral fraction is an important carrier for REE. Cullers et al. (1979), have examined REE in various size fractions of Pennsylvanian-Permian Midcontinent shales. In their study, they showed that in the 2 micron size fraction (normalized), values mimicked the REE patterns for the source area of the shales. Additional results of their study concluded that most REE are present in the less than 2 micron size fraction, but no correlations of REE with clay mineralogy was evident. Also, the nature of the Eu anomalies is similar in all of the size fractions.

Sulfur Isotope Analyses

Sulfur isotopes can aid in the determination of sulfide and metal origins. The values are likely to reflect the biogeochemistry of ancient seawaters and possibly the isotopic composition of sulfate in the ocean at the time of

deposition (Coveney and Shaffer, 1988).

Isotope analyses in this study are from Ag_2S residues stemming from a modified chromium reduction technique in the partitioning of sulfide-sulfur. Representative samples from each black shale unit were sent to Dr. Edward M. Ripley of Indiana University in Bloomington, Indiana. The representative samples were selected to provide a broad cross section of samples from various locations. This type of sampling is beneficial to evaluate the relative importance of sulfide formed in the water column over that formed diagenetically within the sediment. Trends from east to west in the study area thus can be discerned based on the results.

Residues from the chromium reduction technique were combusted with CuO at 1000 ·C and run on a Nuclide 6", 60 · sector stable isotope ratio mass spectrometer. Analytical uncertainty is approximately + or - 0.2%. (E. M. Ripley, personal communication, 1990).

Statistical Analyses

In order to determine which characteristics are most useful in separating Midcontinent Pennsylvanian black shale types, it was necessary to discriminate accurately between the three black shale types defined. Data from samples were treated by stepwise discriminant analysis using the Statistical Package for the Social Sciences (SPSS) (Figure 6).

Figure 6. Flowchart for statistical analyses of geochemical data.

STATISTICAL ANALYSIS OF GEOCHEMICAL DATA

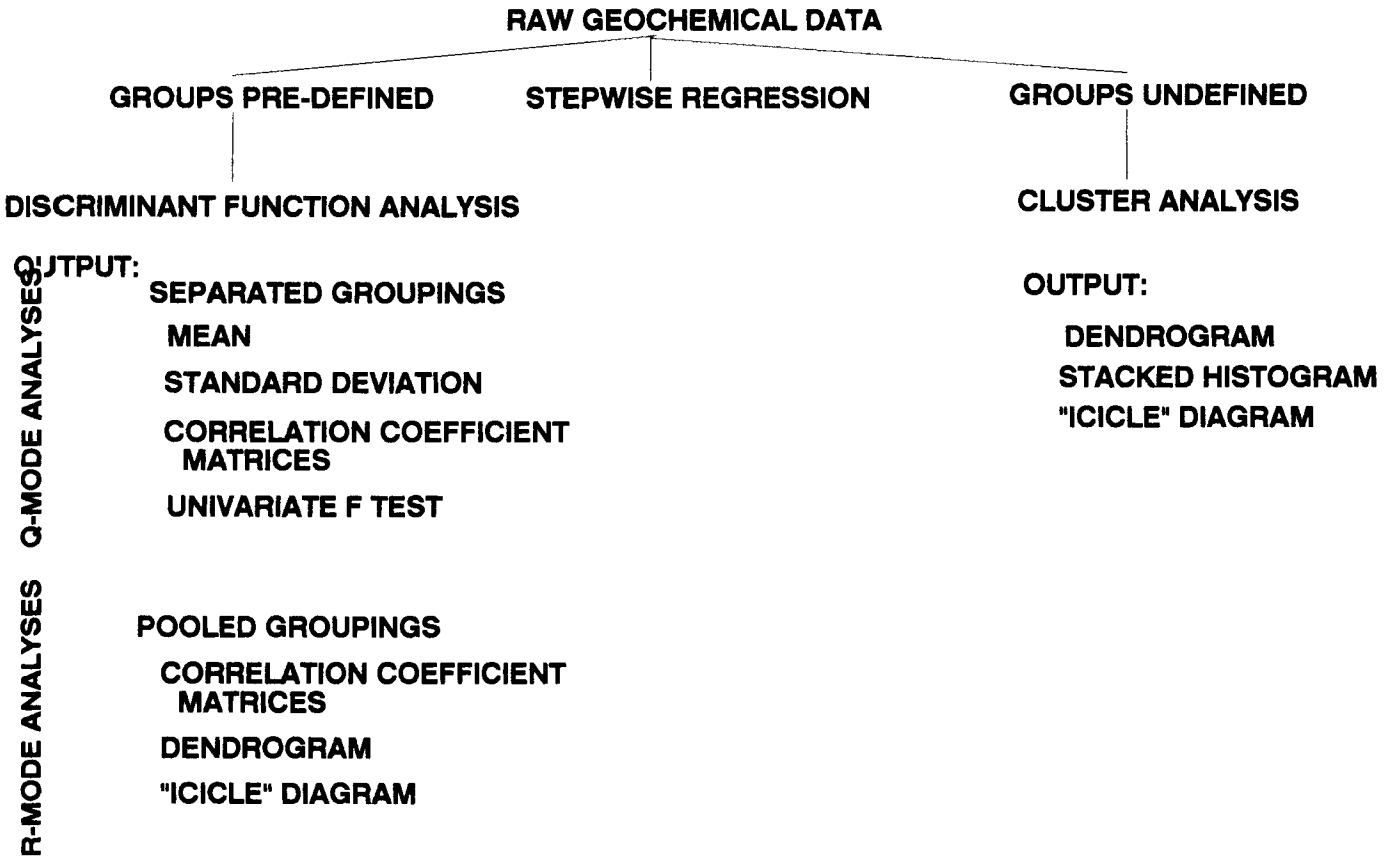

One of the most widely used multivariate procedures in the earth sciences is the discriminant function (Davis, 1986). Discrimination of samples is determining the linear combination of variables that provides the maximum difference between two or more groups (Davis, 1986) or, as defined by Klecka (1975), is a "statistical technique which allows the differences between two or more groups of objects with respect to several variables to be calculated simultaneously." Basic assumptions of the analysis are: (a) the data are members of two or more mutually exclusive groups, (b) the groups are defined such that each case belongs to only one group, (c) no variable is a linear combination of the other discriminating variables, (d) two perfectly correlated variables cannot be used at the same time, and (e) each group is drawn from a population that has a multivariate normal distribution. A function that produces a significant difference can be used to allocate new samples to one or more of the original groups.

Classification is internally based and does not depend on the a priori knowledge of groupings as does the discriminant function. The number of groups in a discriminant function is established prior to the analysis and each sample is treated separately; each sample is provisionally defined as belonging to a specific group. In one sense, a discriminant function can be thought of as a way of collapsing a multivariate problem into a univariate problem.

If one is able to make a few assumptions about the nature of the data involved in the analysis, a test of significance of the separation between the groups can be made. Assumptions include: (a) the observations are randomly selected, and (b) the probability of an unknown belonging to any one group is equal. It is a requirement that variables are normally distributed. An idea of the effectiveness of the variables as discriminators can be gained by computing standardized differences, which can be thought of as a general guide to the discriminating power.

In this study, the groups are represented by three black shale types and the variables are represented by various measured geochemical parameters (major oxide percentages, trace-element quantities, DOP values, % TOC, iron ratios, etc.). Linear combinations of the elements (canonical discriminant functions) are computed and used to maximize separation between the black shale types. The greater the power of the discriminant functions to separate the groups, the greater the ability to classify unknown samples correctly. The maximum number of canonical discriminant functions that can be used is equal to the number of groups, in this example it is three, minus one, or the number of discriminating variables, whichever is less. Only the first two functions that account for the greatest variance within the variables need to be used. The Wilks' Lambda method was used to compute this.

Following the stepwise regression to sort out variables most significant to the separation of the black shale groups, a cluster analysis was used to create groupings based on the stepwise regression analysis. These clusters, in the form of a dendrogram, were compared to the groupings of the a priori groupings in the discriminant function analysis. Thus, in effect, this is the opposite of a discriminant function analysis because there is no a priori assignments of group membership. From this, a comprehensive grouping of black shales was established that classifies any and all Midcontinent Pennsylvanian black shale samples into black shale types.

Chapter 4. Geologic Setting

The bedrock geology of eastern Kansas, southeastern Nebraska, and west-central Missouri is characterized by relatively laterally persistent Middle and Upper Pennsylvanian limestones, 1 to several meters thick with thin marine shale interbeds and separated by thick, silty to sandy shales, from a few to 10's of meters thick and containing local channel sandstone development. The Pennsylvanian units strike generally north-northeast to south-southwest and dip gently west into the subsurface at a dip of at most 10 meters per kilometer. South of the southernmost extent of glaciation (near Lawrence, Kansas), resistant limestones and sandstones are cut by east-flowing rivers and streams causing escarpments, which allow for relatively easy correlation of exposed units. Correlation north of this region, especially north of the Kansas City area, is especially difficult because exposures are limited owing to glacial cover.

The Pennsylvanian System in eastern Kansas comprises 49 formations that are subdivided into 130 formally named members and aggregated into 8 groups and 3 stages of the Middle and Upper Pennsylvanian. In this study, units from the Desmoinesian, Missourian, and Virgilian Stages were studied which make included a total of 12 black shale members from 5 groups. Most of these units are recognized

regionally, with a few exceptions, and were described and defined by R. C. Moore and his coworkers in the 1930's and 1940's. The subdivision of the units was designed by Moore to accommodate the vertical repetition of limestones and shales within the sequence.

At the base of the exposed Pennsylvanian stratigraphic sequence in Kansas, is the Middle Pennsylvanian (Desmoinesian), which consists mainly of shale with thin coal seams, local sand development, and thin limestones (Figure 7). The Missourian Stage (Upper Pennsylvanian) overlies the Desmoinesian (Middle Pennsylvanian). The Virgilian Stage (Upper Pennsylvanian) overlies the Missourian Stage and is characterized by shale, local sandstones, and thin limestones (Figure 8). In the topmost part of the Pennsylvanian section, sandy shales and thick limestones with thin shale members comprise the section. The uppermost Pennsylvanian includes an alternation of thicker and more prominent sandy shales, usually possessing coal seams, and thinner limestone units. The Virgilian Stage is overlain conformably by the Lower Permian sequences that continue the basic shale-limestone cyclicity.

During times of maximum transgression during the Pennsylvanian, west-central Indiana was situated at the eastern margin of an epeiric sea that covered west-central Indiana, central to south-central Illinois, southern Iowa, extreme southeastern Nebraska, northern Missouri, and eastern Kan-

Figure 7. Stratigraphic column for Middle Pennsylvanian of Kansas. Desmoinesian includes "V" shale or black shale within the Verdigris Limestone Member (the lateral equivalent of the Mecca Quarry Shale Member in Indiana). Generalized from Zeller (1968).

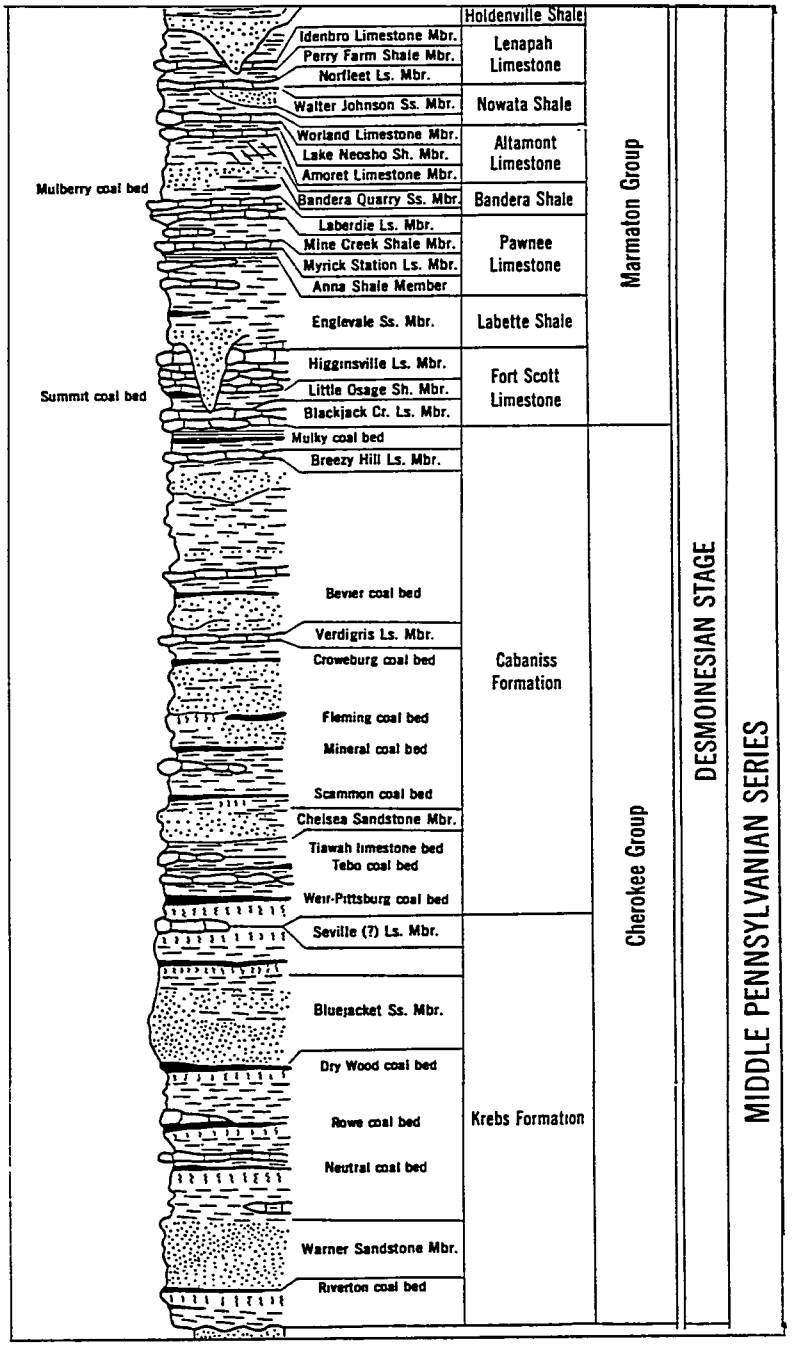
Holdenville Shale
Idenbro Limestone Mbr.
Perry Farm Shale Mbr.
Norfleet Ls. Mbr.
Lenapah Limestone
Walter Johnson Ss. Mbr.
Nowata Shale
Worland Limestone Mbr.
Lake Neosho Sh. Mbr.
Amoret Limestone Mbr.
Altamont Limestone
Mulberry coal bed
Bandera Quarry Ss. Mbr.
Bandera Shale
Laberdie Ls. Mbr.
Mine Creek Shale Mbr.
Myrick Station Ls. Mbr.
Anna Shale Member
Pawnee Limestone
Englevale Ss. Mbr.
Labette Shale
Higginsville Ls. Mbr.
Little Osage Sh. Mbr.
Summit coal bed
Blackjack Cr. Ls. Mbr.
Fort Scott Limestone
Marmaton Group
Mulky coal bed
Breezy Hill Ls. Mbr.
Bevier coal bed
Verdigris Ls. Mbr.
Croweburg coal bed
Fleming coal bed
Mineral coal bed
Scammon coal bed
Chelsea Sandstone Mbr.
Tiawah limestone bed
Tebo coal bed
Weir-Pittsburg coal bed
Cabaniss Formation
Cherokee Group
Seville (?) Ls. Mbr.
Bluejacket Ss. Mbr.
Dry Wood coal bed
Rowe coal bed
Neutral coal bed
Krebs Formation
Warner Sandstone Mbr.
Riverton coal bed
DESMOINESIAN STAGE
MIDDLE PENNSYLVANIAN SERIES

Figure 8. Stratigraphic column for Upper Pennsylvanian of Kansas. Missourian Stage includes Hushpuckney, Stark, Muncie Creek, and Eudora black shale members. Virgilian Stage includes Heebner, Queen Hill, Larsh and Burroak, Holt, and Shanghai Creek black shale members. Generalized from Zeller (1968).

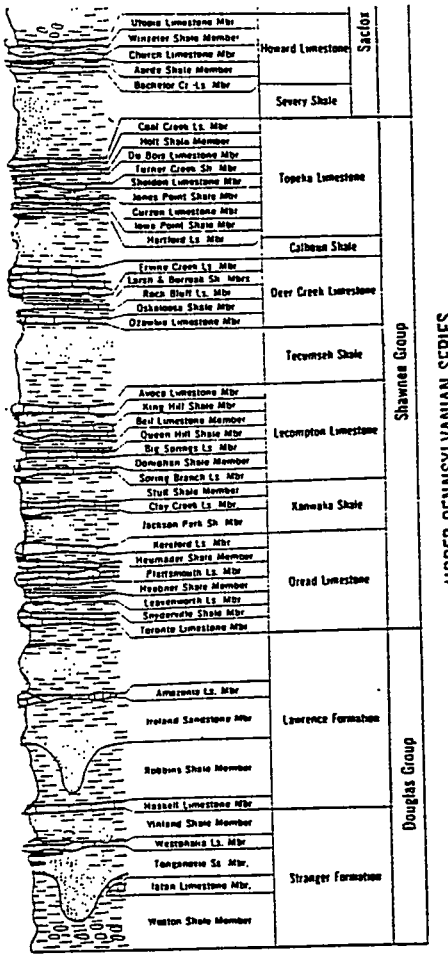
Howard Limestone
Severy Shale
Topeka Limestone
Calhoun Shale
Deer Creek Limestone
Tecumseh Shale
Lecompton Limestone
Kanwaka Shale
Oread Limestone
Lawrence Formation
Stranger Formation
Shawnee Group
Douglas Group
Sacior
UPPER PENNSYLVANIAN SERIES
VIRGILIAN STAGE

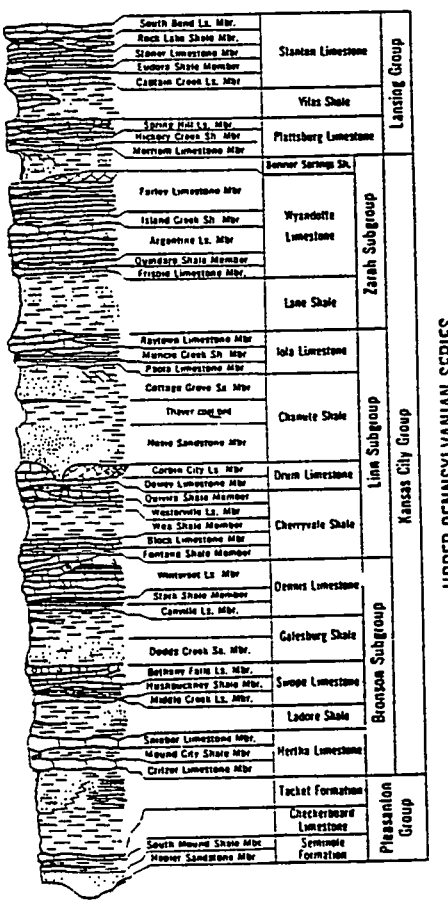
Stanton Limestone
Vilas Shale
Plattsburg Limestone
Lansing Group
Wyandotte Limestone
Lane Shale
Zarah Subgroup
Iola Limestone
Chanute Shale
Drum Limestone
Cherryvale Shale
Linn Subgroup
Dennes Limestone
Galesburg Shale
Swope Limestone
Ladore Shale
Bronson Subgroup
Hertha Limestone
Kansas City Group
Tacket Formation
Checkerboard Limestone
Seminole Formation
Pleasanton Group
UPPER PENNSYLVANIAN SERIES
MISSOURIAN STAGE

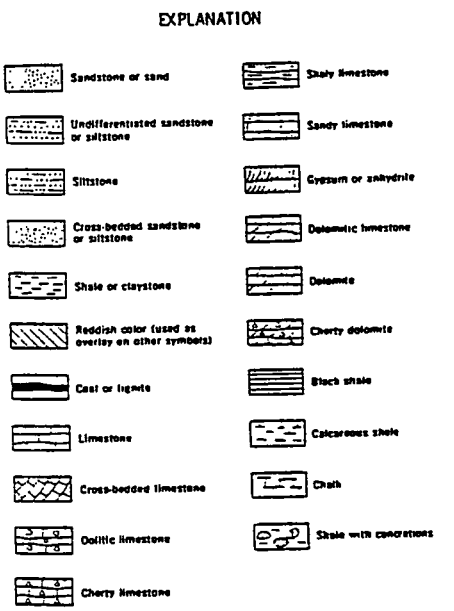
EXPLANATION
Sandstone or sand
Undifferentiated sandstone or siltstone
Siltstone
Cross-bedded sandstone or siltstone
Shale or claystone
Reddish color (used as overlay on other symbols)
Coal or lignite
Limestone
Cross-bedded limestone
Oolitic limestone
Cherty limestone
Shaly limestone
Sandy limestone
Gypsum or anhydrite
Dolomitic limestone
Dolomite
Cherty dolomite
Black shale
Calcareous shale
Chalk
Shale with concretions

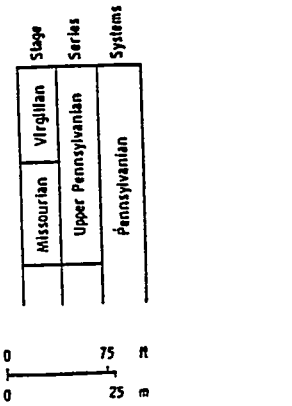
STRATIGRAPHY
Stage
Series
Systems
Virgilian
Missourian
Upper Pennsylvanian
Pennsylvanian
0
75
ft
0
25
m

sas. The west-central Indiana portion of this study is primarily concerned with the Mecca Quarry Shale Member and its lateral equivalents (i.e., the "V" Shale or black shale within the Verdigris Limestone Member in eastern Kansas) (Table 4). Repeatedly, the seas transgressed and regressed over Midcontinent North America, inundating peat swamps and depositing organic-rich, usually metalliferous black shales (Coveney and Shaffer, 1988). Normal seawater (Holland, 1979) or upwelling bottom-waters, as suggested by Heckel (1977), containing metals concentrated by a nutrient trap, provided phosphatic material and metals for the Midcontinent Pennsylvanian black shale units.

Both Hallam (1967) and Heckel (1977) have noted that black shales may be deposited in either deep- or shallow-water conditions. Heckel (1977), who concentrated on Missourian Stage black shales, reported that the organic-rich deposits were deposited at a slow rate of sedimentation in a relatively deep-water regime. However, Heckel focused on the westernmost portion of the Pennsylvanian sea and was opposed by Zangerl and Richardson (1963) who studied the Desmoinesian beds of west-central Indiana (the easternmost extent of the Pennsylvanian sea). They favored extremely rapid deposition in a shallow lagoonal-type sequence for the organic-rich deposits in that region.

According to Coveney and Shaffer (1988) from their study of sulfur isotopes in the Pennsylvanian shales of the

Table 4. Summary of stratigraphic nomenclature for the Mecca Quarry Shale Member and age-equivalent units in the Midcontinent (From Coveney et al., 1987).

	Illinois	Indiana	Iowa	Kansas	Kentucky	Missouri	Oklahoma
Shale Name	Mecca Quarry Shale Member	Mecca Quarry Shale Member	Oakley Shale Member	Verdigris Shale	Mecca Quarry Shale Member	Verdigris Shale	Black shale in Senora Fm.
Subjacent unit	Colchester Coal/ Francis Creek Shale Mbr.	Colchester Coal IIIa	Whitebreast Coal	Cabannis Formation over Croweburg Coal	Schulztown Coal (8b)	Verdigris Fm. over Croweburg Coal	Broken Arrow or Croweburg Coal
Overlying unit	Carbondale Fm./ Oak Grove Ls. Mbr.	Shale and Velpen Limestone Member	Ardmore Limestone Mbr.	Verdigris Limestone Mbr.	Oak Grove Limestone Mbr.	Ardmore Limestone Mbr.	Verdigris Limestone Mbr.

Midcontinent, conditions are more likely to have been uniformly offshore during the Desmoinesian Stage and later in the Missourian Stage when shales were deposited slowly in relatively deep waters. Thus, Upper Pennsylvanian black shales may be differentiated from Middle Pennsylvanian black shales (i.e., the Mecca Quarry Shale Member) based on sedimentation rate and depositional setting. Coveney and Shaffer (1988) also noted that the maximum depths of successive epeiric seas may have increased with time so that Missourian seas were deeper than those of Desmoinesian seas, which fits Wanless and Wright's (1978) suggestion that Desmoinesian black shales were deposited in shallower waters than those of the Upper Pennsylvanian. Schultz (1990) further pointed out that a progressive ventilation with time developed in response to a more open system in the Late Pennsylvanian and into the Permian.

Pennsylvanian Paleoclimate

The temporal and spatial geographic setting of the Midcontinent in the Missourian suggests that it was a time of general drying, expressed as longer drying seasons with shorter wet seasons (Shutter and Heckel, 1985). An analogy between the Missourian paleoclimate and similar transitional climates include: delta areas of India, northern Australia,

and northwestern South America. Vegetation patterns include coastal swamps and marshes, forests on floodplains, and savanna in the hinterland (Shutter and Heckel, 1985). In a river-borne clastic-dominated sequence, a chenier plain might form, while away from clastic influence, carbonate deposition with a range of shallow water depositional sequences would extend offshore adjacent (subparallel) to the shoreline. These types of climates also are typical of adjacent coastal upwelling areas, as in the northwestern coast of South America (Brongersma-Sanders, 1971).

Although the Missourian may have been a time of general drying, it should be noted that this climatic drying was not a sudden event (Shutter and Heckel, 1985). In fact, many of the sedimentological and clay mineralogical features present in the Missourian are present in the Desmoinesian as well.

The apparently wetter Virgilian may not contradict the prevailing drier pattern. Despite the predominance of such notable coals as the Nodaway and Pittsburgh coals of the Midcontinent and eastern Midcontinent, respectively, the Virgilian could represent a relatively wet period reflecting only local changes as a result of tectonic events. The change in coals may reflect slower or no marine transgressions in the Virgilian, giving rise to coal formation, but may not necessarily be related to general climate during that time period (Shutter and Heckel, 1985).

Desmoinesian Stratigraphy

The Mecca Quarry Shale Member and its stratigraphic equivalent shales are located in Illinois, Indiana, Iowa, Kansas, Kentucky, Missouri, and Oklahoma, although "Mecca" is used officially only in Indiana and Illinois (Coveney et al., 1987) (Table 3). In Indiana (type section), Kentucky, and in certain parts of Illinois, the Mecca Quarry Shale Member occurs in the Middle Pennsylvanian Liverpool cyclothem and directly overlies the Colchester Coal Member. The Logan Quarry Shale Member and the Holland Shale (Zangerl and Richardson, 1963) occur strictly as local units known near Parke County, Indiana at the type section of the Mecca Quarry Shale Member. In central and northeastern Illinois, the Francis Creek Shale Member occurs above the Colchester Coal and below the Mecca Quarry Shale Member (Baird et al., 1985). This occurs in Missouri, Kansas, and Oklahoma as well with an unnamed gray shale between the coal and black shale member.

The Middle Pennsylvanian (Desmoinesian) Mecca Quarry Shale Member resembles the Upper Pennsylvanian (Missourian and Virgilian) black shales of the Midcontinent (Heckel, 1977). However, the Upper Pennsylvanian black shales are generally less molybdiferous and possess less organic material than the Desmoinesian deposits. The Mecca Quarry Shale

Member is compositionally not homogeneous as on first inspection. Microstratigraphy reveals various individual beds that range from several to 10's of centimeters thick. Four beds seem to predominate the section that range from dark gray to black and can be traced from western Indiana into Illinois and Kentucky (Zangerl and Richardson, 1963). Missouri, Iowa, and Kansas lack this stratigraphic continuity. Westward into the Midcontinent, the Mecca Quarry Shale and its stratigraphic equivalents increase in phosphatic nodule development and decrease in metal content (Figure 9). Table 3 details the stratigraphic nomenclature of the Mecca Quarry Shale Member and its stratigraphic equivalents in the Midcontinent (Coveney et al., 1987).

Holland Shale Member

The Holland Shale Member is a black to dark gray friable to fissile shale located stratigraphically in the Staunton Formation approximately 1.5 meters above Coal IIA. A type section has not been formally designated, but exposures at Barren Creek and Mine Creek are used as reference sections (Figure 10). The Barren Creek section is located near Rockville, Indiana near the north line of section 33, T. 15 N., R. 8 W. in Parke County, Indiana. The Holland Shale Member is nearly 3 meters thick at this location and rests directly over Coal IIA in the Staunton Formation.

Figure 9. Stratigraphic relations for Desmoinesian black shales in Midcontinent and eastern Midcontinent (after Coveney et al., 1991).

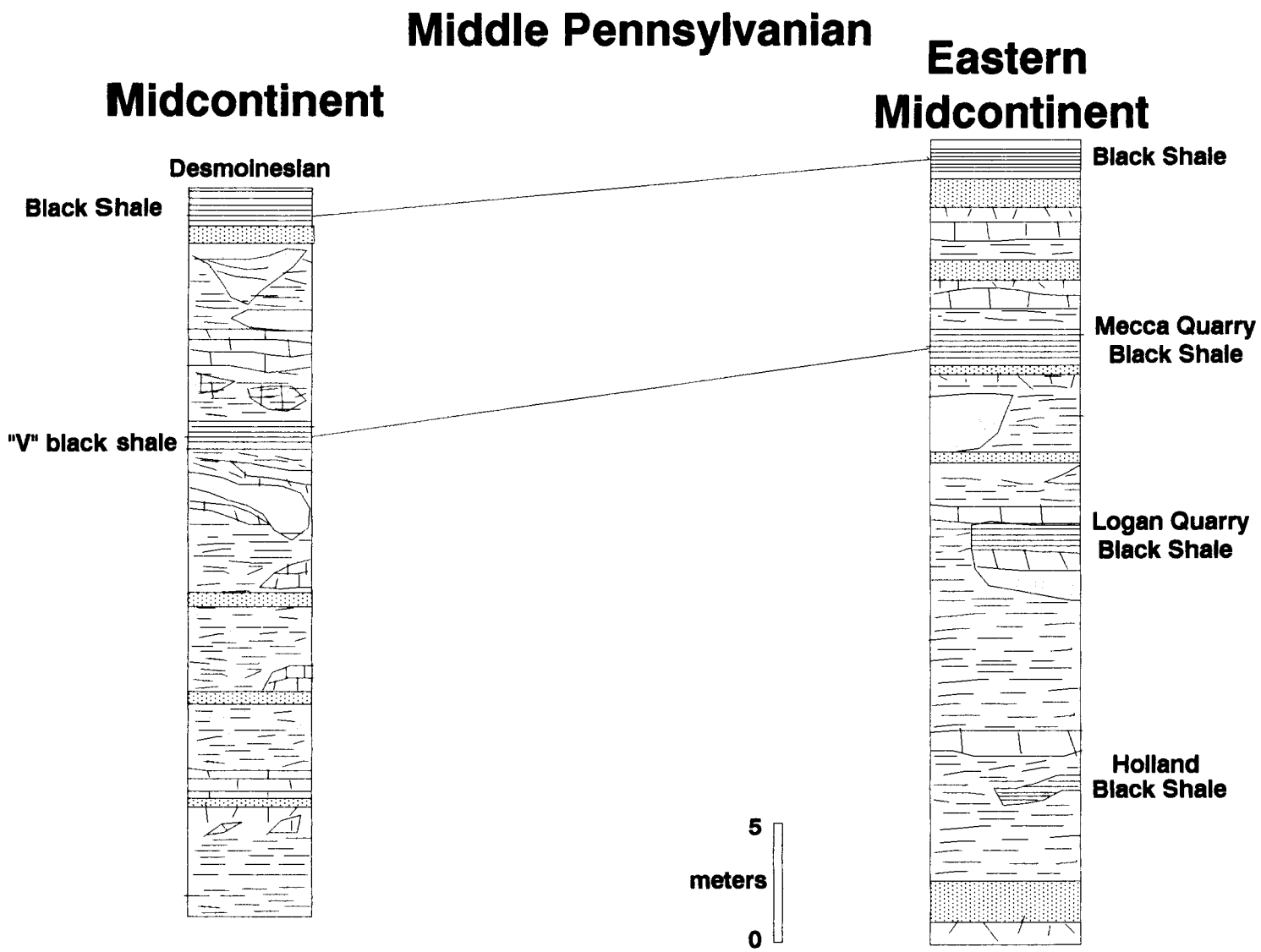

Stratigraphic relations for Desmoinesian black shales in Midcontinent and Eastern Midcontinent (after Coveney, et al., 1991)).

Figure 10. Map of Mecca Quarry region showing localities in text. Major sampling areas included Big Pond Creek (Logan Quarry Shale Member), and Barren Creek (Holland Shale Member). From Zangerl and Richardson (1963).

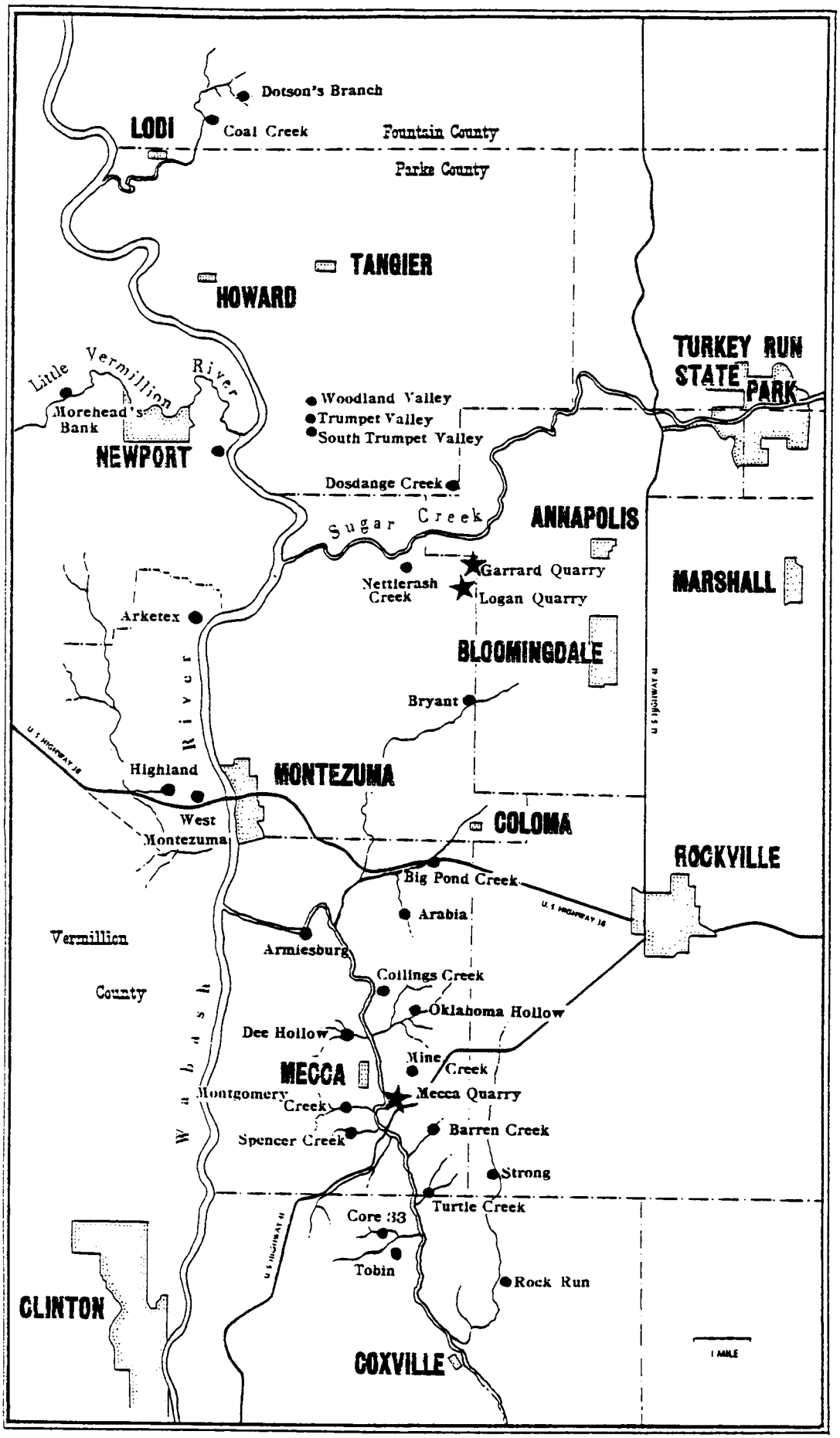
Dotson's Branch
LODI
Coal Creek
Fountain County
Parke County
TANGIER
HOWARD
TURKEY RUN STATE PARK
Little Vermillion River
Morehead's Bank
NEWPORT
Woodland Valley
Trumpet Valley
South Trumpet Valley
Dosdange Creek
Sugar Creek
ANNAPOLIS
Garrard Quarry
Nettlerash Creek
Logan Quarry
MARSHALL
Arketex
BLOOMINGDALE
Bryant
U.S. HIGHWAY 41
U.S. HIGHWAY 36
Highland
MONTEZUMA
West Montezuma
COLOMA
ROCKVILLE
Big Pond Creek
Arabia
Armiesburg
Vermillion County
Collings Creek
Oklahoma Hollow
Dee Hollow
MECCA
Mine Creek
Montgomery Creek
Mecca Quarry
Barren Creek
Spencer Creek
Strong
Turtle Creek
Core 33
Tobin
Rock Run
CLINTON
COXVILLE
1 MILE

Logan Quarry Shale Member

The Logan Quarry Shale Member has been defined as a member of the Staunton Formation by Zangerl and Richardson (1963). It lies above a local coal and approximately 18 meters below Coal IIIA. Not unlike the Mecca Quarry Shale Member, it consists of a sequence of alternating gray and black shale, mostly carbonaceous. The type section for the Logan Quarry Shale Member is located in Reserve Township, Parke County, Indiana (NE1/4, SW1/4, section 9, T. 16 N., R. 8 W.), approximately 2 kilometers east of West Union (Figure 10). A succession of beds at the type section includes interbedded friable to sheety, gray to black shale.

Mecca Quarry Shale Member

The Mecca Quarry Shale Member, originally proposed as a member of the Linton Formation in a study by Wier (1950), consists of evenly bedded alternating sequences of gray and black carbon-rich shale above Coal IIIA and beneath a marine shale and limestone (correlated with the Oak Grove Member in Illinois and the Velpen Limestone Member in Indiana (Wanless, 1939; Zangerl and Richardson, 1963). The shale portion ranges from dark gray to black to a mottled gray. At the type section (Figure 10), there is a bed of 1 cm-thick shale containing calcareous concretions near the base of the

unit, which attains thicknesses of several centimeters. The bottom layer of the Mecca Quarry Shale Member is a fossil hash, transgressive shell breccia, with pyritized shell fragments in a clay-rich matrix lacking bedding. The type locality of the Mecca Quarry Shale Member has been defined by Zangerl and Richardson (1963) to be in Wabash Township, Parke County, Indiana, (SW1/4, NE1/4, section 29, T. 15 N., R. 8 W.), about 1.5 kilometers from the town of Mecca, Indiana (Figure 10).

Missourian Stratigraphy

Missourian strata of Midcontinent North America are characterized by thin cyclic successions of carbonates and siliciclastics (Figure 11), with thicknesses usually less than 25 to 50 meters (Watney, French, and Franseen, 1989). Cyclic sedimentary units or "cyclothems" developed on shelf areas of the Midcontinent generally contain thin widespread transgressive sequences overlain by thicker regressive strata. These cyclothems usually are separated from bounding strata by surfaces associated with diagenetic and textural features indicative of subaerial weathering (Watney and Ebanks, 1978).

Cyclothems are widespread on shelf regions, but not until recently have interbasinal correlations been possible

Figure 11. Stratigraphic relations for Missourian black shales in Midcontinent and eastern Midcontinent (after Coveney et al., 1991).

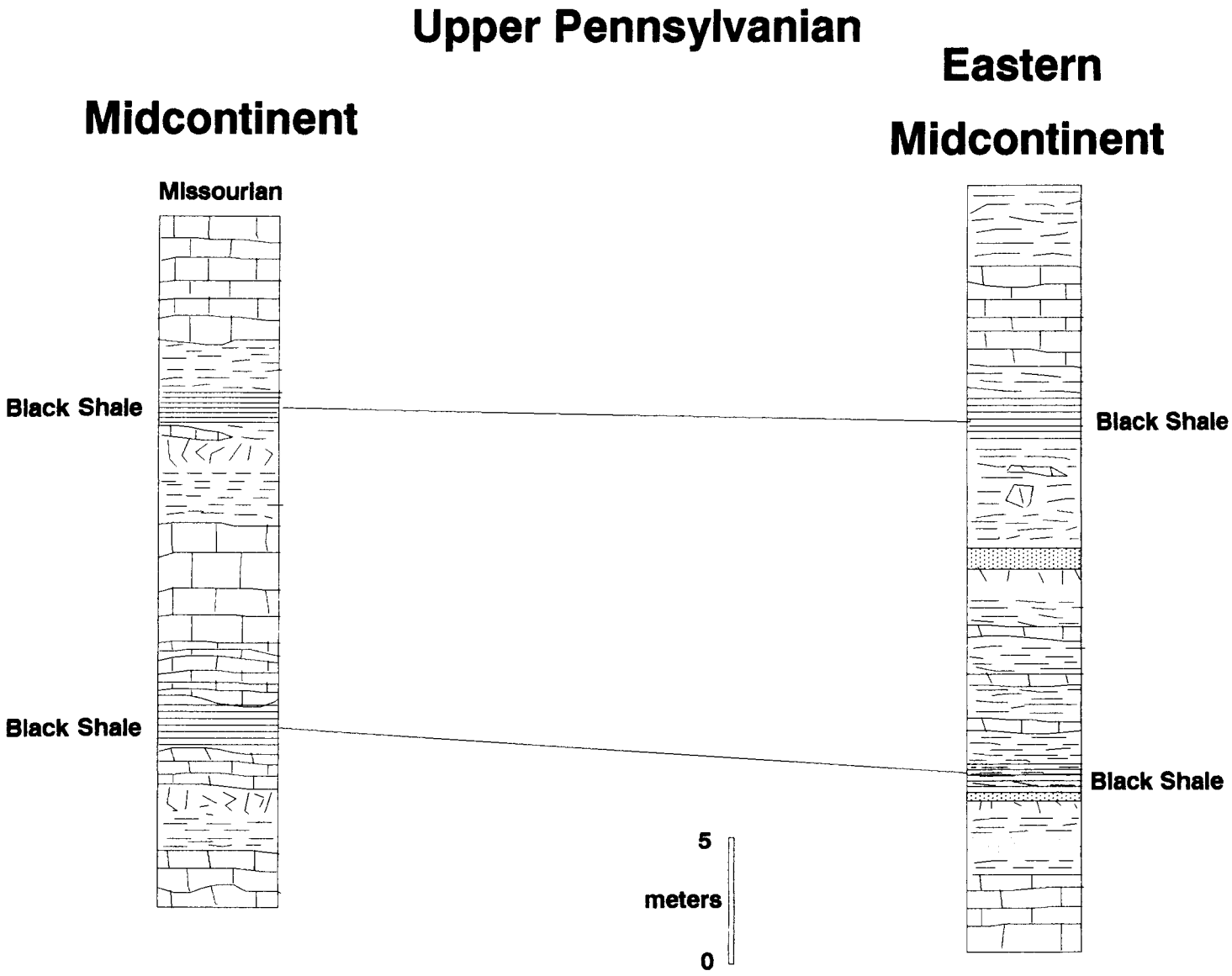

Stratigraphic relations for Missourian black shales in Midcontinent and Eastern Midcontinent (after Coveney, et al. (1991)).

because of durations shorter than accepted levels of biostratigraphic information. Investigations by Boardman and Heckel (1989) provide the basis of correlations for 13 major Virgilian and Missourian cyclothems in the northern Midcontinent. Correlations reflect synchronous marine inundation in both the Midcontinent and Midland Basin regions. Microstratigraphic calculations have been used to extend correlations of similar marine inundations during the Pennsylvanian to a global scale (Ross and Ross, 1987). Both Boardman and Heckel (1989) and Ross and Ross (1987) attributed sealevel fluctuation to late Paleozoic continental glaciation.

The black shales of the Kansas-type cyclothem, generally referred to as core shales by Heckel, overlie the middle transgressive limestone; the black shales are typically thin (0.3-0.9 meters). The black shales are areally extensive units are easily recognizable in outcrop and provide excellent subsurface markers because of their high natural gamma radioactivity (Watney, French, and Franseen, 1989), originally noted in the 1930's. Several units, including the Stark and Hushpuckney of this study, can be traced on the surface from Iowa into Oklahoma. Westward, the units can extend from eastern into western Kansas and into eastern Colorado. Nevertheless, the units change abruptly from black shales to gray, fossil-rich shales in northwestern Kansas and thin gray shales over the structural positive Central Kansas Uplift.

Hushpuckney Shale

The Hushpuckney Shale Member of the Swope Limestone Formation is a laterally persistent shale with the basal section containing few fossils in its black shale. The upper portion of the unit is a blue-gray clay-rich, fossiliferous shale that averages 0.7 meters in thickness. The thickness of the entire Hushpuckney sequence ranges from 1 to 2 meters, and is distinguishable in northwestern Missouri and across eastern portions of Kansas.

Stark Shale Member

The Stark Shale Member of the Dennis Limestone Formation normally contains two part as does the Hushpuckney Shale Member. A lower unit, up to 1 meter thick, is a black, fissile shale and an upper portion, normally up to 1.3 meters thick, consists of gray, clay-rich, fossiliferous shale. The black shale (lower portion) contains plant fragments and conodonts with local phosphatic nodules, whereas the upper gray shale part contains brachiopods and pelecypods.

Muncie Creek Shale Member

The Muncie Creek Shale Member is in the Iola Limestone Formation and contains two lithologic segments. The lower portion contains phosphatic nodules and plant fragments in a black fissile shale. The upper portion is a gray clayshale with several zones of small phosphatic concretions. The type section of the unit is just west of Kansas City, Kansas, where the thickness of the unit is 1 meter. The unit is laterally persistent and is present from eastern Kansas and western Missouri to northern Oklahoma.

Eudora Shale Member

The Eudora Shale Member is present in eastern Kansas, western Missouri, and into northern Oklahoma. It is a member of the Stanton Limestone Formation and possesses two portions. The lower portion, normally 0.5 meters thick, consists of a black, fissile shale that locally contains phosphatic nodules. The upper portion is a gray clayshale with brachiopods, trilobites, and plant fragments. The overall thickness of the unit differs, but averages 1.5 meters.

Virgilian Stratigraphy

Virgilian rocks of Kansas include three major groups (oldest to youngest: Douglas, Shawnee, and Wabaunsee). Limestones alternate regularly with shale vertically and marine sequences alternate vertically with nonmarine sequences. It has been noted by Moore (1949) that no portion of the Pennsylvanian sequence in the northern Midcontinent contains clearer evidence of cyclic sedimentation than the Shawnee and Wabaunsee Groups (upper two groups in the Virgilian) (Figure 12). The Shawnee Group contains the most complete and most complex examples of the cyclic character. Rocks within the Virgilian of the Midcontinent can be described in terms of two major rock types: limestones and shales. Limestones include several types. Major limestone types include: (1) a brownish gray, ferrugenous limestone with few fauna, (2) a dark-blue to gray, dense, hard, limestone with few and "dwarfed" fauna including fusulinids, (3) a light-gray to creamy white limestone with thin wavy bedding and an abundant and variable fauna including algal constituents, and (4) a light-gray finely grained limestone with shale partings. Virgilian shales of the Midcontinent include several types. The shale types, based on color, bedding, composition, weathering character, and thickness are: (1) a light-gray to light-brown clayey to silty shale, generally devoid of fauna and bedded, (2) a reddish clay-

Figure 12. Stratigraphic relations for Virgilian black shales in Midcontinent and eastern Midcontinent (after Coveney et al., 1991).

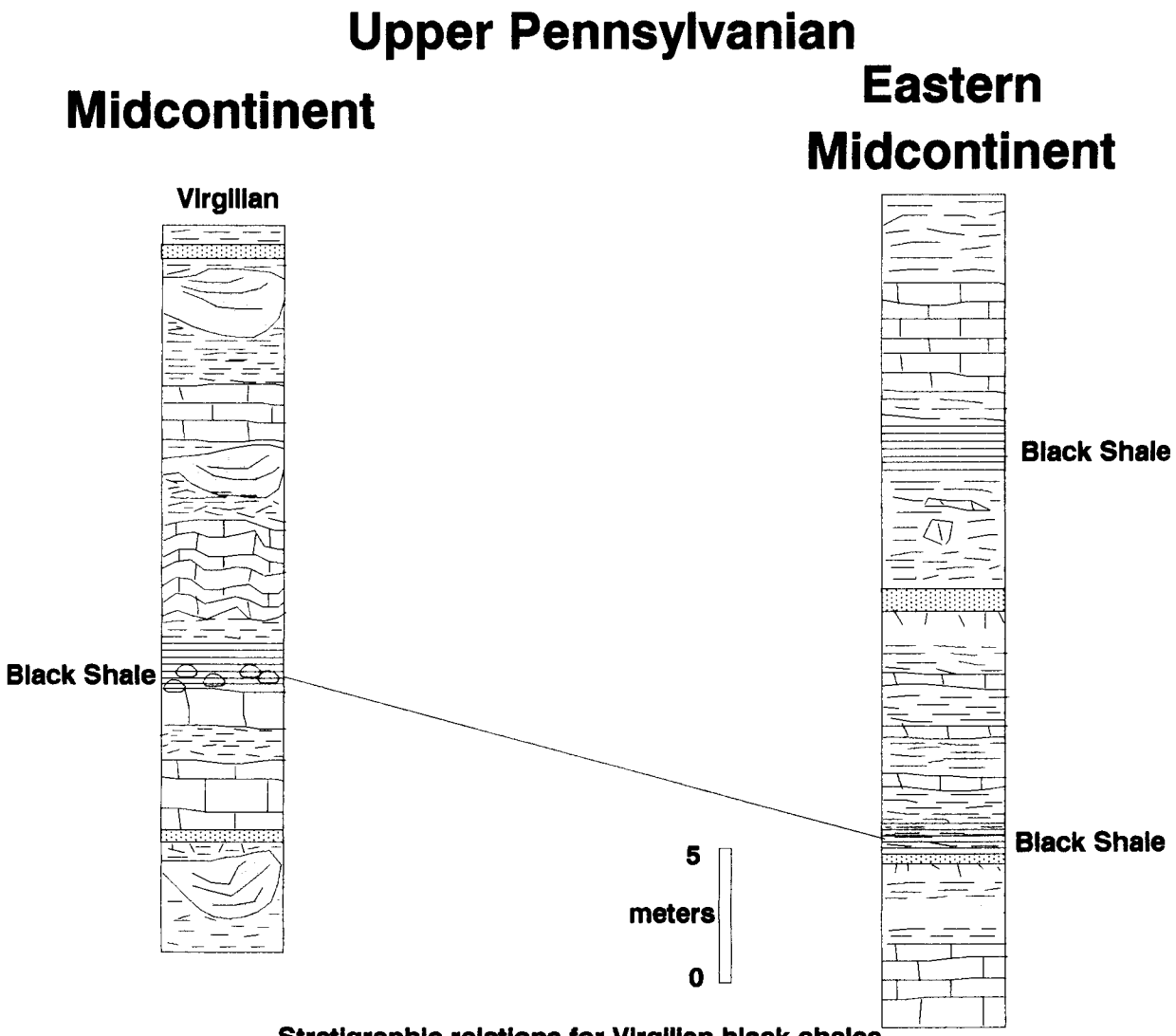

Stratigraphic relations for Virgilian black shales in Midcontinent and Eastern Midcontinent (after Coveney, et al., 1991)).

rich to silty, poorly bedded, nonfossiliferous shale, (3) a blue-gray, laminated marine shale, and (4) a black, fissile, highly carbonaceous shale that contains phosphatic nodules and laminae, fish remains, conodonts, and a few phosphatic brachiopods. Several of the shale units can attain thicknesses of up to 25 meters, but most are only 1 to 3 meters in overall thickness.

Heebner Shale Member

The Heebner Shale Member is a member of the Oread Limestone Formation and contains two parts. The lower part is a typical black, carbon-rich, fissile shale that contains phosphatic nodules, fish remains, and conodonts. The upper part is a gray, marine shale that contains brachiopods and pelecypods. The unit is extremely laterally continuous and is used as a marker bed in subsurface cores (Merriam, 1963). The Heebner Shale Member is constant in thickness at about 1.4 meters.

Queen Hill Shale Member

The Queen Hill Shale Member is a member of the Lecompton Limestone Formation and is laterally persistent. The lower part of the unit is a black, fissile shale with few phosphatic nodules and conodonts. The upper part is a gray

marine shale with brachiopods. Overall thickness of the lower black shale and upper argillaceous shale is 1 to 2 meters.

Larsh and Burroak Shale Members

The Larsh and Burroak Shale Members represent two parts of a single shale unit in Kansas. The lower part is a black, fissile, carbon-rich shale (Larsh) and the upper a gray to yellow, soft clayshale (Burroak). Because this sequence in Kansas is correlative to the Larsh Shale, intervening Haynies Limestone, and overlying Burroak Shale in Nebraska, the sequence in Kansas is referred to as the Larsh-Burroak Shale Member. The Haynies Limestone is absent in Kansas (Moore, 1949). Lower parts of the black shale contain conodonts and phosphatic nodules, whereas the upper gray clayshale part contains mostly calcareous brachiopods and bryozoans. The thickness of the Larsh-Burroak Shale Member in Kansas ranges from 1 to 2 meters.

Holt Shale Member

The Holt Shale Member is characterized by two subdivisions as in other Virgilian black shale units. It is a member of the Topeka Limestone Formation and contains a lower black, fissile shale part and an upper calcareous gray

marine shale sequence with a variety of invertebrate fauna. Overall thickness of the unit is 0.7 to 1 meter. The unit is confined mostly to sections north of Topeka, Kansas, but several localities south of Topeka include a gray shale within the Topeka Limestone Formation that may be correlative to the Holt.

Shanghai Creek Shale Member

The Shanghai Creek Shale Member is a newly named member of the Howard Formation (Wabaunsee Group) in eastern Kansas (Merriam, 1990). The lower part of the unit is a phosphatic, black, fissile shale whereas the upper part is a light gray to tan fossil-rich shale. The unit is generally less than 0.75 meters thick and is confined to southeastern Kansas. The type section of the unit is in southeastern Kansas (Chautauqua County) near the town of Cedar Vale.

Chapter 5. Discussion and Results of Analytical Procedures

The interpretation of environments of deposition of black shales remains a goal of earth scientists for several reasons, but especially for predicting petroleum source rock potential and understanding metal enrichment. Various approaches to this enigmatic problem have been utilized in the past (paleoecological methods, sedimentology, micropaleontological methods, organic geochemical indicators, and a variety of isotopic and mineralogic data) to answer specific questions about depositional settings. This study was designed to answer the question of whether a given organic-rich marine sediment was deposited originally under normal marine (oxygenated bottom water) conditions, or in a euxinic (anoxic, H_2S-containing) basin. Additionally, it is of specific interest to inquire how pyrite forms in these environments and use the relationships of iron, sulfur, and organic carbon to distinguish depositional setting and interpret early diagenetic phases related to metal enrichment.

Results of Whole-Rock XRF Analysis

A Rigaku 3070 X-ray wavelength dispersive spectrometer was used for determining percentages of major oxides and elements in the black shale samples. The purpose of the XRF

analysis is to determine total iron and total sulfur contents accurately and inexpensively preceding colorimetric iron determination (and calculation of DOP). The XRF analyses were used to develop a geochemical baseline for the black shales.

A comparison was made between XRF measurements made at the University of Cincinnati Department of Geology and XRF analyses conducted at XRAL in Ann Arbor, Michigan. SDO-1 (Ohio Devonian Shale Geochemical Standard) was analyzed at both laboratories. Results compared favorably between the two labs, indicative of consistent working conditions and analytical precision (Table 5). Specifically, total iron and total sulfur values compared well between analyses of the two labs.

Heebner-type black shales (Desmoinesian, Missourian, Virgilian) indicated a moderate quantity of total sulfur (avg. = 1.35%) and a relatively high total iron content (4.21%). SiO_2 and Al_2O_3 values were consistent with each other in the Heebner-type samples. Both TiO_2 and MnO_2 were extremely constant in terms of X-ray fluorescence. The amount of CaO differed as a function of position within the basin. Samples closer to the basin center were less enriched in CaO whereas samples closer to basin margins were enriched in CaO. P_2O_5 differed with vertical position within individual units. Samples with phosphatic nodules near the base of the black shale sequences (i.e., QH-3 and

Table 5. A comparison of U.S. Geological Survey geochemical standard SDO-1 (Ohio Devonian Shale). INAA denotes instrumental neutron activation analyses from this study and U.S.G.S. represents published data from Huyck (1991).

Comparison of U. S. G. S. Geochemical Standard SDO–1 and INAA Data from This Study					
INAA:		U.S.G.S.			
Element	Concentrations:				
Boron (ppm)	130.00	B	128.00	LOI	21.70
Sodium (%)	0.32	Na2O	0.38	CO2	1.01
Magnesium (%)	1.53	MgO	1.54	Total Carbon	9.95
Aluminum (%)	12.30	Al2O3	12.27	Organic Carbon	9.68
Silicon (%)	47.50	SiO2	49.28	Er	2.50
Phosphorus (%)	0.10	P2O5	0.11	F	~0.01
Beryllium (ppm)	5.00	Be	3.30	Ga	16.80
Potassium (%)	3.31	K2O	3.35	Hg	0.19
Calcium (%)	1.07	CaO	1.05	Ho	1.10
Scandium (ppm)	12.00	Sc	13.20	In	~0.20
Titanium (%)	0.72	TiO2	0.71	Bi	2.00
Vanadium (ppm)	170.00	V	160.00	Cl	116.00
Chromium (ppm)	110.00	Cr	66.40	Li	28.60
Manganese (%)	0.05	MnO	0.04	Pb	27.90
Iron (%)	9.43	Fe2O3	9.34	Pr	6.00
Cobalt (ppm)	42.00	Co	46.80	Sn	2.90
Nickel (ppm)	97.00	Ni	36.60	Tb	1.20
Zinc (ppm)	63.00	Zn	64.10	Tl	8.30
Copper (ppm)	50.20	Cu	60.20	Tm	0.34
Arsenic (ppm)	61	As	68.50	Y	40.60
Selenium (ppm)	3.00	Se	3.00	Zr	165.00
Bromine (ppm)	6.00	Br	5.00	Dy	5.70
Rubidium(ppm)	150.00	Rb	126.00		
Strontium (ppm)	70.00	Sr	75.10		
Molybdenum (ppm)	160.00	Mo	134.00		
Silver (ppm)	0.50	Ag	0.09		
Cadmium (ppm)	1.00	Cd	~2		
Tin (ppm)	4.60	Sb	4.10		
Cesium (ppm)	6.00	Cs	6.90		
Barium(ppm)	520.00	Ba	397.00		
Lanthanum (ppm)	37.90	La	38.50		
Cerium(ppm)	70.00	Ce	79.30		
Neodymium (ppm)	32.00	Nd	11.40		
Samarium (ppm)	6.30	Sm	7.70		
Europium (ppm)	1.50	Eu	1.60		
Germanium (ppm)	10.00	Ge	1.30		
Gadolinium (ppm)	1.1	Gd	6.50		
Ytterbium (ppm)	3.1	Yb	3.40		
Lutetium (ppm)	0.40	Lu	0.52		
Hafnium (ppm)	4.00	Hf	4.70		
Tantalum (ppm)	1.00	Ta	1.10		
Tungsten (ppm)	3.00	W	3.30		
Iridium (ppb)	30.00				
Gold (ppb)	5.00	Au	0.00		
Thorium (ppm)	8.90	Th	10.50		
Uranium (ppm)	41.50	U	48.80		
Sulfur (%)	5.4	S	5.35		
DOP	0.71	DOP	0.74		

ST-4) reflected high amounts of P_2O_5.

Shanghai-type (Virgilian) shales have abundant total iron and low total sulfur. As in Heebner-type shales, SiO_2, Al_2O_3, TiO_2, and MnO_2 were relatively consistent between samples. P_2O_5 values were low in comparison to Heebner-type deposits. Because INAA data was available for all Mecca-type samples, no XRF analyses were conducted for Mecca-type samples.

Results of Total and Organic Carbon Investigation

A procedure to determine total carbon and total organic carbon (TOC) was carried out to aid in the characterization of black shale types in the Midcontinent Pennsylvanian. Analyses were carried out using a Perkin-Elmer 240 Elemental Analyzer at the University of Cincinnati Department of Geology.

Results indicate a clear distinction between black shale types. Heebner-type black shales (Virgilian, Missourian, Desmoinesian) contained TOC values ranging from 0.01% (HBC-4) to 29.24% (EU-2) with an average value of 12.64% TOC. Most of the total carbon present was determined to be total organic carbon. Only one sample in the study (LB-1) possessed greater than 10% carbonate carbon.

Most Shanghai-type samples contained significantly less TOC (average = 2.92%) than Heebner-type samples. Organic carbon production during late Virgilian time (during the deposition of Shanghai-type units) had decreased such that black shales during this time contain progressively less TOC than earlier Virgilian, Missourian, and Desmoinesian shales.

In contrast to the Heebner-type and Shanghai-type deposits, Mecca-type black shales are enriched in TOC. Average TOC values for Desmoinesian black shales is 25.15% TOC. Once again, most of the total carbon is present as total organic carbon (TOC).

The importance of determining total carbon and total organic carbon (TOC) within these samples is to distinguish organics between the black shale types and to use TOC values as an aid in the computation of degree of pyritization (DOP) versus TOC, a paleoenvironmental indicator of bottom-water oxygenation conditions.

Results of Sulfide-Sulfur Measurements

Sulfur is present as a ubiquitous component of both modern and ancient marine sediments. Specific sulfur components within these settings differ, but sulfur is present as either pyrite, acid-volatile sulfides, elemental sulfur, sulfates, organic sulfur, or a combination of these (Canfield et al., 1986). Sulfur content and composition of

black shales thus can be related to the type of diagenetic environment in which the various sulfur compounds were deposited (Goldhaber and Kaplan, 1974). This is why it is crucial to quantify accurately the sulfur species present within the Midcontinent Pennsylvanian black shales. A chromium reduction technique, modified after Canfield et al. (1986), Liu (1988), and Okita (1987) was used in this study to aid in the separation of black shale types.

Heebner-type shales indicated an average of 0.40 S_{py} (pyritic sulfur) and 0.06% S_{org} (organic sulfur) (Tables 6 and 7). Organic sulfur was calculated as $\%S_{total}$ (measured by XRF) minus S_{py} (measured by the chromium reduction method). This is contrasted by average values of 2.68 and 0.18, respectively for Mecca-type deposits (Table 8), and 0.56 and 0.02, respectively, for Shanghai-type units. These higher values for S_{py} and S_{org} can be interpreted as a more euxinic setting for the Mecca-type shales, as compared with a semieuxinic setting for Heebner-type deposits (intermediate values). Shanghai-type deposits reflect a more aerobic or well-oxygenated environment (low values for pyritic and organic sulfur). Typical values for pyritic sulfur and organic sulfur in euxinic rocks are presented in Pandala et al. (in press).

Table 6. Carbon, iron, and sulfur data for Virgilian black shales (from Schultz and Coveney, in press).

Virgilian Black Shale Samples

(data from Schultz and Coveney, in press)

SAMPLE	%Fet	%St	%TOC	Spy	FeTsol	FePY	DOP
HEEBNER-TYPE SAMPLES							
LB1	6.40	0.88	15.23	0.77	1.75	0.67	0.28
LB2*	5.75	trace	0.06	0.00	2.61	0.00	0.00
LB3	6.08	1.06	16.12	0.95	1.28	0.83	0.39
LB4	6.87	0.67	18.41	0.54	2.09	0.47	0.18
LB5	6.76	2.50	18.53	1.21	1.72	1.06	0.38
QH1	5.04	1.61	15.00	1.51	0.73	1.32	0.64
QH2*	5.31	0.01	1.00	0.00	1.57	0.00	0.00
QH3	4.86	0.86	16.37	0.75	1.18	0.65	0.36
QH4	4.99	0.78	11.19	0.70	1.30	0.61	0.32
QH5*	6.43	trace	0.27	0.00	2.49	0.00	0.00
QH6	5.87	0.05	2.28	0.03	2.59	0.03	0.01
QHC-1	4.44	1.91	3.83	1.88	0.72	1.64	0.70
QHC-2	4.67	1.99	4.00	1.96	0.85	1.71	0.67
QHC-3	3.27	0.84	1.20	0.83	0.64	0.72	0.53
QHC-4*	2.72	0.51	0.18	0.51	0.50	0.44	0.47
QHC-5*	1.77	1.65	0.20	1.65	0.87	1.44	0.62
QHC-6*	3.52	2.60	0.96	2.59	1.33	2.26	0.63
QHC-7*	3.21	1.53	0.31	1.53	1.06	1.33	0.56
QHC-8*	3.49	1.76	0.34	1.76	1.16	1.53	0.57
QHC-9*	5.28	4.37	1.22	4.36	1.68	3.80	0.69
HB1	5.70	1.19	8.80	1.13	1.44	0.99	0.41
HB-2*	6.08	0.02	0.93	0.01	1.09	0.01	0.01
HB3	5.40	0.95	2.18	0.93	1.32	0.81	0.38
HB4	4.69	0.21	3.58	0.18	1.56	0.16	0.09
HBC-1*	0.70	0.16	0.59	0.16	0.50	0.14	0.22
HBC-2*	0.86	0.22	0.71	0.22	0.50	0.19	0.28
HBC-3*	0.83	0.20	0.64	0.20	0.47	0.17	0.27
HBC-4*	1.94	0.13	0.01	0.13	0.48	0.11	0.19
HBC-5*	2.01	0.08	0.07	0.08	0.40	0.07	0.15
HBC-6*	1.51	0.73	1.35	0.72	0.50	0.63	0.56
HBC-7*	0.58	0.13	0.32	0.13	0.28	0.11	0.29
Avg.	4.10	0.95	4.71	0.88	1.18	0.77	0.35
SHANGHAI-TYPE SAMPLES							
SH1	6.13	1.44	4.74	1.41	1.45	1.23	0.46
SH2	6.10	0.05	3.72	0.02	1.93	0.02	0.01
SH3*	6.54	0.03	2.52	0.01	2.47	0.01	0.00
SH4	4.44	0.47	1.40	0.46	1.58	0.40	0.20
SH5	6.27	1.53	10.38	0.86	1.35	0.75	0.36
SHC-1*	2.43	0.81	0.01	0.81	0.75	0.71	0.49
SHC-2*	3.07	0.62	0.26	0.62	1.03	0.54	0.35
SHC-3*	3.07	0.83	1.16	0.82	0.82	0.72	0.47
HO1	5.22	0.04	2.06	0.03	1.96	0.03	0.01
Avg.	4.81	0.65	2.92	0.56	1.48	0.49	0.26

%Fet=total iron from XRF *denotes gray shale

%St=total sulfur from XRF all other samples are black shales

%TOC=% total organic carbon from C analyzer

FeTsol=total acid-soluble iron from colorimetric determination

FePY=pyrite iron, calculated by Spy*0.872

Spy=pyrite sulfur from chromium reduction method

Table 7. Carbon, iron, and sulfur data for Missourian black shales (from Schultz and Coveney, in press).

Missourian Black Shale Samples

data from Schultz and Coveney (in press)

SAMPLE	%Fet	%St	TOC	Spy	Fetsol	FePY	DOP
HEEBNER-TYPE SAMPLES							
EU-1	6.08	1.24	4.30	0.68	2.71	0.59	0.18
EU-2	3.95	1.77	29.24	0.99	1.08	0.86	0.44
MC-1	4.90	0.77	27.89	0.83	2.50	0.72	0.22
MC-2	5.85	1.41	26.88	0.88	1.59	0.77	0.33
MC-3	5.45	0.87	24.77	0.67	2.99	0.58	0.16
ST-1*	6.77	1.30	6.23	0.83	2.73	0.72	0.21
ST-1A	8.29	2.76	20.64	1.34	4.26	1.17	0.22
ST-1B	7.92	3.60	21.76	2.01	3.50	1.75	0.33
ST-1C	7.90	3.01	8.70	1.65	4.43	1.44	0.25
ST-1D	5.89	3.58	3.44	1.77	3.45	1.54	0.31
ST-1E	7.87	3.50	25.36	1.69	3.19	1.47	0.32
ST-1F	6.87	3.46	20.75	1.71	3.01	1.49	0.33
ST-1G*	7.80	3.16	2.48	1.65	3.43	1.44	0.30
ST-1H	6.44	3.51	20.22	1.82	3.12	1.59	0.34
ST-1I	6.66	2.49	10.43	1.13	3.83	0.99	0.20
ST-1J	5.72	2.37	14.40	1.09	2.78	0.95	0.25
ST-1K	7.07	2.15	10.24	1.04	2.96	0.91	0.23
ST-1L	4.03	2.41	18.60	1.12	2.26	0.98	0.30
ST-1M	6.05	1.59	15.17	0.83	2.50	0.72	0.22
ST-1N	6.55	2.04	12.17	0.98	3.54	0.85	0.19
ST-1O	5.27	2.53	20.11	1.06	4.70	0.92	0.16
ST-1P	6.08	1.45	10.30	1.02	2.56	0.89	0.26
ST-2	4.19	1.94	13.08	0.99	1.76	0.86	0.33
ST-3	4.49	1.67	12.63	0.86	1.01	0.75	0.43
HP-3	4.84	0.87	8.93	0.41	0.96	0.36	0.27
HP-4	4.30	1.68	23.18	0.78	1.70	0.68	0.29
Avg.	6.05	2.20	15.84	1.15	2.79	1.00	0.27

%Fet=total iron from XRF

%St=total sulfur from XRF

%TOC=total organic carbon from C analyzer

FeTsol=acid-soluble iron from colorimetric determination

FePY=pyrite iron, calculated by Spy*0.872

Spy=pyrite sulfur from chromium reduction method

DOP=degree of pyritization

EU=Eudora

MC=Muncie Creek

HP=Hushpuckney

ST=Stark

*denotes gray shale

all other samples are black shales

Table 8. Carbon, iron, and sulfur data for Desmoinesian black shales (from Schultz and Coveney, in press).

Desmoinesian Black Shale Samples

data from Schultz and Coveney (in press)

SAMPLE	%Fet	%St	TOC	Spy	FeTsol	FePY	DOP
MECCA-TYPE SAMPLES							
Logan Quarry	12.95	15.60	22.93	8.80	2.36	7.67	0.76
Holland Shale	3.49	2.20	26.91	0.91	1.19	0.79	0.40
MQSB-1	3.50	3.30	39.72	2.39	0.64	2.09	0.77
Velpen A	3.22	2.50	15.35	1.51	0.76	1.31	0.63
Velpen B	3.95	3.00	11.27	1.54	1.25	1.34	0.52
Velpen C*	3.76	2.20	8.60	0.92	1.35	0.80	0.37
Velpen D	11.10	9.70	29.05	6.59	3.71	5.75	0.61
Hesler A1	3.86	3.28	43.74	2.65	0.62	2.31	0.79
Hesler A2	3.86	3.28	32.41	2.67	0.65	2.33	0.78
Hesler A3	3.63	2.80	28.58	2.39	0.65	2.08	0.76
Hesler A4	3.63	2.80	29.41	2.20	0.47	1.92	0.80
Hesler B1	3.38	3.37	29.57	2.06	0.79	1.80	0.69
Hesler B2	3.38	3.37	33.06	2.15	0.65	1.87	0.74
Hesler B3	3.85	2.50	15.33	1.84	1.34	1.60	0.54
Hesler B4	3.75	3.13	34.21	2.12	0.62	1.85	0.75
Hesler C*	4.39	3.53	6.87	2.57	1.60	2.24	0.58
Hesler D	4.75	4.64	20.60	2.19	1.56	1.91	0.55
Avg.	4.73	4.19	25.15	2.68	1.19	2.33	0.65

%Fet=total iron from XRF

%St=total sulfur from XRF

%TOC=total organic carbon from C analyzer

FeTsol=total acid-soluble iron from colorimetric determination

FePY=pyrite iron, calculated by Spy * 0.872

Spy=pyrite sulfur from chromium reduction method

DOP=degree of pyritization

*denotes gray shale

all other samples are black shales

Results of Acid-soluble Iron Determination and DOP

Analyses to determine Fe^{+2}, Fe^{+3}, and DOP were conducted at the University of Cincinnati Department of Geology according to the procedures described in the previous section (see Description of Analytical Procedures: Acid-soluble iron determination and DOP and appendix H). It should be noted that the calculation of DOP was only possible after accurate determinations of total sulfur, total organic carbon, and pyritic sulfur content. The series of calculations for DOP are as follows:

$$\%S_{org} = 0.20^{*} \times \%TOC$$

$$S_{non\text{-}org} = \%S_{total} - \%S_{org}$$

$$Fe_{py} = S_{py} \times (55.85/64.12)$$

$$DOP = Fe_{py} / (Fe_{py} + Fe_{HCl})$$

$^{*}S_{org}/\%TOC = 0.20$ from Bein, Almogi-Labin, and Sass (1990)

Heebner-type samples show an average DOP value of 0.37 indicating a borderline dysaerobic-aerobic bottom-water setting, according to Raiswell et al. (1988). Most of the gray shale samples (i.e., HBC1-7, QH-2) showed lesser values for DOP than did black shale samples. It is important to note that a regional geographic distribution of DOP shows a greater average value for DOP (more euxinic) near the Kansas City, Missouri region where samples reflected a closer

proximity to the basin center.

Shanghai-type samples were indicative of an aerobic setting with an average DOP value of 0.27. These shale samples were taken from southeastern Kansas, which is interpreted a shelf-like setting. Thus, it is postulated that Shanghai-type samples reflect an isolated lagoonal-type setting.

Mecca-type black shales (Desmoinesian) show a dominantly anaerobic bottom-water oxygenation condition, thus indicating a euxinic setting for these deposits. A positive correlation exists in the Mecca-type black shales between S_{py} (pyritic sulfur) and total organic carbon (TOC), pyritic sulfur and degree of pyritization (DOP), and TOC and DOP. As TOC content increases and oxygen supply decreases, more H_2S forms, and increases in disseminated pyrite and DOP values result. This probably is the result of increased organic carbon production during the Desmoinesian when climatic conditions favored the production of organic debris from peat swamps in a nearshore shallow-water setting. In this study, all Mecca-type samples, without exception, possessed DOP values between 0.45 and 0.80, equating with a dysaerobic to anaerobic setting, according to guidelines set forth by Raiswell et al. (1988).

Results of X-ray Diffraction Analyses and Clay Mineralogy

Results of the XRD analyses are summarized in terms of black shale types (Mecca-, Heebner-, and Shanghai-type.) Mecca-type black shales (Desmoinesian) in the powder fraction could be characterized as mostly quartz, feldspars, illite, kaolinite, and organic matter. The 2 mμ fraction reveals a decrease in detrital quartz and feldspars, and shows an asymmetrical basal illite peak (Appendix L.). This may be caused by a poor crystallinity of the illite and may indicate that the illite did not form in situ but was transported along with other clastic constituents. The assymmetrical basal illite peak may also be a result of grinding. With the exception of one sample, the 1 mu fraction shows mostly minute amounts of illite and kaolinite and a total lack of other minerals. Mecca-type powder samples show that kaolinite (d-spacing = 3.12 Å), and illite $2M_1$ polytypes are present.

Heebner-type samples in the powder fraction are characterized by mostly detrital quartz, feldspars, illite, kaolinite, and some organic matter. A decrease in detrital quartz and feldspars is shown in the 2 mu fraction with an asymmetric basal illite peak. Sample MC-3 (Muncie Creek, Missourian) was glycolated to detect any differences in illite-smectite interlayers (Appendix L.). By glycolation, it was shown that the sample was dominantly discrete illite

with little smectite interlayering. Heebner-type powder samples show the presence of chlorite IIb, kaolinite, and $2M_1$ illite as polytypes.

Shanghai-type powder samples also contained mostly quartz, feldspars, illite, kaolinite, as well as some organ ic matter and calcite. The quantity of detrital quartz decreased in the finer fractions and illite and kaolinite increased. Polytypes present in the Shanghai-type black shales include kaolinite and $2M_1$ illite (Appendix L.).

Overall, there is little difference in clay mineralogy between the black shale types. In a study of REE values in Midcontinent Pennsylvanian shales, Cullers et al. (1979) noted that no difference in mineralogy exists between different shale members and no REE to clay mineralogy correlation was evident. This study is consistent with the results of Cullers et al. (1979).

Results of Pyrolysis (Rock-Eval) Analyses

A standard method of source-rock evaluation (Rock-Eval) was used in this study to characterize further the organics within the Midcontinent Pennsylvanian black shales. Several parameters were measured according to the procedures discussed in Description of Analytical Methodology: Pyrolysis (Rock-Eval). Parameters such as S_1, S_2, S_2/TOC or HI (hydrogen index), T_{max}, and $S_1/(S_1 + S_2)$ were measured in

this study. The type of kerogen is characterized by S_2/TOC and is independent of organic matter abundance and related to elemental kerogen composition (Tissot and Welte, 1984). The parameter S_1 represents the fraction of original genetic potential effectively transformed into hydrocarbons while S_2 reflects the residual fraction which has not been used to generate hydrocarbons (Peters, 1986). Therefore, $S_1 + S_2$ evaluates genetic potential and $S_1/(S_1 + S_2)$ represents the transformation ratio where the continual increase with depth makes for a valuable maturation index (Tissot and Welte, 1984). The parameter T_{max} represents the maximum temperature of the hydrocarbon generation during pyrolysis.

Because pyrolysis (Rock-Eval) emphasizes organic-rich samples, low HI indices and high T_{max} values typify Shanghai-type samples whereas high HI indices and low T_{max} values are characteristic of Mecca-type shales (Table 9). Heebner-type shales show intermediate values for these parameters (Table 9). The combination of high T_{max} values, low HI, and high $S_1/(S_1 + S_2)$ values in Shanghai-type deposits correlate with an immature source-rock in terms of temperature history whereas the combination of high HI and low T_{max} values in Mecca-type (and several Heebner-type) shales make for a more mature source-rock in terms of petroleum potential (Table 9). A comparison between Rock-Eval parameters in Midcontinent Pennsylvanian black shales is given in Schultz and Coveney (in press).

Table 9. Rock-Eval data from selected samples of Heebner-, Shanghai-, and Mecca-type black shales in this study. TOC represents total organic carbon. S_1 represents the fraction of original genetic potential effectively transformed into hydrocarbons. S_2 represents the residual portion not yet used to generate hydrocarbons. T_{max} represents maximum temperature of hydrocarbon generation during pyrolysis. S_2/TOC represents HI (hydrogen index). $S_1/(S_1 + S_2)$ evaluates genetic potential, accounting for abundance and type of organic matter. HB1, QH1, LB1, and QHC1 are Heebner-type SH2 and SHC1 are Shanghai-type, and MQB, MQD, and MQSB1 are Mecca-type black shales.

Rock-Eval Data From Selected Samples						
SAMPLE	TOC	S1(ppm)	S2(ppm)	Tmax (°C)	S2/TOC	S1/S1+S2
HB1	10.31	1200.00	49500.00	419.00	0.48	0.02
QH1	22.72	3280.00	137000.00	415.00	0.60	0.02
SH2	5.59	490.00	10900.00	426.00	0.19	0.04
LB1	17.45	1540.00	70300.00	417.00	0.40	0.02
HBC1	19.43	1390.00	83700.00	419.00	0.43	0.02
QHC1	4.89	2060.00	18900.00	428.00	0.39	0.10
SHC1	0.66	250.00	520.00	528.00	0.08	0.32
MQB	14.95	1480.00	41700.00	417.00	0.28	0.03
MQD	36.85	4530.00	176000.00	415.00	0.48	0.03
MQSB1	36.20	5610.00	195000.00	418.00	0.54	0.03

Results of Instrumental Neutron Activation Analyses (INAA)

Selected samples were sent to XRAL Activation Services in Ann Arbor, Michigan for combined XRF-INAA analysis. Most Mecca-type samples were sent to M. D. Glascock of the University of Missouri-Columbia Reactor for INAA. Several Heebner-type samples also were sent to the Missouri Reactor and several Mecca-type samples to XRAL as a check for accuracy. A total of 54 elements were measured by various methods including INAA (instrumental neutron activation analyses) and XRF, depending on the element.

Plots of Midcontinent Pennsylvanian black shales in this study (chondrite-normalized) show three types of REE patterns (Figure 13). Heebner-type shales show the most similarity to NASC patterns. Mecca-type black shales are highest in overall REE's and are thus differentiated from NASC and PAAS. Thirdly, Shanghai-type black shales have low total REE patterns and plot below any other type of shale sample. Mecca-type samples show a strong enrichment in middle REE, not seen in the other types.

Most Mecca-type samples are enriched in various metals as compared with Heebner-type and Shanghai-type shales.

Figure 13. A. Rare Earth Element (REE) distribution for black shale types in this study.
B. REE distribution for shale standards. NASC represents North American Shale Composite. PAAS refers to post-Archean Australian Shales, included for reference. All samples are chondrite-normalized. PAAS data from Nance and Taylor (1976), composite of 23 samples. NASC data from Haskin (1968), composite of 40 samples. Adapted from Schultz and Coveney (in press).

Plot of Rare Earth Elements of Midcontinent Pennsylvanian Black Shales, PAAS, and NASC

A.

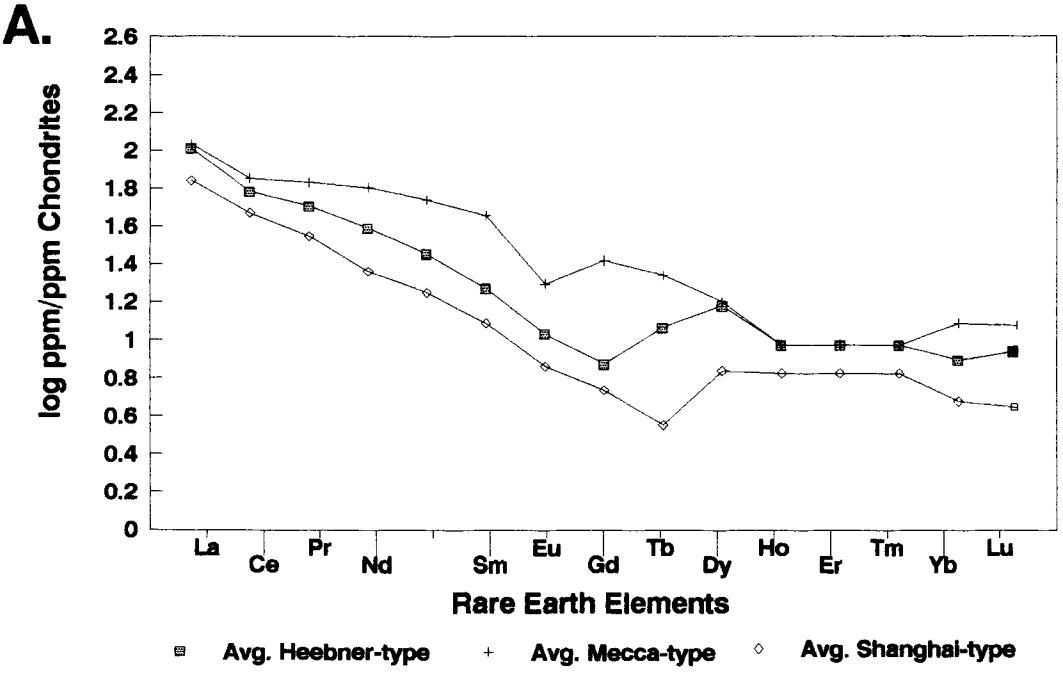

B.

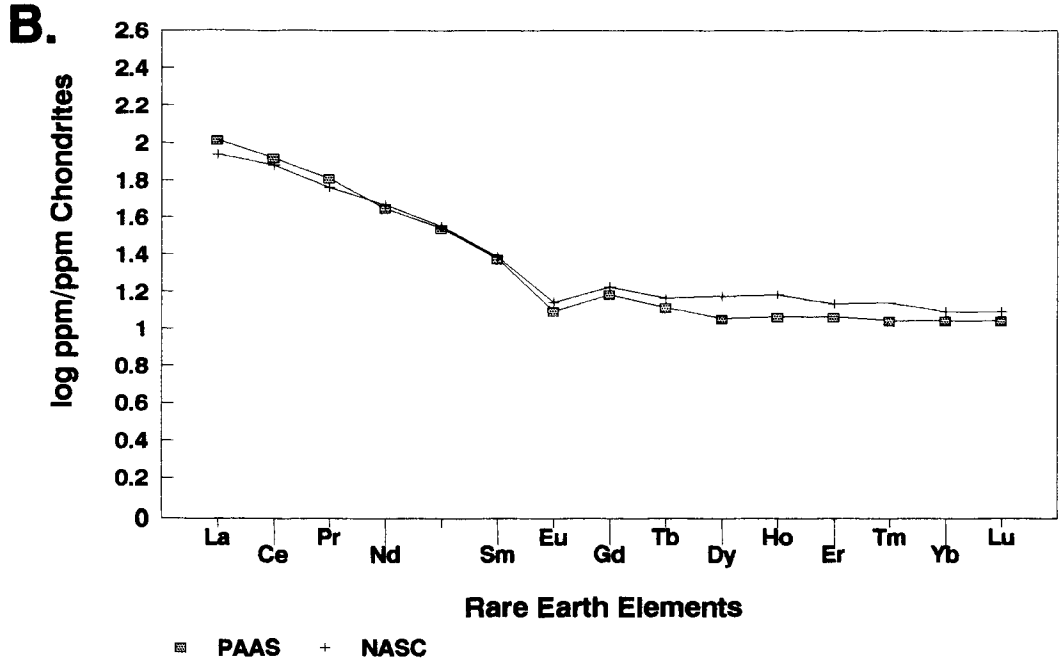

Mecca-type deposits contain elevated values of V (avg. = 1903.5 ppm), Cr (avg. = 371.3 ppm), Sn (avg. = 39.1 ppm), Ni (avg. = 311.0 ppm), Zn (avg. = 1383.9 ppm), Se (avg. = 158.8 ppm), Mo (avg. = 1118.2 ppm), Cd (avg. = 75.2 ppm), and U (avg. = 135.2 ppm) (Table 10). Although these values may not be ore-grade, the values are enriched in comparison to many North American black shales (Vine and Tourtelot, 1970).

Heebner-type black shales are semimetalliferous in comparison to Mecca-type deposits and are enriched in metals in comparison with Shanghai-type samples. Average values for selected metals in Heebner-type deposits are: V (802.5 ppm), Cr (502.3 ppm), Sn (13.5 ppm), Ni (219.6 ppm), Zn (1220.2 ppm), Se (34.3 ppm), Mo (63.5 ppm), Cd (39.7 ppm), and U (51.2 ppm) (Table 10).

Shanghai-type deposits are enriched neither in metals nor organic matter and form the nonmetalliferous end of the Midcontinent Pennsylvanian black shale spectrum. Average values for selected metals include: V (109.5 ppm), Cr (195.5 ppm), Sn (1.0 ppm), Ni (116.8 ppm), Zn (91.8 ppm), Se (4.7 ppm), Mo (3.8 ppm), Cd (1.2 ppm), and U (7.0 ppm) (Table 10).

A plot of metals in Midcontinent Pennsylvanian black shales as compared with SDO-1 shows enrichments of V, Cr, Ni, Zn, and Mo in Mecca-type shales; V, Cr, Ni, Zn, and Sr in Heebner-type shales; and Cr and Zn in Shanghai-type shales (Figure 14).

Figure 14. Plot of metals (in ppm) as compared with metal values in U.S.G.S. Geochemical Standard SDO-1. SDO-1 values from Huyck (1991).

Plot of Metals in Midcontinent Pennsylvanian Black Shales vs. Metals in SDO-1

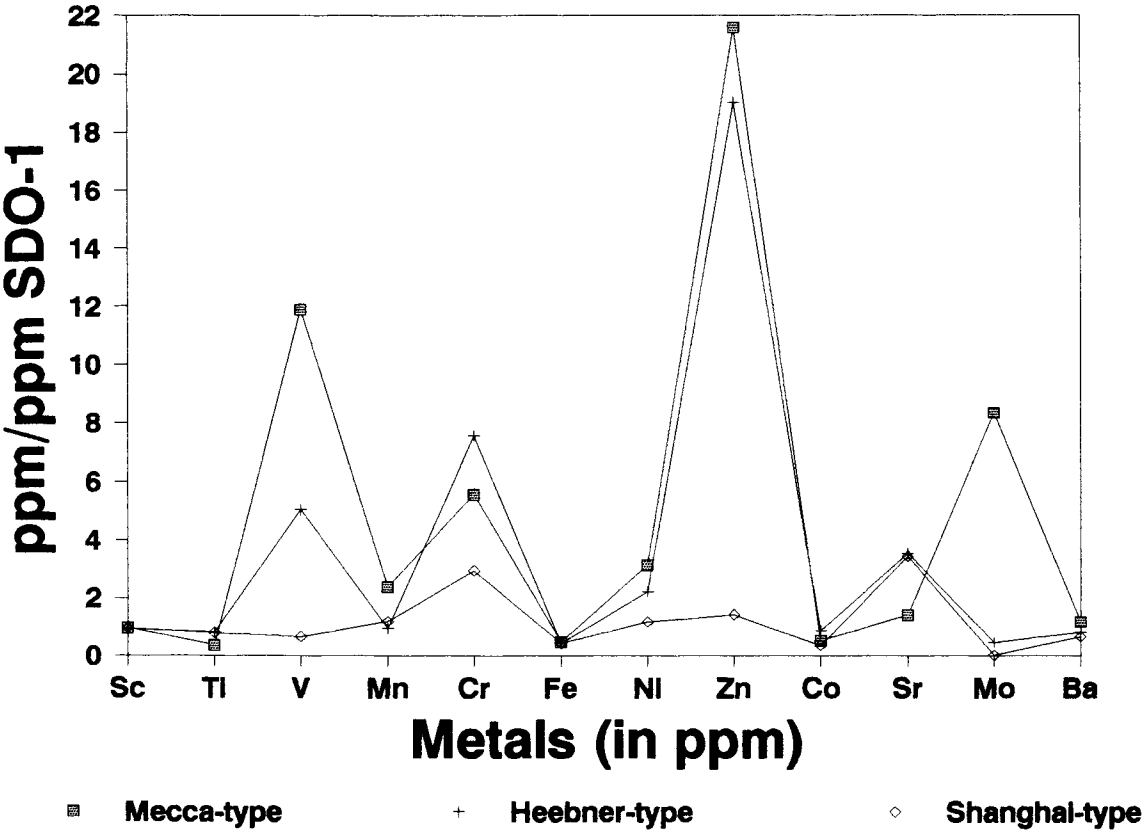

Table 10. Group means and standard deviations of geochemical parameters of all black shales in this study.

GROUP MEANS AND STANDARD DEVIATIONS

	GROUP MEANS			GROUP STANDARD DEVIATIONS		
VARIABLE	GROUP 1 HEEBNER-TYPE	GROUP 2 SHANGHAI-TYPE	GROUP 3 MECCA-TYPE	GROUP 1 HEEBNER-TYPE	GROUP 2 SHANGHAI-TYPE	GROUP 3 MECCA-TYPE
SORG	0.08	0.02	0.18	0.05	0.02	0.08
TOC	10.86	2.47	25.43	7.16	2.11	10.91
FE2SOL	0.70	0.62	0.59	0.41	0.25	0.25
FETSOL	1.28	1.31	1.18	0.68	0.49	0.83
FEPY	1.05	0.63	3.71	0.43	0.50	2.97
SPY	1.01	0.72	2.68	0.50	0.57	2.00
DOP	0.47	0.32	0.75	0.16	0.21	0.09
B	116.92	105.00	100.85	33.26	46.55	26.84
Na	0.63	0.64	0.27	0.26	0.15	0.11
Mg	2.85	1.99	0.80	0.88	0.24	0.30
Al	12.55	13.24	5.66	2.98	6.53	1.49
Si	41.76	37.43	16.19	8.72	15.34	4.78
P	1.41	0.27	2.18	1.97	0.33	1.01
S	1.35	0.74	4.19	0.47	0.57	3.40
Be	3.73	4.00	3.00	1.39	2.31	1.17
K	2.98	2.40	1.95	0.81	1.44	0.52
Ca	8.22	17.18	0.76	9.24	18.26	0.93
Sc	12.37	12.73	12.92	2.93	5.64	2.60
Ti	0.58	0.57	0.27	0.14	0.29	0.07
V	807.54	109.50	1903.47	952.04	71.26	973.51
Mn	0.04	0.05	0.10	0.02	0.02	0.32
Cr	502.31	195.50	371.29	337.00	201.90	163.37
Fe	4.21	4.12	4.63	1.05	1.69	2.84
Sn	13.52	1.00	39.13	9.48	0.80	9.10
Ni	219.62	116.75	311.00	119.46	96.52	141.87
Zn	1220.23	91.75	1383.94	2057.83	89.09	1103.18
Co	40.69	17.25	24.99	29.95	4.19	6.29
As	23.08	11.25	34.98	16.79	10.01	15.07
Se	34.31	4.68	158.78	31.83	3.55	52.81
Br	5.08	10.00	8.57	1.89	7.53	14.47
Rb	131.54	120.00	105.94	38.48	75.28	27.54
Sr	264.62	257.50	106.47	158.67	114.71	34.98
Mo	63.46	3.75	1118.24	83.83	1.50	526.96
Ag	0.92	1.25	5.55	0.50	1.84	2.07
Cd	37.92	1.20	75.24	59.26	1.22	79.25
Ba	321.54	265.00	469.29	93.71	188.06	253.09
La	39.33	28.75	37.09	28.51	14.79	14.26
Ce	63.38	52.50	66.17	47.65	24.01	31.35
Nd	28.77	21.50	44.11	24.09	13.92	42.61
Sm	5.40	3.90	10.11	5.09	2.91	11.80
Eu	1.15	0.88	1.84	1.22	0.64	2.33
Yb	2.50	1.75	3.02	1.33	0.86	0.59
Hf	2.75	2.75	2.52	0.83	1.50	0.73
Ta	0.85	0.75	0.98	0.20	0.30	0.23
W	10.64	10.55	5.87	7.49	9.19	2.82
Ir	39.00	14.00	2.35	57.80	2.16	2.12
Au	3.40	1.80	2.95	1.47	1.85	1.23
Th	8.25	8.38	8.68	1.85	4.82	1.76
U	51.15	7.00	138.24	74.16	6.00	150.98

Based on the results of INAA analyses, it is evident that metals such as V, Cr, Sn, Ni, Zn, Se, Mo, Cd, and U had an opportunity to be fixed in Desmoinesian black shales (mainly Mecca-type shales). As organic carbon production decreased through the Missourian and Virgilian, metal fixation decreased and the quantity of metals present in Missourian and Virgilian black shales decreased dramatically.

Results of Sulfur Isotope Analyses

The conditions of sedimentation of Midcontinent Pennsylvanian black shales affected sulfur isotopes in both coarse-grained sulfides and in dispersed sulfides, as measured on aliquots of Ag_2S from chromium reduction precipitates. High, variable $\delta^{34}S$ values are typical of sediments deposited in shallow anoxic waters, analogous to Desmoinesian black shales (Coveney and Shaffer, 1988), whereas Missourian and Virgilian black shales formed under deeper anoxic to dysaerobic conditions and thus contain sulfur with lighter, more constant $\delta^{34}S$ values.

According to Schwarz and Burnie (1973), sulfur isotope ratio distributions in clastic, nonvolcanic sediments can be accounted for in two models: (1) an open-system reduction of seawater sulfate under steady-state conditions with $\delta^{34}S$ values approaching -50 per mil, or (2) a closed system

reduction of a limited sulfate pool with $\delta^{34}S$ values ranging from -3 to -25 per mil. The latter condition apparently develops in nearshore sedimentary settings where organic supply is greater than bacterial consumption, that is, the Mecca Quarry Shale Member.

In this study, $\delta^{34}S$ values of Mecca-type shales average approximately -14 per mil, but range from -42 to -5 per mil (Table 11). This is suggestive of a nearshore setting, with a relatively rapid rate of sedimentation. Organic nutrient supply probably exceeded bacterial consumption rate, thus providing for relatively heavy and erratic $\delta^{34}S$ values.

Heebner-type shales average approximately -30 per mil, and range from -42 to -27 per mil (Table 11), indicative of a more offshore setting with a slower rate of deposition. The less variable $\delta^{34}S$ values can be accounted for by a more uniform condition offshore because of an open diffusion of sulfate from seawater into the sediment, allowing greater bacterial fractionation (Schultz and Coveney, in press).

Shanghai-type deposits display a heavy $\delta^{34}S$ average value (Table 11), pointing to a more nearshore setting. Although few samples were used in this study, values for Shanghai-type shales are heavy and erratic, similar to Mecca-type shales, but without the tremendous organic content present in Mecca-type units.

Thus, in a Desmoinesian to Virgilian time frame, Pennsylvanian black shales show an overall decrease in organic

Table 11. Sulfur isotope data from sulfides. Note increase through Virgilian and relatively heavy, yet erratic, values for gray and black Desmoinesian shales. Values from Coveney and Shaffer (1988) are from individual sulfide minerals whereas all other values are for extracted sulfides (from Schultz and Coveney, in press).

Sulfur Isotope Data from Sulfides				
Stratigraphy	Avg. Value	Location	Samples	Lithology
Virgilian Series black shales			19	
Shanghai-type:				
Shanghai Creek Shale Member	+3.0	Forest City Basin	4	black shales
Holt Shale Member	–5.3	Forest City Basin	3	dark gray shale
Heebner-type:				
Larsh/Burroak Shale Member	–29.2	Forest City Basin	4	black shale
Queen Hill Shale Member	–36.5	Forest City Basin	3	black shale
Heebner Shale Member	–36.6	Forest City Basin	5	black shale
Missourian Series black shales			11	
Heebner-type:				
Eudora Shale Member	–41.8	Forest City Basin	2	dark gray shale
Muncie Creek Shale Member	–40.8	Forest City Basin	2	dark gray shale
Stark Shale Member	–26.6*	Illinois/F.C. Basin	3	black shale
Hushpuckney Shale Member	–27.7*	Forest City Basin	4	black shale
Desmoinesian black shales			31	
Heebner type:				
Unofficial "V" shale over Croweburg Coal Mbr. (Desmoinesian Heebner-type)	–14.5*	Western Interior Coal basin	10	black shale
Mecca-type:				
Anna Shale Member	–9.6*	Illinois Basin	1	gray shale
Mecca Quarry Shale Member	–10.2*	Illinois Basin	15	black shale
Logan Quarry Shale Member	–4.8	Illinois Basin	2	black shale
Holland Shale Member	–42.2	Illinois Basin	3	black shale
Desmoinesian gray shales	+14.1*	Illinois Basin	4	gray shale

*denotes values for individual grains of sulfide minerals from Coveney and Shaffer (1988).
data from Schultz and Coveney (in press)

carbon production, a deepening of seas towards the western Midcontinent, and a progressive ventilation with time, as indicated by falling DOP values, accounting for the isotopically light $\delta^{34}S$ values during the Missourian and early Virgilian. Later, as conditions became drier in the late Virgilian and early Permian, $\delta^{34}S$ values become more erratic as organic production decreased dramatically and bacterial fractionation decreased.

Results of Statistical Analyses

Statistical analyses of geochemical parameters from the Midcontinent Pennsylvanian black shales in this study include: multiple discriminant analysis, cluster analysis, and principal components analysis. The initial step that was done in the multivariate analysis of these data is the formation of a Pearson correlation coefficient matrix between all geochemical parameters (variables) within groups (black shale types) (Tables 12 and 13). The purpose of the construction of correlation coefficient matrices is to form a preliminary working model showing which variables are most important in separating black shale types. From the correlation coefficient matrices, Heebner-type and Mecca-type deposits show good correlations among DOP, Fe_{py}, and S_{py}, indicating that pyrite formation is an important event

Table 12. Correlation coefficient matrix for geochemical parameters of Heebner-type black shales. Five fractions are present in the samples: detrital, carbonate, P/REE, heavy metals, and organics.

Group 1: Heebner-type

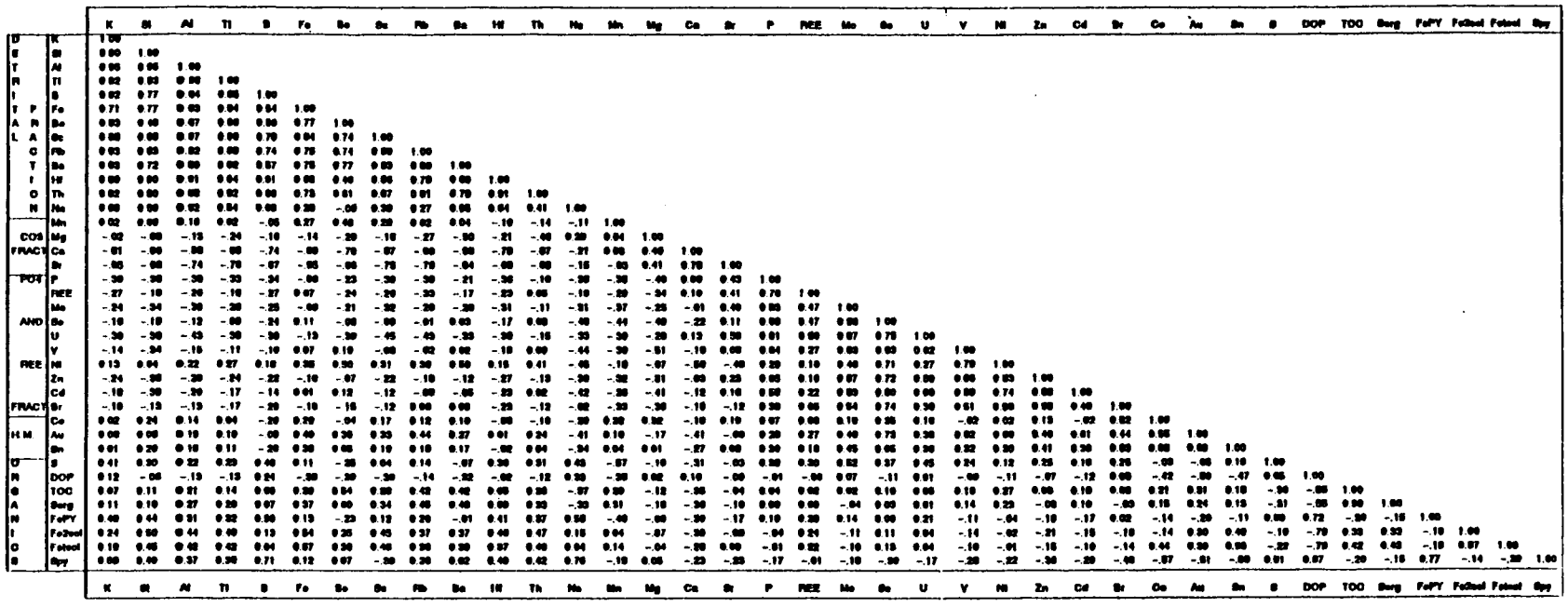

Table 13. Correlation coefficient matrix for geochemical parameters of Mecca-type black shales. Four fractions are present in the samples: detrital, carbonate (weak), heavy metals, and organics. Although a weak REE fraction is present, it does not correlate with P as in the Heebner-type shale samples because of a lack of P in Mecca-type black shale samples.

Group 3: Mecca-type

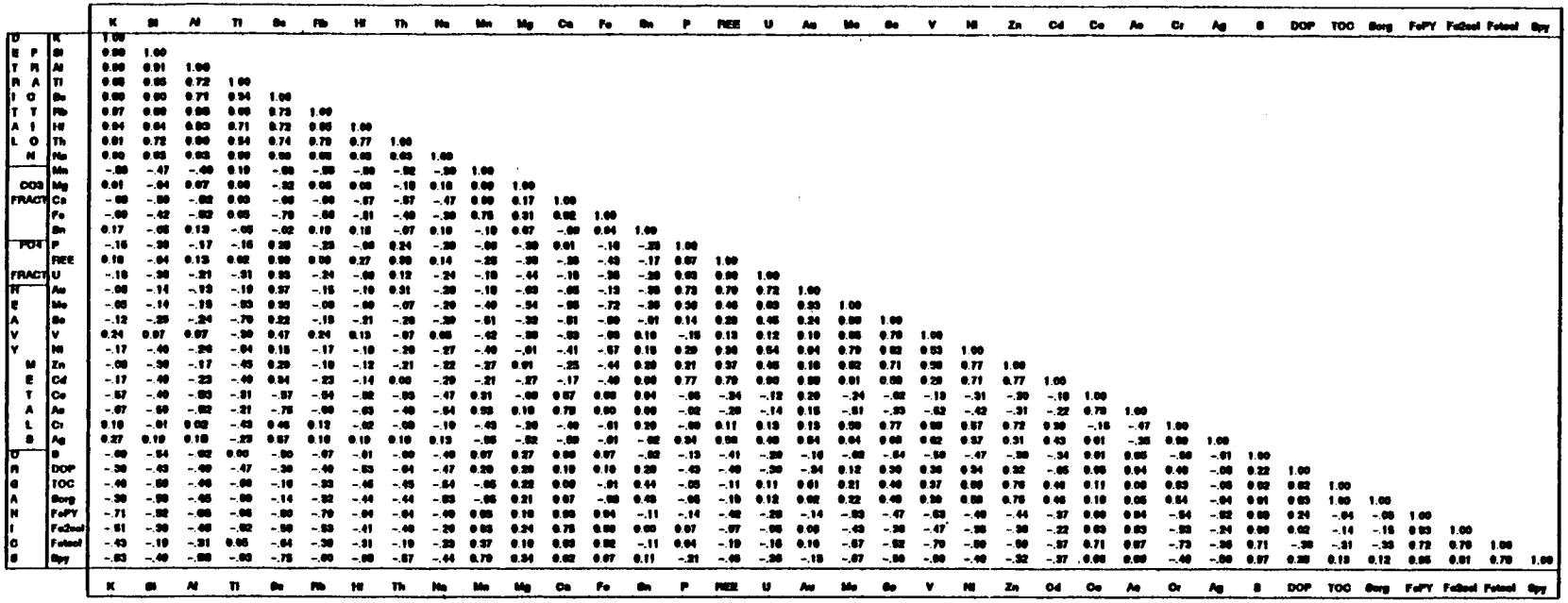

during black shale diagenesis. Relatively high DOP values in Heebner-type deposits and high DOP values in Mecca-type shales verify this interpretation. Mecca-type shales show positive correlations between TOC and many metals (including V, Cr, Ni, and Zn), thus indicating that metals are attracted to sediments with higher TOC contents.

Based on the correlation coefficient matrices of both Heebner- and Mecca-type black shales (Shanghai-type samples were not included because there were too few samples), it is evident that several fractions of elements and geochemical parameters are present in each type of deposit. The differences in the fractions of the two black shale types indicate that different sedimentological and geochemical processes occurred during diagenesis of the shales and reflect different depositional settings of the black shales.

Heebner-type black shales show five major fractions or groupings of elements and geochemical parameters. The fractions are summarized in Table 14 and include: detrital, carbonate, phosphate and REE, heavy metals, and organics associated with pyrite formation under reducing conditions. The detrital fraction of the Heebner-type shales includes detrital elements K, Si, Al, Ti, Sc, Rb, Hf, Th, and Na. However, additional elements are included in this fraction of Heebner-type black shales based on their high positive correlation coefficients, and include: Be, B, and Fe. The Fe is mostly present as iron coatings on clay minerals in

Table 14. Summary of fractions present in Heebner-type black shales and Mecca-type black shales based on correlation coefficient matrices.

Fractions of Black Shale Types Based on Correlation Coefficients (> 0.65)	
Group 1: Heebner-type	
Elements:	Fraction:
K, Si, Al, Ti, B, Fe, Be, Sc, Rb, Ba, Hf, Th, Na	Detrital
Mn, Mg, Ca, Sr	Carbonate
P, REE, Mo, Se, U, V, Ni, Zn, Cd, Br	P/REE
Co, Au, Sn	Heavies
S, DOP, TOC, Sorg	Organics and
Fepy, Fe2sol, FeTsol, Spy	pyrite-formation
Group 2: Mecca-type	
Elements:	Fraction:
K, Si, Al, Ti, Sc, Rb, Hf, Th, Na	Detrital
Mn, Mg, Ca, Sn (weak)	Carbonate
S, Dop, TOC, Sorg, Fepy, Fe2sol, FeTsol, Spy	Organics, pyrite-formation and others (reducing conditions)
Mn, As, Co, As, Ca, Zn, Cd	
REE, P, U, Au	P/REE (weak)

this fraction of Heebner-type shales whereas scanning electron microscopy indicates that Fe is present mostly in sulfides (i.e., pyrite) in Mecca-type shales (Coveney and Glascock, 1989). The Heebner-type carbonate fraction consists of Mn, Ca, Mg, and Sr, although the correlations are rather weak. It is postulated that the carbonate production process is a secondary process in the diagenesis of these shales. Phosphate and REE correlations in Heebner-type shales suggest a rather strong relationship among P, REE, Mo, Se, U, V, Ni, Zn, Cd, and Br. The abundant phosphatic nodules in Heebner-type samples most likely are a sink for REE and other metals (i.e., U, V, and Cd). The heavy metal fraction in the Heebner-type samples consists of Au, Sn, and Co, although correlations are rather weak in this fraction. Lastly, organics and pyrite-forming elements (iron and sulfur) comprise the organic fraction under reducing conditions. Based on the correlation coefficient matrix for S, DOP, TOC, S_{org}, Fe_{py}, and S_{py}, pyrite formation under reducing conditions is an important activity during diagenesis of the Heebner-type black shales, but did not control the distribution of metals such as Mo, Ni, and Zn, which correlate with the P fraction.

Mecca-type black shales contain four major fractions or groupings of elements and geochemical parameters based on the correlation coefficient matrices: detrital, carbonate, heavy metals, and organics (Table 14). The detrital frac-

tion of Mecca-type shales is similar to the detrital fraction of the Heebner-type shales and includes K, Si, Al, Ti, Sc, Rb, Hf, Th, and Na. Note that Fe is not contained in this fraction, unlike the Heebner-type shales, and indicates that iron is not present as coatings on clay minerals, but is concentrated in the sulfide-organic fraction during the formation of pyrite. This indicates that the relative importance of pyrite formation in Mecca-type shales is greater than that of Heebner-type shales. Thus, DOP values are greater in the Mecca-type shales. Unlike the Heebner-type shales, carbonate production is relatively unimportant in Mecca-type shales as evidenced by the low correlations among Mn, Ca, and Mg. Because of the lack of the REE/P fraction in the Mecca-type black shales, metals normally associated with phosphatic deposits as in Heebner-type shales (i.e., Mo, U, V, Ni, Zn, and Cd) are present in other fractions in Mecca-type black shales. Sulfides and pyrite nodules become sinks for other metals In Mecca-type black shales as evidenced by the association of Mo with framboidal pyrite (Coveney and Glascock, 1989). Mo, V, Ni, and REE are included in the heavy metal fraction whereas Zn, Cd, and Co are included in the organic (pyrite-formation under reducing conditions) fraction.

To quantitatively determine which geochemical parameters (i.e., S_{py}, DOP, TOC, REE) in Pennsylvanian black shales best discriminate between black shale types, the

stepwise discriminant analysis in SPSS was used. Groups were predefined by lithologic character (i.e., Mecca-, Heebner-, and Shanghai-type) and the variables were represented by the various geochemical parameters. Linear combinations of the parameters, referred to as canonical discriminant functions, were computed and maximized separation between black shale groupings (Table 15). Only the number of functions that account for the greatest variance within the variables need to be computed because the functions are derived in order of their power to discriminate between groupings.

Variables that account for the greatest discriminating power between groups are represented by the variables with the greatest Wilks' Lambda, or multivariate measure of group difference. Parameters with the greatest values for Wilks' Lambda include: Sn, Mg, Cr, Mo, V, Sr, TOC, Fetsol, Zn, Fe_{tot}, and DOP (Table 16).

Following the stepwise discriminant function analysis and calculation of canonical discriminant functions, a cluster analysis was conducted that used the previously calculated variables, most powerful in terms of discriminating power. A factor analysis separated variables into clusters and a subsequent Wards' minimum variance cluster program provided an "icicle diagram" that divided clusters into five major groupings (Figure 15). These groupings corresponded to Heebner-type samples, Shanghai-type samples,

Table 15. Eigenvalues, variance, canonical correlation, and Wilks' Lambda values for statistical analysis. Note that after only one discriminant function pass, 97.22% of the variance was accounted for, thus only one discriminant function was used throughout the study.

FUNCTION	EIGENVALUE	PERCENT OF VARIANCE	CUMULATIVE PERCENT	CANONICAL CORRELATION	AFTER FUNCTION	WILKS' LAMBDA	CHI-SQUARED	D.F.	SIGNIF.
					0	0.023226	109.110	10	0.000
1	23.3645	97.22	97.22	0.9800892	1	0.589107	15.345	4	0.004
2	0.69748	2.78	100.00	0.6410093					

Table 16. Summary of stepwise regression analysis. Step represents importance of variable in terms of discriminating between black shale types.

STEPWISE REGRESSION SUMMARY TABLE			
STEP	ACTION ENTERED	VARS IN	WILKS' LAMBDA
1	Sn	1	0.24501
2	Mg	2	0.09505
3	Cr	3	0.05199
4	Mo	4	0.03570
5	V	5	0.02311
6	Sr	6	0.02311
7	Sorg	7	0.02310
8	TOC	8	0.02289
9	Fetsol	9	0.02230
10	Zn	10	0.02230
11	Fet	11	0.02200
12	DOP	12	0.01809

Figure 15. Ward's minimum variance cluster analysis of black shale geochemical parameters. Note that here is a good progression between Heebner-type and Shanghai-type black shales, but a clear distinction exists in Mecca-type samples. The outlier represents Holland Shale Member. Metal-rich Mecca-type represents metalliferous Mecca-type black shales, and Mecca-type gray shales are Hesler C and Velpen C samples.

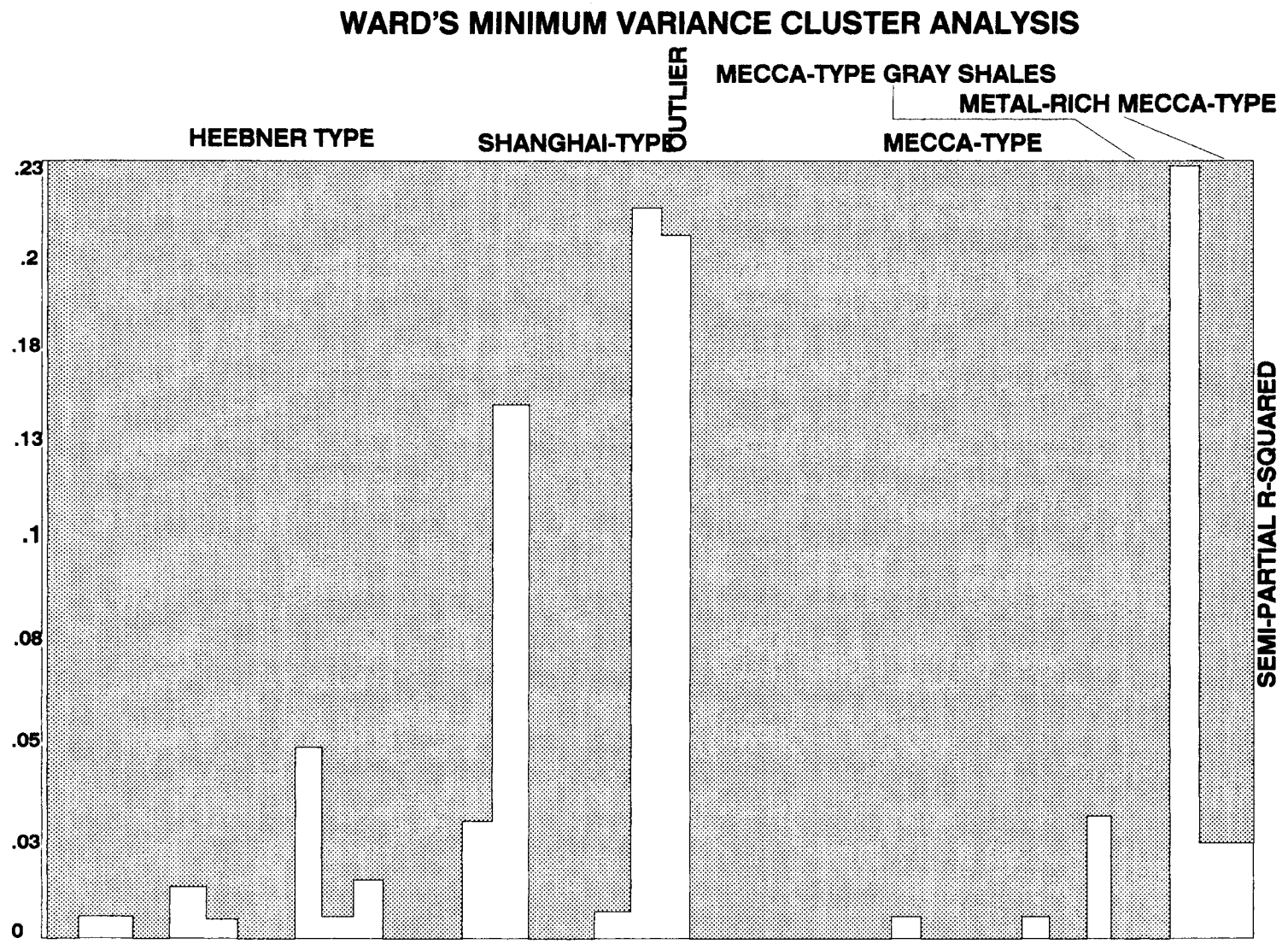
WARD'S MINIMUM VARIANCE CLUSTER ANALYSIS
OUTLIER
MECCA-TYPE GRAY SHALES
METAL-RICH MECCA-TYPE
HEEBNER TYPE
SHANGHAI-TYPE
MECCA-TYPE
.23
.2
.18
.13
.1
.08
.05
.03
0
SEMI-PARTIAL R-SQUARED

Mecca-type samples, the most metal-rich Mecca-type samples, and one outlier (Holland Shale Member).

Lastly, a principal components analysis showed groups (in three dimensions) were separated by geochemical parameters. A good separation between Mecca-type shales and other types exists indicating at least two distinct black shale types (Table 17). However, a significant overlap is present between Shanghai- and Heebner-type units. This shows that there is a progression from distinct Missourian black shales to Virgilian black shales, but an overlap exists within Virgilian black shales between Heebner-type and Shanghai-type samples (Figures 16 and 17). Thus, in effect, distinct metal-rich Mecca-type black shales and Missourian Heebner-type deposits plot in separate groups and there is good evidence for a separation of these types of black shales (Figure 18), but questionable evidence for the differentiation between late Heebner-type deposits (Virgilian) and Shanghai-type units (Virgilian) (Figure 19). Further study and more careful microstratigraphic sampling will aid in the clarification of this problem.

To simplify the problem of clustering, a second analysis was conducted using only 12 variables. The variables were selected on the basis of the stepwise regression analysis. Figures 20 and 21 represent clusters of factor scores 1 vesus factor scores 2 and 3, respectively. Note the better separation of the Mecca-type samples from the Heeb-

Table 17. Summary of classification results in statistical analysis. Note overlap between Heebner-type and Shanghai-type samples, but no overlap with Mecca-type black shale samples. Percent of "grouped" cases correctly classified refers to the number of unknown samples that plotted in "correct" or predefined groupings.

CLASSIFICATION RESULTS				
ACTUAL GROUP	NO. OF CASES	PREDICTED GROUP MEMBER SHIP		
		1	2	3
GROUP 1	13	11	2	0
HEEBNER–TYPE		84.6%	15.4%	0.0%
GROUP 2	6	2	4	0
SHANGHAI–TYPE		33.3%	66.7%	0.0%
GROUP 3	17	0	0	17
MECCA–TYPE		0.0%	0.0%	100.0%

PERCENT OF "GROUPED" CASES CORRECTLY CLASSIFIED: 94.44%

Figure 16. Plot of regression factor score 1 versus regression factor score 2. Note the overlap of Heebner-type and Shanghai-type samples, but no overlap of Mecca-type black shale samples.

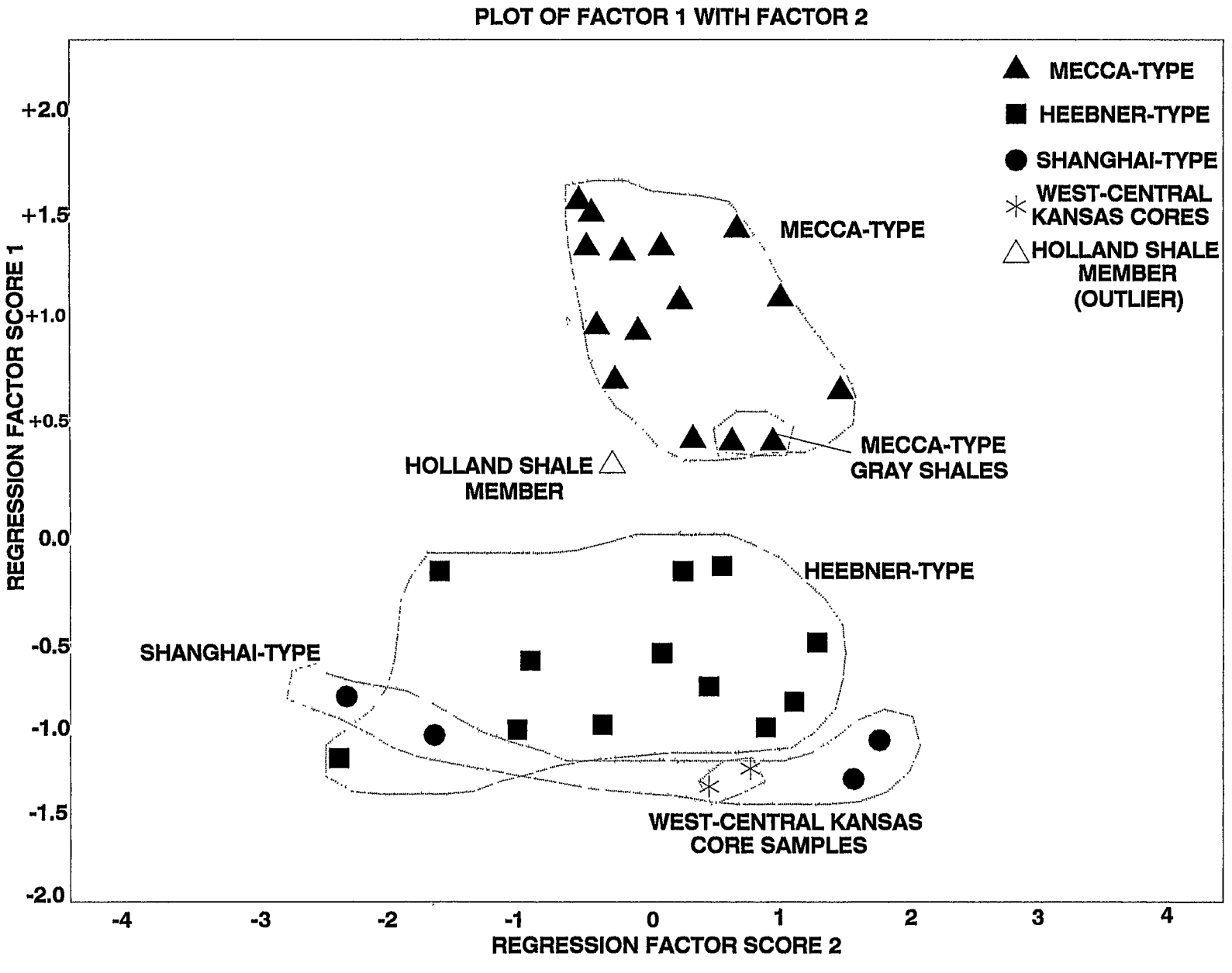
PLOT OF FACTOR 1 WITH FACTOR 2
MECCA-TYPE
HEEBNER-TYPE
SHANGHAI-TYPE
WEST-CENTRAL KANSAS CORES
HOLLAND SHALE MEMBER (OUTLIER)
MECCA-TYPE
MECCA-TYPE GRAY SHALES
HOLLAND SHALE MEMBER
HEEBNER-TYPE
SHANGHAI-TYPE
WEST-CENTRAL KANSAS CORE SAMPLES
REGRESSION FACTOR SCORE 1
+2.0
+1.5
+1.0
+0.5
0.0
-0.5
-1.0
-1.5
-2.0
-4
-3
-2
-1
0
1
2
3
4
REGRESSION FACTOR SCORE 2

Figure 17. Plot of regression factor score 1 versus regression factor score 3. Note the close proximity of Heebner-type and Shanghai-type samples, but relatively isolated Mecca-type black shale samples.

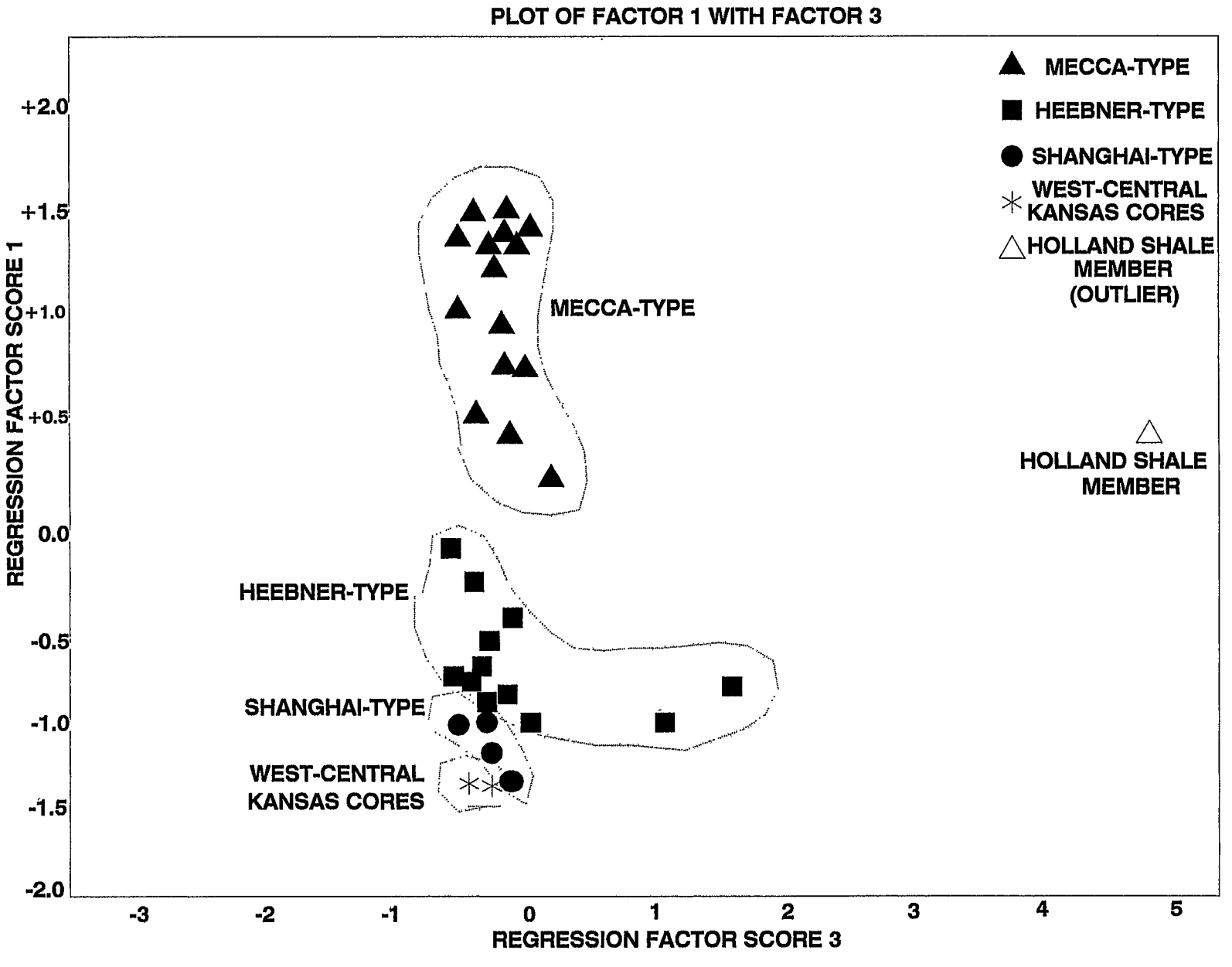
PLOT OF FACTOR 1 WITH FACTOR 3
MECCA-TYPE
HEEBNER-TYPE
SHANGHAI-TYPE
WEST-CENTRAL KANSAS CORES
HOLLAND SHALE MEMBER (OUTLIER)
HOLLAND SHALE MEMBER
MECCA-TYPE
HEEBNER-TYPE
SHANGHAI-TYPE
WEST-CENTRAL KANSAS CORES
REGRESSION FACTOR SCORE 1
+2.0
+1.5
+1.0
+0.5
0.0
-0.5
-1.0
-1.5
-2.0
-3
-2
-1
0
1
2
3
4
5
REGRESSION FACTOR SCORE 3

Figure 18. Stacked histogram of all black shale samples in statistical analysis. Centroids represent center of groupings. Heebner- and Shanghai-type samples overlap indicative of a progression of black shales, whereas Mecca-type black shale samples are isolated and do not overlap other black shale samples.

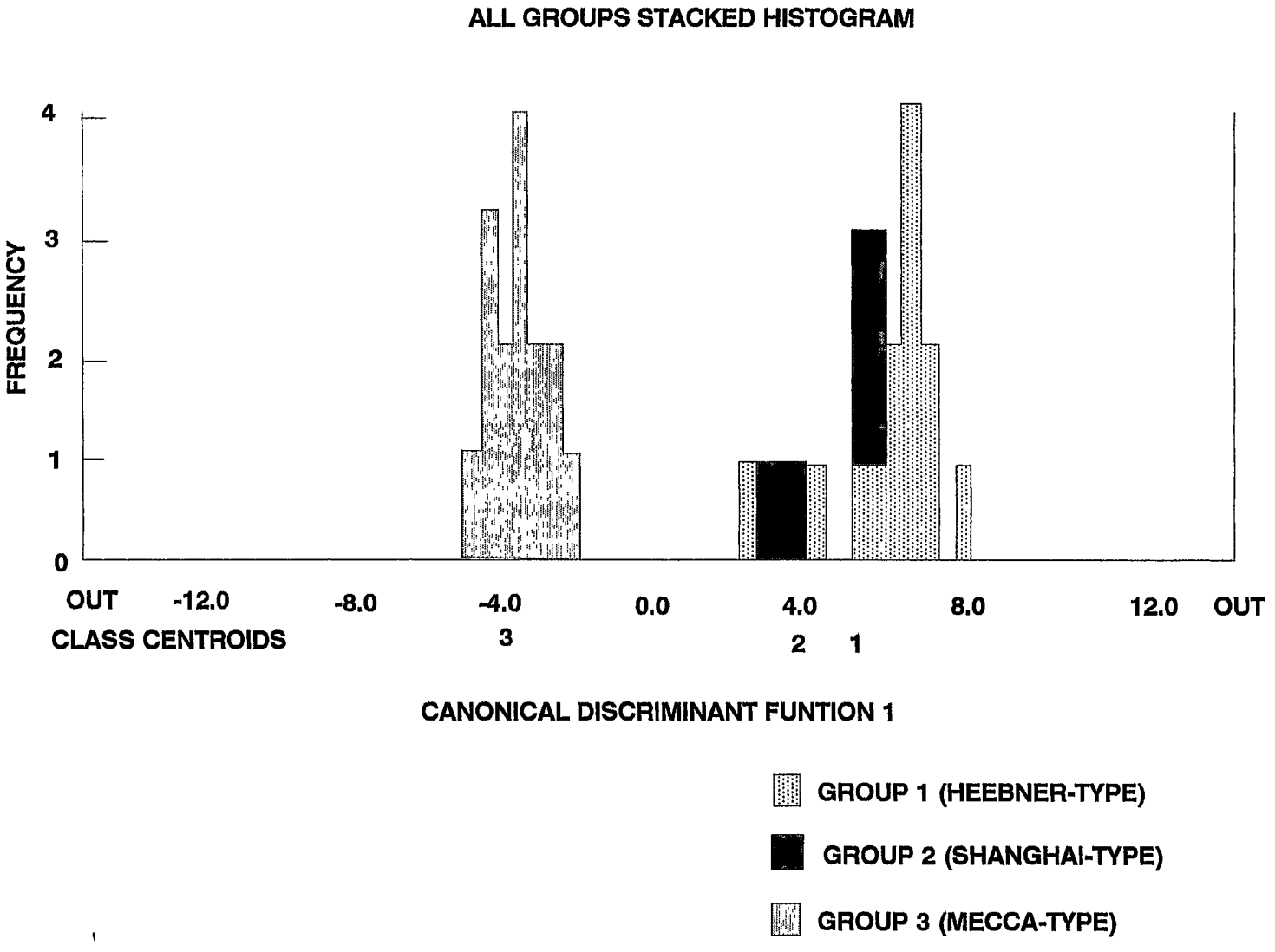
ALL GROUPS STACKED HISTOGRAM
FREQUENCY
4
3
2
1
0
OUT
-12.0
-8.0
-4.0
0.0
4.0
8.0
12.0
OUT
CLASS CENTROIDS
3
2
1
CANONICAL DISCRIMINANT FUNTION 1
GROUP 1 (HEEBNER-TYPE)
GROUP 2 (SHANGHAI-TYPE)
GROUP 3 (MECCA-TYPE)

Figure 19. Dendrogram of samples based on centroid method of SPSS (Statistical Package for the Social Sciences). The grouping of samples in the left column is based on cluster analysis.

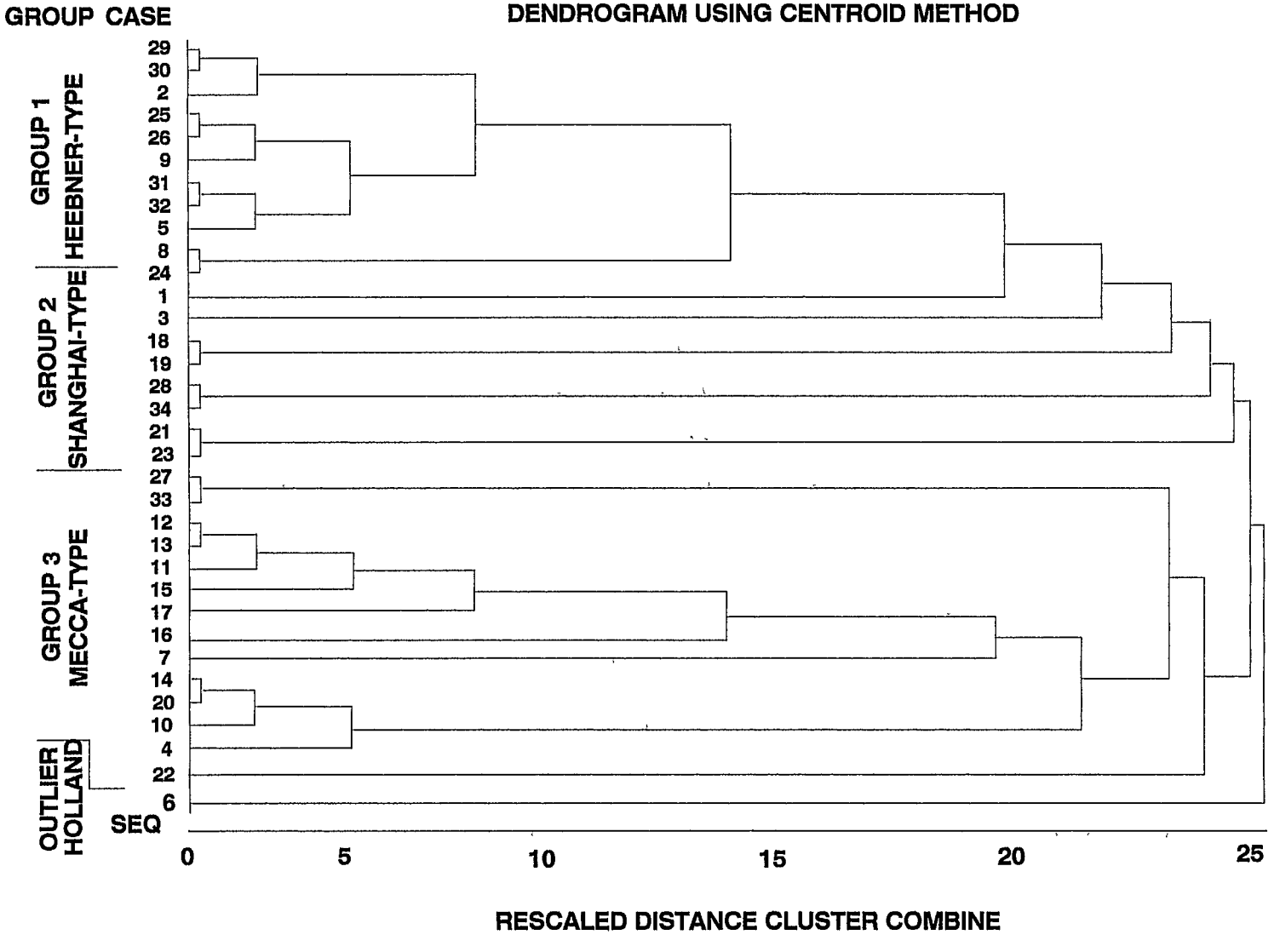
GROUP CASE
DENDROGRAM USING CENTROID METHOD
GROUP 1 HEEBNER-TYPE
GROUP 2 SHANGHAI-TYPE
GROUP 3 MECCA-TYPE
OUTLIER HOLLAND
29
30
2
25
26
9
31
32
5
8
24
1
3
18
19
28
34
21
23
27
33
12
13
11
15
17
16
7
14
20
10
4
22
6
SEQ
0
5
10
15
20
25
RESCALED DISTANCE CLUSTER COMBINE

Figure 20. Plot of regression factor score 1 versus regression factor score 2 using 12 variables. Note the increased separation of the Mecca-type samples from the Heebner- and Shanghai-type samples, but a poor separation between Heebner- and Shanghai-type samples.

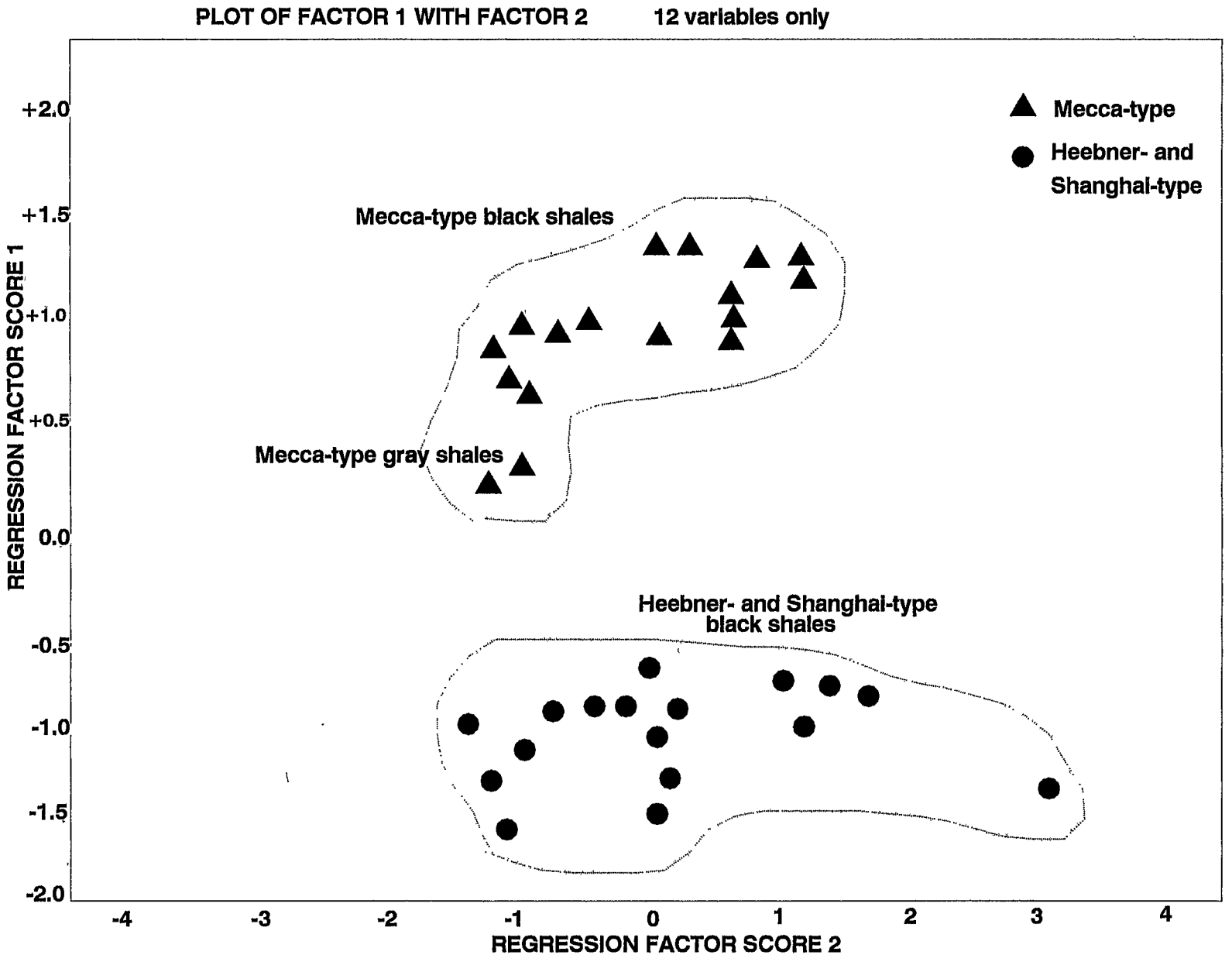
PLOT OF FACTOR 1 WITH FACTOR 2
12 variables only
Mecca-type
Heebner- and Shanghai-type
Mecca-type black shales
Mecca-type gray shales
Heebner- and Shanghai-type black shales
REGRESSION FACTOR SCORE 1
+2.0
+1.5
+1.0
+0.5
0.0
-0.5
-1.0
-1.5
-2.0
-4
-3
-2
-1
0
1
2
3
4
REGRESSION FACTOR SCORE 2

Figure 21. Plot of regression factor score 1 versus regression factor score 3 using 12 variables. Note the separation of Mecca-type gray shales, but the close clustering of Heebner- and Shanghai-type samples. Outliers represent Logan Quarry Shale Member and Holland Shale Member.

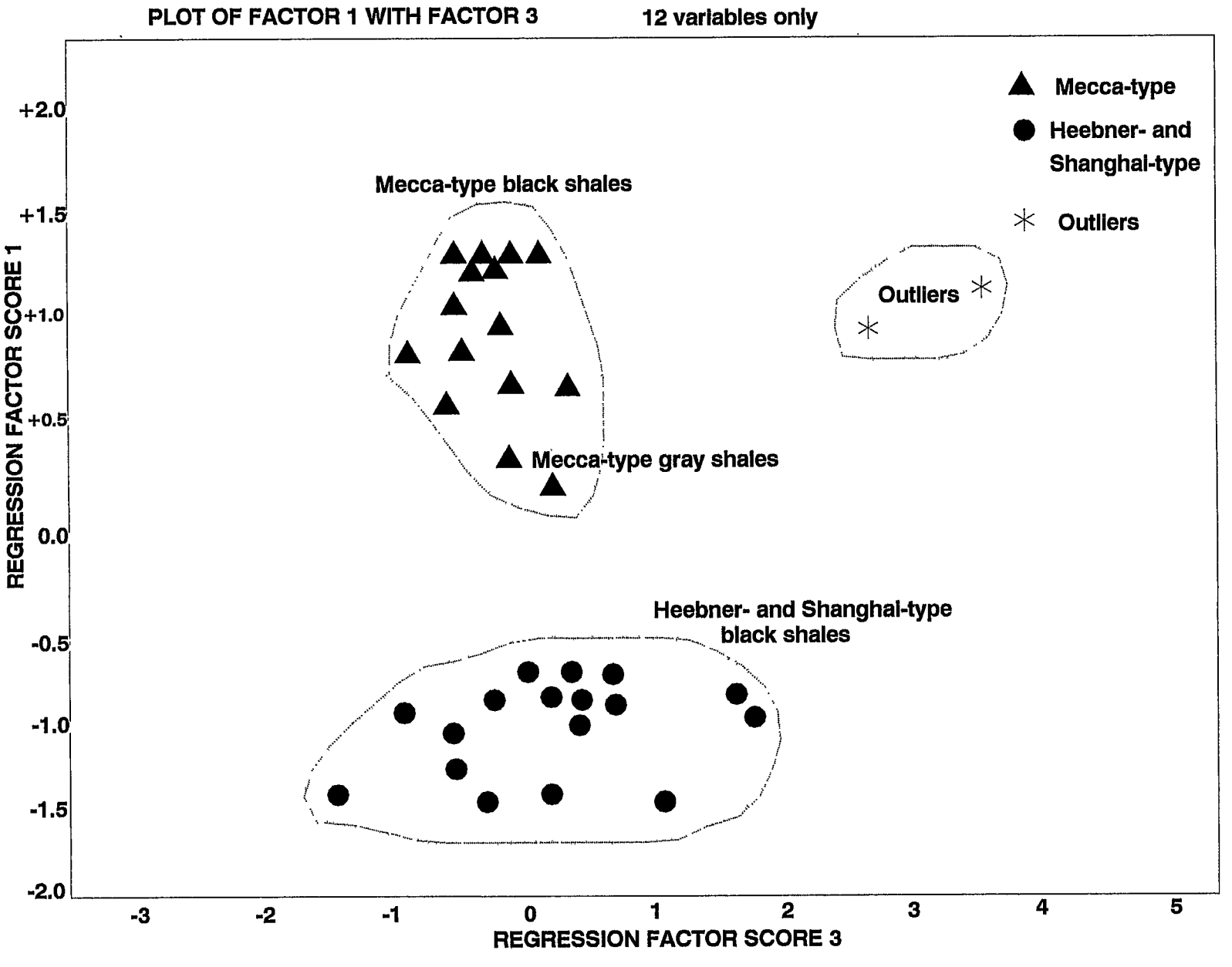
PLOT OF FACTOR 1 WITH FACTOR 3
12 variables only
Mecca-type
Heebner- and Shanghai-type
Outliers
Mecca-type black shales
Outliers
Mecca-type gray shales
Heebner- and Shanghai-type black shales
REGRESSION FACTOR SCORE 1
+2.0
+1.5
+1.0
+0.5
0.0
-0.5
-1.0
-1.5
-2.0
-3
-2
-1
0
1
2
3
4
5
REGRESSION FACTOR SCORE 3

ner- and Shanghai-type samples, but a poor separation of Heebner- and Shanghai-type samples. It is evident that to separate Heebner- and Shanghai-type samples from each other, more variables are required. Ward's minimum variance cluster shows the separation of Mecca-type samples, Logan Quarry Shale Member, Holland Shale Member, and Heebner- and Shanghai-type shale samples, although the Heebner- and Shanghai-type samples are poorly separated (Figure 22). A summary table of values for the cluster analysis is depicted in Table 18.

Figure 22. Ward's minimum variance cluster analysis using 12 variables. Note the separation of the Mecca-type shale samples, Logan Quarry Shale Member, and the Logan Quarry Shale Member, but the close proximity of Heebner- and Shanghai-type samples.

Ward's Minimum Variance Cluster Analysis

12 variables only

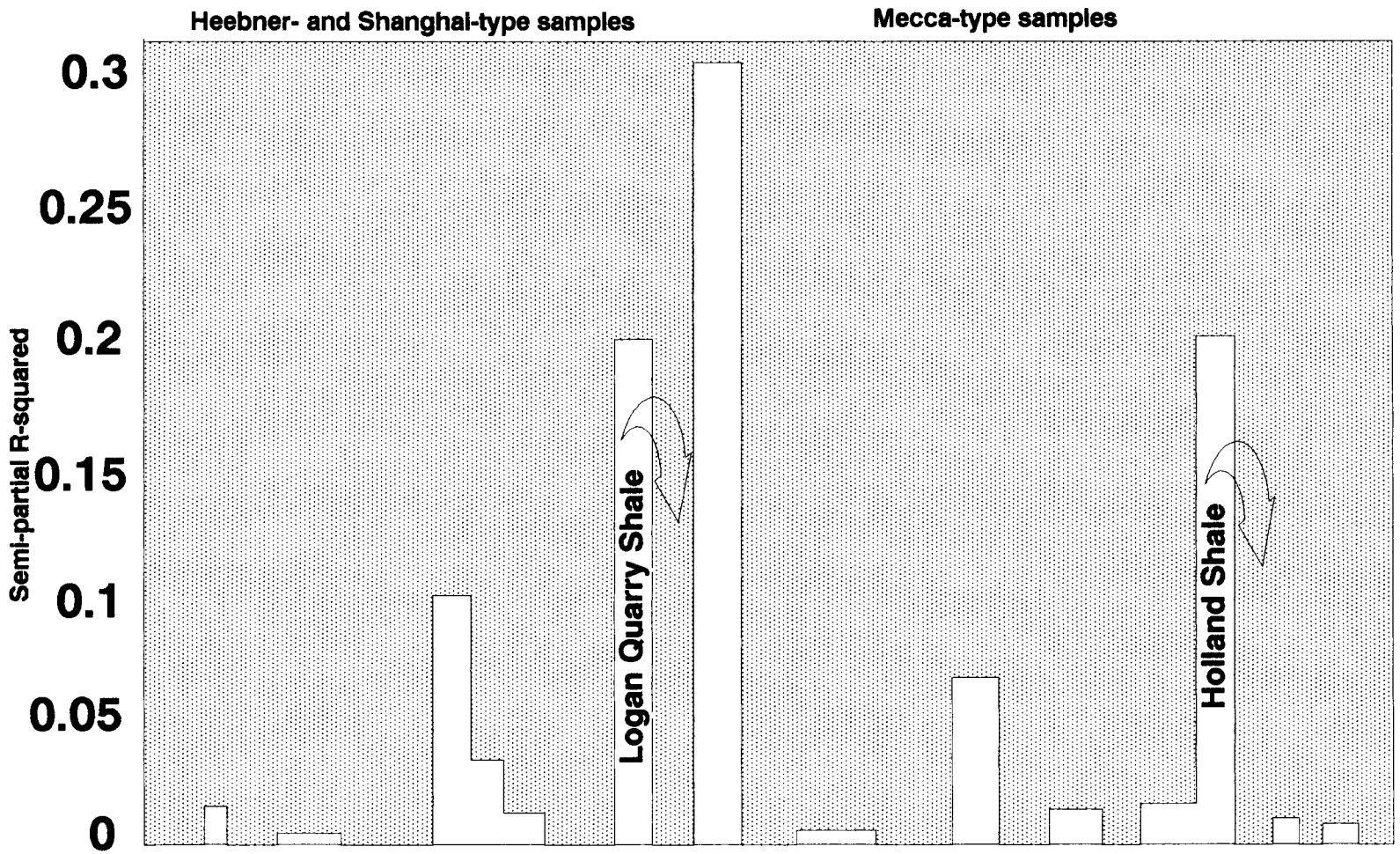

Table 18. Summary table for values in cluster analyses. Values are included for the analysis with all variables and the second analysis with 12 variables.

Values for Cluster Analysis						
	Analysis of all variables			Analysis of 12 variables only		
Sample	Factor 1	Factor 2	Factor 3	Factor 1	Factor 2	Factor 3
EU1	-0.53484	1.27109	-0.35642	-0.75638	-0.27311	1.34293
HBC6	-1.19854	-2.43054	-0.33063	-1.45991	-1.06765	-1.56042
HB1	-0.94567	0.82669	0.95444	-0.61455	-0.06341	0.50796
HLD1	0.31207	-0.29348	5.11358	0.91786	-0.00776	-0.70886
HP3	-0.79860	-0.36880	-0.63328	-1.19638	0.13587	0.09339
HP4	-1.07671	-0.92451	-0.00017	-1.28307	3.14043	-0.39091
LB3	-0.74054	1.03108	-0.08430	-0.69572	1.68705	0.43805
LOG1	-0.35860	-1.40198	-0.23342	0.83187	-0.95777	2.63069
MC1	-0.22738	0.28999	-0.39348	-0.93155	0.13244	1.42536
MQHA1	1.60015	-0.34892	-0.18695	1.30350	1.05433	-0.11022
MQHA2	1.43143	0.51983	-0.24734	1.17768	0.49117	-0.42360
MQHA3	1.24149	0.05006	-0.19453	1.00385	0.52434	-0.44775
MQHA4	1.21234	0.20070	-0.23623	1.09881	0.45694	-0.55846
MQHB1	1.41159	-0.40918	-0.28441	1.23440	1.10613	-0.48444
MQHB2	1.28089	-0.21218	-0.36727	1.30630	0.03993	-0.47756
MQHB3	0.92223	0.98369	-0.53487	0.66030	-0.08447	-0.21993
MQHB4	1.24152	0.02550	-0.37675	1.30659	-0.08847	-0.39509
MQHC	0.22904	1.07865	0.14179	0.24802	-1.18493	0.03966
MQHD	0.72579	-0.24876	-0.27956	0.72933	-0.98916	0.29185
MQSB	1.43964	-0.48915	0.28798	1.31200	0.74114	-0.60158
MQVA	0.34413	0.21916	-0.26574	0.62108	-0.85306	-0.77005
MQVB	0.79286	-0.45338	-0.04299	0.92352	-0.79988	-1.17871
MQVC	0.32262	0.61711	-0.01962	0.29021	-0.97078	-0.42069
MQVD	0.71652	-0.32339	-0.13023	1.01775	-0.56443	3.37458
QHC1	-1.40684	0.57039	-0.32086	-0.80933	-0.91205	-0.41829
QHC2	-1.38250	0.94094	0.15863	-0.99330	-0.99756	-0.66628
QH1	-0.71856	0.48827	-0.43575	-0.62451	1.23996	-0.14923
QH3	-0.56041	0.24346	-0.37638	-0.94737	1.09023	0.22746
SHC2	-1.09144	-1.61447	-0.53378	-1.17455	-1.22877	-0.66080
SHC3	-0.85568	-2.51442	-0.54329	-0.94074	-1.46747	-1.12808
SH1	-1.09483	1.69762	0.30442	-0.84286	-0.50252	0.33227
SH2	-1.30563	1.53926	0.02888	-1.28820	0.00276	0.89478
ST2	-0.70888	-0.96543	1.50323	-0.83207	0.17983	0.06711
ST3	-0.21864	0.40508	-0.76744	-0.59259	0.99068	0.10487

Provenance and Weathering

One goal in examining the chemical composition of clastic sedimentary rocks (i.e., black shales) is to ascertain provenance or source area. Sources of clastic rocks, according to Taylor and McLennan (1985) are:

1. "Primary" igneous rocks and their metamorphosed equivalents, derived from the mantle through partial melting stages.
2. "Secondary" igneous rocks derived from the remelting of crustal rocks.
3. Recycled sedimentary and metasedimentary rocks.

The provenance of many sediments is usually made up of recycled crustal material implying large-scale mixing of upper crustal rocks (Taylor and McLennan, 1985). Sedimentation involves several complex chemical and physical processes, including, among others, weathering. Because rare-earth elements' behavior during weathering is not well-understood, it is important to attempt a quantification of the chemical effects of weathering on shales, black shales in particular. Three major stages of weathering have been recognized by Chesworth (1973):

1. Early Stage - formation of chlorite, smectite, vermiculite, and illite with high cation exchange capacity (CEC).

2. Intermediate Stage - clay fraction composed mostly of smectite, with lesser amounts of illite.

3. Late Stage - clay fraction dominated by kaolinite-gibbsite-quartz, iron oxides, low CEC.

High rates of mechanical erosion necessary to form clastic sediments such as black shales, usually follow periods of significant uplift, therefore it is inappropriate to associate clastic sediments from extremely weathered sources (i.e., late stage) with clastics in this study. Considering weathering effects of shales in this study, the early and intermediate stages seem most germane.

Under early stages of weathering, large cations (Rb, Cs, Ba) are adsorbed on clays (Nesbitt and Young, 1984) and immobile elements include: Al, Ga, Ti, Zr, Hf, REE's, Th, and Nb. Some Ni and V mobility is apparent, according to Kronberg et al., (1979), especially important in black shales.

Nesbitt and Young (1982) have developed a quantitative assessment of weathering effects on sedimentary rock composition referred to as chemical index of alteration (CIA):

$$CIA = [Al_2O_3/(Al_2O_3 + CaO + Na_2O + K_2O)] \times 100$$

Because feldspar makes up approximately 50% of the upper crust, this index measures with a good degree of accuracy, the degree of feldspar to clay mineral alteration during weathering. A typical value for an average shale is 70 to 75, as compared with 50 for the average upper continental crust (Nesbitt and Young, 1982). The 70 to 75 values for shales indicate that weathering has not progressed to the stage where alkalis are removed from the clays. Black shales in the Midcontinent possess CIA values within the 70 to 75 range, indicative of early to intermediate weathering phases.

Chapter 6. Discussion of Black Shale Types and Depositional Models

Pennsylvanian black shales of the Midcontinent can be differentiated on geochemical parameters. Three Midcontinent black shale types are differentiated on: variation in inorganic geochemistry (metal contents), type and abundance of organic constituents, sulfur isotope variation, and inferred fluctuations in bottom-water oxygenation conditions during depositional processes (Schultz, 1990). Paleontological and sedimentological characteristics further characterize the black shale types. The three types of black shale sequences are referred to as: Mecca-type, Heebner-type, and Shanghai-type (Figure 23).

Mecca-type Black Shales

The prototype Mecca Quarry Shale Member, along with other Mecca-type black shales (Desmoinesian) including the Holland Shale Member and the Logan Quarry Shale Member, contain elevated TOC values, typically between 20% and 40%, usually of terrestrial origin, as shown by Rock-Eval analyses (Coveney, Watney, and Maples, 1991) (Table 19). Metal values also are high with Mo between 500 ppm and 3000 ppm (Coveney, Watney, and Maples, 1991), including a value of 2000+ ppm in Mecca Quarry Shale samples from Velpen, Indiana.

Figure 23. Black shale types of the Midcontinent Pennsylvanian (from Schultz and Coveney, in press).

BLACK SHALE TYPES

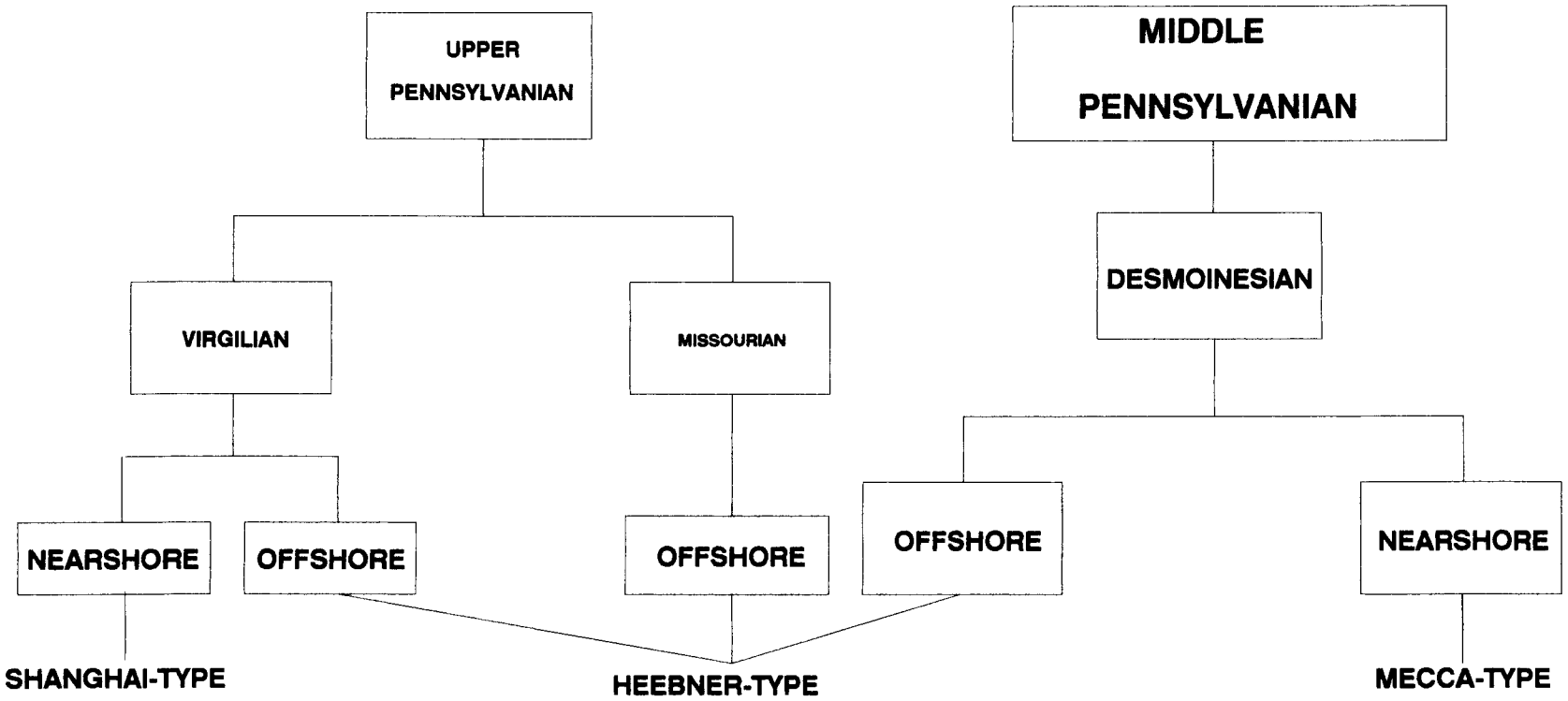

Table 19. Characteristics of black shale types in the Midcontinent Pennsylvanian (from Schultz and Coveney, in press).

Characteristics of Black Shale Types

Parameters	Mecca–type	Heebner–type	Shanghai–type
Organic matter type and quantity	> 20%, terrestrial–type (1)	< 20%, marine–type, (2)	< 15%, mixed marine– and terrestrial types
Inorganic geochemistry	> 100 ppm U > 500 ppm Mo (3) < 0.3 % P2O5 (4)	< 100 ppm U < 200 ppm Mo > 0.3% P2O5	<< 50 ppm U < 10 ppm Mo > 0.5% P2O5
S isotopes	erratic, heavy (5)	constant, light (5)	erratic, heavy
Sedimentary	siliciclastic association carbonate nodules abundant, well–preserved fossils colors: N2–N3	carbonate association phosphatic nodules few fossils colors: N3–N4	siliciclastic association few phosphatic nodules abundant, phosphatic fossils colors: N4–N5
Depositional environment	nearshore	offshore	isolated, lagoonal
Bottom–water conditions (DOP)	inhospitable (DOP > 0.70)	restricted (0.17 < DOP < 0.70)	aerobic (DOP < 0.35)
Quantitative TOC vs. Spy	high C/S ratios below normal marine	low C/S ratios above normal marine	low C/S ratios slightly below normal marine
Examples	Mecca Quarry, Logan Quarry, Holland	Heebner, Queen Hill, Stark, Hushpuckney, Muncie Ck., Eudora, Larsh/Burroak.	Shanghai Creek, Holt.

data from Schultz and Coveney (in press)

(1) Shaffer and Leininger, 1985; Coveney, et al., 1987

(2) Wenger and Baker, 1986

(3) Coveney, et al., 1987

(4) Coveney, et al., 1991

(5) Coveney and Shaffer, 1988

Uranium values are generally 100+ ppm. Phosphate values are low, mostly less than 0.3 weight percent P_2O_5 (Coveney, Watney, and Maples, 1991). Not surprisingly, phosphatic nodules in Mecca-type deposits are rare and $\delta^{34}S$ values are variable: Coveney and Shaffer (1988) have reported average values for Mecca-type black shales of -12.9 per mil, but note that erratic values are typical for shallow-water deposits. DOP values for Mecca-type units average greater than 0.75, indicative of anaerobic bottom-water conditions during deposition, as defined by Raiswell et al., (1988). Finally, total REE values are large in Mecca-type units in comparison with PAAS and NASC and the distribution shows an enrichment in middle REE with a Eu anomaly comparable to the shale standards (Figure 13B).

Heebner-type Black Shales

Heebner-type black shales are generally, although not always, metalliferous (Leventhal in Huyck, 1991), and include several units Missourian and Virgilian in age. Heebner-type black shales in this study include: the prototype Heebner Shale Member, Stark Shale Member, Hushpuckney Shale Member, Eudora Shale Member, Muncie Creek Shale Member, Queen Hill Shale Member, and the Larsh/Burroak Shale Members. TOC values are mostly less than 20% and reflect marine-type organic matter (Coveney, Watney, and Maples,

1991). Typical values for TOC are 10-15% (Table 19). Metal values are intermediate in comparison with Mecca-type units, with less than 500 ppm of Mo and 100 ppm of U present (Coveney, Watney, and Maples, 1991). Phosphate values are high with weight percent of P_2O_5 usually greater than 0.3% (Table 19). One sample of the Stark Shale Member in eastern Kansas contains 5.43% weight percent P_2O_5. Phosphatic nodules are abundant in these units and ^{34}S values are light, yet relatively constant. Coveney and Shaffer (1988) reported an average of -27.2 per mil for midwestern Missourian black shales. Values of -40.0 per mil have been determined for Virgilian black shales in this study, suggestive of a more distal (to shore) origin for the Heebner-type deposits. DOP values average between 0.45 and 0.75, indicative of dysaerobic bottom-water conditions (Schultz, 1989). REE total abundances and the chondrite-normalized distribution are similar to NASC and PAAS values, but totals are low in comparison with Mecca-type shales. A Gd anomaly is present (Figure 13).

Shanghai-type Black Shales

The third type of black shale delineated in the Pennsylvanian section is the Shanghai-type black shale. The unit has been defined to include the prototype Shanghai Creek Shale Member and the Holt Shale Member of southeastern

and eastern Kansas (Schultz, 1989). TOC values are low, averaging 1.98%, with extreme values of 0.01 and 4.74 (Schultz, 1990). Rock-Eval results indicate a mostly terrestrial, although somewhat mixed terrestrial and marine origin for the organic material (Table 19). Metal values are exceptionally low, with Mo values generally less than 120 ppm and U values less than 20 ppm. The quantity of P_2O_5 present is generally moderate, but quantities can exceed 0.75 weight percent. Phosphatic nodules are sparse, but phosphatic brachiopods are abundant. $\delta^{34}S$ values average -29.2 per mil with little variation, possibly indicative of sediments deposited in marine to brackish waters where deposition was fairly slow. DOP values are low in general, with values ranging from 0.46 to 0.01 (average 0.15), suggesting an aerobic setting for bottom waters (Schultz, 1989). Finally, total REE values are low in comparison with PAAS, NASC, Mecca-type deposits, and Heebner-type black shales. The Eu anomaly also is small in Shanghai-type units. Despite several differences between Shanghai- and Heebner-type units, the statistical analyses show that the two types are gradational (Table 19). Table 20 depicts a representative sampling across the Midcontinent Pennsylvanian in terms of metal supply.

Table 20. INAA (instrumental neutron activation analysis) data for 45 elements in Pennsylvanian black shales. The data represent the most metal-rich black shale samples. Sample locations are arranged from east (left) to west (right). Note that Desmoinesian black shales are enriched in Mo, U, Se, V, and Cd, and formed near shore. Metal contents decrease westward where depositional environment changes to fully marine. The 1989 average refers to 74 samples of black, dark gray, and gray shales reported by Coveney and Glascock (1989). From Schultz and Coveney (in press).

Representative Black Shale INAA Data

	Desmoinesian (M. Penn.)						Missourian (U. Penn.)		Virgilian (U. Penn.)				1989	Typical
	Mecca-type Black Shales			Transitional	Heebner-type Shales		Heebner-type Shales		Heebner-type Shales		Shanghai-type Shales		Shale Avg	Anal. Error
sample no.	73	21	18	61	55	44	79	80	HB5	QH1	SH1	SH2		
Element														
B	85	63	84	94	92	103	95	94	103	140	160	120	102	5
Na	2350	2000	1540	2070	2780	3800	3920	3590	4010	4500	6800	6800	2950	44
Mg	9060	11000	10000	11500	11300	12900	15100	14300	15600	22700	21700	21800	10500	940
Al	46600	43000	43000	39500	44300	68900	69000	67800	67400	127000	186000	190000	60600	2500
Si	121000	132000	98000	117000	127000	210000	185000	192000	216000	418000	502000	503000	173000	5300
S	33700	28000	32000	22400	18500	22500	13600	16700	22200	8400	14400	500	36800	3000
Cl	240	360	490	200	290	250	260	150	150	175	98	75	200	100
K	17100	13500	15800	14700	17500	21700	21400	21600	22200	27500	36400	36200	20100	450
Ca	5480	4400	4300	87400	56700	46400	46700	25200	36800	24200	20100	14600	22700	1100
Sc	12	11	11	9	10	14	13	12	14	12	18	17	13	0.3
Ti	1990	1950	2350	1620	1800	2500	3510	3170	3300	5900	8000	8300	274	300
V	2850	3170	1410	2800	1300	400	790	1050	930	1100	180	160	1300	60
Cr	610	490	300	370	920	500	540	570	660	910	360	380	17	10
Mn	130	360	120	500	290	260	190	150	200	400	400	300	36	6
Fe	33800	32000	37000	25200	28000	35000	33400	33600	38400	40600	55400	54600	43800	400
Co	23	21	25	11	12	22	14	12	14	12	19	11	20	0.4
Ni	530	450	420	360	410	290	200	270	300	330	190	210	270	100
Zn	3350	3020	520	3270	1360	1860	1620	1930	2220	1800	84	220	1300	70
Ga	16	15	18	11	12	15	17	18	16	13	11	9	17	2
As	35	38	40	27	14	28	39	25	41	13	26	9	36	0.6
Se	230	250	210	180	110	78	76	100	120	30	10	2	130	10
Br	10	7	8	3	9	4	8	7	7	6	4	3	7	2
Rb	85	81	83	71	75	113	115	97	120	150	180	190	110	4
Sr	<80	<130	<110	<66	<60	420	244	<65	<70	100	170	150	140	70
Mo	1430	2260	1840	910	170	60	80	86	67	83	5	5	855	240
Cd	150	110	21	170	50	20	54	55	56	48	1	3	54	12
Sb	52	69	56	51	11	8	15	15	17	8	2	1	28	0.2
Cs	5	4	4	4	5	7	7	6	7	6	9	10	6	1
Ba	300	290	<240	155	200	360	190	260	340	370	400	450	320	50
La	42	31	31	44	31	42	39	40	33	26	46	37	38	0.8
Ce	59	54	52	63	61	81	80	66	2	48	85	56	68	1
Nd	49	34	27	45	38	46	48	42	58	21	41	22	41	4
Sm	8.5	7.1	5.1	8.6	7.8	8.4	9	8.8	5.7	3.9	8.2	3.2	8.4	0.2
Eu	1.8	1.4	1.1	1.9	1.6	1.8	2	1.7	2	0.7	1.8	0.8	1.8	0.03
Gd	8.4	7.8	4.9	9.6	8.5	8.6	8.7	8.7	5.2	4.3	3.2	2.1	8.4	0.2
Tb	1.1	1.3	0.8	1.4	1.1	1.3	1.2	1.2	1.1	0.5	1.2	0.4	1.3	0.07
Dy	7.7	9.4	4.1	8.3	7.2	7.1	7.9	7.7	5.5	3.4	3.3	2.2	7	0.3
Yb	3.6	3.2	2.4	4.3	4.1	4.7	3.5	3.4	2.9	2	2.9	1.9	3.7	0.1
Lu	0.6	0.5	0.3	0.7	0.8	0.9	0.6	0.5	0.5	0.1	0.05	0.02	0.6	0.02
Hf	2	1.9	1.7	1.8	2	3.5	3.1	2.9	3.2	3	4	4	2.6	0.06
Ta	1.4	0.5	0.8	0.6	0.7	1.2	0.9	0.9	1	1	1	1	0.9	0.04
W	15	2.5	4.9	2.6	3.3	6.1	3.2	4.1	2.1	2.1	2.6	2.2	4.9	0.7
Au	2	3.7	<2.6	1.7	2.9	1.9	1.7	1.8	1.8	0.9	0.5	0.2	2.5	0.5
Th	6.5	6.5	6.2	5.6	7	10.1	8.7	7.6	8.7	9	12	13	8.4	0.1
U	165	140	125	134	58	39	64	80	35	43	14	10	85	4

Sample Descriptions

73. Mecca-type shale; Mecca Quarry mbr., Hesler Farm, Mecca, IN, upper 8.5 cm, Bed B

21. Mecca-type shale; Mecca Quarry mbr., stream near town cemetery, Velpen, IN, bed B, lowe 8 cm

18. Mecca-type shale; Logan Quarry mbr., Midway, IN, hard bed E of Zangerl and Richardson (1963)

61. Transitional shale; Oakley mbr. (Mecca-equivalent), Polk Co., IA, basal 7.5 cm of Iowa Geol. Survey core CP47

55. Heebner-type shale; shale in Verdigris Limestone (Mecca-equivalent), Randolph Co., Missouri Dept. of Nat. Res. core ORC19 (32 cm)

44. Heebner-type shale; Mecca Quarry mbr., Bill's Coal Mine, Bourbon Co., KS, 7.6 cm

79. Heebner-type shale; Hushpuckney mbr., roadcut, Unity Village, Jackson Co., Kansas City, MO, bottom 36 cm

80. Heebner-type shale; Stark mbr., roadcut, Unity Village, Jackson Co., Kansas City, MO, bottom 41 cm

HB5 Heebner-type shale; Heebner mbr., Clinton Lake dam spillway, Douglas Co., KS, 89 cm

QH1 Heebner-type shale; Queen Hill mbr., roadcut, Kansas Turnpike, Douglas Co., KS, 44 cm

SH1 Shanghai-type shale; Shanghai Creek mbr., roadcut, US-166, Chautauqua Co., KS, 22 cm

SH2 Shanghai-type shale; Shanghai Creek mbr., roadcut, US-166, Chautauqua Co., KS, 13 cm

data from Baltzer and Caveney (in press)

Depositional Regime

The origin of marine, organic-rich, and generally metal-rich, black shales is not understood fully and several models have been proposed for their formation. Wignall (1991) noted that in epicontinental basins, the problem of black shale origin is compounded by the lack of modern analogues. The Baltic Sea is a proposed analog for the Pennsylvanian Midcontinent and will be discussed in a later section. Black shales typically are confined to basin centers where bathymetric centers double as depocenters in which the greatest thicknesses of sediment collects (Wignall, 1991). Depths of black shale deposition on continental crust range from a few to hundreds of meters (Hallam, 1967).

The black shales of the Midcontinent Pennsylvanian are unquestionably extremely complex units in origin and difficult to explain with any simple, all-encompassing theory of deposition. However, several models seem to fit the pattern that is consistent with the results of this study. Four principal publications provide the framework for insight into the origin of these shales. Factors germane to this point include: sedimentation rate, organic matter quantity and type, sedimentary structures, sulfur isotope values, and most importantly, the timing of fixation of heavy metals in the black shales. Studies by Zangerl and Richardson (1963) on the Mecca Quarry Shale units, Heckel (1977) on the origin

of the phosphatic black shale facies in the Midcontinent Pennsylvanian, Brongersma-Sanders (1966, 1971) on the postulate of upwelling waters leading to phosphate development, and by Coveney et al. (1991) on a model for black shale deposition for Pennsylvanian black shales based on molybdenum abundances, are keys to the understanding of the origin for black shales in the Pennsylvanian Midcontinent.

Black Shale Models

Zangerl and Richardson (1963) proposed that Midcontinent black shales originated chiefly by rapid deposition, in a shallow-water marine setting. Near the water surface, Zangerl and Richardson (1963) envisioned a floating mat (or flotant) of algal materials that impeded wave action and added a tremendous quantity of organic-rich material to the underlying sediment. R. C. Moore envisioned this flotant in the Pennsylvanian Midcontinent as well. This notion fits well with the Middle Pennsylvanian (Desmoinesian) shales of Indiana, which have been proposed to have formed nearshore in a shallow-water environment. Additionally, the correlations between metal concentrations in these shales and seawater composition reported by Holland (1970) point towards a syngenetic deposition from seawater for these deposits.

An additional syngenetic model for development of metalliferous black shales in a marine setting was postulated by Brongersma-Sanders (1966, 1971) that involved phosphate and heavy metal-rich bottom waters upwelling to invade platforms beneath a thermocline. Heckel (1977) used this model to argue for a similar situation in the Midcontinent Pennsylvanian. Conodont correlations, phosphatic nodule and laminae development, and other paleontological and sedimentary criteria were used to support this argument.

Cannon and Force (1983) have invoked a "bath-tub ring model" for the deposition of manganese around the margins of basins with black shale development in their center. Because most black shales, including those in this study, are relatively low in manganese (Vine and Tourtelot, 1970), it seems that Mn has been lost. Unlike the Cannon and Force model, however, Mn has been lost even from nearshore shales, at least in the Mecca situation. However, similar to manganese deposits, phosphatic-rich units are to be expected at the margins of anoxic basins, and their proximity to a redox interface may be a focal point for the location of metal-rich deposits (Kucha, 1982). The location of such an interface is crucial in the understanding of ancient shorelines and paleogeographic reconstructions of units such as the metal-rich Midcontinent Pennsylvanian black shales.

Recently, Coveney et al. (1991) have proposed a model for metal-rich black shales of the Midcontinent that may

resolve the dichotomy between the offshore model of Heckel (1977) and the nearshore model of Zangerl and Richardson (1963). The Coveney et al. (1991) model has the advantage of explaining differing black shale types and points out that molybdenum abundances can be used to segregate nearshore and offshore black shale types. The model includes an accumulation of abundant peat debris from shallow acidic waters during the Desmoinesian (Middle Pennsylvanian). Black shales rich in Mo, V, Se, and U were deposited during this time adjacent to the ancient shoreline and characterized by association with deltaic siliciclastic deposits and coal swamps. Surface waters maintained pH values less than 6.0 and less than 5.0 in pore fluids. Offshore during this time, less organic material was present and waters were less acidic, thus metal enrichment (i.e., Mo, U, Se, and V) was lower offshore. Later, in the Late Pennsylvanian, climates became drier, vegetation production had declined, and slower rates of sedimentation were present. Uniform anoxic conditions prevailed, and deeper waters allowed upwelling which led to phosphatic-rich black shales that were less enriched in Mo, Se, V, and U (Coveney et al., 1991).

Problems associated with Zangerl and Richardson's (1963) model include their requirement for an extremely rapid deposition, which is difficult to accommodate assuming a syngenetic origin for the metals. They invoked a time-span of four years for the deposition of the Mecca Quarry

Shale, which is inconsistent with the high metal values determined for metal emplacement. A theory of longer deposition or post-depositional epigenetic accumulation of these units could alleviate this difficulty (Coveney and Glascock, 1989).

Upwelling waters are unlikely to have been associated with the nearshore Mecca Quarry Shale units in Indiana, as indicated by low PO_4, and water depth may have been too shallow for a thermocline to develop. A nearshore redox interface was probably present based on DOP. In addition to the vertical sequence, the nature of the organic matter present and the sulfur isotope variability point to a nearshore origin for the shallow-water Mecca Quarry Shale deposits.

Source for Metal Constituents

The concentration of elements scavenged from seawater into carbon-rich sediments can be used to monitor the geochemical behavior of the elements in the exogenic cycle (Holland, 1984). Holland (1984) suggests that the processes that control metal enrichment in carbonaceous sediments have not changed dramatically during the past 2 b.y. Thus, it is appropriate to compare changes in seawater chemistry with

metal constituents in metalliferous black shales and the operation of the exogenic cycle during the past 600 m.y.

The best-studied modern example of an anoxic basin is the Black Sea. But, because the Black Sea is a rather isolated body of water and communicates with the open ocean only via the Mediterranean Sea, the Dardanelles, the Sea of Marmara, and the Bosporus (Holland, 1984), it represents a poor analog of the Midcontinent Pennsylvanian. The Black Sea contains abnormally saline water near the Bosporus as a result of evaporation en route from the Atlantic Ocean. Additionally, the upper 200 meters of the Black Sea are oxygenated; oxygen is absent below this level and H_2S is present. Thus, organic matter is not destroyed as completely as in settings overlain by oxygenated water columns. A suggestion for a better modern analog for the Midcontinent Pennsylvanian is the Baltic Sea, where topography varies little, and euxinic sediments are present in isolated "pods". Other regions in the Baltic Sea are closely similar to the Midcontinent Pennsylvanian in terms of its anoxicity.

The enrichment of trace metals in black shales is variable in the oceans today (Holland, 1984). The variability is a result of biological removal processes in shallow waters, but the release of biologically sequestered metals during organic matter oxidation is the cause for variability in deeper waters (Holland, 1984). Therefore, release patterns differ from metal to metal and from basin to basin.

Table 21. Mean concentration of trace elements in seawater as calulated by Holland (1979). Other references as listed.

Mean concentration of trace elements in Sea Water (ug/kg)	
Element	Measurement Value
Ag	0.04 (1)
Cr	0.3 (1)
Au	0.08
Mo	10 (1)
Ni	0.6 (2)
V	2.5 (1)
Zn	3 (1)

(1) Brewer (1975)
(2) Sclater et al. (1976)

P50 Enrichment Factor = P50 (in ppm) / (Measurement Value * (100))
P95 Enrichment Factor = P95 (in ppm) / (Measurement Value * (100))

However, a few metals behave consistantly (i.e., Mo and U).

Holland (1979) compared the mean concentration of trace metals in seawater (Table 21) to various carbonaceous deposits. Using the same method, calculations were made on Shanghai-, Heebner-, and Mecca-type shales in this study (Table 22).

Based on the calculations, Shanghai-type samples were rather depleted in important trace metals, with the exception of Cr. Most elements plot well below the enrichment factor indicative of a depletion of these metals in the shale with respect to seawater (Figure 24). However, Cr plots near the enrichment factor indicating that Cr in the black shales may have originated from seawater.

Heebner-type black shales are depleted in Ag, Au, and Mo, but, similar to Shanghai-type shales, show an enrichment in Cr, and to a certain extent Zn. Cr, Zn, Ni, and V plot near the enrichment factor leading to the conclusion that these elements originated from seawater (Figure 25). However, Mo plots well below the enrichment factor leading to the conclusion that the relative deficiency of Mo in Heebner-type shales is a result of an inefficient extraction of Mo from seawater by the black shales, or that a lower Mo content in Midcontinent seawater existed at the time of deposition. Because Mo is readily absorbed by black shales (and organic matter) (Coveney and Glascock, 1989), the latter explanation is more probable.

Table 22. Summary of metal enrichment values for median and 95th percentile of 7 metals. Values are present for Shanghai-type, Heebner-type, and Mecca-type black shale samples in this study.

Shanghai-type				
Element	Highest median of 17 sets of black shale samples (in ppm)	Enrichment Factor ($\times 10^5$)	Highest 95th percentile of 17 sets of black shale samples (in ppm)	Enrichment Factor ($\times 10^5$)
Ag	0.3	0.08	0.5	0.13
Cr	380	12.7	590	19.7
Au	0.2	0.03	0.5	0.06
Mo	4	0.004	47	0.05
Ni	190	3.2	210	3.5
V	180	0.7	270	1.1
Zn	84	0.3	220	0.7

Heebner-type				
Element	Highest median of 15 sets of black shale samples (in ppm)	Enrichment Factor ($\times 10^5$)	Highest 95th percentile of 15 sets of black shale samples (in ppm)	Enrichment Factor ($\times 10^5$)
Ag	1	0.25	2	0.5
Cr	757	25.2	990	33
Au	0.005	0.0006	0.006	0.0008
Mo	76	0.08	200	0.2
Ni	270	4.5	460	7.7
V	1100	4.4	2400	9.6
Zn	1800	6	3400	11.3

Mecca-type				
Element	Highest median of 17 sets of black shale samples (in ppm)	Enrichment Factor ($\times 10^5$)	Highest 95th percentile of 17 sets of black shale samples (in ppm)	Enrichment Factor ($\times 10^5$)
Ag	4.3	1.1	8.8	2.2
Cr	366	12.2	564	18.8
Au	0.003	0.0004	0.004	0.0005
Mo	1023	1.02	2016	2.02
Ni	300	5	505	8.42
V	1799	7.2	2941	11.8
Zn	860	2.9	2868	9.6

Figure 24. Plot of concentration in seawater (ppb) versus concentration in shale (ppm) for Shanghai-type black shale samples. Note the relative depletion in most metals and the position of Cr and Zn relative to the enrichment factor, indicating that Cr and Zn may have originated from seawater.

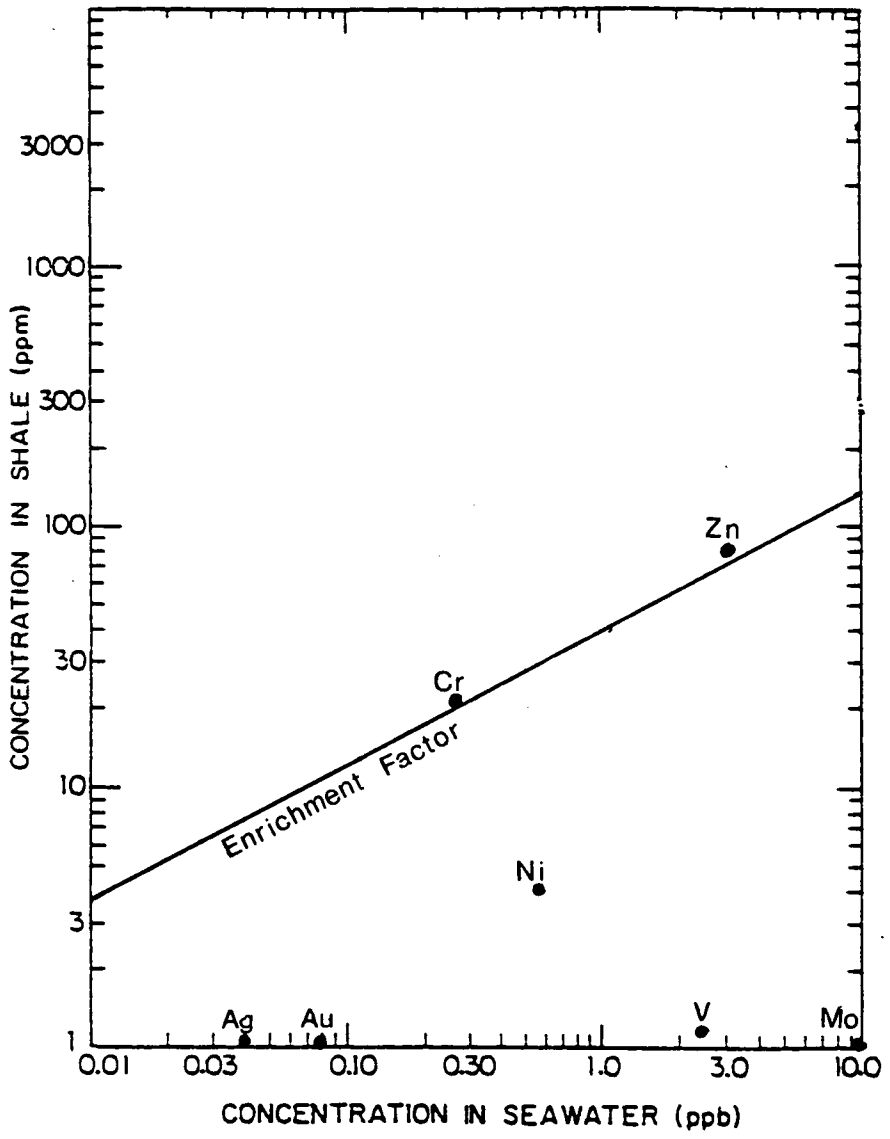
3000
1000
300
100
30
10
3
1
CONCENTRATION IN SHALE (ppm)
Zn
Cr
Enrichment Factor
Ni
Ag
Au
V
Mo
0.01
0.03
0.10
0.30
1.0
3.0
10.0
CONCENTRATION IN SEAWATER (ppb)

Figure 25. Plot of concentration in seawater (ppb) versus concentration in shale (ppm) for Heebner-type black shale samples. Note the relative depletion in Mo, Ag, and Au, but the close proximity of Ni, Cr, Zn, and V to the enrichment factor indicating that these metals may have originated from seawater.

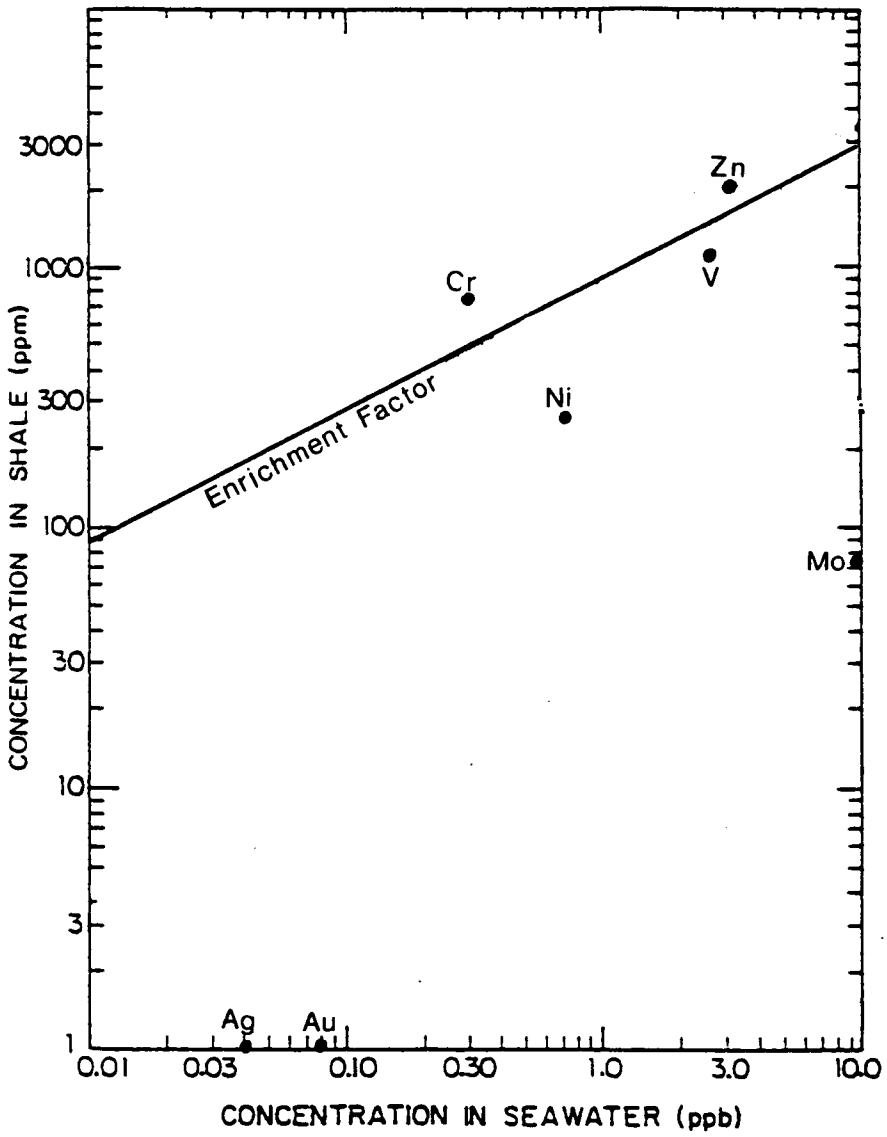
3000
1000
300
100
30
10
3
1
CONCENTRATION IN SHALE (ppm)
Zn
V
Cr
Ni
Mo
Enrichment Factor
Ag
Au
0.01
0.03
0.10
0.30
1.0
3.0
10.0
CONCENTRATION IN SEAWATER (ppb)

Mecca-type shales are enriched in Ni, Cr, V, Zn, and Mo, but depleted in Au and Ag. Origin of the metals is likely to have been via a complex interaction of shale with seawater, connate waters, meteoric fluids, and basinal brines (Coveney and Glascock, 1989). It would indeed be unlikely that enrichment in metals occurred from seawater alone, based on the calculations of Allen (1986). Additionally, it would be even more unlikely that deposition of the Mecca Quarry Shale occurred in a 4 year interval as proposed by Zangerl and Richardson (1963). An incredible change in seawater chemistry would have to have occurred for this to happen. Figure 26 depicts a plot of the relative enrichment of metals in Mecca-type black shales in this study.

Pennsylvanian black shales, at various stages between their deposition and today, have been in contact with essentially three types of genetically distinct fluids (Coveney and Glascock, 1989). These fluids include: brackish seawater, basinal brines, and recent groundwater (Coveney and Glascock, 1989), although the proposed "deeper water" Heebner-type black shales were in contact with normal seawater as well. Each of these three types of fluids may have had the opportunity to add or remove metals from the black shales (Coveney and Glascock, 1989). A summary of the complexity of determining black shale metal origins is contained in Vine and Tourtelot (1970) in which they proclaim that enrichment of metals is cumulative where organic

Figure 26. Plot of concentration in seawater (ppb) versus concentration in shales (ppm) for Mecca-type black shales. Note the abundance of Ni, Cr, V, Zn, and Mo in terms of enrichment.

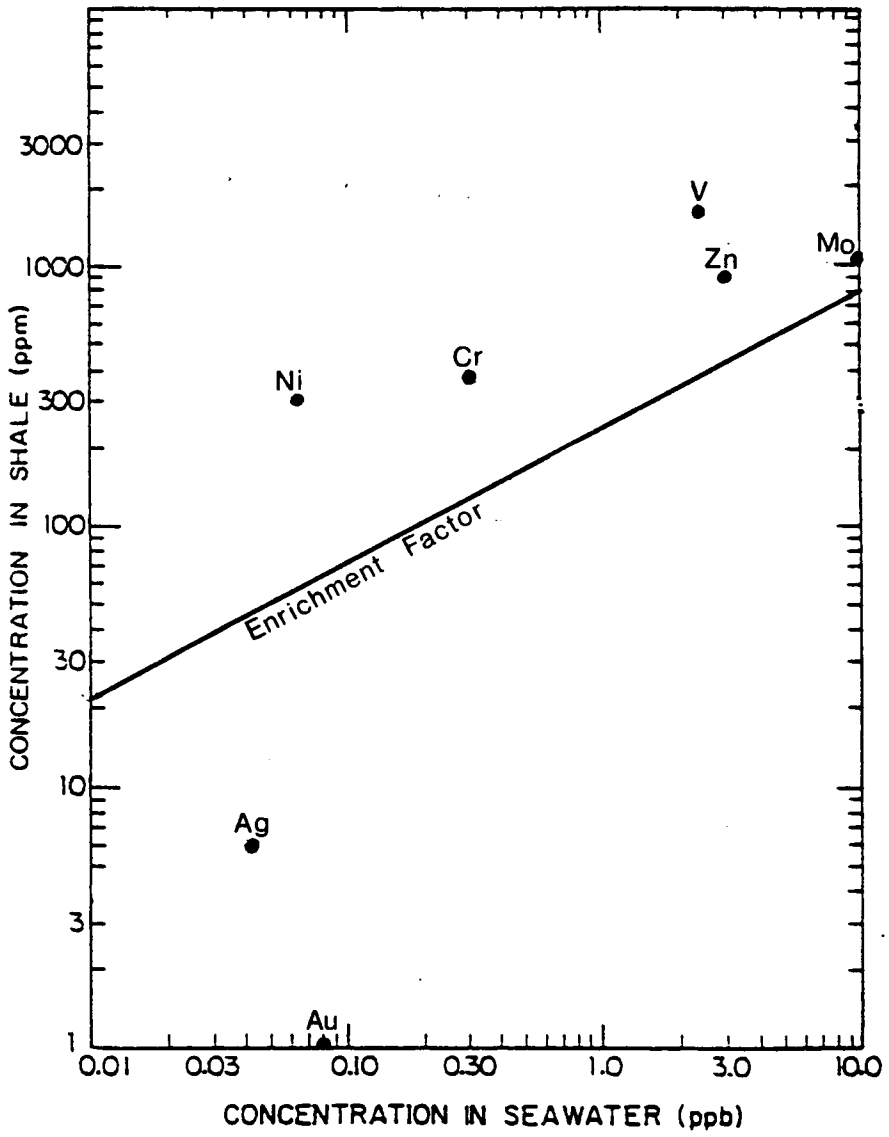
3000
1000
300
100
30
10
3
1
V
Zn
Mo
Cr
Ni
Ag
Au
Enrichment Factor
0.01
0.03
0.10
0.30
1.0
3.0
10.0
CONCENTRATION IN SHALE (ppm)
CONCENTRATION IN SEAWATER (ppb)

matter plays an important role in absorbing metals from solutions in contact with it all throughout diagenesis. They add, however, that the timing of the main period of this sorption process is difficult to pinpoint, but that the late addition of metals is likely, as pointed out by Coveney and Goebel (1985). Such addition could occur from warm, migrating formational waters known to have flowed through Midwestern basins (Coveney and Goebel, 1985). Considering the lateral persistence of the black shale units and the differences in depositional settings across the Midcontinent, United States, it is highly likely that the metals within the black shales have a complex origin.

From this study, it seems likely that, based on the lateral heterogeneity of the black shales in terms of metal enrichment, Midcontinent metal-rich black shales were enriched in metals in several stages, including contact with metal-enriched basinal brines at various localities. The high molybdenum content in Mecca-type shales near Mecca, Indiana ensued as a result of acidic conditions in response to nearby swamp drainage. Thus, metals were probably fixed syngenetically during early diagenesis. Temporal and spatial relations suggest that the possibility exists such that sphalerite in some shales was enriched during the early stages of deposition as well. Further work on fluid inclusions would be helpful in determining the time and temperature of sphalerite emplacement. Coveney et al. (1987) imply

that Mecca-type metal enrichments formed as a result of a complex interaction between shale constituents and seawater, connate fluids, basinal brines, and meteoric waters, and rule out supergene enrichment because of "ambiguous timing". However, despite timing ambiguities, metal associations between molybdenum and pyrite in Mecca-type samples suggest a possible role for supergene enrichment, although unlikely. Thus, a model for syngenetic metal emplacement and later basinal brine involvement is invoked here for the fixation of metals in Mecca-type shales.

A further observation in this study is the correlation of DOP with metal enrichment. DOP or degree of anoxicity in a given area plays an insignificant role until it reaches approximately 0.60-0.70. This is the approximate boundary defined by Raiswell et al. (1988) between dysaerobic and inhospitable bottom-water oxygenation conditions. In order for metal enrichment to occur in a black shale, not only do favorable depositional conditions have to be present, but significant quantities of metals, perhaps more than can be supplied by seawater, must be available to be absorbed by abundant organic material. This may not apply to all regions; the Henryville Bed of the New Albany Shale is a counterexample. However, in the Midcontinent Pennsylvanian, conditions favorable for metal enrichment are a semieuxinic to euxinic basinal setting (DOP values between 0.70 and 1.00) (Figure 27), presence of available metal constituents

Figure 27. Plot of DOP values for all samples in this study. Mecca-type samples have DOP values that range from approximately 0.60 to 0.90, and possess the greatest enrichment of metals. Heebner-type samples have DOP values that range from approximately 0.20 to 0.70 and possess a moderate enrichment of metals in comparison with Mecca-type samples. Shanghai-type samples contain DOP values ranging from 0.10 to 0.40 and possess the least enrihment values in terms of metal abundance as compared with other black shale types.

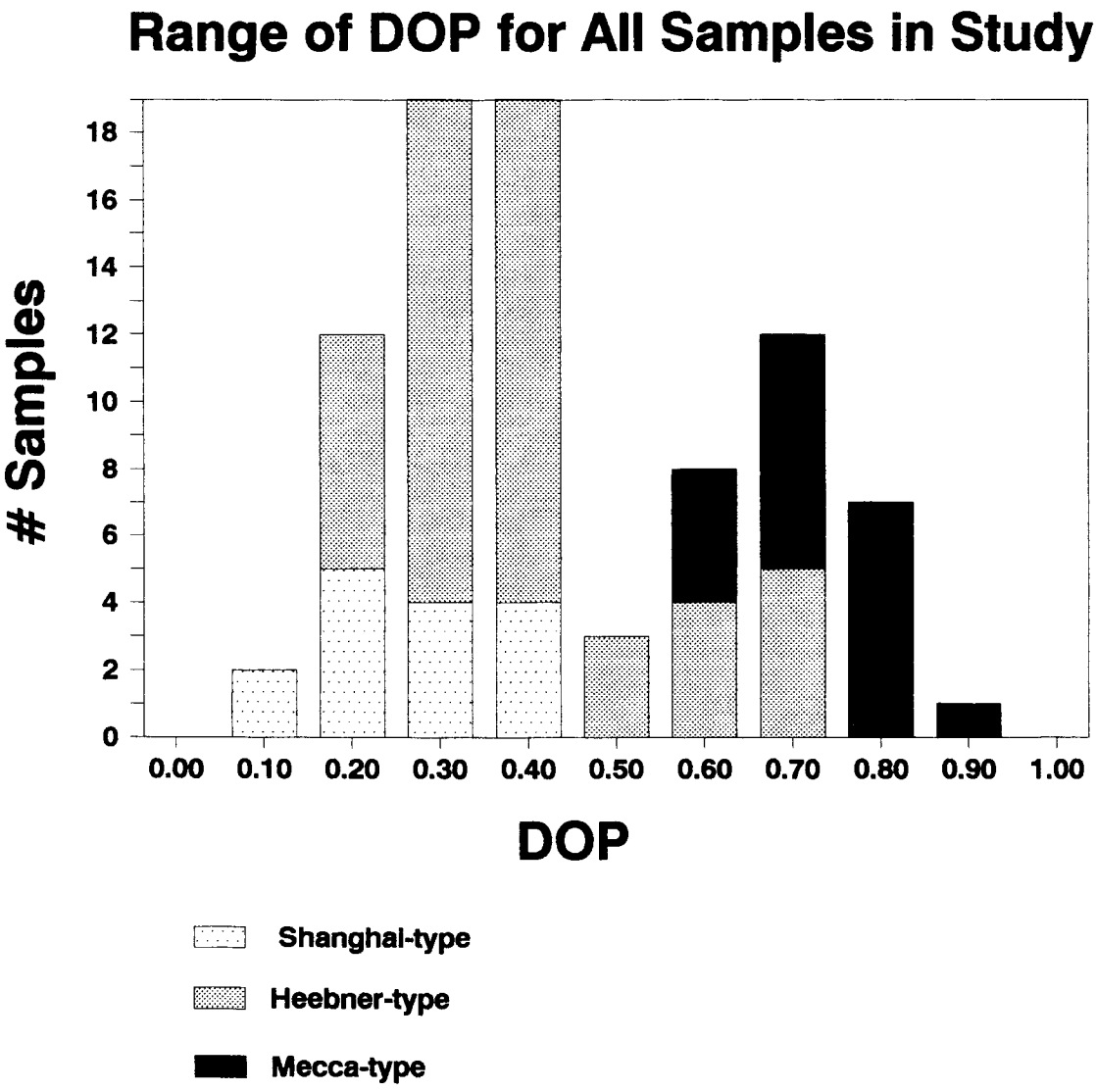
Range of DOP for All Samples in Study
Samples
18
16
14
12
10
8
6
4
2
0
0.00
0.10
0.20
0.30
0.40
0.50
0.60
0.70
0.80
0.90
1.00
DOP
Shanghai-type
Heebner-type
Mecca-type

in proximity to low pH swamps, and ample organic matter to absorb the metals. Phosphatic nodules and laminae provide a good sink for several elements (i.e., REE) in Heebner-type black shales and framboidal pyrite hosts Mo in Mecca-type shales (Coveney and Glascock, 1989).

Proposed Black Shale Model

At times of maximum transgression during the Pennsylvanian, epeiric seas covered the Midcontinent. The seas repeatedly transgressed and regressed over the region, inundating Midcontinent peat swamps and depositing organic-rich metalliferous black shales. Desmoinesian shales, such as the Mecca Quarry Shale Member, Holland Shale Member, and Logan Quarry Shale Member of this study, were deposited in nearshore settings as indicated by their spatial orientation to deltaic sequences (Baird et al., 1985) and tremendous quantity of terrestrial organic constituents derived from peat swamps and storm events (Coveney et al., 1991). Humic-type organic matter was dispersed by freshwater plumes migrating seaward above a halocline (Coveney et al., 1987). Normal seawater concentrated by a nutrient trap (Heckel, 1977) may have provided abundant phosphatic material (in the form of nodules and laminae in western exposures) and some metals for the sediment precursors of the Pennsylvanian

black shales (i.e., Heebner-type black shale units). Much phosphatic material however, may have originated from plant debris as suggested by Coveney et al. (1991).

In closer proximity to the shore, peat swamp effluents induced a brackish, acidic condition reflected in the presence of marcasite (Reynolds and Goldhaber, 1983). The pH conditions in this area at this time would have approached 5.0 or below (Murrowchick and Barnes, 1986). Farther west, where conditions were less acidic and less organic matter was present, smaller amounts of metals were fixed in the black shales, with the exception of Zn and U, which remained relatively enriched because of slightly reducing conditions.

Thus, based on fluctuations of geochemical parameters as discussed in this study, black shales of the Midcontinent Pennsylvanian show a change in character through the Middle (Desmoinesian) to Late (Virgilian) Pennsylvanian (Figure 28) that can be summed up in the following series of Pennsylvanian geologic and geochemical events:

Figure 28. Plots of various geochemical parameters in Midcontinent Pennsylvanian black shales as changes occur from Middle to Late Pennsylvanian. Metals decrease with time, DOP reflects a sharp increase in bottom-water oxygenation conditions with time, and TOC (amount of total organic carbon) decreases with time. HI represents the hydrogen index (grams of pyrolized hydrocarbons divided by the weight percent of TOC). Rock-Eval data from Coveney et al. (1987), Schultz (1990), and Schultz and Coveney (in press).

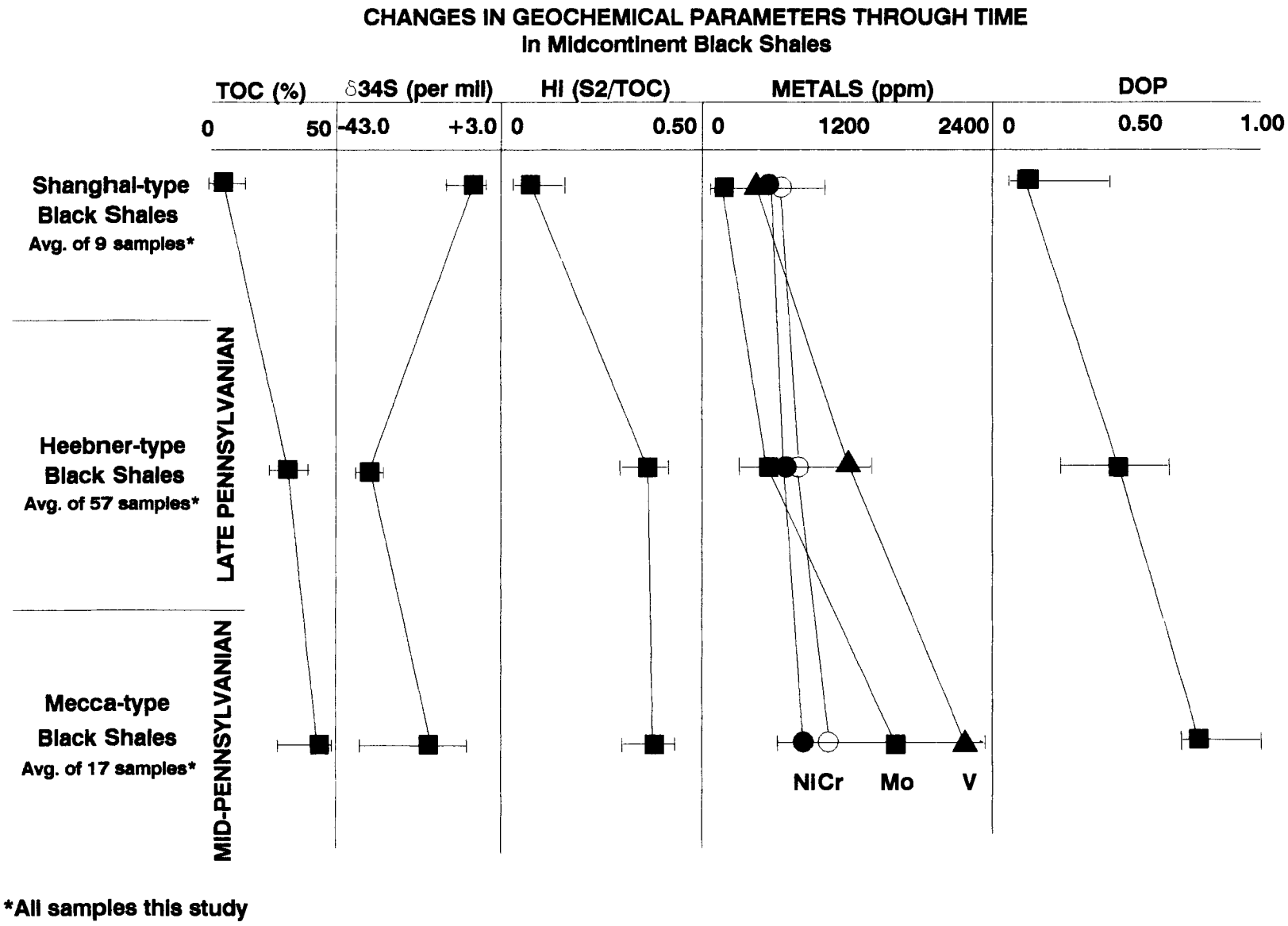

*All samples this study

1. Desmoinesian black shales were deposited in relatively shallow water over extensive peat swamps which accommodated abundant organic matter. Variations in Eh and pH caused geochemical fluctuations nearshore where a redox interface existed between anoxic bottom-waters and oxygen-rich surface waters. Molybdenum abundances were elevated in these deposits at this time as a result of swamp drainage. Black shales that developed from organic-rich muds reflect repeated contact of organic matter with molybdenum-rich fluids. Offshore, in somewhat deeper water, Heebner-type shales were deposited, with moderately high DOP values and metal values.

2. The maximum depths of successive epeiric seas increased with time such that Missourian (Upper Pennsylvanian) seas were deeper than Desmoinesian (Middle Pennsylvanian) seas. A uniform geochemical condition existed offshore during the Missourian so that Heebner-type shales were deposited more slowly and in deeper waters (Coveney and Glascock, 1989). Metal values and DOP values are moderate in these Missourian units compared to Desmoinesian sequences.

3. A progressive ventilation or opening of the system during the Virgilian provided for the continuance towards lower DOP values and a decline in metal contents with time.

Based on results from this study and a compilation of other factors from published work, it is postulated that Mecca-type shales were deposited in a nearshore, shallow water setting where accumulations of organic material in proximity to to redox interface prompted the deposition of high quantities of metals (i.e., Mo, Se, U, and V). Heebner-type shales were deposited in an offshore setting, during maximum transgression, in relatively deep waters with a slow rate of deposition. Upwelling may have provided for the accumulation of phosphate nodules and laminae in these deposits.

Chapter 7. Comparison of Midcontinent to Other Areas

Several well-studied black shale units stand out as being particularly metal-rich and thus form a comparison to the metalliferous Mecca Quarry Shale (Desmoinesian) and semimetalliferous Upper Pennsylvanian black shales of Midcontinent North America (Schultz, 1991). Among the well-studied units are the Alum Shale of Scandinavia, New Albany Shale of Indiana, and several Cambrian Chinese black shale units. These units are important mainly because of their enrichment in U, V, Mo, Pb, Cu, Ni, and Zn contents.

Alum Shale

The Alum Shale and its lateral equivalents are marine black shales, Middle to Late Cambrian and Ordovician in age, that are famous for their high carbon and uranium content. For the most part, its outcrop is confined to Scandinavia and was deposited on stable continental basement (Thickpenny and Leggett, 1987). The present-day outcrop probably represents much of the original depositional area, but some Alum Shale equivalents have been thrust eastward, implying an original basinal extension west of the present-day Norwegian coast. Sediment thickness is approximately 10-20 meters, although exposures of complete sections are relatively rare, especially to the east (Thickpenny and Leggett, 1987).

Mudstones rich in organic matter (~20% TOC) are the dominant lithotype with some intermittent concretionary carbonates (Thickpenny and Leggett, 1987). Local beds of white, kerogen-free, biocalcarenite are present that are perhaps storm deposits (Bergstrom, 1980). Thus, deposition was below normal wave base, but in water shallow enough for the bottom to be stirred by major storms. The Alum Shale overlies an areally restricted clastic sequence thought to have been deposited in a rift basin (Bjorlykke and Englund, 1979), so that the Alum, which covers a wider area and lies directly on basement in many sections, may represent the first stage of basin fill in a cratonic interior basin successor to a rift.

Chemistry of the Alum Shale has been described by Armands (1972), Andersson et al.(1983), and by Lewan and Buchardt (1989). Uranium concentration is usually in excess of 100 ppm, and may reach 400 ppm in the richest strata. As with other metalliferous shales, a number of other metals are present in anomalously high concentrations. Total organic carbon (TOC) is also high, approaching 20 percent in many of the samples (Lewan and Buchardt, 1989). The high metal values may be related to the slow rate of deposition; Bjorlykke and Englund (1979) calculated the rate to be as low as 1 mm/1000 yrs.

New Albany Shale

The New Albany Shale of Indiana, U.S., is late Devonian-early Mississippian in age and is a portion of an extensive sequence of organic-rich shales within the Illinois, Appalachian, and Michigan Basins. The New Albany outcrop occupies a semicontinuous arcuate band from west-central Indiana to south-central Kentucky. Underlying and overlying sequences imply a stable, cratonic-interior setting with epeiric seas. Lithology of the shale sequences alternates between well-laminated black shales and poorly laminated gray shales, differences that apparently result from changes in the position of the redox interface in the water column (Ettensohn and Elam, 1985), possibly related to sea-level changes. These shale units differ considerably in thickness ranging from 15-125 meters (Hasenmueller et al., 1983).

Beier and Hayes (1989) have documented two types of black shale within the New Albany sequence. The first type has TOC values of 5 to 6 percent, with S about 2 percent, and a good correlation between C and S, passing through the origin in a C vs. S plot. The second type has TOC at 10 to 15 percent, S at 2 to 6 percent, and a poor correlation between the two. Sulfur isotopes are lighter in the second type, with values as low as -40 per mil, suggestive of syngenetic sulfate reduction within the water column. DOP averages about 0.55 in the first type, 0.75 in the second,

confirming a more anoxic environment for the deposition of the more carbon-rich shales.

Although metal enrichment in the sequence coincides with high-organic content, the presence of organic matter does not necessarily signify metal enrichment. In the New Albany, the most metal-rich shale occurs at the top of the Formation in the Henryville Bed, which is rich in organic matter, but the underlying Clegg Creek Member possesses TOC values of 10-15 percent, and lacks significant metal enrichment (Shaffer and Chen, 1981). Other units within the shale sequence that are high in TOC similarly lack metal enrichment, including all those in the Appalachian Basin, where the rate of deposition seems to have been greater than in the Illinois Basin (Maynard, 1980). Thus, it is clear, as stated previously by Tourtelot (1979), that some process beyond organic matter accumulation must operate in order for a metalliferous sediment to result.

Enriched metal values in the Henryville Bed as reported by Shaffer et al. (1983), include Cu (1700 ppm), Mo (535 ppm), Ni (837 ppm), Pb (835 ppm), and V (4455 ppm). One sample of the Henryville Bed contained Pb concentrations in excess of 9000 ppm. TOC values averaged about 24 percent in the samples studied.

Chinese Black Shales

Lower Cambrian black shales are distributed widely in southern China and are associated with argillaceous and siliceous rocks (Fan Delian, 1983). The shales are rich in organic matter and sulfides, and are black. Black shale units include mudstones, black argillaceous siliceous rocks, black cherts, and siltstones, with TOC values ranging from about 5 to 15 percent (Fan Delian, 1983). The units range from 40 to 50 meters in thickness and in places are associated with manganese carbonate beds (Fan Delian, 1989). It is thought that the various black shales series of China reflect a euxinic environment associated with possibly volcanic-sourced Mn and Ba (Fan Delian, 1989; Wang Zhongcheng and Li Guizhi, in press).

Metal enrichment values reported by Fan Delian (1983) and Coveney and Nansheng (1989) include the black shale host and thin, cm-scale bands of "polyelement" sulfide mineralization with up to 7 percent Mo, 4 percent Ni, 2 percent Zn, and nearly 1 ppm Au. Fan Delian (1983) suggested that submarine hot springs related to basement faulting contributed metals to the water column during deposition of the sediment. Coveney and Nansheng (1989), however, suggested a nonsyngenetic component to the mineralization based on sulfur isotope values being heavier in the more metal-rich portion of the samples.

For the most part, the Alum Shale, New Albany Shale, and Chinese Black Shales were deposited on stable continental platforms, far from active plate margins. The Chinese black shales are a possible exception, but problems concerning their tectonic setting setting are far from resolved. All of the shales seem to have been deposited in relatively quiet water, below clear-weather wave base. Additionally, all are associated with high values of TOC (Table 23), but similar organic-rich beds in the same section may lack metal-enrichment. In comparison with the Midcontinent Pennsylvanian black shales of this study, it seems likely that the degree of anoxia, as reflected in the DOP value, is an important control. An additional factor of importance may be the rate of deposition, with slow sedimentation in a stable setting favoring extraction of metals from fluids.

Table 23. Summary of various geochemical parameters in metalliferous black shales around the world (from Schultz, 1991).

Concentrations of some metals of economic interest in metalliferous black shales*						
Shale:	Alum	New Albany	Chinese	Mecca	Heebner	Shanghai
Ag		9.00	1.00	7.00	1.00	0.50
Au	0.01			0.00	0.00	0.00
Ba	110.00	450.00	1520.00	300.00	320.00	140.00
Co	25.00	244.00	9.00	23.00	17.00	20.00
Cu	110.00	236.00	187.00		56.00	15.00
Mo	340.00	793.00	160.00	1400.00	44.00	5.00
Ni	200.00	1050.00	160.00	530.00	130.00	37.00
Pb	14.00	972.00	12.00		82.00	4.00
U	300.00			165.00	12.00	2.00
V	750.00	4920.00	417.00	2850.00	190.00	63.00
Zn	130.00	9200.00		3350.00	100.00	36.00
DOP	0.78	0.94		0.82	0.70	0.34
Corg	15.50	21.80		39.70	3.80	0.30
St	7.00	2.80		3.30	1.90	0.60

Corg=organic carbon

St=total sulfur

*values in ppm except for Corg and St, in %

Sources:

Alum: Andersson et al. (1983)

New Albany: Ripley et al (in press), DOP from Schultz (in progress)

Cambrian shales of China: Fan Delian (1983)

Mecca Quarry Shale: Coveney and Glascock (1989)

Upper Pennsylvanian black shales: Schultz (1990)

Chapter 8. Summary and Conclusions

The study of black shales has been difficult and usually with ambiguous results until recently. Theories of black shale origin have been limited to the simple explanation that organic-rich deposits formed in euxinic settings (anoxic, H_2S-containing) under reducing conditions. Recently, geochemistry has played an important role in understanding the behavior of both organic and inorganic constituents, widening the scope of inferences drawn on these enigmatic units.

This study of the Midcontinent Pennsylvanian black shales has strived to present new geochemical data for the deposits. Included in this study are data for separate species (organic C, acid-soluble Fe, and pyritic S), whole-rock X-ray fluorescence (XRF) of major oxides, values for degree of pyritization (DOP) (important for the paleoenvironmental determination of inferred bottom-water oxygenation conditions), X-ray diffraction data (XRD) characterizing the clay mineralogy of the black shales, instrumental neutron activation analyses (INAA) providing a quantitative assessment of metal enrichment, sulfur isotope data, and a statistical analysis including correlation coefficient matrices for black shale groups, a stepwise regression analysis, a discriminant function and canonical function analysis, a cluster analysis, and a principal components analysis to characterize further the black shale types in the Midconti-

nent Pennsylvanian.

Conclusions of this study are:

1. Desmoinesian black shales were deposited in relatively shallow water when extensive peat swamps accommodated abundant organic matter. Variations in Eh and pH caused geochemical fluctuations nearshore where a redox interface existed between anoxic bottom-waters and oxygen-rich surface waters. Offshore, in somewhat deeper water, Heebner-type shales (i.e, Stark Shale Member), with relatively high DOP values and metal values, were deposited (Figure 29).

2. The maximum depths of successive epeiric seas increased with time such that Missourian (Upper Pennsylvanian) seas were deeper than Desmoinesian (Middle Pennsylvanian) seas. A uniform geochemical condition existed offshore during the Missourian so that Missourian Heebner-type shales were deposited more slowly and in deeper waters (Coveney, 1989). Metal values and DOP values are moderate in these Missourian units compared to Desmoinesian sequences.

3. A progressive ventilation or opening of the system during the Virgilian provided for the continuance towards lower DOP values and a decline in metal contents. Sediment supply was either decreasing or was diverted elsewhere during this time interval.

Figure 29. Model for Midcontinent Pennsylvanian black shale formation. Note the presence of PO_4-rich zone where upwelling may occur, and the presence of organic input from above the thermocline. Anoxic-oxic differentiation is gradual.

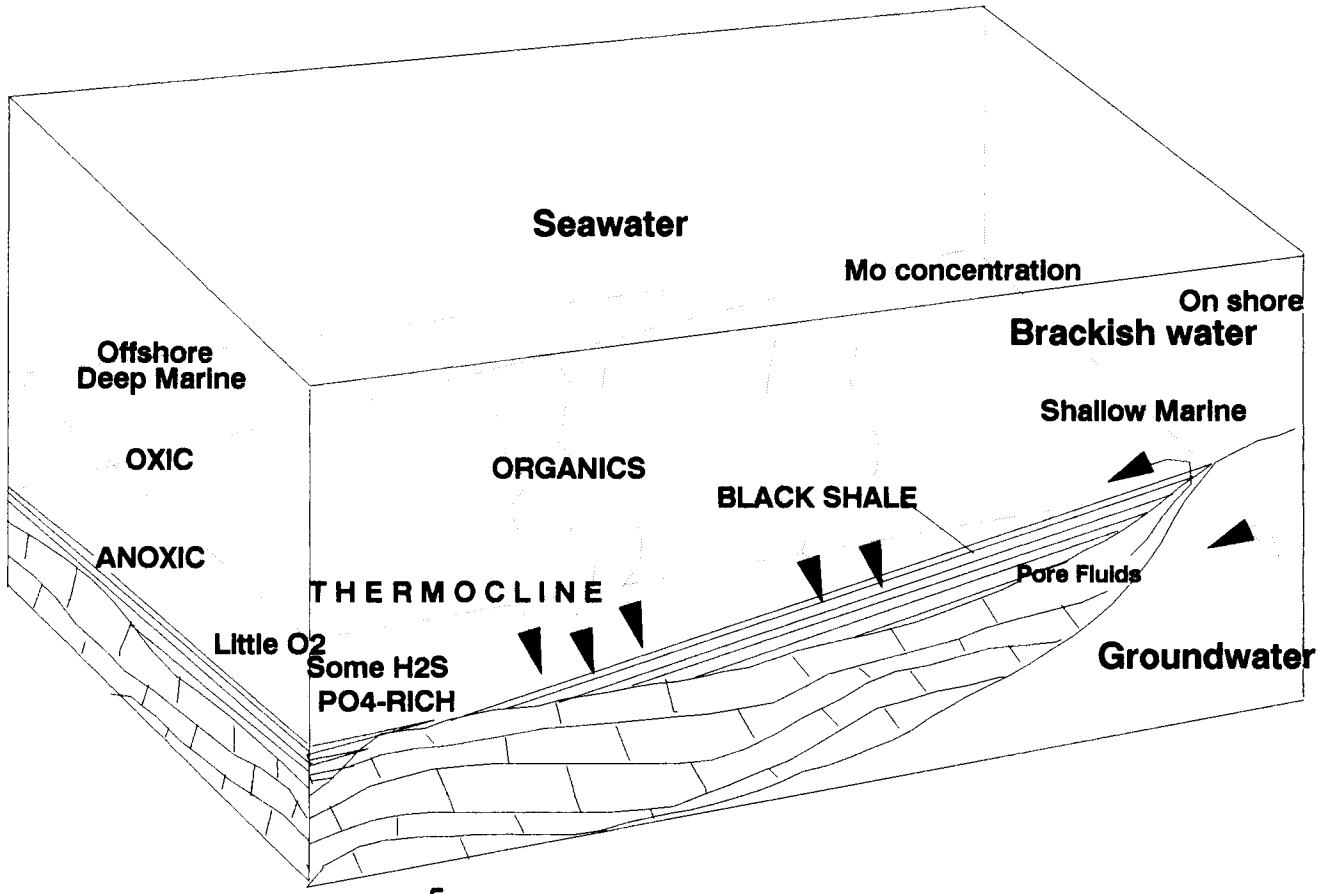

Model for Midcontinent Pennsylvanian Black Shale Formation

4. Midcontinent black shales can be separated into at least two and possibly three major types based on geochemical and sedimentological parameters. A statistical analysis indicates that nearly 94% of black shales can be classified "correctly" according to the procedures outlined in this study.

5. Mecca-type black shales are characterized by greater than 20% TOC (mostly terrestrial-type), high metal contents (especially V, Cr, Ni, Mo, U, and Sn), erratic and heavy $\delta^{34}S$ values, high DOP values, and an association with underlying coals and siliciclastics.

6. Heebner-type black shales are characterized by less than 20% TOC (mostly marine-type and phosphatic, although somewhat mixed), moderate metal contents, light, stable ^{34}S values, moderate DOP values, and an association with phosphatic nodules at the base of the unit. A sedimentary association with siliciclastics (Missourian) and carbonates (Virgilian) also is evident.

7. Shanghai-type deposits are characterized by less than 15% TOC (mostly mixed terrestrial and marine types), low metal contents, erratic and heavy $\delta^{34}S$ values, low DOP values, and a mostly phosphatic fauna.

8. Metal constituents in the Mecca-type shales developed in response to repeated contact of black shales and organic matter with various types of fluids: brackish seawater, basinal brines, and modern groundwater. It is probable that a redox interface existed such that metals present in fluids were attracted to the nearshore organic matter in Mecca-type (Desmoinesian) shales.

9. A geochemical and tectonic comparison can be made between the Pennsylvanian Midcontinent black shales and other well-studied black shales, including: the Alum Shale of Scandinavia, the New Albany Shale of Indiana, and various metal-rich Chinese shales of Cambrian age. The black shales were, so far as can be determined from the literature, deposited on stable continental platforms. All were deposited in quiet water below clear-weather wave base, and are associated with high values of TOC, although similar organic-rich beds in the same section may lack metal enrichment. The degree of anoxia seems to be an important control for the black shale metal extraction, supplemented by a slow rate of sedimentation in a stable setting.

10. A model for time-dependent changes of Midcontinent Pennsylvanian black shales is offered that shows a progressive ventilation from the Desmoinesian through the

Virgilian in the Midcontinent such that metal supplies, DOP values, and TOC contents decrease with time.

11. Conditions favorable for metal enrichment in Pennsylvanian black shales are: a semieuxinic to euxinic basinal setting, DOP values between 0.70 and 1.00, the presence of available metals, ample organic matter to absorb the metals, and a predominance of quiscence to promote metal fixation. Phosphatic nodules and laminae in Heebner-type black shales provide a source for elements (i.e., REE), whereas pyrite framboids provide a host for Mo coatings in Mecca-type black shales.

REFERENCES CITED

Allen, A. V., 1986, Geochemistry of the Mecca Quarry Shale and Colchester Coal, Linton Formation (Middle Pennsylvanian) in Parke and Vermillion counties, Indiana: Unpubl. Masters thesis, Univ. of Missouri-Kansas City, 79 p.

Andersson, A., Dahlman, B., and Gee, D. G., 1983, Kerogen and uranium resources in the Cambrian Alum Shales of the Billingen-Falbygden and Narke areas, Sweden: Geologiska Foren. Forhand., v. 104, p. 197-209.

Armands, G., 1972, Geochemical studies of uranium, molybdenum, and vanadium in the Swedish Alum Shale: Stockholm Contributions Geol., v. 22, p. 1-148.

Baird, G. C., Shabica, C. W., Anderson, J. L., and Richardson, E. S., Jr., 1985, Biota of a Pennsylvanian muddy coast: habitats within the Mazonian delta complex, northeast Illinois: Journ. Paleo., v. 59, p. 253-281.

Barker, C., 1974, Pyrolysis techniques for source-rock evaluation: Amer. Assoc. Petrol. Geol. Bull., v. 58, p. 2294-2361.

Beier, J. A., and Hayes, J. M., 1989, Geochemical and isotopic evidence for paleoredox conditions during deposition of the Devonian-Mississippian New Albany Shale, southern Indiana: Geol. Soc. America Bull., v. 101, p. 774-782.

Bein, A., Almogi-Labin, A., and Sass, E., 1990, Sulfur sinks and organic carbon in Cretaceous organic-rich carbonates: implications for evaluation of oxygen-poor depositional environments: Amer. Journ. Sci., v. 290, p. 882-911.

Bergstrom, J., 1980, Middle and Upper Cambrian biostratigraphy and sedimentation in south-central Jamtland, Sweden: Geoligiska Freningens Frhandlingar, v. 102, p. 373-376.

Berner, R. A., 1970, Sedimentary pyrite formation: Amer. Journ. Sci., v. 268, p. 1-23.

Berner R. A., 1971, Principles of chemical sedimentology: New York, McGraw-Hill Book Co., 240 p.

Berner, R. A., 1984, Sedimentary pyrite formation: an update: Geochim. et Cosmochim. Acta, v. 48, p. 605-615.

Berner, R. A., 1987, Models for carbon and sulfur cycles and atmospheric oxygen: application to Paleozoic geologic history: Amer. Journ. Sci., v. 287, p. 177-196.

Berner, R. A., and Raiswell, R., 1983, Burial of organic carbon and pyrite sulfur in sediments over Phanerozoic time: a new theory: Geochim. et Cosmochim. Acta: v. 47, p. 855-862.

Berner, R. A., and Raiswell, R., 1984, C/S method for distinguishing freshwater from marine sedimentary rocks: Geology, v. 12, p. 365-368.

Bjorlykke, K., and Englund, J. O., 1979, Geochemical response to Upper Precambrian rift basin sedimentation and Lower Paleozoic epicontinental sedimentation in south Norway: Chem. Geology, v. 27, p. 271-295.

Boardman, D. R., and Heckel, P. H., 1989, Glacial-eustatic sea-level curve for early Upper Pennsylvanian sequence in north-central Texas and biostratigraphic correlation with curve for midcontinent North America: Geology, v. 17, p. 802-805.

Brewer, P. G., 1975, Minor elements in seawater, in Riley, J. P., and Skirrow, G., eds., Chemical oceanography, 2nd ed., New York, Academic Press, p. 415-496.

Brongersma-Sanders,, M., 1969, Origin of trace metal enrichment in bituminous shales in Hobson, G. D., and Speers, C. C., eds., Advances in organic geochemistry, Third International Congress Proceedings: Oxford, Pergamon Press, p. 231-236.

Brongersma-Sanders, M., 1971, Origin of major cyclicity of evaporites and bituminous rocks: an actualistic model: Marine Geology, v. 11, p. 123-144.

Bulman, O. M. D., 1955, Graptolithinia, Part V, in Moore, R. C., ed., Treatise on Invertebrate Paleontology: Lawrence, Kansas, Geological Society of America and University of Kansas Press, p. V3-V109.

Byers, C. W., 1977, Biofacies patterns in euxinic basins: a general model: Soc. Econ. Paleontol. and Mineral., Special Publication 25, p. 5-17.

Canfield, D. E., 1988, Sulfate reduction and diagenesis of iron in anoxic marine sediments: un publ. Ph.D. dissertation, Yale Univ.

Canfield, D. E., 1989, Reactive iron in marine sediments: Geochim. et Cosmochim. Acta: v. 53, p. 619-632.

Canfield, D. E., Raiswell, R., Westrich, J. T., Reaves, C. M., and Berner, R. A., 1986, The use of chromium reduction in the analysis of reduced inorganic sulfur in sediments and shales: Chem. Geol., v. 54, p. 149-155.

Cannon. W. F., and Force, E. R., 1983, Potential for high-grade shallow-marine manganese deposits in North America, in Shanks, W. C., III, ed., Cameron volume on unconventional mineral deposits: New York, Society of Econ. Geol. and Society of Mining Engineers, p. 175-189.

Chesworth, W., 1973, The residua system of chemical weathering: a model for the chemical breakdown of silica rocks at the surface of the earth: Journ. Soil Sci., v. 24, p. 69.

Claypool, G. E., and Read, P. R., 1976, Thermal analysis technique for source-rock evaluation: quantitative estimate of organic richness and effects of lithologic variation: Amer. Assoc. Petrol. Geol. Bull., v. 60, p. 608-612.

Coryell, C. G., Chase, J. W., and Winchester, J. W., 1963, A procedure for geochemical interpretation of terrestrial rare-earth abundance patterns: Journ. Geophys. Res., v. 68, p. 559-566.

Coveney, R. M., Jr., and Goebel., E. D., 1985, Fluid inclusions in midcontinent country rocks: [abst.]: Geol. Soc. of Amer. Abstr. with Prog., v. 17, p. 154-155.

Coveney, R., M., Jr., Leventhal, J. S., Glascock, M. D., and Hatch, J. R., 1987, Origins of metals and organic matter in the Mecca Quarry Shale Member and stratigraphically equivalent beds across the Midwest: Econ. Geol., v. 82, p. 915-933.

Coveney, R. M., Jr., and Shaffer, N. R., 1988, Sulfur isotope variations in Pennsylvanian shales of the midwestern United States: Geology, v. 16, p. 18-21.

Coveney, R. M., Jr., and Glascock, M. D., 1989, A review of the origins of metal-rich Pennsylvanian black shales, central U.S.A., with an inferred role for basinal brines: Applied Geochem., v. 4, p. 347-367.

Coveney, R. M., Jr., and Nansheng, C., 1989, Ni-Mo-PGE-Au-rich shales of southern China: a new ore type with possible analogs for the Pennsylvanian of the U.S.A.: Abstracts for 28th Intern. Geol. Cong., Washington, D.C., v. 1, p. A335-A336.

Coveney, R. M., Jr., Watney, W. L., and Maples, C. G., 1991, Contrasting depositional models for Pennsylvanian black shale discerned from molybdenum abundances: Geology, v. 19, p. 147-150.

Cullers, R. L., Chaudhuri, S., Kilbane, N., and Koch, R., 1979, Rare-earths in size fractions and sedimentary rocks of Pennsylvanian-Permian age from the mid-continent of the U.S.A.: Geochimica et Cosmochim. Acta, v. 43, p. 1285-1301.

Davis, J. C., 1986, Statistics and data analysis in geology: John Wiley and Sons, Inc., 646 p.

Dean, W. E., and Arthur, M. A., 1989, Iron-sulfur-carbon relationships in organic-carbon-rich sequences I: Cretaceous Western Interior Seaway: Amer. Journ. Sci., v. 289, p. 708-743.

Espitalie, J., Laporte, J. L., Madec, M., Marquis, F., Leplat, P., Paulet, J., and Boutefeu, A., 1977, Methode rapide de characterisation des roches meres, de leur potential petrolier et de leur degre d'evolution: Revue de l'Institut Francais du Petrole, v. 32, p. 23-42.

Ettensohn, F. R., and Elam, T. D., 1985, Defining the nature and location of a Late Devonian-Early Mississippian pycnocline in eastern Kentucky: Geol. Soc. Amer. Bull., v. 96, p. 1313-1321.

Evensen, N. M., Hamilton, P. J., and O'Nions, R. K., 1978, Rare earth abundances in chondrite meteorites: Geochimica et Cosmochimica Acta, v. 42, p. 1199-1212.

Fan Delian, 1983, Ployelements in the Lower Cambrian black shale series in southern China, in The significance of trace elements in solving petrogenetic problems and controversies: Athens, Greece, Theophrastus Publ., p. 447-474.

Fan Delian, 1989, The Sinian-Ordovician metalliferous black shale series in Yangtze Platform in China, in Proceedings of the IGCP #254 Inagural Meeting: Prague, Czechoslovak Geological Survey, p. 25-28.

Fisher, I. St. J., and Hudson, J. D., 1987, Pyrite formation in Jurassic shales of contrasting biofacies, in Brooks, J. and Fleet, A. J., eds., Marine petroleum source rocks Geological Society Special Publ. No. 26, p. 69-78.

Garrels, R. M., and Christ, C. L., 1965, Solutions, minerals, and equilibria: New York, Harper and Row, 450 p.

Goldhaber, M. B., and Kaplan, I. R., 1974, The sulfur cycle,in Goldberg, E. D., ed., The Sea: New York, Wiley, v. 5, p. 569-655.

Hallam, A., 1967, The depth of shales with bituminous laminae: Marine Geology, v. 5, p. 481-493.

Hasenmueller, N. R., Kepferle, R. C., Matthews, R. D., and Pollock, R., 1983, Foerstia (Protosalvinia) in the Devonian Shale of the Appalachain, Illinois, and Michigan Basins, Eastern United States, in Proceedings 1983 Eastern Oil Shale Symposium, p. 41-59,

Haskin, L. A., 1968, An accurate procedure for the determination of rare earths by neutron activation: Journ. Radioanal. Chem., v. 1, p. 337.

Heckel, P. H., 1977, Origin of phosphatic black shale facies in Pennsylvanian cyclothems of mid-continent North America: Amer. Assoc. Petrol. Geol. Bull., v. 61, p. 1045-1068.

Holland, H. D., 1979, Metals in black shales: a reassessment: Econ. Geol., v. 74, p. 1676-1680.

Holland, H. D., 1984, The chemical evolution of the atmosphere and oceans: Princeton University Press, Princeton, New Jersey, 582 p.

Huyck, H. L. O., 1991, When is a metalliferous black shale not a black shale? in Grauch, R. I., and Huyck, H. L. O., eds., Metalliferous black shales and related ore deposits - Proceedings, 1989 United States Working Group Meeting, International Geological Correlation Program Project 254: U.S. Geological Survey Circular 1058, p. 42-56.

Klecka, W. R., 1975, Discriminant analysis in Nie, N. H., Hull, C. H., Jenkins, J. G., Steinbrenner, K., and Bent, D. H., eds., Statistical package for the Social Sciences (SPSS): McGraw-Hill, New York, 675 p.

Kronberg, B. I., 1979, The chemistry of some Brazilian soils: element mobility during intense weathering: Chemical Geology, v. 24, p. 211.

Kucha, H., 1982, Platinum-group metals in the Zechstein copper deposits, Poland: Econ. Geol., v. 77, p. 1578-1591.

Leventhal, J. S., 1983a, An interpretation of carbon and sulfur relationships in Black Sea sediments as indicators of environments of deposition: Geochimica et Cosmochimica Acta, v. 47, p. 133-137.

Leventhal, J. S., 1983b, Organic carbon, sulfur, and iron relationships in ancient shales as indicators of environments of deposition: EOS, v. 64, p. 739.

Leventhal, J. S., 1987, Carbon and sulfur relationships in Devonian Shales from the Appalachian Basin as an indicator of environment of deposition: Amer. Journ. Sci., v. 287, p. 33-49.

Leventhal, J. S., and Taylor, C., 1990, Comparison of methods to determine degree of pyritization: Geochimica et Cosmochima Acta, v. 54, p. 2621-2625.

Lewan. M. D., and Buchardt, B., 1989, Irradiation of organic matter by uranium decay in the Alum Shale, Sweden: Geochimica et Cosmochimica Acta: v. 53, p. 1307-1322.

Liu, T., 1988, C-S-Fe correlation of shales hosting sedimentary manganese deposits: Unpubl. doctoral dissert., Univ. of Cincinnati, 300 p.

Maynard, J. B., 1980, Sulfur isotopes of iron sulfides in Devonian-Mississippian shales of the Appalachian Basin: control by rate of sedimentation: Amer. Journ. Sci., v. 280, p. 772-786.

Merriam, D. F., 1963, The geologic history of Kansas: Kansas Geol. Surv. Bull. 163, 317 p.

Merriam, D. F., 1990, Shanghai Creek Shale Member of the Howard Formation (Wabaunsee Group, Upper Pennsylvanian) in eastern Kansas: Trans. Kasnas Acad. Sci., v. 92, p. 107-112.

Moore, R. C., 1949, Divisions of the Pennsylvanian System in Kansas: Kansas Geol. Surv. Bull. 83, 203 p.

Moore, D. M., and Reynolds, R. C., Jr., 1989, X-ray diffraction and the identification and analysis of clay minerals: New York, Oxford Univ. Press, 332 p.

Murrowchick, J. B., and Barnes, H. L., 1986, Marcasite precipitation from hydrothermal solutions: Geochimica et Cosmochmica Acta: v. 50, p. 2615-2629.

Nance, W. B., and Taylor, S. R., 1976, Rare earth element patterns and crustal evolution - I. Australian post-Archean sedimentary rocks: Geochmica et Cosmochimica Acta, v. 40, p. 1539.

Nesbitt, H. W., and Young, G. M., 1982, Early Proterozoic climates and plate motions inferred from major element chemistry of lutites: Nature, v. 299, p. 715.

Okita, P. M., 1987, Geochemistry and mineralogy of the Molango manganese orebody, Hidalgo State, Mexico, Unpubl. Doctoral dissert., Univ. of Cincinnati, 362 p.

Pandala, H. S., Changkakoti, A., Krouse, H. R., and Gunalan, N., 1991, A study of the relationship between carbon, sulfur, and pyritic iron in the Proterozoic Amjhore pyrite deposit, Bihar, India: Econ. Geol., in press.

Pedersen, T. F., and Calvert, S. E., 1990, Anoxia vs. productivity: what controls the formation of organic-carbon-rich sediments and sedimentary rocks?: Amer. Assoc. Petrol. Geol. Bull., v. 74, p. 454-466.

Peters, K. E., 1986, Guidelines for evaluating petroleum source rock using programmed pyrolysis: Amer. Assoc. Petrol. Geol. Bull., v. 70, p. 318-329.

Pettijohn, F. J., 1949, Sedimentary rocks: New York, Harper and Bros., 526 p.

Raiswell, R., 1982, Pyrite texture, isotopic composition, and the availability of iron: Amer. Journ. Sci., v. 282, p. 1244-1263.

Raiswell, R., and Berner, R. A., 1985, Pyrite formation in euxinic and semi-euxinic sediments: Amer. Journ. Sci., v. 285, p. 710-724.

Raiswell, R., and Berner, R. A., 1986, Pyrite and organic matter in Phanerozoic normal marine shales: Geochimica et Cosmochimica Acta: v. 50, p. 1967-1976.

Raiswell, R., Buckley, F., Berner, R. A., and Anderson, T. F., 1988, Degree of pyritization as a paleoenvironmental indicator of bottom-water oxygenation: Journ. Sediment. Petrol., v. 58, p. 812-819.

Reynolds, R. L., and Goldhaber, M. B., 1983, Iron disulfide minerals and the genesis of roll-type uranium deposits: Econ. Geol., v. 78, p. 105-120.

Ross, C. A., and Ross, J. R. P., 1987, Late Paleozoic sea levels and depositional sequences in Ross, C. A., and Haman, D., eds., Timing and depositional history of eustatic sequences, Cushman Foundation for Foraminiferal Research Spec. Publ. 24, p. 137-149.

Schultz, R. B., 1989, Geochemical characteristics and inferred depositional environments of Upper Pennsylvanian (Virgilian) black shales in eastern Kansas: The Compass, v. 67, p. 47-54.

Schultz, R. B., 1990, A characterization of Midcontinent Pennsylvanian black shales: evidence based on geochemical parameters: Geol. Soc. Amer. Abst. with Prog., v. 22, p. A12.

Schultz, R. B., 1991, Metalliferous black shales: accumulation of carbon and metals in cratonic basins in Force, E. R., Eidel, J. J., and Maynard, J. B., eds., Sedimentary and diagenetic mineral deposits: a basin analysis approach to exploration, Reviews in Econ. Geol., v. 5, p. 171-176.

Schultz, R. B., and Coveney, R. M., Jr., in press, Time-dependent changes for Midcontinent black shales: Chem. Geology.

Sclater, F. R., Boyle, E., and Edmond, J. M., 1976, On the marine geochemistry of nickel: Earth Planet. Sci. Letters, v. 31, p. 119-128.

Schwarz, H. P., and Burnie, S. W., 1973, Influence of sedimentary environments on sulfur isotope ratios in clastic rocks: a review: Mineralium Deposita, v. 8, p. 264-277.

Shaffer, N. R., and Chen, P. Y., 1981, Mineralogy and petrology in Hasenmueller, N. R., and Woodard, G. S., eds., Studies of the New Albany Shale (Devonian and Mississippian) and equivalent strata in Indiana: Morgantown, W. V., Final Report by the Indiana State Geological Survey to the U.S. DOE under contract DE-AC21-76MC05204, p. 34-44.

Shaffer, N. R., Leininger, R. K., and Gilstrap, M. S., 1983, Composition of the uppermost beds of the New Albany Shale in southeastern Indiana, in Proceedings 1983 Eastern Oil Shale Symposium, p. 195-205.

Shutter, S. S., and Heckel, P. H., 1985, Missourian (Early Late Pennsylvanian) climate in Midcontinent North America: Intern. Journ. of Coal Geology, v. 5, p. 111-140.

Strom. K. M., 1939, Land-locked waters and the deposition of black muds in Recent Marine Sediments: Tulsa, Amer. Assoc. Petrol. Geol., p. 356-372.

Sweeney, R. E., 1972, Pyritization during diagenesis of marine sediments: Unpubl. Doctoral dissert., Univ. of California, Los Angeles, 184 p.

Taras, M. J., 1971, Standard methods for the examination of water and wastewater: Amer. Public Health Assoc., 13th ed., 874 p.

Taylor, S. R., 1964, Abundance of chemical elements in the continental crust: a new table: Geochmica et Cosmochimica Acta: v. 28, p. 1273.

Taylor, S. R., and McLennan, S. M., 1985, The continental crust: its composition and evolution, Blackwell, Oxford.

Taylor, S. R., and McLennan, S. M., 1988, The continental crust: its composition and evolution: an examination of the geochemical record preserved in sedimentary rocks: 2nd ed., Blackwell Press, Oxford, 312 p.

Thickpenny, A. and Leggett, J. K., 1987, Stratigraphic distribution and paleo-oceanographic significance of European early Paleozoic organic-rich sediments in Brooks, J., and Fleet, A. J., eds., Marine Petroleum Source Rocks: London, Geological Society, Special Publ. 26, p. 231-247.

Tissot, B. P., and Welte, D. H., 1984, Petroleum formation and occurrence: New York, Springer-Verlag, 699 p.

Tourtelot, H. A., 1979, Black shale-its deposition and diagenesis: Clays and Clay Minerals, v. 27, p. 100-104.

Vine J. D., and Tourtelot, E. B., 1970, Geochemistry of black shales-a summary report: Econ. Geol., v. 65, p. 253-273.

Wang Zhongchen and Li Guizhi, in press, Barite and witherite deposits in Lower Cambrian shales of south China: stratigraphic distribution and geochemical characterization: Econ. Geol.

Wanless, H. R., 1939, Pennsylvanian correlations in the Eastern Interior and Appalachian coal fields: Geol. Soc. Amer. Spec. Paper 17, 130 p.

Wanless, H. R., and Wright, C. R., 1978, Paleoenvironmental maps of Pennsylvanian rocks, Illinois Basin, and northern Midcontinent region: Geol. Soc. Amer. Map Series MC-23.

Watney, W. L., and Ebanks, W. J., Jr., 1978, Early subaerial exposure and freshwater diagenesis of the Upper Pennsylvanian cyclic sediments in northern Kansas and southern Nebraska: [abst.]: Amer. Assoc. Petrol. Geol., Bull, v. 62, p. 570-571.

Watney, W. L., French, J. A., and Franseen, E. K., 1989, Sequence stratigraphic interpretations and modeling of cyclothems in the Upper Pennsylvanian (Missourian) Lansing, and Kansas City groups in eastern Kansas: Kansas Geol Soc. 41st Ann. Fieldtrip Guidebook, 211 p.

Wier, C. E., 1950, Geology and coal deposits of the Jasonville Quadrangle, Clay, Greene, and Sullivan counties, Indiana: U. S. Geol. Surv., Coal, Inv. Map C1.

Wignall, P. B., 1991, Model for transgressive black shales?: Geology, v. 9, p. 167-170.

Williams, N., 1978, Studies of the base metal sulfide deposits at McArthur River, Northern Territory, Australia: II The sulfide-S and organic-C relationships of the concordant deposits and their significance: Econ. Geol., v. 73, p. 1036-1056.

Zangerl, R., and Richardson, E. S., 1963, The paleoecologic history of two Pennsylvanian blck shales: Chicago Nat. History Museum, Fieldiana Geol. Mem. 4, 352 p.

OTHER REFERENCES

Anderson, T. F., Kruger, J., and Raiswell, R., 1987, C-S-Fe relationships and the isotopic composition of pyrite in the New Albany Shale of the Illinois Basin, U.S.A.: Geochimica et Cosmochimica Acta, v. 51, p. 2795-2805.

Boesen, C. and Postma, D., 1988, Pyrite formation in anoxic environments of the Baltic: Amer. Journ. Sci., v. 288, p. 575-603.

Berner, R. A., 1981, A new geochemical classification of sedimentary environments: Journ. Sediment. Petrol., v. 51, p. 359-365.

Berner, R. A., and Westrich, J. T., 1985, Bioturbation and the early diagenesis of carbon and sulfur: Amer. Journ. Sci., v. 285, p. 193-206.

Coveney, R. M., Jr., 1979, Sphalerite concentrations in Mid-continent Pennsylvanian black shales of Missouri and Kansas: Econ. Geol., v. 74, p. 131-140.

Coveney, R. M., Jr., 1985, Temporal and spatial variations in Pennsylvanian black shale geochemistry in Watney, W. L., Kaesler, R. L., and Newell, K. D., eds., Recent interpretations of Late Paleozoic cyclothems, Kansas Geological Survey, p. 247-266.

Coveney, R. M., Jr., 1986, Origins of metal values in Middle Pennsylvanian black shales: [abst.]: Geol. Soc. Amer. Abstracts with Programs, v. 18, p. 572-573.

Coveney, R. M., Jr., and Martin, S. P., 1983, Molybdenum and other heavy metals of the Mecca Quarry and Logan Quarry shales: Econ. Geol., v. 78, p. 132-149.

Coveney, R. M., Jr., Goebel, E. D., and Ragan, V. M., 1987, Pressures and temperatures for aqueous fluid inclusions in sphalerite from midcontinent country rocks: Econ. Geol., v. 82, p. 740-751.

Coveney, R. M., Jr., Watney, W. L., and Maples, C. G., 1989, Rates and durations for accumulations of Pennsylvanian black shales in the midwestern United States in Sedimentary modeling: computer simulation of depositional sequences: Kansas Geol. Surv. Subsurf. Geol. Series 12, p. 73-76.

Cubitt, J. M., 1975, A computer analysis of the geochemistry and mineralogy together with the petrology of the Upper Pennsylvanian and Lower Permian shales of Kansas, U.S.A.: Unpubl. Doctoral dissert., Univ. Leicester (U.K.), 366 p.

Cubitt, J. M., 1979, Geochemistry, mineralogy, and petrology of the Upper Paleozoic shales of Kansas: Kansas Geol. Surv. Bull. 217, 117 p.

Cubitt, J. M., and Merriam, D. F., 1984, Geochemical distributions in Pennsylvanian cyclic sediments of the Midcontinent (U.S.A.) in Geldsetzer, H. H. J., and others, eds., Sedimentology and geochemistry, pt. 3, Intern. Carbonif. Congress on Strat. and Geology, v. 9, p. 633-640.

Davison, W., Lishman, J. P., and Hilton, J., 1985, Formation of pyrite in freshwater sediments: implications for C/S ratios: Geochmica et Cosmochimica Acta, v. 49, p. 1615-1620.

Eslinger, E., and Pevear, D., 1988, Clay minerals for petroleum geologists and engineers: S.E.P.M. Short Course Notes No. 22, Tulsa, OK.

Evans, J. K., 1967, Depositional environment of a Pennsylvanian black shale (Heebner) in Kansas and adjacent states: unpubl. doctoral dissert., Rice Univ., 134 p.

Force, E. R., and Cannon, W. F., 1988, Depositional model for shallow-marine manganese deposits around black shale basins: Econ. Geol., v. 83, p. 93-117.

Franseen, E. K., and Watney, W. L., eds., 1989, Sedimentary modeling: computer simulation of depositional sequences: Kansas Geol. Surv. Subsurf. Geol. Series 12, 84 p.

Glascock, M. D., and Coveney, R. M., Jr., 1988, MQSB-1, a new metal-rich black shale analytical standard from southern Indiana, U.S.A.: [abst.]: IAS Intern. Sympos. on Sedimentology Related to Mineral Deposits, Beijing, p. 66-67.

Heckel, P. H., 1979, Pennsylvanian cyclic platform deposits of Kansas and Nebraska: 9th Intern. Carbonif. Congress on Strat. and Geology, Guidebook Series 4, p. 1-79.

Heckel, P. H., 1984, Changing concepts of midcontinent Pennsylvanian cyclothems: IX Intern. Carbonif. Congress Compte Rendu, v. 3, p. 535-553.

Heckel, P. H., 1986, Sea-level curve for Pennsylvanian eustatic marine transgressive-regressive depositional cycles along midcontinent outcrop belt, North America: Geology, v. 14, p. 330-334.

Holser, W. T., Schidlowski, M., Mackenzie, F. T., and Maynard, J. B., 1988, Biogeochemical cycles of carbon and sulfur in Gregor, C. B., Garrels, R. M., Mackenzie, F. T., and Maynard, J. B., eds., Chemical cycles in the evolution of the Earth: New York, John Wiley & Sons, p. 105-174.

James, C. W., 1970, Stratigraphic geochemistry of a Pennsylvanian black shale (Excello) in the mid-continent and Illinois Basin: Unpubl. Doctoral dissert., Rice University, Houston, TX.

Kaplan, I. R., Emery, K. O., and Rittenberg, S. C., 1963, The distribution and isotopic abundance of sulphur in recent marine sediments off southern California: Geochimica et Cosmochimica Acta, v. 27, p. 297-331.

Kidder, D. L., 1985, Petrology and origin of phosphatic nodules from the midcontinent Pennsylvanian epicontinental sea: Journ. Sediment. Petrol., v. 55, p. 809-816.

Klein, G. deV., 1990, Pennsylvanian time scales and cyclic periods: Geology,v. 18, p. 455-457.

Klein, G. deV., and Willard, D. A., 1989, Origin of the Pennsylvanian coal-bearing cyclothems: Geology, v. 17, p. 152-155.

Leeder, M., Raiswell, R., Al-Biatty, H., McMahon, A., and Hartman, M., 1990, Carboniferous stratigraphy and correlation of well 48/3-3 in the southern North Sea Basin: integrated use of palynology, natural gamma/sonic logs and carbon/sulphur geochemistry: Journ. Geol. Soc., London, v. 147, p. 287-300.

Leventhal, J. S., Crock, J. G., Mountjoy, W., Thomas, J. A., Shaw, V. E., Briggs, P. H., Wahlberg, J. S., and Malcolm, M. J., 1978, Preliminary analytical results a new U. S. Geological Survey Devonian Ohio shale analytical standard SDO-1: U. S. Geol. Surv. Openfile Rept. 78-447.

Lewan, M. D., 1985, Evaluation of petroleum by hydrous pyrolysis experimentation: Phil. Trans. R. Sco. Lond., Part A, v. 315, p. 123-134.

Lewan, M. D., and Maynard, J. B., 1982, Factors controlling enrichment of vanadium and nickel in the bitumen of organic sedimentary rocks: Geochmica et Cosmochimica Acta, v. 46, p. 2547-2560.

Magaritz, M., and Holser, W. T., 1990, Carbon isotope shifts in Pennsylvanian seas: Amer. Journ. Sci., v. 290, p. 977-994.

Maples, C. G., 1986, Enhanced paleoecological and paleo-environmental interpretations result from analysis of early diagenetic concretions in Pennsylvanian shales: Palaios, v. 1, p. 512-516.

Martin, S. P., 1982, Trace elements in the Pennsylvanian-age Hushpuckney and Mecca Quarry shales, Midcontinent, U.S.A.: Unpubl. Masters thesis, Univ. of Missouri-Kansas City.

Maynard, J. B., 1982, Extension of Berner's "new geochemical classification of sedimentary environments" to ancient sediments: Journ. Sediment. Petrol., v. 52, p. 1325-1331.

Maynard, J. B., 1983, Geochemistry of sedimentary ore deposits: New York, Springer-Verlag, 305 p.

Merriam, D. F., ed., 1964, Symposium on cyclic sedimentation: Kansas Geol. Surv. Bull 169, Parts I and II.

Merriam, D. F., 1986, Geology of the Shawnee Group (Virgilian Stage, Upper Pennsylvanian) in eastern Kansas and its relation to the cyclothem theory: Kansas Geol. Soc. 38th Ann. Fieldtrip Guidebook, p. 1-51.

Merriam, D. F., 1989, The Wauneta Limestone, a new member of the Howard Limestone (Wabaunsee Group, Upper Pennsylvanian) in eastern Kansas: Trans. Kansas Acad. Sci., v. 92, p. 107-112.

Moore, R. C., 1936, Stratigraphic classification of the Pennsylvanian rocks of Kansas: Kansas Geol. Surv. Bull. 22, 256 p.

Potter, P. E., Maynard, J. B., and Pryor, W. A., 1980, Sedimentology of Shale: New York, Springer-Verlag, 305 p.

Raiswell, R., and Berner, R. A., 1987, Organic carbon losses during burial and thermal maturation of normal marine shales: Geology, v. 15, p. 853-856.

Raiswell, R., and Al-Biatty, H. J., 1989, Depositional and diagenetic C-S-Fe signatures in early Paleozoic normal marine shales: Geochmica et Cosmochimica Acta, v. 53, p. 1147-1152.

Schultz, R. B., 1987, Mineral determination of the Heebner Shale Member (Shawnee Group, Upper Pennsylvanian) in southeastern Kansas using X-ray diffraction techniques: The Compass, v. 64, p. 149-159.

Vail, P. R., Mitchum, R. M., Jr., and Thompson, S., III, 1977, Seismo-stratigraphy and global changes of sea level: Amer. Assoc. Petrol. Geol. Mem. 26, p. 83-97.

Watney, W. L., 1980, Cyclic sedimentation of the Lansing-Kansas City Groups in northwestern Kansas and southwestern Nebraska: Kansas Geol. Surv. Bull. 220, 72 p.

Wenger, L. M., and Baker, D. R., 1986, Variations in organic geochemistry of anoxic-oxic black shale-carbonate sequences of the Midcontinent: Adv. Org. Geochem., v. 10, p. 85-92.

Westrich, J. T., and Berner, R. A., 1984, The role of organic matter in bacterial sulfate reduction: the G model tested: Limnol, Oceanogr., v. 29, p. 236-249.

Zeller, D. E., ed., 1968, The stratigraphic succession in Kansas: Kansas Geol. Surv. Bull 189, 81 p.

Appendix A. Whole-rock XRF Procedure: Powder Mounts

A method for preparing powder mounts for the XRF using minimal sample material (particularly valuable when using standards that are in limited supply) with SPEX 3624B X-Press.

1. Attach the base to the die and insert one of the polished discs with the polished side up.

2. Add enough microcrystalline cellulose to fill approximately one-half of the die. Level the cellulose.

3. Insert the die plunger (upside-down) with the bevelled edge down.

4. Place the die assembly in the press, center it, tighten the press with the hand screw (on top of the press), and press the cellulose to no more than two tons (the upside-down position with the bevelled edge of the plunger is not designed for high stresses). To operate the press, first, turn the handle on the right side of the press clockwise until snug (not too tight). This seals the hydraulic system. Now depress the switch at the front of the unit until the desired pressure is achieved. To release the pressure, turn the handle at the right side slowly counter-clockwise. Never release pressure too quickly. After opening the pressure release, depress the front button to lower the press.

5. Release the pressure, remove the die assembly, and extract the plunger with a slight twist. Never pull the plunger off. A cellulose pellet with a slightly raised rim should remain. Get rid of any loose cellulose particles left, if they are present.

6. Insert the homemade plastic liner into the die assembly and add enough sample so that the surface area is smooth and covered, but not too much sample so that piles are created. The smoother the sample area is, the smoother the pellet will be without clumps. The sample should be a fine, homogeneous powder prepared in the shatterbox or SPEX mill (a powder ground in the shatterbox is preferred over the SPEX mill because of its smaller grain size and homogeneity). Make sure the sample is level and smooth. Remove the plastic liner.

7. Insert the top polished disc, polished side towards the sample, and the plunger with bevelled edge up this time. The flat edge of the plunger should be on top of the sample.

8. Return the die assembly to the press and press to the maximum load. The press is pre-set to about 20 tons, so you can press no farther than that. Allow die assembly to remain under pressure for approximately 30 seconds to one minute.

9. Slowly release the pressure as before (in 15-20 seconds) and remove the die from the press. Remove the base from the die, and put the aluminum cup into the bottom of the die assembly.

10. Invert the entire die assembly and return it to the press in the upside-down position. Use the hand crank on top to begin the extraction process. After turning the hand crank one or two rotations, remove the die assembly and press out the pellet and discs by hand into the foam pad. The aluminum cup should be up at this point with the plunger fitting into the hole in the foam pad. Carefully extract pellet without jarring to avoid damage to the pellet and discs.

Cleanliness: Before, during, and after the process, keep all parts of the assembly and press clean. Keeping things free of particles and dust prevents cross-contamination and minimizes wear and tear on the die assembly. Kim-wipes and puffs of air do a satifactory job in this respect. Never use water to clean the parts; acetone is best for cleaning. Store all parts in a desiccator.

Appendix B. Geochemical Standards for XRF

GEOCHEMICAL STANDARDS USED FOR XRF (from U.S.G.S./NIST)

STANDARDS	%SiO2	%TiO2	%Al2O3	%Fe2O3	%MnO2	%MgO	%CaO	%Na2O	%K2O	%P2O5	%S	Error
SDO-1	49.800	0.670	12.620	9.330	0.046	1.550	1.040	0.420	3.300	0.110	5.310	-0.00072
ST-41	51.190	0.750	16.460	6.980	0.100	3.130	1.380	3.910	3.720	0.180	0.430	0.14098
ST-28	73.470	0.278	13.800	1.890	0.040	0.280	1.150	4.120	4.350	0.050	0.010	-0.00024
ST-21	66.150	1.000	15.750	6.850	0.120	1.700	1.390	2.100	3.240	0.180	0.067	0.00958
SY-2	60.100	0.140	12.120	6.270	0.320	2.700	7.980	4.340	4.480	0.430	0.011	0.01691
ST-14	70.330	0.310	14.740	2.350	0.050	0.680	2.180	3.800	3.510	0.110	0.000	0.01364
ST-15	74.110	0.280	12.650	2.730	0.030	0.080	0.580	2.850	5.100	0.130	0.000	0.11395
SHP-1	60.650	1.030	17.530	7.230	0.100	1.930	0.590	1.470	3.280	0.190	0.000	-0.00371
ST-25	65.930	0.620	16.370	4.290	0.090	1.040	3.240	4.230	3.630	0.260	0.000	0.01305
1413	82.770	0.110	9.900	0.240	0.000	0.060	0.740	1.750	3.940	0.040	0.000	0.00946
69B	13.43	1.900	48.800	7.140	0.110	0.085	0.130	0.025	0.068	0.118	0.630	-0.39142
97B	42.380	2.390	39.210	2.380	0.010	0.190	0.030	0.130	1.240	0.140	0.000	0.04045
278	73.050	0.245	14.150	2.040	0.052	0.230	0.983	4.840	4.160	0.038	0.000	0.00127
688	48.400	1.170	17.360	10.350	0.167	8.400	12.170	2.150	0.187	0.134	0.000	0.02502
QUARTZ	100.000	0.000	0.000	0.000	0.000	0.000	0.000	0.000	0.000	0.000	0.000	0.00005
690	3.710	0.022	0.180	95.580	0.230	0.180	0.200	0.003	0.003	0.011	0.003	-0.00021
C690	78.052	0.005	0.041	21.786	0.052	0.041	0.046	0.001	0.001	0.004	0.001	0.00344
ST-31	49.900	2.690	13.850	12.230	0.170	7.310	11.330	2.290	0.540	0.280	0.011	-0.00169
St-32	59.660	0.130	18.440	5.210	0.220	0.100	1.090	8.950	4.290	0.160	0.000	0.00243
70A	67.100	0.010	17.900	0.070	0.000	0.000	0.110	2.500	11.800	0.000	0.000	-0.00090
99A	65.200	0.007	20.500	0.060	0.000	0.020	2.140	6.230	5.200	0.020	0.000	0.00155
SIND-2	46.000	0.580	11.200	5.300	0.012	0.940	0.350	0.360	3.390	0.110	2.750	0.00015
MAG-1	51.190	0.750	16.460	6.980	0.100	3.130	1.380	3.910	3.720	0.180	0.430	-0.12145
SCo-1	63.390	0.620	13.700	5.220	0.050	2.760	2.640	0.950	2.820	0.220	0.066	0.02154
SGR-1	28.300	0.240	6.490	2.980	0.032	4.570	8.320	3.020	1.630	0.290	1.560	0.24515

Appendix C. SDO-1 Geochemical Standard

SDO-1 GEOCHEMICAL STANDARD

	%Fe	%S	%Sorg	%TOC	Fe2sol	FeTsol	FePY	Spy	DOP	Fe2sol/FeTsol	Spy/TOC
SDO-1	9.213	5.307	.048	6.90	1.53	1.87	4.58	5.26	.71	.82	.762

*%Fe and %S are measured by XRF
*%Sorg is organic sulfur
*Fe2sol is ferrous iron content
*FeTsol is ferric iron content
*FePY is pyrite iron
*Spy is pyrite sulfur or inorganic sulfur
*DOP is degree of pyritization

**Sorg measured by sulfide-sulfur determinations
**%TOC measured by Carbon analyzer
**Fe2sol and FeTsol measured by colorimetric iron determ.
**FePY=Spy*55.85/64.12
**DOP=FePY/(FePY+FeTsol)

Appendix D. XRF Data

SAMPLE	Si%	Ti%	Al%	Fe%	Mn%	Mg%	Ca%	Na%	K%	P%	S%	TOTAL
HB1	45.45	0.68	14.20	5.70	0.04	1.98	5.28	0.65	3.22	3.06	1.19	81.45
HB2	49.78	0.70	14.84	6.08	0.04	1.92	1.11	0.56	3.15	1.12	0.02	79.31
HB3	47.76	0.70	14.00	5.40	0.06	2.01	1.87	0.99	3.33	1.00	0.95	78.06
HB4	46.30	0.97	15.26	4.69	0.07	2.31	5.78	0.71	4.27	0.03	0.21	80.60
QH1	44.96	0.85	15.37	5.04	0.05	3.70	3.81	0.71	4.25	1.08	1.61	81.44
QH2	49.56	0.97	16.17	5.31	0.06	4.71	1.95	0.89	5.06	0.07	0.01	84.78
QH3	40.80	0.61	12.30	3.94	0.03	1.85	4.09	0.55	2.75	2.20	0.84	69.96
QH4	43.02	0.71	13.54	4.99	0.05	2.20	6.79	0.67	3.31	2.00	0.78	78.06
QH5	46.37	0.79	14.06	6.43	0.06	4.05	1.18	0.59	5.32	1.68	0.00	80.51
QH6	47.88	0.78	15.11	5.87	0.06	3.79	1.66	1.00	4.23	1.00	0.05	81.43
LB1	48.90	0.99	17.92	6.40	0.05	3.47	2.49	0.70	4.70	0.56	0.88	85.06
LB2	47.28	0.90	16.89	5.75	0.07	3.85	0.98	0.68	4.13	0.95	0.00	81.47
LB3	39.60	0.67	14.30	6.06	0.04	2.11	0.82	0.50	3.44	0.20	1.06	68.82
LB4	40.40	0.64	14.60	6.87	0.03	1.97	3.29	0.50	3.13	1.59	0.67	73.69
HO1	46.20	0.97	19.86	5.22	0.05	4.61	5.10	0.68	4.80	0.35	0.04	87.88
SH1	50.20	0.80	18.60	6.13	0.04	2.17	2.01	0.68	3.64	0.76	1.44	86.47
SH2	50.30	0.83	19.00	6.10	0.03	2.18	1.46	0.68	3.62	0.18	0.05	84.43
SH3	49.54	0.99	20.80	6.54	0.08	3.64	2.29	0.67	3.72	0.56	0.03	88.86
SH4	48.50	0.88	18.58	4.44	0.10	3.19	11.66	0.59	3.88	0.03	0.47	92.30
HBC1	21.70	0.28	5.49	0.70	0.04	3.85	44.46	0.73	1.20	0.31	0.73	79.28
HBC2	23.14	0.31	5.17	0.86	0.05	3.56	45.27	0.74	1.36	0.11	0.20	80.79
HBC3	22.46	0.27	5.82	0.83	0.05	3.30	52.56	0.63	1.30	0.11	0.13	87.45
HBC4	41.16	0.29	4.96	1.94	0.04	3.68	14.54	0.78	2.02	0.04	0.08	69.53
HBC5	41.22	0.33	5.83	2.01	0.04	3.66	14.51	0.89	3.29	0.03	0.00	71.89
HBC6	20.40	0.24	4.84	1.51	0.03	3.43	36.21	0.45	1.00	0.55	0.73	69.40
HBC7	22.25	0.22	4.44	0.58	0.04	3.93	54.15	0.45	1.96	0.45	0.13	88.59
QHC1	48.30	0.67	14.41	4.44	0.03	3.45	5.84	1.13	3.91	0.11	1.91	84.22
QHC2	49.23	0.68	14.81	4.67	0.03	3.68	7.18	1.17	4.12	0.17	1.99	87.73
QHC3	45.68	0.86	17.80	3.27	0.05	3.58	8.97	1.18	5.70	0.33	0.84	88.05
QHC4	43.65	0.77	16.75	2.72	0.04	3.69	12.07	1.42	5.75	0.35	0.51	87.71
QHC5	32.43	0.56	7.88	1.77	0.06	6.73	22.98	0.79	2.31	0.04	1.65	77.20
QHC6	34.43	0.68	14.33	3.52	0.06	6.00	13.76	1.30	4.04	0.13	2.60	80.86
QHC7	40.56	0.80	15.37	3.21	0.06	4.98	11.80	1.39	4.08	0.06	1.53	83.81
QHC8	42.34	0.87	16.56	3.49	0.06	5.06	9.89	1.49	4.25	0.06	1.76	85.82
QHC9	45.05	0.79	13.92	5.28	0.06	8.81	12.14	1.54	3.87	0.05	4.37	95.88
SHC1	46.71	0.59	14.09	2.43	0.07	4.57	13.82	1.05	3.87	0.02	0.81	88.04
SHC2	29.50	0.40	9.11	3.07	0.06	1.94	27.71	0.78	1.48	0.07	0.62	74.75
SHC3	19.71	0.24	6.26	3.07	0.06	1.66	37.54	0.42	0.86	0.08	0.83	70.75

OUTCROP SAMPLES												
Sample	%SiO2	%TiO2	%Al2O3	%Fe2O3	%MnO2	%MgO	%CaO	%Na2O	%K2O	%P2O5	%S	Total
SH-5	52.37	0.89	17.55	6.27	0.05	2.86	4.47	0.79	3.90	0.38	1.53	91.05
LB-5	50.16	0.85	15.47	6.76	0.03	3.26	2.34	0.61	4.00	0.43	2.50	86.40
HP-3	53.03	0.58	13.69	4.84	0.07	5.39	11.57	0.51	3.50	0.05	0.87	94.10
HP-4	47.15	0.62	12.68	4.30	0.02	2.65	9.46	0.80	3.53	5.80	1.68	88.69
EU-1	60.48	0.89	17.87	6.08	0.04	3.54	2.55	0.73	3.87	0.06	1.24	97.35
EU-2	42.83	0.54	10.43	3.95	0.01	1.27	10.37	0.44	2.78	4.99	1.77	79.39
ST-1	59.96	0.95	18.01	6.77	0.04	4.02	0.92	0.76	4.16	0.09	1.30	96.98
ST-1A	50.67	0.88	13.23	8.29	0.02	2.44	0.66	0.48	3.58	0.12	2.76	83.13
ST-1B	53.42	0.87	14.04	7.92	0.03	2.73	0.37	0.63	3.47	0.11	3.60	87.20
ST-1C	56.69	0.90	15.47	7.90	0.03	2.86	0.35	0.76	3.63	0.10	3.01	91.69
ST-1D	42.92	0.63	10.98	5.89	0.02	1.82	8.58	0.54	3.00	5.58	3.58	83.55
ST-1E	45.83	0.79	11.46	7.87	0.02	2.02	2.74	0.58	3.22	1.62	3.50	79.65
ST-1F	48.31	0.79	12.84	6.87	0.02	2.35	3.44	0.55	3.41	2.20	3.46	84.23
ST-1G	50.86	0.85	14.01	7.80	0.03	2.68	1.43	0.56	3.61	0.75	3.16	85.75
ST-1H	43.74	0.64	11.28	6.44	0.02	1.87	8.13	0.55	3.04	4.77	3.51	84.01
ST-1I	56.05	0.86	16.34	6.66	0.03	2.90	0.84	0.67	4.08	0.35	2.49	91.27
ST-1J	50.64	0.74	13.75	5.72	0.02	2.60	6.31	0.55	3.48	3.43	2.37	89.60
ST-1K	56.78	0.88	16.64	7.07	0.03	2.98	0.36	0.66	4.14	0.06	2.15	91.73
ST-1L	39.04	0.47	9.78	4.03	0.01	1.47	14.48	0.61	2.67	8.64	2.41	83.61
ST-1M	54.07	0.80	15.48	6.05	0.02	2.71	2.13	0.57	4.02	1.09	1.59	88.54
ST-1N	56.26	0.88	15.81	6.55	0.03	3.06	1.73	0.66	3.82	0.89	2.04	91.71
ST-1O	42.51	0.60	10.93	5.27	0.02	1.74	9.00	0.54	3.05	4.87	2.53	81.06
ST-1P	56.29	0.86	16.87	6.08	0.04	3.88	3.46	0.69	4.16	0.37	1.45	94.13
ST-2	50.62	0.55	11.71	4.19	0.03	2.95	12.26	0.54	2.87	5.42	1.94	93.05
ST-3	61.07	0.80	16.43	4.49	0.02	2.89	0.58	0.55	4.02	0.12	1.67	92.63
MC-1	55.88	0.70	16.44	4.90	0.05	5.42	9.44	0.65	3.85	0.16	0.77	98.26
MC-2	54.95	0.82	14.70	5.85	0.02	2.66	0.63	0.63	3.68	0.07	1.41	85.42
MC-3	57.81	0.75	16.08	5.45	0.05	4.32	7.72	0.75	3.74	0.22	0.87	97.74
Avg.	51.80	0.76	14.28	6.08	0.03	2.91	4.87	0.62	3.58	1.88	2.18	89.00
CORE SAMPLES												
MC Cores												
0-3.5	56.14	0.70	16.70	4.52	0.01	5.41	9.77	0.64	3.81	0.19	0.57	98.46
3.5-7	59.43	0.79	16.41	5.67	0.05	4.04	6.65	0.85	3.65	0.12	0.79	98.45
Avg.	57.79	0.75	16.56	5.10	0.03	4.73	8.21	0.75	3.73	0.16	0.68	98.46

Appendix E. Organic Carbon Measurement

Elemental Carbon Analyzer Procedures

Samples were ground to -400 mesh in a shatterbox. Samples were not sieved so as not to exclude any minerals as a result of preferential size variations. The Perkin-Elmer 240 Elemental Analyzer was used for the analysis of carbon content. The Elemental analyzer was calibrated using two blanks and two standards of U.S. Geological Survey geochemical standard SDO-1, which contains 10.48% total carbon and 10.13% total organic carbon (TOC). Samples were then weighed to the nearest .001 milligram using a microbalance, and immediatly analyzed on the Perkin-Elmer Elemental Analyzer. The calculations for total carbon are as follows:

1. Standard sample (in mg) x 0.1048 = mg of C standard

2. Mg of C standard / (standard C reading in mV - blank reading in mV) = K_C value for standard SDO-1

3. Mg of C_{sample} = sample reading in mV x K_C

4. Mg of C_{sample} / sample in mg = % total carbon in sample

For a determination of the total organic carbon (TOC) present, 100 milligram samples were washed with 4 ml of concentrated HCl followed by filtering and washing with distilled water. Filter paper collected the remaining meterial and was dried at not more than 80° C overnight in an oven. These samples were then analyzed in the Perkin-Elmer Elemental Analyzer as in the total carbon investigation. Calculations for total organic carbon are as follows:

1. Standard sample (in mg) x 0.1013 = mg of organic C in SDO-1

2. Mg of $TOC_{standard}$ / (standard reading in mV - blank reading in mV = K_{TOC} value for SDO-1 standard

3. Mg of TOC_{sample} = sample reading in mV x K_{TOC}

4. Mg of TOC_{sample} / sample in mg = %TOC in sample

Appendix F. Total Organic Carbon Data

SUMMARY OF CARBON INVESTIGATION				
SAMPLE	% TOTAL C	%CO3 C	% TOC	% H2O
SDO-1 W	10.48	0.35	10.13	1.31
SDO-1 R	10.48	0.35	10.13	1.31
OUTCROP SAMPLES				
HB-1 W	11.75	2.95	8.80	1.64
HB-2 R	4.09	3.16	0.93	0.62
HB-3 W	9.72	7.54	2.18	0.11
HB-4 R	8.10	4.52	3.58	1.06
QH-1 W	15.07	0.07	15.00	1.19
QH-2 R	3.62	2.62	1.00	2.57
QH-3 W	16.67	0.30	16.37	4.09
QH-4 R	17.62	6.43	11.19	1.37
QH-5 W	3.24	2.97	0.27	0.01
QH-6 R	7.45	5.17	2.28	0.73
LB-1 W	27.22	11.99	15.23	0.01
LB-2 R	4.21	4.15	0.06	0.59
LB-3 W	23.54	7.42	16.12	0.30
LB-4 R	22.36	3.95	18.41	1.49
HO-1 W	6.94	4.88	2.06	0.14
SH-1 R	6.48	1.74	4.74	0.74
SH-2 W	8.10	4.38	3.72	0.03
SH-3 R	3.82	1.30	2.52	0.03
SH-4 W	6.48	5.08	1.40	0.01
SDO-1 R	10.48	0.35	10.13	1.31
SDO-1 W	10.48	0.35	10.13	1.31
CORE SAMPLES				
HBC-1 R	7.25	6.66	0.59	0.54
HBC-2 W	10.52	9.81	0.71	0.62
HBC-3 R	7.43	6.79	0.64	0.20
HBC-4 W	3.08	3.07	0.01	0.03
HBC-5 R	2.16	2.09	0.07	0.31
HBC-6 W	4.86	3.51	1.35	0.59
HBC-7 R	9.29	8.97	0.32	0.02
QHC-1 W	4.59	0.76	3.83	0.77
QHC-2 R	5.47	1.47	4.00	2.66
QHC-3 W	2.88	1.68	1.20	0.50
QHC-4 R	2.49	2.31	0.18	0.50
QHC-5 W	8.01	7.81	0.20	0.50
QHC-6 R	4.58	3.62	0.96	0.18
QHC-7 W	2.88	2.57	0.31	0.22
QHC-8 R	3.52	3.18	0.34	0.60
QHC-9 W	5.17	3.95	1.22	1.04
SHC-1 R	5.95	5.94	0.01	0.87
SHC-2 W	2.93	2.67	0.26	0.47
SHC-3 R	6.04	4.88	1.16	0.40
MQSB-1 W	31.48	1.22	30.26	3.39

SAMPLE	%TOC
LB–5	18.53
HB–5	20.76
HP–3	8.93
HP–4	23.18
EU–1	4.3
EU–2	29.24
MC–1	27.89
MC–2	26.88
MC–3	24.77
ST–1	6.23
ST–1A	20.64
ST–1B	21.76
ST–1C	8.7
ST–1D	3.44
ST–1E	25.36
ST–1F	20.75
ST–1G	2.48
ST–1H	20.22
ST–1I	10.43
ST–1J	14.4
ST–1K	10.24
ST–1L	18.6
ST–1M	15.17
ST–1N	12.17
ST–1O	20.11
ST–1P	10.3
ST–2	13.08
ST–3	12.63
SH–5	10.38

Sample	Total C	CO3 C	%TOC
MQSB–1	43.72	4.00	39.72
Logan Q.	25.22	2.29	22.93
Holland Sh.	29.91	3.00	26.91
Hesler A1	47.54	3.80	43.74
Hesler A2	35.62	3.21	32.41
Hesler A3	31.76	3.18	28.58
Hesler A4	32.32	2.91	29.41
Hesler B1	32.49	2.92	29.57
Hesler B2	35.94	2.88	33.06
Hesler B3	17.03	1.70	15.33
Hesler B4	37.18	2.97	34.21
Hesler C	7.72	0.85	6.87
Hesler D	22.64	2.04	20.60
Velpen A	17.06	1.71	15.35
Velpen B	12.54	1.27	11.27
Velpen C	9.77	1.17	8.60
Velpen D	31.58	2.53	29.05

where Kc ave. for Total C=.00420395

and Kc ave. for TOC=.003777362

Appendix G. Sulfide-Sulfur Determination

Chromium Reduction in Analysis of Inorganic Sulfur

The proposed technique is used to convert sulfur compounds (i.e., pyrite) in a shale sample to a silver sulfide precipitate, which can later be used for sulfur isotope analyses.

Initially, acid digestion liberates acid-soluble sulfide materials. The procedure then involves utilizing 1 to 2 grams of shale sample in two portions. First, carbonates and acid-soluble sulfides are removed using 6 N HCl (heated at medium temperature setting, just shy of boiling). Secondly, conversion of pyrite to H_2S gas is accomplished by adding $CrCl_3$ solution and heating at medium setting (not boiling) for a minimum of 2 hours. The H_2S gas is bubbled into a silver nitrate solution and converted to silver sulfide (precipitate). A nitrogen atmosphere is maintained throughout the conversion process.

Chemicals:

-Ethanol
-6 N HCl
-Zinc shot (Fisher Chemical Z-12)
-$AgNO_3$ (Fisher Chemical S-181)
-Chromic chloride (Fisher Chemical C-325)
N_2 tank
-Deionized water

Hardware:

-Stirring hot plate with stir bar
-Three (3) split ring stands
-Finger clamps for ring stands
-45 micron filter papers
-Millipore filtering apparatus
-Black hole covers for flasks and rubber o-rings

Glassware:

-250 ml beakers
-Glass tubing
-Three (3) 3-way stopcocks
-Two (2) 250 ml condensing columns with stopcocks
-Test tube with outlet pipe
-Disposable Pasteur pipettes
-3-hole reaction vessel (3-necked flask)

Appararus Setup:

Assemble the apparatus as shown in the figure. It is much easier and more efficient to use this setup than suggested by Canfield, et al. (1986). Acid can easily be added to the

system, $CrCl_3$ can be added slowly (a great advantage), and there are no complications resulting from syringe usage as in the technique offered by Canfield, et al. (1986).

Solution Preparation:

5% $AgNO_3$ solution:

5 grams $AgNO_3$ + 100 ml deionized water
*Make sure the water is clean or a cloudy precipitate will form.

Chromic chloride solution:

2 grams $CrCl_3$ + 50 ml 6 N HCl
*Put the $CrCl_3$ in a 100 ml beaker and add the acid to it slowly under the hood. Store covered under the hood.

Reduction of zinc:

Add 10 ml 6 N HCl + 60 ml deionized water to 10 grams of zinc shot. Do not add the $CrCl_3$ at this time. Add the acid solution slowly. The reaction must continue for at least 10 minutes or until bubbling decreases.

Procedure:

I. Sample setup

1. Place 1 to 2 grams of sample material into the reaction vessel (add more if the sample is low in total sulfur, less if the sample is high in total sulfur).

2. Carefully add the stir bar into the reaction vessel.

3. Add 5 ml of ethanol into the reaction vessel.

4. Make all connections to the reaction vessel. Double check to be certain all connections are tight.

5. Vessel must be secure with good seals on o-rings.

II. Purging the system of air

1. Purge the reaction vessel of air by slowly turning on the N_2 gas and allowing it to permeate the system for one minute.

2. Turn on the hot plate to low-medium heat, but do not boil. Do not turn on stirring system at this time.

3. Slowly begin the flow of N_2 into the vessel. Adjust the flow rate if necessary.

4. Place the disposable pipette into the test tube of $AgNO_3$ solution (precipitate trap). Again adjust the flow rate of the N_2 so that one bubble per second is being released into the $AgNO_3$ trap.

III. Acid digestion

1. Add 25 ml of 6 N HCl to the reaction vessel by turning the appropriate stopcock. Make sure not to allow the N_2 to escape by opening the wrong stopcock.

2. Turn on the stir bar system to a low speed.

3. Allow reaction to continue for at least 10 minutes.

4. Adjust the N_2 flow rate if necessary.

IV. $CrCl_3$ digestion

1. While the HCl digestion is occurring, reduce the $CrCl_3$

2. Drain acid solution from the zinc shot into a 250 ml beaker and discard.

3. Slowly add the green $CrCl_3$ solution to the zinc shot. Be careful when adding the solution because the reaction is very exothermic and if added too quickly will foam up over the glassware. It is normal for the glassware to be slightly warm after adding the $CrCl_3$ solution.

4. The solution is reduced when it turns from the original green color to a cobalt blue and the amount of bubbling decreases. This may take 15-20 minutes.

V. Precipitate recovery

1. While keeping the N_2 gas on, remove the disposable pipette from the $AgNO_3$ trap. A black precipitate should be present at the bottom of the test tube trap.

2. Remove the test tube and carefully filter the $AgNO_3$ solution through the Millipore setup.

3. Dry the filtrate overnight by placing filter paper with precipitate on a petri dish. Immediatly label the sample.

4. Using the attached sulfide-sulfur measurement data chart, calculate the sulfide weight percent in the whole rock.

SULFIDE-SULFUR MEASUREMENT DATA CHART

Date:_____

Sample Number:_____

Sample weighing:

1. Paper weight:_____gm
2. Paper + sample:_____gm
3. Paper weight (after use):_____gm
4. Sample weight:_____gm

Silver sulfide weighing:

1. Filter paper weight:_____gm
2. Sulfide + paper:_____gm
3. Silver sulfide weight:_____gm

Sulfide weight percent in the whole rock:

$AgNO_3$ weight * 12.9381% / Sample weight = Sulfide Weight Percent

_____gm * 12.9381% / _____gm = _____%

Notes/Calculations:

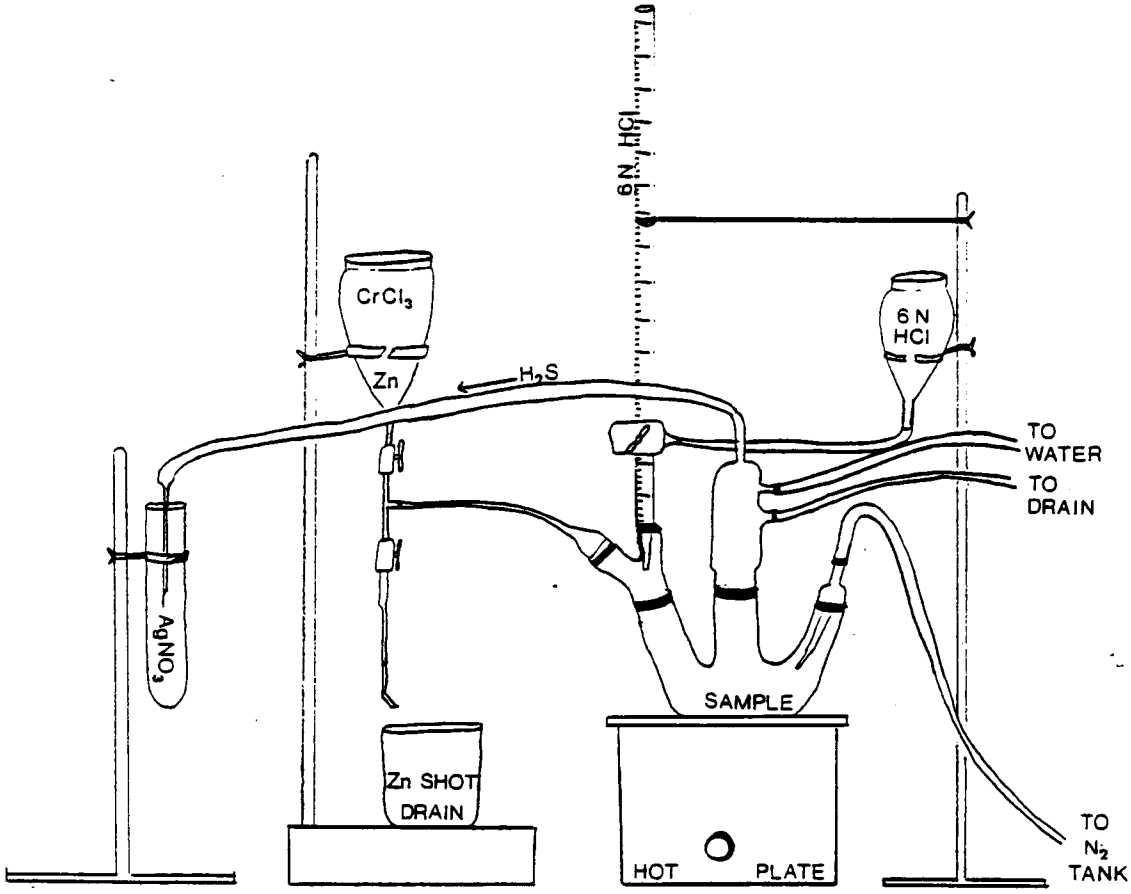

General setup for chromium reduction of reduced inorganic sulfur compounds.

Appendix H. Acid-Soluble Iron Determination (DOP)

Colorimetric Determination of Iron in Shales

Reagents:

-Concentrated HCl

-Hydroxyl amine solution: 10 gm in 100 ml distilled water. Store in 125 Erlenmeyer flask.

-Ammonium acetate buffer solution: dissolve 250 gm of ammonium acetate in 150 ml of distilled water and add 700 ml of glacial acetic acid. Store in 3.8 liter container.

-Phenanthroline solution: dissolve 200 mg (0.20 gm) in 100 ml of distilled water with two drops of concentrated HCl. Store in 100 ml volumetric flask.

-Stock iron solution: dissolve 108.90 mg (0.1089 gm) of $FeSO_4$ in 200 ml of distilled water to yield 200 mg/l iron concentration. Store in 1000 ml volumetric flask.

-Working standards: dilute stock iron solution to 1, 2, 4, and 10 mg/l concentrations. Use 0.5 ml, 1 ml, 2 ml, and 5 ml portions. Prepare fresh daily. Store in separate 100 ml volumetric flasks.

-Blank solutions: prepare two reagent blamks that include 10 ml of ammonium buffer solution and 5 ml of the phenanthroline solution. To <u>one</u> of the blanks, add 1 ml of hydroxylamine solution. It will turn slightly orange. Use 50 ml volumetric flasks.

Equipment:

Accurate balance (up to 0.001 gm)
Weighing paper
125 ml Erlenmeyer flask
10 ml graduated cyclinder
Hot plate
Filter paper
Funnel
Four (4) 50 ml volumetric flasks
Two (2) 150 ml volumetric flasks
1000 ml volumetric flask
Access to a nearby sink
100 ml volumetric flask
Wash bottle
10 ml pipette
5 ml pipette
1 ml pipette
Pipette bulbs
Ring stand
Disposable pipettes
3.8 l container
Paper towels
Spectrophotometer
Distilled water

Procedure:

1. Weigh out exactly 100 mg (0.10 gm) of powdered sample material. Transfer the sample to a 125 ml Erlenmeyer flask and add 4 ml of concentrated HCl; if the sample effervesces freely, add 4 additional ml of concentrated HCl.

2. Bring mixture to a boil on a hot plate (setting 5 or medium high) and boil for <u>exactly</u> one minute.

3. Filter the mixture into a 100 ml volumetric flask, being careful to thoroughly wash the Erlenmeyer flask and the filter paper. When finished, dilute the filtration solution to 100 ml with distilled water.

4. In two 50 ml volumetric flasks, add 10 ml of ammonium acetate solution and 5 ml of phenanthroline solution to each. Add 1 ml of hydroxyl amine solution to <u>one</u> of the flasks. Add 10 ml of the filtrate solution to each of the two flasks (not the blanks). Dilute to 50 ml with distilled water. At this point, there will be two blanks and two sample solutions. (four 50 ml volumetric flasks in all). Allow the color to develop for at least 15 minutes before measuring on the spectrophotometer. Shake the solutions a few times to help with color development.

5. Pipette each of the four volumetric flasks into the four cells of the spectrophotometer being careful not to spill on the cell walls. Use kmi-wipes to thoroughly clean the sides of the spectrophotometer cells. Use the blank without the hydroxyl amine in slot #1, the blank with the hydroxyl amine in slot #2, the sample filtrate without the hydroxyl amine in slot #3, and the filtrate solution with the hydroxyl amine in slot #4. Calibrate the spectrophotometer based on slot #1 at 510 u.

6. Slot #1 will provide a zero standard. Slot #2 will furnish a difference between samples with the hydroxyl amine solution and without the solution by taking the difference between the reading in slot #2 from the zero reading in slot #1. Slot #3 will provide the Fe^{++} and slot #4 will furnish the total acid-soluble iron.

7. The DOP is then calculated as follows:

$$\%S_{org} = 0.20^{*} \times \%TOC$$

$$S_{non\text{-}organic} = \%S_{total} - \%S_{organic}$$

$$Fe_{py} = S_{py} \times (55.85/64.12)$$

$$DOP = Fe_{py} / (Fe_{py} + Fe_{HCl})$$

*$S_{org}/TOC = 0.20$ from Bein, Almogi-Labin, and Sass (1990)

Appendix I. Fe-S-TOC Data

Desmoinesian Black Shale Samples

SAMPLE	%Fet	%St	%Sorg	TOC	Fe2sol	Fetsol	FePY	Spy	DOP	Fe2sol/FeTsol	FeTsol+FePY/%Fet	Spy/TOC
MECCA-TYPE SAMPLES												
Logan Quarry	12.95	15.60	0.16	22.93	1.21	2.36	7.67	8.80	0.76	0.51	0.77	0.38
Holland Shale	3.49	2.20	0.19	26.91	0.62	1.19	0.79	0.91	0.40	0.52	0.57	0.03
MQSB-1	3.50	3.30	0.28	39.72	0.43	0.64	2.09	2.39	0.76	0.66	0.78	0.06
Velpen A	3.22	2.50	0.11	15.35	0.27	0.76	1.31	1.51	0.63	0.36	0.64	0.10
Velpen B	3.95	3.00	0.08	11.27	0.74	1.25	1.34	1.54	0.52	0.59	0.66	0.14
Velpen C*	3.76	2.20	0.06	8.60	0.40	1.35	0.80	0.92	0.37	0.30	0.57	0.11
Velpen D	11.10	9.70	0.20	29.05	1.07	3.71	5.75	6.59	0.61	0.29	0.85	0.23
Hesler A1	3.86	3.28	0.31	43.74	0.48	0.62	2.31	2.65	0.79	0.77	0.76	0.06
Hesler A2	3.86	3.28	0.23	32.41	0.57	0.65	2.33	2.67	0.78	0.88	0.77	0.08
Hesler A3	3.63	2.80	0.20	28.58	0.50	0.65	2.08	2.39	0.76	0.78	0.75	0.08
Hesler A4	3.63	2.80	0.21	29.41	0.38	0.47	1.92	2.20	0.80	0.81	0.66	0.07
Hesler B1	3.38	3.37	0.21	29.57	0.45	0.79	1.80	2.06	0.69	0.57	0.76	0.07
Hesler B2	3.38	3.37	0.23	33.06	0.50	0.65	1.87	2.15	0.74	0.77	0.75	0.07
Hesler B3	3.85	2.50	0.11	15.33	0.51	1.34	1.60	1.84	0.54	0.38	0.76	0.12
Hesler B4	3.75	3.13	0.24	34.21	0.56	0.62	1.85	2.12	0.75	0.91	0.66	0.06
Hesler C*	4.39	3.53	0.05	6.87	0.90	1.60	2.24	2.57	0.58	0.56	0.87	0.37
Hesler D	4.75	4.64	0.14	20.60	0.39	1.56	1.91	2.19	0.55	0.25	0.73	0.11
Avg.	4.73	4.19	0.18	25.15	0.59	1.19	2.33	2.68	0.66	0.58	0.73	0.11

%Fet=total iron from XRF

%St=total sulfur from XRF

%Sorg=organic sulfur

%TOC=total organic carbon from C analyzer

Fe2sol=acid-soluble ferrous iron from colorimetric determination

Fetsol=total acid-soluble iron from colorimetric determination

FePY=pyrite iron, calculated from Spy*0.872

Spy=pyrite sulfur from chromium reduction method

DOP=degree of pyritization

Sorg/TOC=0.20 from Bein, Almogi-Labin, and Sass (1990)

*denotes gray shale

all other samples are black shales

data from Schultz and Coveney (in press)

Missourian Black Shale Samples

SAMPLE	%Fet	%St	%Sorg	TOC	Fe2sol	Fetsol	FePY	Spy	DOP	Fe2sol / FeTsol	FeTsol+FePY / %FeT	Spy/TOC
HEEBNER-TYPE SAMPLES												
EU-1	6.08	1.24	0.03	4.30	1.67	2.71	0.59	0.68	0.18	0.62	0.54	0.16
EU-2	3.95	1.77	0.20	29.24	0.82	1.08	0.86	0.99	0.44	0.76	0.49	0.03
MC-1	4.90	0.77	0.20	27.89	1.33	2.50	0.72	0.83	0.22	0.53	0.66	0.03
MC-2	5.85	1.41	0.19	26.88	0.89	1.59	0.77	0.88	0.33	0.56	0.40	0.03
MC-3	5.45	0.87	0.17	24.77	1.16	2.99	0.58	0.67	0.16	0.39	0.66	0.03
ST-1*	6.77	1.30	0.04	6.23	1.73	2.73	0.72	0.83	0.21	0.63	0.51	0.13
ST-1A	8.29	2.76	0.14	20.64	1.08	4.26	1.17	1.34	0.22	0.25	0.65	0.06
ST-1B	7.92	3.60	0.15	21.76	1.24	3.50	1.75	2.01	0.33	0.35	0.66	0.09
ST-1C	7.90	3.01	0.06	8.70	1.25	4.43	1.44	1.65	0.25	0.28	0.74	0.19
ST-1D	5.89	3.58	0.02	3.44	1.45	3.45	1.54	1.77	0.31	0.42	0.85	0.51
ST-1E	7.87	3.50	0.18	25.36	1.69	3.19	1.47	1.69	0.32	0.53	0.59	0.07
ST-1F	6.87	3.46	0.15	20.75	1.20	3.01	1.49	1.71	0.33	0.40	0.66	0.08
ST-1G*	7.80	3.16	0.02	2.48	1.18	3.43	1.44	1.65	0.30	0.34	0.62	0.67
ST-1H	6.44	3.51	0.14	20.22	1.33	3.12	1.59	1.82	0.34	0.43	0.73	0.09
ST-1I	6.66	2.49	0.07	10.43	1.24	3.83	0.99	1.13	0.20	0.32	0.72	0.11
ST-1J	5.72	2.37	0.10	14.40	1.44	2.78	0.95	1.09	0.25	0.52	0.65	0.08
ST-1K	7.07	2.15	0.07	10.24	0.83	2.96	0.91	1.04	0.23	0.28	0.55	0.10
ST-1L	4.03	2.41	0.13	18.60	1.28	2.26	0.98	1.12	0.30	0.57	0.80	0.06
ST-1M	6.05	1.59	0.11	15.17	1.07	2.50	0.72	0.83	0.22	0.43	0.53	0.05
ST-1N	6.55	2.04	0.09	12.17	1.43	3.54	0.85	0.98	0.19	0.40	0.67	0.08
ST-1O	5.27	2.53	0.14	20.11	0.96	4.70	0.92	1.06	0.16	0.20	1.07	0.05
ST-1P	6.08	1.45	0.07	10.30	1.83	2.56	0.89	1.02	0.26	0.71	0.57	0.10
ST-2	4.19	1.94	0.09	13.08	1.07	1.76	0.86	0.99	0.33	0.61	0.63	0.08
ST-3	4.49	1.67	0.09	12.63	0.52	1.01	0.75	0.86	0.43	0.51	0.39	0.07
HP-3	4.84	0.87	0.06	8.93	0.39	0.96	0.36	0.41	0.27	0.41	0.27	0.05
HP-4	4.30	1.68	0.16	23.18	1.16	1.70	0.68	0.78	0.29	0.68	0.55	0.03
Avg.	6.05	2.20	0.11	15.84	1.20	2.79	1.00	1.15	0.26	0.47	0.62	0.12

%FeT=total iron from XRF
%St=total sulfur from XRF
%Sorg=organic sulfur
%TOC=total organic carbon from C analyzer
Fe2sol=ferrous iron content from colorimetric determination
Fetsol=acid soluble iron from colorimetric determination
FePY=pyrite iron, calculated by Spy * 0.872
Spy=pyrite sulfur from chromium reduction method
DOP=degree of pyritization
Sorg/TOC=0.20 from Bein, Almogi-Labin, and Sass (1990)

EU=Eudora
MC=Muncie Creek
ST=Stark
HP=Hushpuckney

*denotes gray shale
all other samples are black shales

data from Schultz and Coveney (in press)

Virgilian Black Shale Samples

Sample	%Fe	%S	%Sorg	%TOC	Fe2sol	FeTsol	FePY	Spy Snon-org	DOP	Fe2sol FeTsol	FeTsol+FePY %Fe	Spy/TOC
HEEBNER-TYPE SAMPLES												
LB1	6.40	0.88	0.11	15.23	0.81	1.75	0.67	0.77	0.28	0.46	0.39	0.051
LB2*	5.75	trace	0.00	0.06	0.19	2.61	0.00	0.00	0.00	0.07	0.61	0.000
LB3	6.08	1.06	0.11	16.12	0.69	1.28	0.83	0.95	0.39	0.54	0.36	0.059
LB4	6.87	0.67	0.13	18.41	0.89	2.09	0.47	0.54	0.18	0.43	0.39	0.030
LB5	6.76	2.50	0.13	18.53	1.13	1.72	2.06	1.21	0.54	0.66	0.56	0.065
QH1	5.04	1.61	0.11	15.00	0.49	0.73	1.31	1.51	0.64	0.66	0.41	0.100
QH2*	5.31	0.01	0.01	1.00	0.81	1.57	0.00	0.00	0.00	0.52	0.30	0.003
QH3	4.86	0.86	0.11	16.37	0.64	1.18	0.65	0.75	0.36	0.54	0.40	0.046
QH4	4.99	0.78	0.08	11.19	0.87	1.30	0.61	0.70	0.32	0.67	0.39	0.063
QH5*	6.43	trace	0.00	0.27	0.25	2.49	0.00	0.00	0.00	0.10	0.39	0.000
QH6	5.87	0.05	0.02	2.28	1.22	2.59	0.03	0.03	0.01	0.47	0.46	0.015
QHC-1	4.44	1.91	0.03	3.83	0.44	0.72	1.64	1.88	0.70	0.61	0.53	0.492
QHC-2	4.67	1.99	0.03	4.00	0.57	0.85	1.71	1.96	0.67	0.68	0.54	0.491
QHC-3	3.27	0.84	0.01	1.20	0.39	0.64	0.72	0.83	0.53	0.60	0.42	0.693
QHC-4*	2.72	0.51	0.00	0.18	0.25	0.50	0.44	0.51	0.47	0.50	0.36	2.826
QHC-5*	1.77	1.65	0.00	0.20	0.31	0.87	1.44	1.65	0.62	0.36	1.33	8.243
QHC-6*	3.52	2.60	0.01	0.96	0.35	1.33	2.26	2.59	0.63	0.26	1.01	2.701
QHC-7*	3.21	1.53	0.00	0.31	0.35	1.06	1.33	1.53	0.56	0.33	0.74	4.928
QHC-8*	3.49	1.76	0.00	0.34	0.40	1.16	1.53	1.76	0.57	0.35	0.76	5.169
QHC-9*	5.28	4.37	0.01	1.22	0.39	1.68	3.80	4.36	0.69	0.23	1.02	3.575
HB1	5.70	1.19	0.06	8.80	0.70	1.44	0.98	1.13	0.41	0.49	0.43	0.128
HB-2*	6.08	0.02	0.01	0.93	0.37	1.09	0.01	0.01	0.01	0.34	0.19	0.015
HB3	5.40	0.95	0.02	2.18	0.78	1.32	0.81	0.93	0.38	0.59	0.40	0.429
HB4	4.69	0.21	0.03	3.58	0.71	1.56	0.16	0.18	0.09	0.45	0.38	0.052
HBC-1*	0.70	0.16	0.00	0.59	0.45	0.50	0.14	0.16	0.21	0.90	1.00	0.264
HBC-2*	0.86	0.22	0.00	0.71	0.29	0.50	0.19	0.22	0.27	0.58	0.97	0.303
HBC-3*	0.83	0.20	0.00	0.64	0.22	0.47	0.17	0.20	0.27	0.47	0.94	0.306
HBC-4*	1.94	0.13	0.00	0.01	0.19	0.48	0.11	0.13	0.19	0.41	0.34	
HBC-5*	2.01	0.08	0.00	0.07	0.22	0.40	0.07	0.08	0.15	0.54	0.27	1.136
HBC-6*	1.51	0.73	0.01	1.35	0.25	0.50	0.63	0.72	0.56	0.51	0.80	0.534
HBC-7*	0.58	0.13	0.00	0.32	0.09	0.28	0.11	0.13	0.29	0.32	0.94	0.399
Avg.	4.10	0.95	0.03	4.71	0.51	1.18	0.80	0.88	0.35	0.47	0.58	1.068
SHANGHAI-TYPE SAMPLES												
SH1	6.13	1.44	0.03	4.74	0.98	1.45	1.23	1.41	0.46	0.67	0.44	0.297
SH2	6.10	0.05	0.03	3.72	0.55	1.93	0.02	0.02	0.01	0.29	0.33	0.006
SH3*	6.54	0.03	0.02	2.52	0.96	2.47	0.01	0.01	0.00	0.39	0.39	0.005
SH4	4.44	0.47	0.01	1.40	1.03	1.58	0.40	0.46	0.20	0.65	0.45	0.329
SH5	6.27	1.53	0.07	10.38	0.58	1.35	1.27	0.86	0.48	0.43	0.42	0.083
SHC-1*	2.43	0.81	0.00	0.01	0.38	0.75	0.71	0.81	0.49	0.50	0.61	
SHC-2*	3.07	0.62	0.00	0.26	0.55	1.03	0.54	0.62	0.34	0.54	0.52	2.378
SHC-3*	3.07	0.83	0.01	1.16	0.41	0.82	0.72	0.82	0.47	0.51	0.51	0.709
HO1	5.22	0.04	0.01	2.06	0.44	1.96	0.02	0.03	0.01	0.23	0.39	0.012
Avg.	4.81	0.65	0.02	2.92	0.65	1.48	0.55	0.56	0.27	0.47	0.45	0.424

**Sorg/TOC=0.20 from Bein, Almogi-Labin, and Sass (1990)

%TOC=% total organic carbon

Fe2sol=ferrous iron content

FeTsol=ferric iron content

FePY=pyritic iron

Spy=pyrite sulfur

*denotes gray shale

all other samples are black shales

(data from Schultz and Coveney, in press)

SAMPLE	%Fet	%St	%Sorg	Total C	TOC	Cnon-org	Snon-org	Fe2sol	Fetsol	FePY	Spy	C/S ratio	DOP
SH-5	6.27	1.53	0.0727	15.33	10.38	4.95	1.457	0.58	1.35	0.75	0.86	6.78	0.36
LB-5	6.76	2.50	0.1297	22.36	18.53	3.83	2.370	1.13	1.72	1.06	1.21	7.41	0.38
HP-3	4.84	0.87	0.0625	15.34	8.93	6.41	0.808	0.39	0.96	0.36	0.41	10.26	0.27
HP-4	4.30	1.68	0.1623	28.68	23.18	5.50	1.518	1.16	1.70	0.68	0.78	13.80	0.29
EU-1	6.08	1.24	0.0301	7.34	4.30	3.04	1.209	1.67	2.71	0.59	0.68	3.47	0.18
EU-2	3.95	1.77	0.2047	37.33	29.24	8.09	1.975	0.82	1.08	0.86	0.99	16.52	0.44
ST-1	6.77	1.30	0.0436	7.85	6.23	1.62	1.256	1.73	2.73	0.72	0.83	4.79	0.21
ST-1A	8.29	2.76	0.1444	21.25	20.64	0.61	2.904	1.08	4.26	1.17	1.34	7.48	0.22
ST-1B	7.92	3.60	0.1523	22.01	21.76	0.25	3.448	1.24	3.50	1.75	2.01	6.04	0.33
ST-1C	7.90	3.01	0.0609	8.95	8.70	0.25	2.949	1.25	4.43	1.44	1.65	2.89	0.25
ST-1D	5.89	3.58	0.0241	7.34	3.44	3.90	3.556	1.45	3.45	1.54	1.77	0.96	0.31
ST-1E	7.87	3.50	0.1775	27.14	25.36	1.78	3.323	1.69	3.19	1.47	1.69	7.25	0.32
ST-1F	6.87	3.46	0.1453	22.88	20.75	2.13	3.315	1.20	3.01	1.49	1.71	6.00	0.33
ST-1G	7.80	3.16	0.0174	5.22	2.48	2.74	3.143	1.18	3.43	1.44	1.65	0.79	0.30
ST-1H	6.44	3.51	0.1415	27.18	20.22	6.96	3.368	1.33	3.12	1.59	1.82	5.76	0.34
ST-1I	6.66	2.49	0.0730	11.88	10.43	1.45	2.417	1.24	3.83	0.99	1.13	4.19	0.20
ST-1J	5.72	2.37	0.1008	20.56	14.40	6.16	2.269	1.44	2.78	0.95	1.09	6.08	0.25
ST-1K	7.07	2.15	0.0717	11.34	10.24	1.10	2.078	0.83	2.96	0.91	1.04	4.76	0.23
ST-1L	4.03	2.41	0.1302	28.45	18.60	9.85	2.280	1.28	2.26	0.98	1.12	7.72	0.30
ST-1M	6.05	1.59	0.1062	17.94	15.17	2.77	1.484	1.07	2.50	0.72	0.83	9.54	0.22
ST-1N	6.55	2.04	0.0852	14.22	12.17	2.05	1.955	1.43	3.54	0.85	0.98	5.97	0.19
ST-1O	5.27	2.53	0.1408	28.44	20.11	8.33	2.389	0.96	4.70	0.92	1.06	7.95	0.16
ST-1P	6.08	1.45	0.0721	12.45	10.30	2.15	1.378	1.83	2.56	0.89	1.02	7.10	0.26
ST-2	4.19	1.94	0.0916	22.58	13.08	9.50	1.848	1.07	1.76	0.86	0.99	6.74	0.33
ST-3	4.49	1.67	0.0884	13.02	12.63	0.39	1.582	0.52	1.01	0.75	0.86	7.56	0.43
MC-1	4.90	0.77	0.1952	35.89	27.89	8.00	0.575	1.33	2.50	0.72	0.83	36.22	0.22
MC-2	5.85	1.41	0.1882	28.93	26.88	2.05	1.600	0.89	1.59	0.77	0.88	19.06	0.33
MC-3	5.45	0.87	0.1734	31.99	24.77	7.22	0.697	1.16	2.99	0.58	0.67	28.47	0.16

%FeT=total iron from XRF
%St=total sulfur from XRF
%Sorg=organic sulfur
%TOC=total organic carbon from C analyzer
Cnon-org=non-organic carbon (Total C - TOC)
Snon-org=non-organic sulfur (%St - Sorg)
Fe2sol=ferrous iron content from colorimetric determination
Fetsol=acid soluble iron from colorimetric determination
FePY=pyrite iron
Spy=pyrite sulfur from chromium reduction method
DOP=degree of pyritization
Sorg/TOC=0.20 from Bein, Almogi-Labin, and Sass (1990)

HP=Hushpuckney
SH=Shanghai Creek
ST=Stark
EU=Eudora
LB=Larsh/Burroak
MC=Muncie Creek

Appendix J. INAA (Instrumental Neutron Activation Analyses)

Member	Mecca Quarry	Mecca Quarry	Mecca Quarry	Mecca Quarry	Mecca Quarry	Mecca Quarry	Mecca Quarry
Location	Hesler	Hesler	Hesler	Hesler	Hesler	Hesler	Hesler
Bed	A1 upper	A2 lower	B1 upper	B3 lower	B4 lower	C	D
Thickness	8.9 cm	8.9 cm	9.0 cm	9.0 cm	9.0 cm	8.8 cm	4.2 cm
Element	Concentrations:						
Boron (ppm)	93	118	85	128	109	135	146
Sodium (ppm)	2089	3392	2348	4490	2857	5084	2772
Magnesium (ppm %)	11409	1	9062	1	10289	13643	10081
Aluminum (ppm %)	53797	7	46599	8	60078	81850	60523
Silicon (ppm %)	143960	20	120840	21	158900	236290	149450
Phosphorus (ppm %)	~20000	~2	~20000	~2	~20000	~20000	~20000
Sulfur (ppm %)	32780	3	33680	3	31320	35320	46390
Chlorine (ppm)	203	~50	237	~50	147	136	133
Potassium (ppm %)	18134	2	17134	3	21283	28357	17129
Calcium (ppm %)	6525	0	5476	0	4621	16270	3629
Scandium (ppm)	14	16	12	16	12	15	10
Titanium (ppm %)	1889	0	1982	0	2811	3759	2609
Vanadium (ppm)	2180	2855	2849	2905	1799	804	439
Chromium (ppm)	564	522	609	424	353	146	182
Manganese (ppm)	167	200	127	192	167	271	192
Iron (ppm %)	38556	4	33768	4	37531	43923	47519
Cobalt (ppm)	24	28	23	29	20	18	25
Nickel (ppm)	457	274	530	153	455	197	300
Zinc (ppm)	2868	1720	3349	860	1457	220	464
Gallium (ppm)	15	16	16	23	18	20	17
Arsenic (ppm)	29	30	35	28	26	35	31
Selenium (ppm)	190	162	231	147	165	95	130
Bromine (ppm)	5	4	10	3	8	~3.4	2
Rubidium(ppm)	105	124	85	150	115	145	95
Strontium (ppm)	~81	~99	~74	~96	~70	168	137
Molybdenum (ppm)	1248	1023	1433	869	1259	519	855
Silver (ppm)		9		6			
Cadmium (ppm)	117	83	151	36	76	10	38
Antimony (ppm)	45	33	52	33	40	19	16
Cesium (ppm)	5	7	5	9	6	8	5
Barium(ppm)	340	764	298	887	301	519	318
Lanthanum (ppm)	31	40	42	40	33	47	23
Cerium(ppm)	59	63	59	65	54	91	49
Neodymium (ppm)	42	30	49	27	35	50	29
Samarium (ppm)	6	6	9	5	5	10	6
Europium (ppm)	1	1	2	1	1	2	1
Gadolinium (ppm)	6	3	8	4	5	10	7
Terbium (ppm)	1	1	1	1	1	1	1
Dysprosium (ppm)	5	5	8	4	4	8	4
Ytterbium (ppm)	3	4	4	3	3	4	2
Lutetium (ppm)	1	1	1	0	0	1	0
Hafnium (ppm)	2	3	2	4	3	4	2
Tantalum (ppm)	1	1	1	1	1	1	1
Tungsten (ppm)	5	3	15	5	7	6	5
Iridium (ppm)		~1.1		~1.1			
Gold (ppb)	2	4	2	3	2	2	1
Thorium (ppm)	8	9	7	11	8	11	8
Uranium (ppm)	129	114	165	77	122	85	62

Member	Holland Shale	Logan Quarry Shale	Mecca Quarry	Mecca Quarry	Mecca Quarry	Mecca Quarry	Mecca Quarry
Location	Barren Creek	Big Pond Creek	Velpen	Velpen	Velpen	Velpen	Velpen
Bed	Bed 5	Bed Kb	A	B	C	D	B
Thickness			14 cm	15 cm	23 cm	2.5 cm	MQSB-1
Element	Concentrations:						
Boron (ppm)	75	62	90	68	97	149	70
Sodium (ppm)	1602	1411	2523	2011	4311	1013	2000
Magnesium (%)	0.3	0.9	0.4	0.3	0.7	1	0.7
Aluminum (%)	4.44	2.82	6.64	4.42	7.86	3.79	4.9
Silicon (%)	9.2	7.5	21.3	17.2	25	13	13.5
Phosphorus (%)	6	~2	~2	~2	~2	~2	1
Sulfur (%)	2.2	15.6	2.5	3	2.2	9.7	3.3
Chlorine (ppm)	50	89	339	149	~50	161	18.5
Potassium (%)	1.57	0.88	2.36	1.6	2.51	1.23	1.7
Calcium (%)	0.7	3.97	~.18	~.17	0.66	1.98	0.4
Scandium (ppm)	15.6	7.6	14.7	12.1	14.4	7.7	12
Titanium (%)	0.212	~.32	0.305	0.173	0.403	0.188	0.223
Vanadium (ppm)	1601	328	1370	2941	1191	474	2984
Chromium (ppm)	337	100	366	459	196	163	461
Manganese (ppm)	212	13376	310	74	1525	347	695
Iron (%)	2.49	12.95	3.22	2.95	3.76	11.1	3.5
Cobalt (ppm)	23.4	32.5	15.3	30.7	20.4	42.2	24
Nickel (ppm)	505	95	146	380	195	132	417
Zinc (ppm)	2690	202	109	187	775	246	2830
Gallium (ppm)	17.6	9	20.1	14.1	19.5	11.3	15
Arsenic (ppm)	33.9	65.5	27.9	33.2	21.4	80.5	35
Selenium (ppm)	208.3	54.2	105.4	239.5	103	121.8	232
Bromine (ppm)	3.6	3.2	9.8	64	4.3	5.3	4.2
Rubidium(ppm)	78	47	123	83	142	74	95
Strontium (ppm)	~143	186	~84	~120	131	~88	
Molybdenum (ppm)	2016	180	916	2182	999	335	1655
Silver (ppm)	8.3	~1.2	4.3	9.1	4.2	4.2	
Cadmium (ppm)	331	10	5	18	33	7	103
Antimony (ppm)	46.9	12	29.5	63.8	21.1	13.4	62
Cesium (ppm)	4.23	2.59	6.64	4.11	7.81	3.53	4.7
Barium(ppm)	~296	~243	~196	938	803	~196	733
Lanthanum (ppm)	85.3	23.5	28.8	34.1	42.2	24.7	29
Cerium(ppm)	180.5	45.8	53.2	53.1	75.5	50	55
Neodymium (ppm)	207	24	25.6	32	34	26.6	35
Samarium (ppm)	49.73	4.56	5.77	6.52	6.1	5.43	30
Europium (ppm)	10.81	1.125	1.107	1.352	1.333	1.153	1.2
Gadolinium (ppm)	49.6	5.4	4.1	7	5.8	5.2	5.9
Terbium (ppm)	7.86	0.89	0.55	1.36	1.06	1.04	0.93
Dysprosium (ppm)	35.4	4.2	3.2	5.9	4.9	4.4	5
Ytterbium (ppm)	13.34	2.67	2.02	3.35	3.41	2.18	3
Lutetium (ppm)	1.778	0.412	0.264	0.512	0.558	0.326	0.45
Hafnium (ppm)	2.17	1.23	2.54	1.87	3.79	1.64	2
Tantalum (ppm)	0.623	0.77	1.152	0.9	0.983	0.851	0.6
Tungsten (ppm)	2.5	6.1	7.4	6	4.1	7.8	
Iridium (ppb)	~7.2	~2.4	~2.5	~1.4	~8.4	~1.6	
Gold (ppb)	6.6	2.1	3.6	3.2	~2.3	4	3
Thorium (ppm)	10.04	5.11	11.99	6.83	10.27	7.83	7.2
Uranium (ppm)	704.2	36.7	43.5	173.4	112.1	48.6	125

Member Location	SDO–1	Stark Shale ST–2	Stark Shale ST–3	Hushpuckney Shale HP–3	Hushpuckney Shale HP–4	Eudora Shale EU–1	Muncie Ck. Shale MC–1
Element	Concentrations:						
Boron (ppm)	130.00	80.00	120.00	90.00	90.00	130.00	110.00
Sodium (%)	0.32	0.47	0.48	0.42	0.57	0.80	0.64
Magnesium (%)	1.53	2.50	2.12	4.60	2.46	2.57	3.98
Aluminum (%)	12.30	9.56	14.30	11.80	10.00	16.00	14.00
Silicon (%)	47.50	36.70	48.40	41.10	31.70	54.20	45.20
Phosphorus (%)	0.10	5.43	0.15	0.04	5.21	0.07	0.13
Beryllium (ppm)	5.00	2.00	3.00	4.00	3.00	4.00	5.00
Potassium (%)	3.31	2.21	3.42	2.73	2.39	3.46	3.13
Calcium (%)	1.07	12.30	0.57	10.10	10.40	2.20	9.43
Scandium (ppm)	12.00	9.00	13.60	12.40	10.10	15.70	13.90
Titanium (%)	0.72	0.46	0.63	0.52	0.47	0.77	0.60
Vanadium (ppm)	170.00	1500.00	550.00	120.00	3000.00	200.00	100.00
Chromium (ppm)	110.00	290.00	990.00	450.00	780.00	290.00	150.00
Manganese (ppm, %	0.05	240.00	140.00	0.08	160.00	270.00	0.06
Iron (%)	9.43	4.08	3.87	4.49	3.78	5.42	4.78
Cobalt (ppm)	42.00	22.00	21.00	22.00	26.00	27.00	18.00
Nickel (ppm)	97.00	240.00	270.00	190.00	330.00	230.00	78.00
Zinc (ppm)	63.00	1500.00	820.00	250.00	7700.00	530.00	91.00
Copper (ppm)	50.20	61.10	73.20	97.60	58.60	63.80	64.70
Arsenic (ppm)	61	19.00	11.00	39.00	38.00	20.00	4.00
Selenium (ppm)	3.00	89.00	55.00	22.00	92.00	42.00	3.00
Bromine (ppm)	6.00	6.00	9.00	6.00	8.00	5.00	3.00
Rubidium(ppm)	150.00	90.00	180.00	110.00	100.00	160.00	160.00
Strontium (ppm)	70.00	530.00	90.00	260.00	430.00	130.00	410.00
Molybdenum (ppm)	160.00	200.00	36.00	25.00	280.00	15.00	7.00
Silver (ppm)	0.50	1.00	1.50	0.50	2.00	0.50	0.50
Cadmium (ppm)	1.00	74.00	8.00	3.00	180.00	4.00	1.00
Tin (ppm)	4.60	15.00	7.80	11.00	31.00	3.90	1.00
Cesium (ppm)	6.00	5.00	9.00	7.00	6.00	9.00	10.00
Barium(ppm)	520.00	230.00	400.00	290.00	260.00	410.00	340.00
Lanthanum (ppm)	37.90	123.00	19.40	19.80	40.50	30.90	22.90
Cerium(ppm)	70.00	185.00	27.00	29.00	57.00	45.00	39.00
Neodymium (ppm)	32.00	88.00	10.00	11.00	27.00	16.00	16.00
Samarium (ppm)	6.30	17.90	1.60	1.60	5.60	2.50	2.70
Europium (ppm)	1.50	3.80	0.40	0.30	1.10	0.50	0.50
Germanium (ppm)	10.00	10.00	10.00	10.00	10.00	10.00	10.00
Gadolinium (ppm)	1.1	2.90	0.50	0.50	0.80	0.50	0.50
Ytterbium (ppm)	3.1	6.30	1.50	1.60	2.80	1.90	1.80
Lutetium (ppm)	0.40	0.88	0.24	0.25	0.38	0.33	0.28
Hafnium (ppm)	4.00	2.00	3.00	2.00	2.00	4.00	3.00
Tantalum (ppm)	1.00	1.00	1.00	1.00	1.00	1.00	1.00
Tungsten (ppm)	3.00	24.00	17.00	16.00	11.00	13.00	11.00
Iridium (ppb)	30.00	200.00	20.00	20.00	130.00	20.00	20.00
Gold (ppb)	5.00	5.00	5.00	5.00	5.00	5.00	5.00
Thorium (ppm)	8.90	7.80	8.70	6.10	6.90	10.00	8.30
Uranium (ppm)	41.50	253.00	11.70	10.40	169.00	8.70	4.60

Member Location Bed Thickness	Heebner Shale HB-1	Shanghai Ck. Shale SH-1	Shanghai Ck. Shale SH-2	Larsh/Burroak Shale LB-3	Larsh/Burroak Shale LB-4	Queen Hill Shale QH-1	Queen Hill Shale QH-3
Element	Concentrations:						
Boron (ppm)	130.00	160.00	120.00	140.00	140.00	140.00	120.00
Sodium (%)	0.65	0.68	0.68	0.50	0.50	0.45	0.55
Magnesium (%)	1.98	2.17	2.18	2.11	1.97	2.27	1.85
Aluminum (%)	14.20	18.60	19.00	14.30	14.60	12.70	12.30
Silicon (%)	45.50	50.20	50.30	39.60	40.40	41.80	40.80
Phosphorus (%)	3.06	0.76	0.18	0.20	1.59	2.20	1.00
Sulfur (%)	1.19	1.44	0.05	1.06	0.67	1.61	0.84
Beryllium (ppm)	5.00	6.00	6.00	6.00	5.00	5.00	4.00
Potassium (%)	3.22	3.64	3.62	3.44	3.13	2.94	2.75
Calcium (%)	5.28	2.01	1.46	0.82	3.29	2.42	4.09
Scandium (ppm)	14.60	18.10	17.00	15.30	14.10	11.80	12.70
Titanium (%)	0.68	0.80	0.83	0.67	0.64	0.59	0.61
Vanadium (ppm)	600.00	180.00	160.00	2400.00	1100.00	1100.00	600.00
Chromium (ppm)	460.00	360.00	380.00	870.00	790.00	910.00	890.00
Manganese (ppm)	0.04	0.04	0.03	0.04	0.03	0.04	0.03
Iron (%)	5.31	5.54	5.46	5.01	5.49	4.06	3.94
Tin (ppm)	9.10	2.10	1.10	11.00	6.30	8.10	2.90
Nickel (ppm)	200.00	190.00	210.00	470.00	460.00	330.00	260.00
Zinc (ppm)	65.00	84.00	220.00	1900.00	3400.00	1800.00	830.00
Cobalt (ppm)	25.00	19.00	11.00	16.00	22.00	12.00	17.00
Arsenic (ppm)	29.00	26.00	9.00	18.00	15.00	13.00	9.00
Selenium (ppm)	15.00	10.00	<3	65.00	98.00	30.00	19.00
Bromine (ppm)	4.00	4.00	3.00	5.00	4.00	6.00	4.00
Rubidium(ppm)	140.00	180.00	190.00	170.00	140.00	150.00	130.00
Strontium (ppm)	150.00	170.00	150.00	120.00	220.00	100.00	190.00
Molybdenum (ppm)	10.00	<5	5.00	76.00	35.00	83.00	13.00
Silver (ppm)	1.00	<0.5	<0.5	<0.5	1.00	1.50	1.00
Cadmium (ppm)	<1	<1	3.00	140.00	58.00	48.00	31.00
Copper (ppm)	60.00	97.00	110.00	110.00	130.00	73.00	74.00
Cesium (ppm)	8.00	9.00	10.00	8.00	7.00	6.00	7.00
Barium(ppm)	400.00	400.00	450.00	380.00	360.00	370.00	430.00
Lanthanum (ppm)	72.00	45.50	36.70	32.50	53.10	26.10	38.20
Cerium(ppm)	150.00	85.00	56.00	51.00	108.00	48.00	57.00
Neodymium (ppm)	75.00	41.00	22.00	23.00	63.00	21.00	26.00
Samarium (ppm)	15.00	8.20	3.20	3.00	10.00	3.90	5.60
Europium (ppm)	3.40	1.80	0.80	0.70	2.30	0.70	1.20
Lead (ppm)	50.00	28.00	78.00	100.00	160.00	52.00	48.00
Terbium (ppm)	2.20	1.20	<.5	0.50	1.30	0.50	0.70
Niobium (ppm)	<10	10.00	20.00	<10	20.00	10.00	10.00
Ytterbium (ppm)	4.10	2.90	1.90	2.10	3.70	2.00	2.50
Scandium (ppm)	14.60	18.10	17.00	15.30	14.10	11.80	12.70
Hafnium (ppm)	3.00	4.00	4.00	3.00	3.00	3.00	3.00
Tantalum (ppm)	<1	1.00	1.00	1.00	1.00	1.00	1.00
Tungsten (ppm)	9.00	<3	<3	<3	<3	<3	20.00
Iridium (ppb)	<20	<20	<20	<20	<20	<20	<20
Gold (ppb)	<5	<5	<5	6.00	9.00	<5	<5
Thorium (ppm)	9.80	12.00	13.00	10.00	10.00	9.00	8.90
Uranium (ppm)	31.40	14.10	9.90	27.00	48.70	49.00	42.90
Zirconium (ppm)	140.00	150.00	160.00	130.00	130.00	130.00	120.00

Member Location	Queen Hill Core QHC-1	Queen Hill Core QHC-2	Heebner Core HBC-6	Shanghai Ck. Core SHC-2	Shanghai Ck. Core SHC-3	Queen Hill QH-1	Queen Hill QH-3
Element	Concentrations:						
Boron (ppm)	140.00	180.00	50.00	90.00	50.00	140.00	120.00
Sodium (%)	1.13	1.17	0.45	0.78	0.42	0.45	0.55
Magnesium (%)	3.45	3.68	3.43	1.94	1.66	2.27	1.85
Aluminum (%)	14.40	14.80	4.84	9.10	6.26	12.70	12.30
Silicon (%)	48.30	49.20	20.40	29.50	19.70	41.80	40.80
Phosphorus (%)	0.11	0.17	0.55	0.07	0.08	2.20	1.00
Sulfur (%)	1.91	1.99	0.73	0.62	0.83	1.61	0.84
Beryllium (ppm)	4.00	2.50	1.00	2.00	2.00	5.00	4.00
Potassium (%)	3.91	4.12	1.00	1.48	0.86	2.94	2.75
Calcium (%)	5.84	7.18	36.20	27.70	37.50	2.42	4.09
Scandium (ppm)	12.60	14.10	5.00	8.80	7.00	11.80	12.70
Titanium (%)	0.67	0.68	0.24	0.40	0.24	0.59	0.61
Vanadium (ppm)	190.00	97.00	41.00	63.00	35.00	1100.00	600.00
Chromium (ppm)	200.00	150.00	100.00	33.00	<10	910.00	890.00
Manganese (ppm)	0.03	0.03	0.03	0.06	0.06	0.04	0.03
Iron (%)	4.99	3.68	1.36	3.42	2.06	4.06	3.94
Tin (ppm)	5.30	2.80	0.50	0.40	0.40	8.10	2.90
Nickel (ppm)	130.00	94.00	37.00	37.00	30.00	330.00	260.00
Zinc (ppm)	100.00	47.00	230.00	36.00	27.00	1800.00	830.00
Cobalt (ppm)	17.00	19.00	4.00	20.00	19.00	12.00	17.00
Arsenic (ppm)	61.00	36.00	3.00	5.00	5.00	13.00	9.00
Selenium (ppm)	8.00	3.00	3.00	<3	<3	30.00	19.00
Bromine (ppm)	3.00	3.00	4.00	17.00	16.00	6.00	4.00
Rubidium(ppm)	150.00	130.00	40.00	60.00	50.00	150.00	130.00
Strontium (ppm)	220.00	290.00	520.00	380.00	330.00	100.00	190.00
Molybdenum (ppm)	44.00	35.00	<5	<5	<5	83.00	13.00
Silver (ppm)	1.00	0.50	<.5	<0.5	<.5	1.50	1.00
Cadmium (ppm)	<1	<1	2.00	<1	<1	48.00	31.00
Copper (ppm)	56.00	31.00	7.60	15.00	9.10	73.00	74.00
Cesium (ppm)	8.00	11.00	39.00	5.00	4.00	6.00	7.00
Barium(ppm)	320.00	250.00	100.00	140.00	70.00	370.00	430.00
Lanthanum (ppm)	28.30	27.50	30.20	18.30	14.50	26.10	38.20
Cerium(ppm)	47.00	50.00	39.00	37.00	32.00	48.00	57.00
Neodymium (ppm)	18.00	21.00	22.00	12.00	11.00	21.00	26.00
Samarium (ppm)	3.20	4.00	3.60	2.20	2.00	3.90	5.60
Europium (ppm)	0.60	0.90	0.80	0.40	0.50	0.70	1.20
Lead (ppm)	82.00	28.00	24.00	4.00	2.00	52.00	48.00
Terbium (ppm)	0.50	0.60	<0.5	<0.5	<.5	0.50	0.70
Niobium (ppm)	20.00	10.00	<10	<10	<10	10.00	10.00
Ytterbium (ppm)	2.00	2.30	1.60	1.20	1.00	2.00	2.50
Scandium (ppm)	12.60	14.10	5.00	8.80	7.00	11.80	12.70
Hafnium (ppm)	3.00	4.00	1.00	2.00	1.00	3.00	3.00
Tantalum (ppm)	<1	<1	<1	<1	<1	1.00	1.00
Tungsten (ppm)	11.00	<3	<3	18.00	19.00	<3	20.00
Iridium (ppb)	<20	<20	<20	<20	<20	<20	<20
Gold (ppb)	<5	<5	<5	<5	<5	<5	<5
Thorium (ppm)	8.10	10.00	3.60	5.00	3.50	9.00	8.90
Uranium (ppm)	11.50	22.50	22.20	2.10	1.70	49.00	42.90
Zirconium (ppm)	140.00	130.00	40.00	70.00	30.00	130.00	120.00

LOCATION:	Jackson Cty., MO 31st St. Hushpuckney Sh. HP-1	Jackson Cty., MO Unity Village Hushpuckney Sh. < 36 cm HP-2	Jackson Cty., MO Unity Village Hushpuckney Sh. < 41 cm HP-2A	Douglas Cty., KS Clinton Lake Heebner Sh. 39 cm HB-5
ELEMENT	Concentrations:			
Boron (ppm)	105.00	94.80	94.10	103.20
Sodium (ppm)	5705.00	3916.00	3592.00	4007.00
Magnesium (%)	1.20	1.51	1.43	1.51
Aluminum (%)	5.89	6.90	6.78	6.75
Silicon (%)	19.00	18.51	19.24	21.56
Phosphorus (%)	2.00	2.00	2.00	2.00
Sulfur (%)	1.50	1.36	1.67	2.22
Chlorine (ppm)	565.00	259.00	148.00	147.00
Potassium (%)	2.25	2.14	2.16	2.22
Calcium (%)	4.27	4.67	2.52	3.68
Scandium (ppm)	13.40	12.88	11.96	13.68
Titanium (%)	0.32	0.35	0.32	0.33
Vanadium (ppm)	584.00	790.00	1146.00	925.00
Chromium (ppm)	757.00	538.90	572.20	656.00
Manganese (ppm)	175.00	191.30	148.80	202.40
Iron (%)	2.86	3.34	3.36	3.84
Cobalt (ppm)	12.30	14.30	12.20	13.90
Nickel (ppm)	174.00	199.00	265.00	299.00
Zinc (ppm)	1077.00	1616.00	1926.00	2221.00
Gallium (ppm)	16.60	16.50	18.30	15.50
Arsenic (ppm)	32.70	38.70	24.70	41.00
Selenium (ppm)	72.80	75.90	103.10	118.10
Bromine (ppm)	8.80	7.50	7.00	7.30
Rubidium (ppm)	111.00	115.00	97.00	118.00
Strontium (ppm)	360.00	244.00	65.00	70.00
Molybdenum (ppm)	86.00	79.00	86.00	67.00
Silver (ppm)	5.50			
Cadmium (ppm)	23.00	53.90	55.30	55.70
Antimony (ppm)	15.20	14.89	15.11	16.89
Cesium (ppm)	6.96	7.10	6.32	7.18
Barium (ppm)	368.00	192.00	259.00	336.00
Lanthanum (ppm)	40.90	39.30	40.00	33.30
Cerium (ppm)	72.00	79.90	66.10	92.10
Neodymium (ppm)	44.60	47.80	42.20	57.50
Samarium (ppm)	7.68	8.98	8.81	5.68
Europium (ppm)	1.68	2.00	1.74	1.95
Gadolinium (ppm)	7.20	8.66	8.70	5.18
Terbium (ppm)	1.35	1.16	1.18	1.14
Dysprosium (ppm)	6.60	7.87	7.69	5.51
Ytterbium (ppm)	3.75	3.46	3.37	2.88
Lutetium (ppm)	0.55	0.56	0.47	0.55
Hafnium (ppm)	3.03	3.12	2.88	3.17
Tantalum (ppm)	0.84	0.93	0.85	0.99
Tungsten (ppm)	1.80	3.20	4.10	2.10
Iridium (ppm)	1.40			
Gold (ppb)	3.20	1.70	1.80	1.80
Thorium (ppm)	8.94	8.70	7.63	8.72
Uranium (ppm)	49.60	64.40	80.40	35.10

Member Location	Muncie Ck. Shale MC–1	Muncie Ck. Shale MC–2	Muncie Ck. Shale MC–3	Shanghai Ck. Shale SH–5
Element Concentration:				
Boron (ppm)	110.00	110.00	120.00	150.00
Sodium (%)	0.64	0.58	0.64	0.78
Magnesium (%)	3.98	2.02	3.85	2.41
Aluminum (%)	14.00	12.60	14.00	16.30
Silicon (%)	45.20	41.30	45.80	44.20
Phosphorus (%)	0.13	0.10	0.25	0.35
Beryllium (ppm)	5.00	3.00	4.00	4.00
Potassium (%)	3.13	2.84	3.10	3.31
Calcium (%)	9.43	0.49	8.92	3.69
Scandium (ppm)	13.90	13.20	14.10	16.40
Titanium (%)	0.60	0.59	0.62	0.74
Vanadium (ppm)	100.00	1100.00	100.00	270.00
Chromium (ppm)	150.00	1100.00	160.00	590.00
Manganese (ppm, %)	0.06	130.00	0.06	0.06
Iron (%)	4.78	4.10	4.62	5.42
Cobalt (ppm)	18.00	14.00	21.00	17.00
Nickel (ppm)	78.00	340.00	95.00	160.00
Zinc (ppm)	91.00	1900.00	98.00	70.00
Copper (ppm)	64.70	65.50	67.30	72.30
Arsenic (ppm)	4.00	13.00	4.00	11.00
Selenium (ppm)	3.00	100.00	4.00	23.00
Bromine (ppm)	3.00	11.00	3.00	5.00
Rubidium(ppm)	160.00	150.00	150.00	150.00
Strontium (ppm)	410.00	60.00	360.00	170.00
Molybdenum (ppm)	7.00	56.00	7.00	47.00
Silver (ppm)	0.50	1.00	0.50	0.50
Cadmium (ppm)	1.00	44.00	1.00	1.00
Tin (ppm)	1.00	9.10	1.10	1.70
Cesium (ppm)	10.00	7.00	9.00	9.00
Barium(ppm)	340.00	390.00	320.00	410.00
Lanthanum (ppm)	22.90	16.40	24.10	43.00
Cerium(ppm)	39.00	24.00	42.00	72.00
Neodymium (ppm)	16.00	8.00	18.00	33.00
Samarium (ppm)	2.70	1.20	3.30	6.30
Europium (ppm)	0.50	0.20	0.70	1.60
Germanium (ppm)	10.00	10.00	10.00	10.00
Gadolinium (ppm)	0.50	0.50	0.50	0.90
Ytterbium (ppm)	1.80	1.20	1.80	2.70
Lutetium (ppm)	0.28	0.19	0.28	0.40
Hafnium (ppm)	3.00	3.00	3.00	4.00
Tantalum (ppm)	1.00	1.00	1.00	1.00
Tungsten (ppm)	11.00	15.00	7.00	14.00
Iridium (ppb)	20.00	20.00	20.00	20.00
Gold (ppb)	5.00	5.00	5.00	5.00
Thorium (ppm)	8.30	8.00	8.40	11.00
Uranium (ppm)	4.60	22.10	5.60	28.10

Appendix K. Rare Earth Element (REE) Data

	PAAS	NASC	Avg. Heebner (n=22)	Avg. Mecca (n=17)	Avg. Shanghai (n=6)
La	38.00	32.00	36.29	37.42	25.31
Ce	80.00	73.00	60.29	68.39	47.22
Pr	8.90	7.90	7.17	9.32	5.16
Nd	32.00	33.00	29.81	46.02	18.62
	18.80	19.35	17.43	28.48	11.06
Sm	5.60	5.70	5.05	10.94	3.50
Eu	1.10	1.24	1.16	1.98	0.83
Gd	4.70	5.20	2.99	9.02	2.26
Tb	0.77	0.85	0.85	1.45	0.30
Dy	4.40	5.80	6.90	7.24	3.48
Ho	1.00	1.04	1.02	1.02	0.77
Er	2.90	3.40	3.00	2.99	2.24
Tm	0.40	0.50	0.43	0.43	0.32
Yb	2.80	3.10	2.56	3.71	1.61
Lu	0.43	0.48	0.43	0.56	0.23
Eu/Eu*	0.65	0.70	0.91	0.61	0.90

REE in NASC and PAAS compared with Pennsylvanian black shales of this study. Values in ppm. PAAS and NASC values from Taylor and McLennan (1985). Eu/Eu* defined as: Eu/[(Sm)(Gd)]1/2 where all values are chondrite-normalized. (from Schultz and Coveney, in press)

Appendix L. X-ray Diffraction (XRD): Samples and Representative Diffractograms

XRD Samples		
File	SAMPLE	FRACTION
RBS001	LB-5	POWDER
RBS002	EU-2	POWDER
RBS003	MC-3	POWDER
RBS004	HP-4	POWDER
RBS005	HB-5	POWDER
RBS006	QH-1	POWDER
RBS007	ST-1	POWDER
RBS008	SH-1	POWDER
RBS009	SH-5	POWDER
RBS010	HO-1	POWDER
RBS011	VELPEN B	POWDER
RBS012	HESLER A1	POWDER
RBS013	HESLER B1	POWDER
RBS014	HOLLAND	POWDER
RBS015	LOGAN Q.	POWDER
RBS016	HESLER B1	2mu
RBS017	VELPEN B	2mu
RBS018	HO-1	2mu
RBS019	LOGAN Q.	2mu
RBS020	SH-1	2mu
RBS021	EU-2	2mu
RBS022	MC-3	2mu
RBS023	HP-4	2mu
RBS024	SH-5	2mu
RBS025	HOLLAND	2mu
RBS026	QH-1	2mu
RBS027	ST-1	2mu
RBS028	HESLER A1	2mu
RBS029	HB-5	2mu
RBS030	LOGAN Q.	1mu
RBS031	VELPEN B	1mu
RBS032	SH-1	1mu
RBS033	HP-4	1mu
RBS034	ST-1	1mu
RBS035	MC-3	1mu
RBS036	EU-2	1mu
RBS037	QH-1	1mu
RBS038	LB-5	1mu
RBS039	HO-1	1mu
RBS040	HOLLAND	1mu
RBS041	HESLER B1	1mu
RBS042	SH-5	1mu
RBS043	QH-1	< 1mu
RBS044	EU-2	< 1mu
RBS045	HO-1	< 1mu
RBS046	ST-1	< 1mu
RBS047	HP-4	< 1mu
RBS048	HOLLAND	< 1mu
RBS049	MC-3	< 1mu
RBS050	SH-5	< 1mu
RBS051	MC-3	2mu GLY
RBS052	MC-3	1mu GLY
RBS053	MC-3	< 1mu GLY

Key Peaks on XRD Trace						
File	2Theta	D-spacing	Integ. I (%)	Integ. I	Max I	FWHM
RBS016	8.785	10.0567	100.0	2538	242	0.523
	9.362	9.4383	50.1	1273	84	0.754
	12.362	7.1539	7.8	198	38	0.260
	17.785	4.9830	1.1	28	30	0.047
	20.844	4.2579	5.3	135	44	0.152
	26.677	3.3387	18.8	477	98	0.244
RBS009	8.261	10.6935	11.5	247	74	0.168
	11.935	7.4090	10.6	227	80	0.142
	17.245	5.1377	7.3	156	27	0.290
	19.270	4.6022	15.2	326	69	0.235
	20.400	4.3497	17.4	375	69	0.271
	21.548	4.1205	7.2	155	33	0.239
	26.203	3.3980	100.0	2148	412	0.260
	27.480	3.2430	15.1	325	47	0.343
	28.971	3.0793	10.5	225	55	0.206
	34.289	2.6130	20.3	436	54	0.402
	34.519	2.5961	13.4	287	50	0.288
	36.119	2.4847	12.2	261	48	0.273
	39.089	2.3019	7.2	155	22	0.348
	42.029	2.1480	14.3	307	37	0.419
	49.771	1.8304	8.2	175	40	0.220
RBS003	8.779	10.0645	3.2	151	43	0.177
	12.277	7.2032	0.7	34	21	0.083
	19.521	4.5435	3.1	147	47	0.155
	19.754	4.4904	6.5	307	64	0.241
	20.834	4.2600	18.2	852	196	0.217
	25.175	3.5345	5.6	261	52	0.249
	25.369	3.5078	4.0	189	48	0.196
	26.615	3.3463	100.0	4688	1360	0.172
	27.819	3.2042	4.8	226	61	0.184
	29.420	3.0334	24.8	1163	301	0.193
	30.681	2.9115	26.0	1219	229	0.267
	33.040	2.7088	2.9	137	37	0.187
	34.585	2.5913	7.3	341	64	0.267
	34.719	2.5816	3.3	153	69	0.111
	36.019	2.4913	4.2	197	58	0.171
	36.518	2.4584	5.8	274	89	0.154
	39.444	2.2825	10.1	472	128	0.184
	40.233	2.2396	2.6	122	32	0.189
	40.901	2.2045	8.3	388	67	0.291
	42.427	2.1287	7.8	365	77	0.238
	43.204	2.0922	2.4	115	35	0.162
	44.669	2.0269	2.2	105	35	0.151
	45.768	1.9808	2.3	110	46	0.120

Key Peaks on XRD Trace						
File	2Theta	D-spacing	Integ. I (%)	Integ. I	Max I	FWHM
RBS017	8.647	10.2174	100.0	251	70	0.178
	12.299	7.1905	49.7	125	46	0.135
RBS004	8.355	10.5742	16.6	278	88	0.158
	12.008	7.3640	3.7	62	37	0.084
	19.339	4.5858	17.8	298	48	0.313
	20.428	4.3437	21.0	351	70	0.249
	25.402	3.5034	13.4	225	57	0.196
	26.213	3.3968	100.0	1672	351	0.239
	27.475	3.2435	12.8	215	34	0.316
	28.098	3.1731	8.9	150	36	0.206
	30.425	2.9355	21.3	356	48	0.368
	31.527	2.8353	75.2	1258	175	0.359
	32.692	2.7368	37.5	627	113	0.277
	33.685	2.6585	10.6	177	35	0.250
	36.158	2.4821	8.6	144	26	0.277
	38.943	2.3107	4.1	68	23	0.150
	39.673	2.2699	17.3	289	44	0.324
	40.668	2.2166	7.1	118	21	0.281
	42.021	2.1483	22.2	371	38	0.493
	46.482	1.9520	12.2	205	43	0.240
	47.154	1.9258	19.6	329	58	0.285
	49.171	1.8513	14.7	247	51	0.243
	49.774	1.8303	10.4	175	39	0.222
RBS001	8.714	10.1383	9.9	441	69	0.318
	11.543	7.6596	7.6	338	66	0.255
	12.332	7.1711	9.5	426	56	0.381
	17.620	5.0292	8.8	393	42	0.469
	19.678	4.5077	21.6	965	113	0.429
	20.744	4.2783	23.4	1047	220	0.238
	25.174	3.5346	12.9	576	48	0.595
	26.557	3.3536	100.0	4476	1028	0.218
	27.811	3.2051	8.7	390	78	0.250
	29.016	3.0747	7.3	327	69	0.237
	29.837	2.9920	7.1	317	42	0.378
	30.891	2.8922	12.2	546	59	0.464
	31.969	2.7971	3.6	162	28	0.291
	34.811	2.5750	32.6	1458	106	0.685
	36.470	2.4616	7.6	341	71	0.241
	37.454	2.3991	4.6	207	24	0.431
	39.396	2.2852	5.0	223	50	0.221
	40.198	2.2415	6.5	291	42	0.343
	42.393	2.1303	5.5	247	66	0.188
	44.601	2.0299	3.5	159	17	0.454
	48.317	1.8821	3.2	145	26	0.281

Key Peaks on XRD Trace						
File	2Theta	D-spacing	Integ. I (%)	Integ. I	Max I	FWHM
RBS025	8.762	10.0829	100.0	1757	158	0.557
	12.353	7.1593	9.4	165	54	0.154
RBS014	2.877	30.6848	12.3	349	67	0.262
	8.726	10.1254	16.0	453	55	0.415
	12.334	7.1699	12.3	349	52	0.336
	17.769	4.9873	5.7	162	26	0.305
	19.745	4.4924	16.9	480	75	0.321
	20.806	4.2657	12.8	364	102	0.179
	21.988	4.0390	3.4	96	36	0.134
	26.598	3.3484	100.0	2842	710	0.200
	28.532	3.1258	6.7	190	42	0.226
	31.897	2.8033	28.9	822	96	0.429
	33.030	2.7097	17.5	497	91	0.272
	34.135	2.6244	2.1	61	20	0.152
	34.849	2.5723	9.9	281	41	0.342
	39.460	2.2816	5.3	151	44	0.172
	40.747	2.2125	5.8	165	42	0.197
	42.412	2.1294	6.8	193	55	0.176
	45.783	1.9802	4.3	123	33	0.186
	47.444	1.9147	6.5	183	35	0.262
RBS013	3.447	25.6094	2.1	60	18	0.163
	8.712	10.1413	10.7	306	92	0.167
	12.323	7.1767	5.6	160	38	0.211
	17.599	5.0351	2.5	71	39	0.092
	19.634	4.5177	6.2	177	43	0.207
	19.712	4.4999	4.9	140	71	0.098
	20.823	4.2623	12.3	353	108	0.163
	24.854	3.5794	5.4	154	60	0.129
	26.612	3.3467	100.0	2868	772	0.186
	27.905	3.1946	3.6	102	49	0.105
	28.523	3.1267	11.6	334	108	0.155
	33.023	2.7102	15.6	447	142	0.157
	34.494	2.5979	5.7	162	37	0.219
	34.619	2.5888	2.6	74	35	0.107
	36.519	2.4583	6.7	193	51	0.188
	37.056	2.4240	10.6	305	81	0.187
	39.407	2.2846	3.2	91	33	0.140
	40.748	2.2124	9.7	278	63	0.221
	42.444	2.1279	5.3	152	45	0.170
	47.429	1.9152	8.7	250	68	0.184

Key Peaks on XRD Trace						
File	2Theta	D-spacing	Integ. I (%)	Integ. I	Max I	FWHM
RBS022	6.111	14.4504	0.3	123	166	0.037
	8.578	10.2992	100.0	38211	1107	1.726
	12.276	7.2037	6.7	2552	277	0.461
	17.621	5.0289	4.6	1752	169	0.518
	20.714	4.2845	0.1	44	77	0.029
	24.998	3.5590	2.6	1009	89	0.565
	26.655	3.3414	17.9	6855	390	0.879
	45.330	1.9989	5.1	1942	97	0.998
RBS023	2.732	32.3077	11.4	145	34	0.217
	8.664	10.1976	100.0	1276	133	0.478
	10.732	8.2368	12.6	160	35	0.228
	12.225	7.2335	5.7	72	36	0.102
	20.687	4.2899	9.9	126	44	0.144
	21.730	4.0863	14.4	184	35	0.263
	26.516	3.3587	28.1	359	64	0.280
	31.819	2.8100	26.8	341	102	0.167
	33.006	2.7116	34.6	441	130	0.169
	33.982	2.6359	15.0	191	29	0.331
	39.942	2.2552	11.5	147	33	0.224
	46.962	1.9332	9.0	114	31	0.187
RBS016	8.728	10.1230	100.0	624	164	0.190
	9.440	9.3607	9.1	57	52	0.055
	12.362	7.1539	31.7	198	38	0.260
	20.844	4.2579	21.6	165	44	0.152
	26.677	3.3387	76.3	477	98	0.244
RBS024	6.056	14.5806	15.9	231	65	0.178
	8.669	10.1909	100.0	1447	244	0.297
	12.224	7.2345	58.8	851	124	0.342
	17.591	5.0374	21.1	305	41	0.368
	24.756	3.5933	17.5	254	47	0.272
	26.518	3.3584	48.9	707	111	0.320
RBS034	4.303	20.5184	3.4	675	110	0.307
	6.080	14.5249	5.5	1098	93	0.592
	8.607	10.2641	100.0	19800	806	1.228
	12.323	7.1764	13.1	2598	283	0.458
	17.655	5.0193	6.8	1343	158	0.425
	18.655	4.7500	2.1	421	60	0.351
	19.675	4.5083	0.8	152	70	0.109
	20.736	4.2799	4.5	892	200	0.223
	25.085	3.5469	6.5	1281	145	0.441
	26.569	3.3521	33.2	6581	1091	0.302
	29.810	2.9946	2.3	452	73	0.310
	34.875	2.5704	2.8	551	38	0.721
	45.374	1.9971	6.8	1352	103	0.653

Key Peaks on XRD Trace						
File	2Theta	D-spacing	Integ. I (%)	Integ. I	Max I	FWHM
RBS035	6.261	14.1040	0.2	82	145	0.028
	8.756	10.0909	100.0	41601	1410	1.475
	12.544	7.0505	6.2	2591	233	0.557
	17.862	4.9615	7.0	2931	167	0.876
	18.800	4.7161	0.5	197	86	0.114
	25.230	3.5268	2.1	880	89	0.495
	26.981	3.3018	17.4	7259	346	1.050
	45.545	1.9899	4.0	1684	86	0.982
RBS032	3.012	29.3088	90.7	1065	170	0.313
	4.039	21.8554	100.0	1175	173	0.340
	4.638	19.0348	51.6	606	77	0.392
	8.906	9.9207	2.3	27	29	0.046
	12.444	7.1069	18.6	219	43	0.255
	26.715	3.3340	15.2	178	41	0.218
RBS031	8.825	10.0121	69.5	2681	294	0.457
	12.351	7.1602	5.0	193	83	0.116
	20.037	4.4276	4.6	176	53	0.167
	20.994	4.2280	14.8	571	198	0.144
	26.770	3.3274	100.0	3858	1032	0.187
	28.050	3.1784	4.7	180	67	0.135
	33.171	2.6984	6.4	247	78	0.159
	36.681	2.4479	6.5	250	79	0.159
	40.433	2.2289	3.0	116	36	0.161
	42.566	2.1221	4.7	181	49	0.183
RBS030	11.505	7.6850	100.0	505	125	0.201
	20.641	4.2994	83.6	423	116	0.182
RBS049	8.756	10.0908	100.0	8609	813	0.529
	12.439	7.1098	13.3	1142	96	0.594
	17.802	4.9782	16.6	1432	85	0.843
	25.084	3.5471	4.8	417	44	0.475
	26.846	3.3181	42.9	3696	180	1.025
	45.442	1.9942	11.7	1007	51	0.994

Key Peaks on XRD Trace: Glycolated Samples						
File	2Theta	D-spacing	Integ. I (%)	Integ. I	Max I	FWHM
RBS051	2.122	41.5954	100.0	54287	1851	1.467
	6.112	14.4491	0.3	169	139	0.061
	6.589	13.4030	7.2	3887	140	1.389
	8.628	10.2392	33.1	17958	781	1.149
	12.328	7.1735	4.5	2441	235	0.521
	17.623	5.0282	2.7	1492	125	0.598
	20.659	4.2957	0.2	99	87	0.057
	26.588	3.3497	12.1	6565	525	0.625
	45.366	1.9974	2.1	1129	71	0.799
RBS052	6.322	13.9676	5.8	792	127	0.312
	8.906	9.9210	100.0	13722	727	0.944
	12.516	7.0665	17.8	2436	205	0.593
	17.800	4.9788	13.9	1904	118	0.805
	25.236	3.5260	4.6	629	68	0.460
	26.858	3.3166	40.8	5595	380	0.735
	45.414	1.9954	5.7	783	50	0.779
RBS053	6.847	12.8980	3.5	334	91	0.184
	7.368	11.9875	4.3	408	123	0.165
	8.787	10.0545	100.0	9444	538	0.878
	12.433	7.1131	14.1	1334	107	0.621
	17.714	5.0028	4.4	420	68	0.310
	18.882	4.6957	4.5	425	38	0.567
	25.111	3.5433	3.5	332	44	0.376
	26.758	3.3289	38.2	3604	238	0.757
	45.401	1.9959	8.1	769	34	1.137

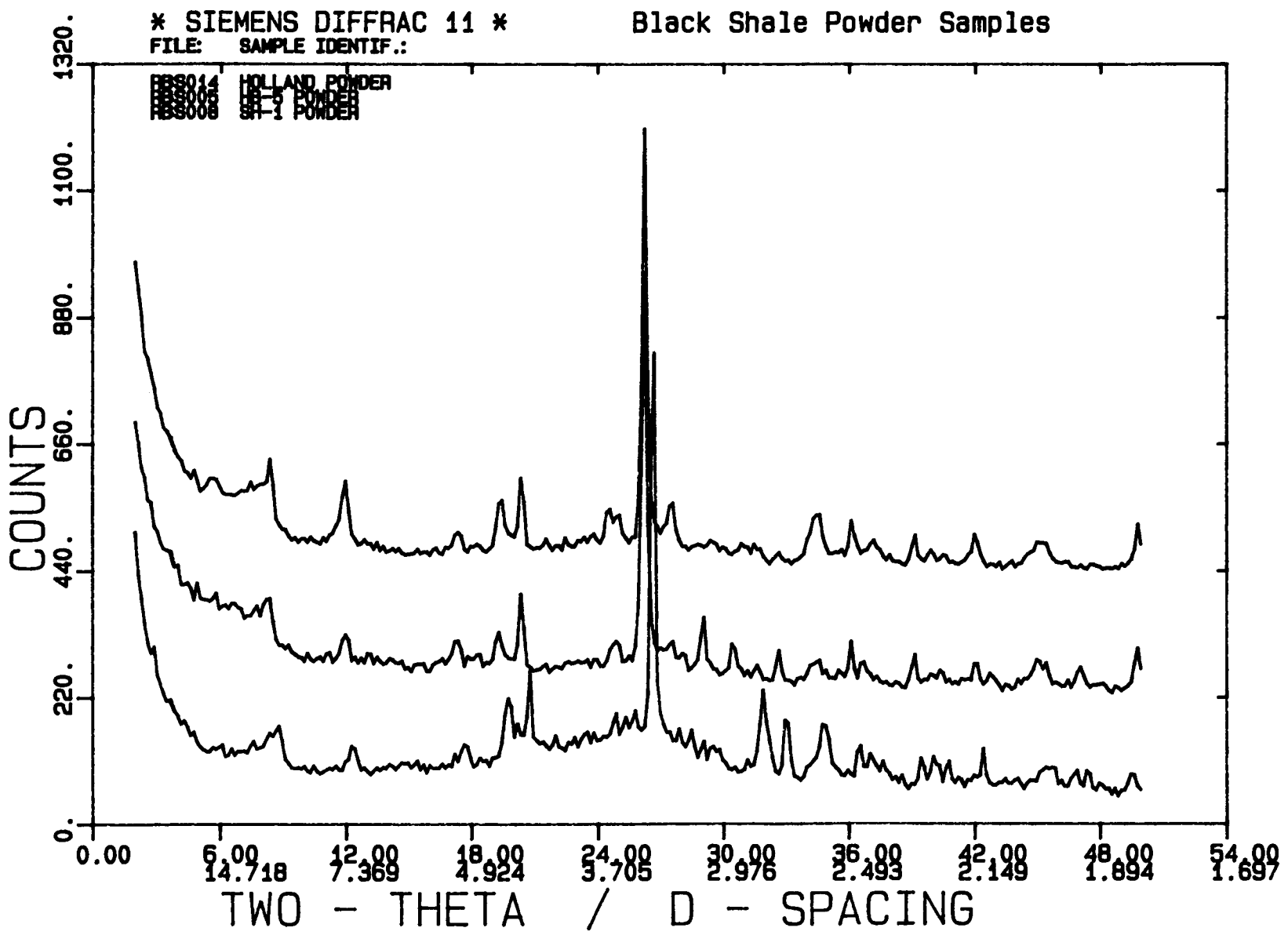
* SIEMENS DIFFRAC 11 *
Black Shale Powder Samples
FILE: SAMPLE IDENTIF.:
RBS014 HOLLAND POWDER
RBS008 SH-1 POWDER
COUNTS
1320.
1100.
880.
660.
440.
220.
0.
0.00
6.00
12.00
18.00
24.00
30.00
36.00
42.00
48.00
54.00
14.718
7.369
4.924
3.705
2.976
2.493
2.149
1.894
1.697
TWO - THETA / D - SPACING

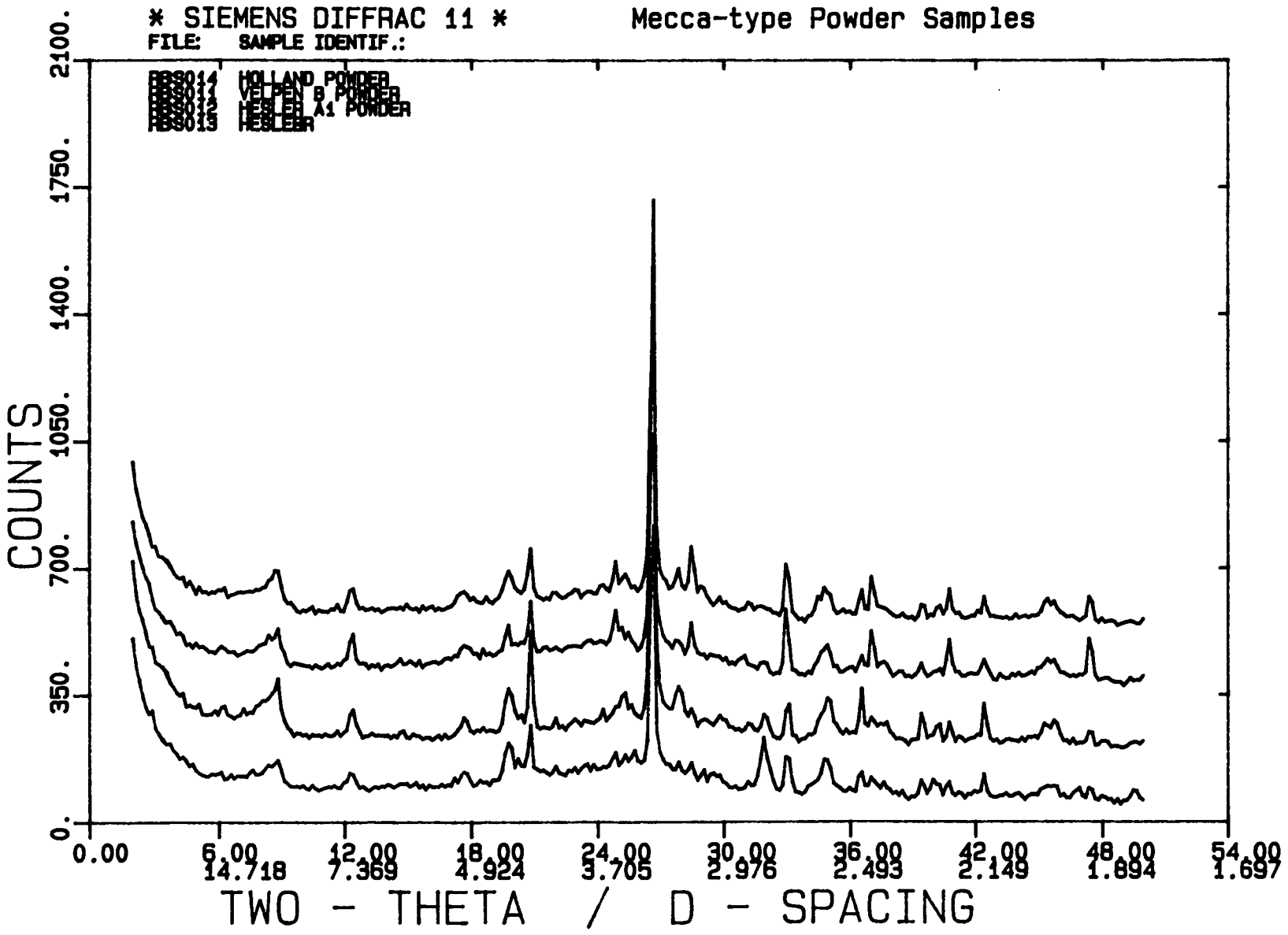
* SIEMENS DIFFRAC 11 *
Mecca-type Powder Samples
FILE: SAMPLE IDENTIF.:
RBS014 HOLLAND POWDER
RBS012 VELPEN B POWDER
RBS013 HESLEER
COUNTS
2100.
1750.
1400.
1050.
700.
350.
0.
0.00
6.00
12.00
18.00
24.00
30.00
36.00
42.00
48.00
54.00
14.718
7.369
4.924
3.705
2.976
2.493
2.149
1.894
1.697
TWO - THETA / D - SPACING

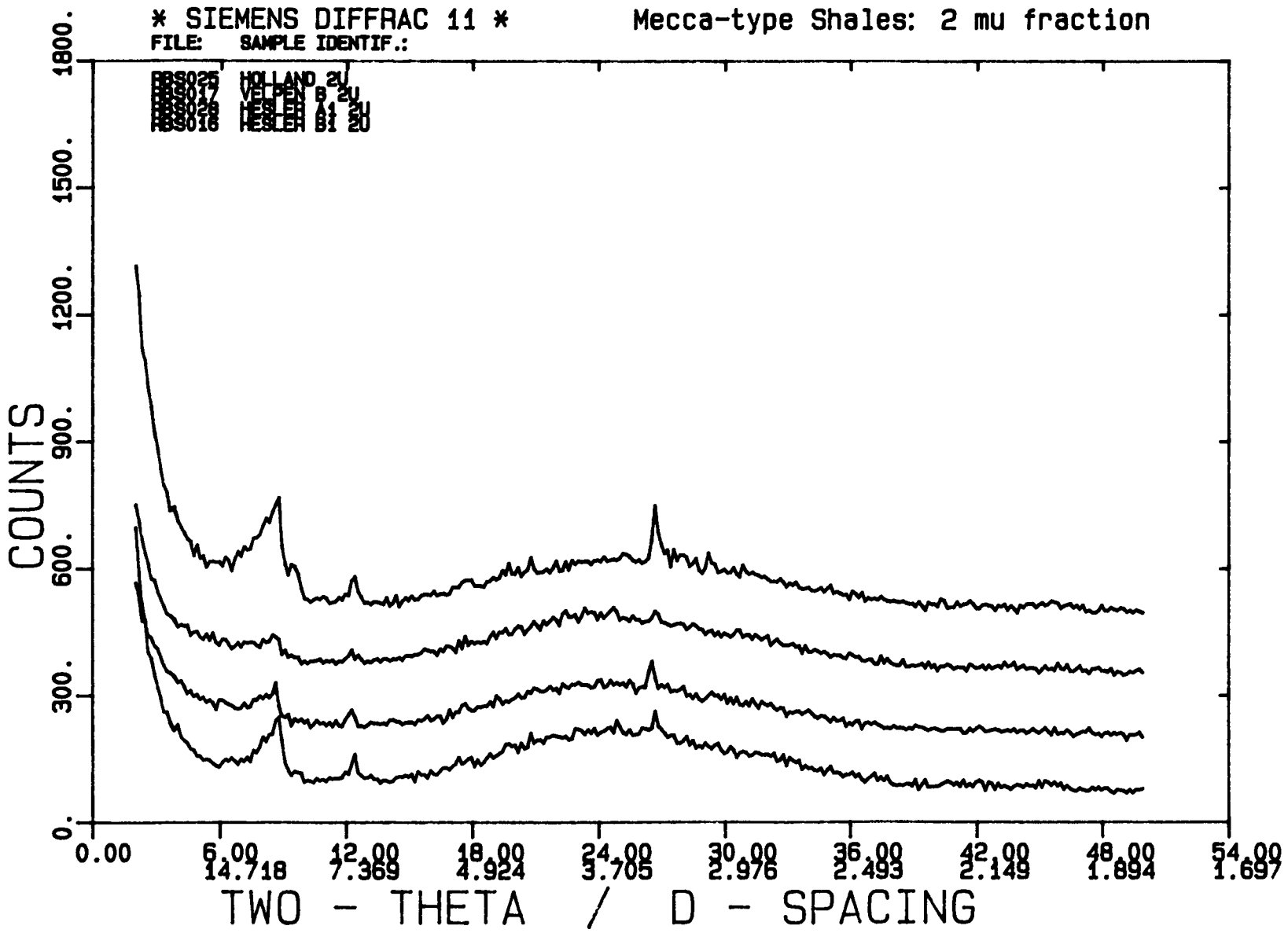
* SIEMENS DIFFRAC 11 *
Mecca-type Shales: 2 mu fraction
FILE: SAMPLE IDENTIF.:
RBS025 HOLLAND 2U
RBS017 VELPEN B 2U
RBS028 HESLER A1 2U
RBS016 HESLER B1 2U
COUNTS
0.
300.
600.
900.
1200.
1500.
1800.
0.00
6.00
12.00
18.00
24.00
30.00
36.00
42.00
48.00
54.00
14.718
7.369
4.924
3.705
2.976
2.493
2.149
1.894
1.697
TWO - THETA / D - SPACING

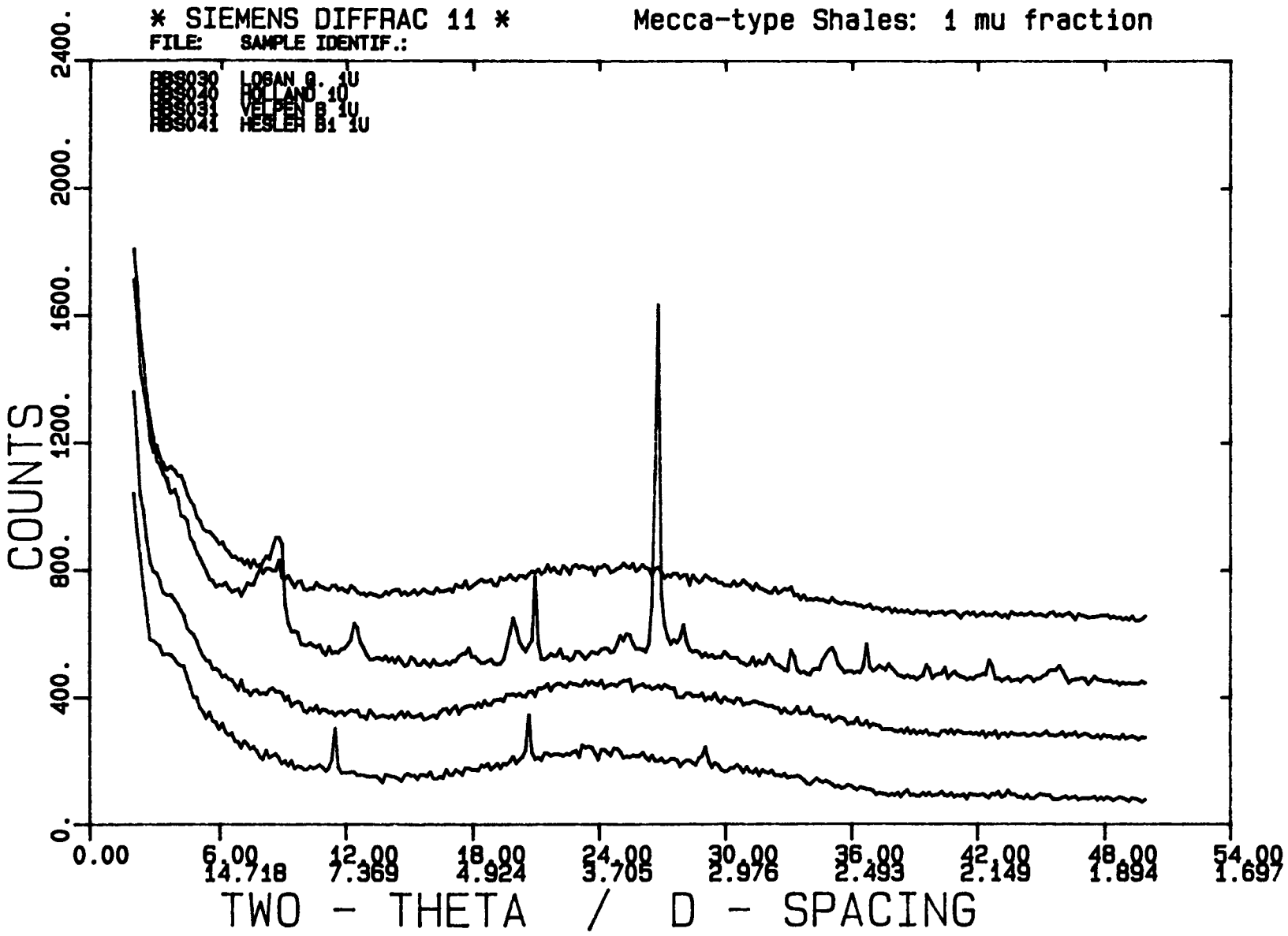
* SIEMENS DIFFRAC 11 *
Mecca-type Shales: 1 mu fraction
FILE: SAMPLE IDENTIF.:
RBS030 LOGAN B. 1U
RBS040 HOLLAND 10
RBS031 VELPEN B 1U
RBS041 HESLER B1 1U
COUNTS
0.
400.
800.
1200.
1600.
2000.
2400.
0.00
6.00
14.718
12.00
7.369
18.00
4.924
24.00
3.705
30.00
2.976
36.00
2.493
42.00
2.149
48.00
1.894
54.00
1.697
TWO - THETA / D - SPACING

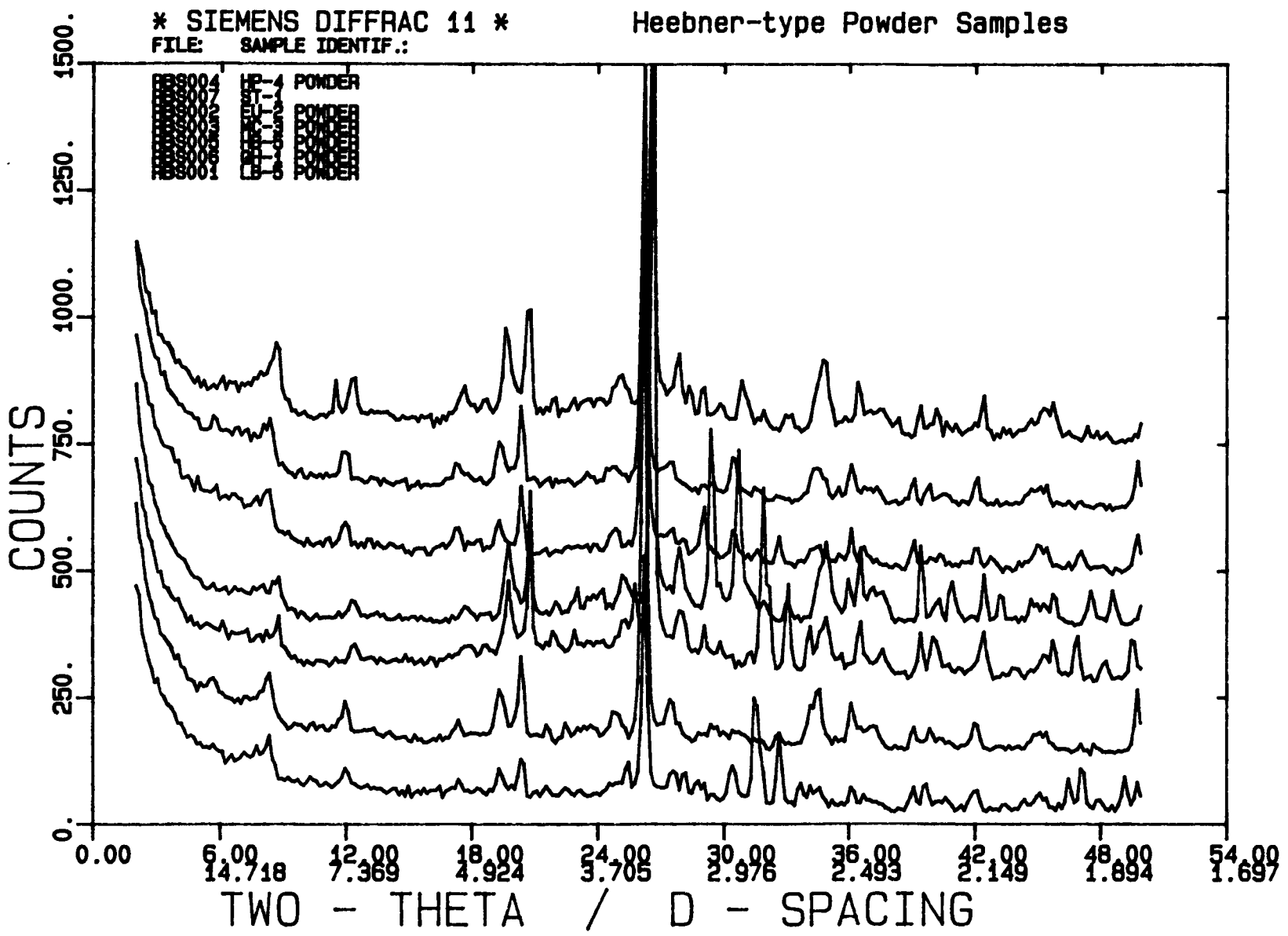
* SIEMENS DIFFRAC 11 *
Heebner-type Powder Samples
FILE: SAMPLE IDENTIF.:
HP-4 POWDER
COUNTS
0.
250.
500.
750.
1000.
1250.
1500.
0.00
6.00
12.00
18.00
24.00
30.00
36.00
42.00
48.00
54.00
14.718
7.369
4.924
3.705
2.976
2.493
2.149
1.894
1.697
TWO - THETA / D - SPACING

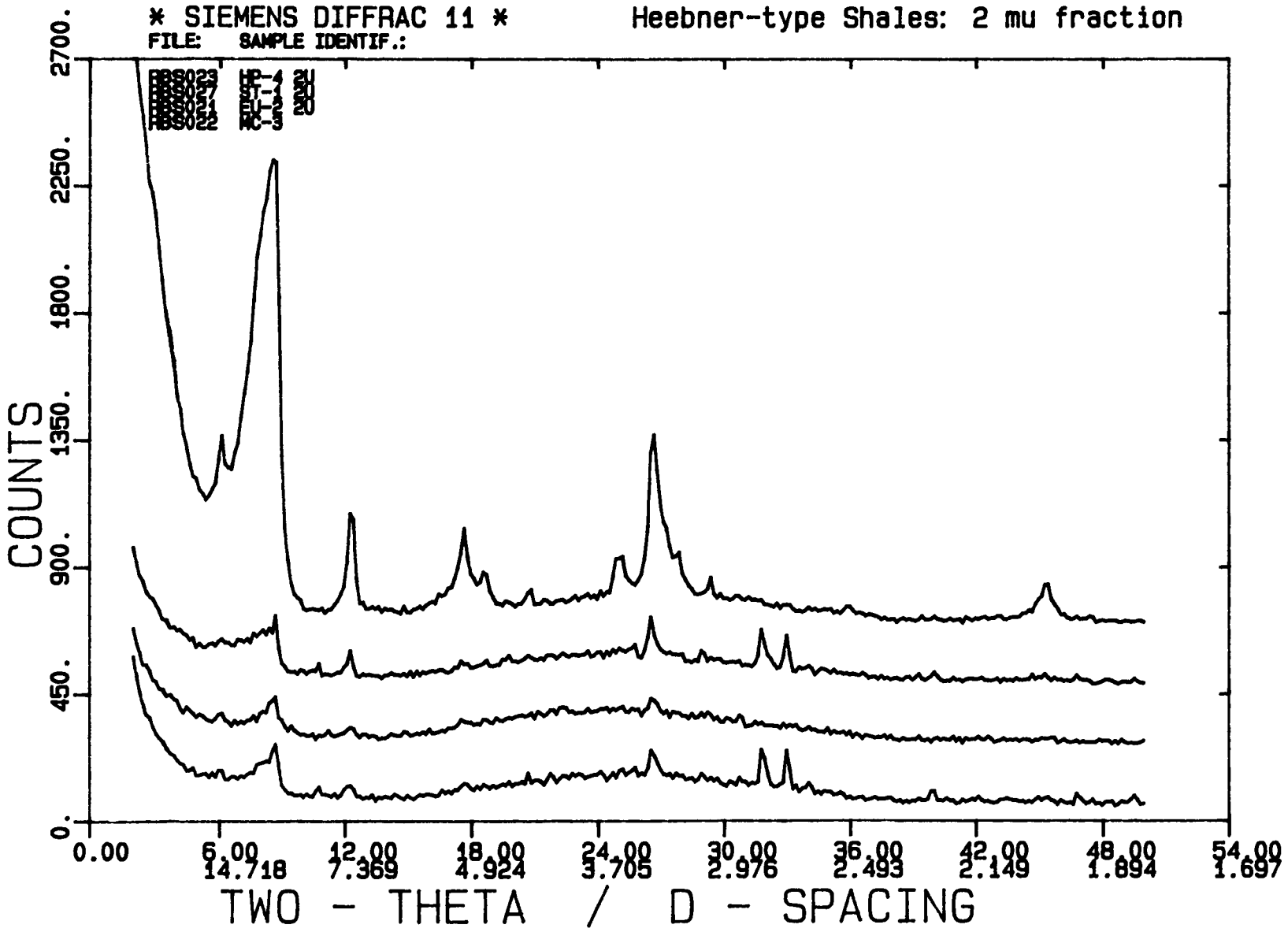
* SIEMENS DIFFRAC 11 *
Heebner-type Shales: 2 mu fraction
FILE: SAMPLE IDENTIF.:
ABS023 HP-4 2U
ABS027 ST-1 2U
ABS021 FT-2 2U
ABS022 MC-3
COUNTS
2700.
2250.
1800.
1350.
900.
450.
0.
0.00
6.00
12.00
18.00
24.00
30.00
36.00
42.00
48.00
54.00
14.718
7.369
4.924
3.705
2.976
2.493
2.149
1.894
1.697
TWO - THETA / D - SPACING

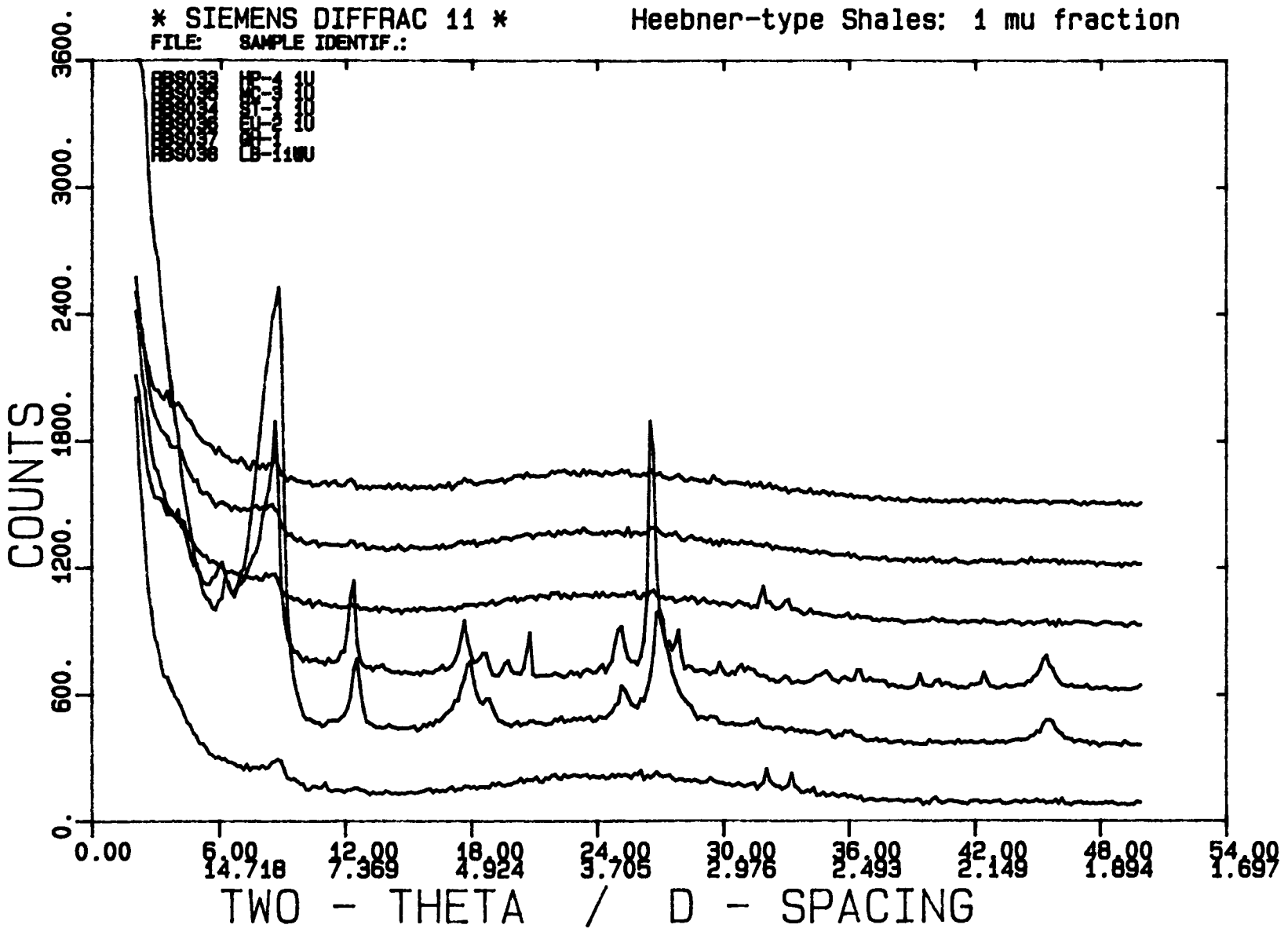
* SIEMENS DIFFRAC 11 *
Heebner-type Shales: 1 mu fraction
FILE: SAMPLE IDENTIF.:
COUNTS
0.
600.
1200.
1800.
2400.
3000.
3600.
0.00
6.00
12.00
18.00
24.00
30.00
36.00
42.00
48.00
54.00
14.718
7.369
4.924
3.705
2.976
2.493
2.149
1.894
1.697
TWO - THETA / D - SPACING

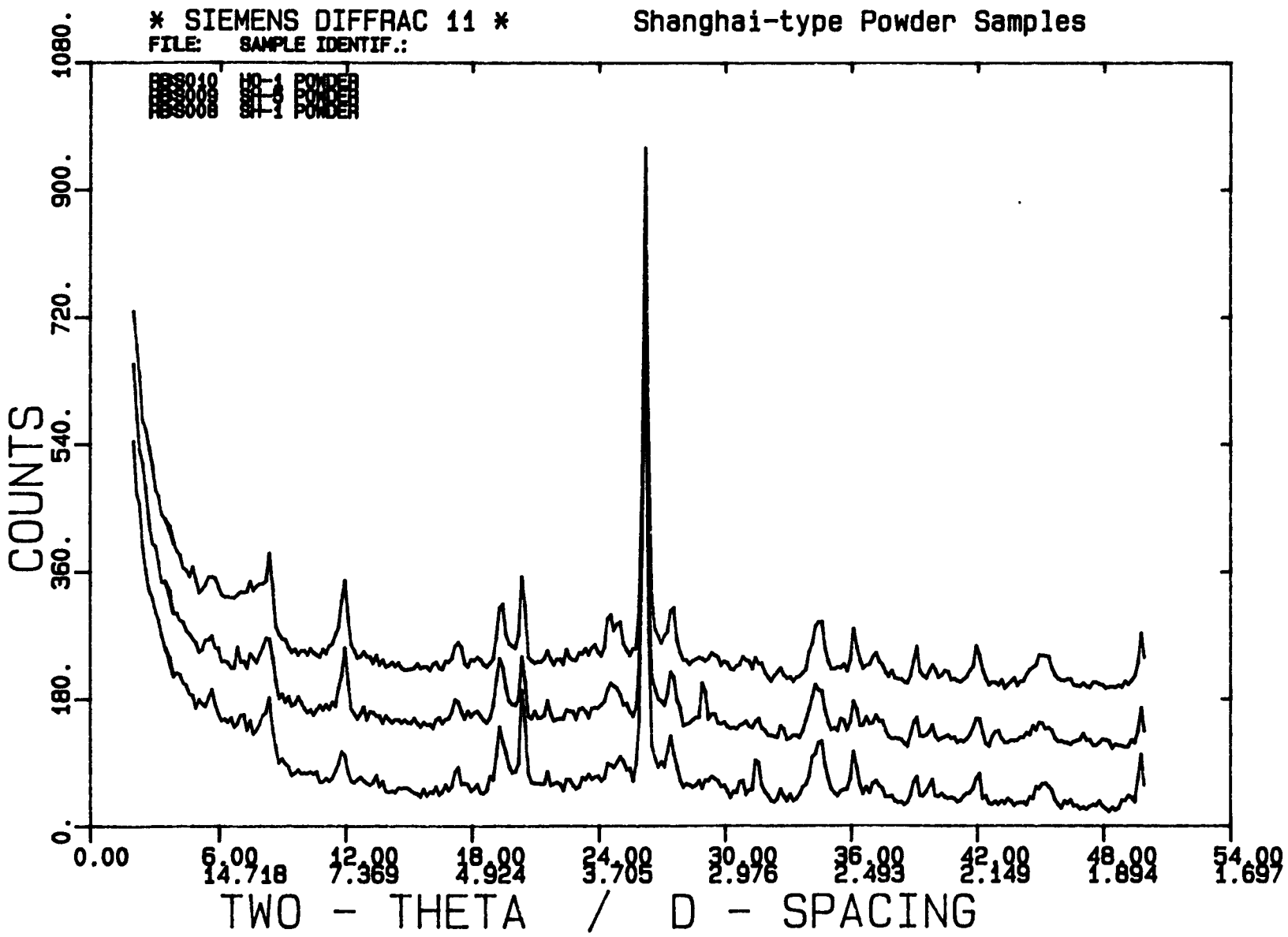
* SIEMENS DIFFRAC 11 *
Shanghai-type Powder Samples
FILE: SAMPLE IDENTIF.:
RDS010 HO-1 POWDER
RDS009 SH-2 POWDER
RDS008 SH-1 POWDER
COUNTS
1080.
900.
720.
540.
360.
180.
0.
0.00
6.00
12.00
18.00
24.00
30.00
36.00
42.00
48.00
54.00
14.718
7.369
4.924
3.705
2.976
2.493
2.149
1.894
1.697
TWO - THETA / D - SPACING

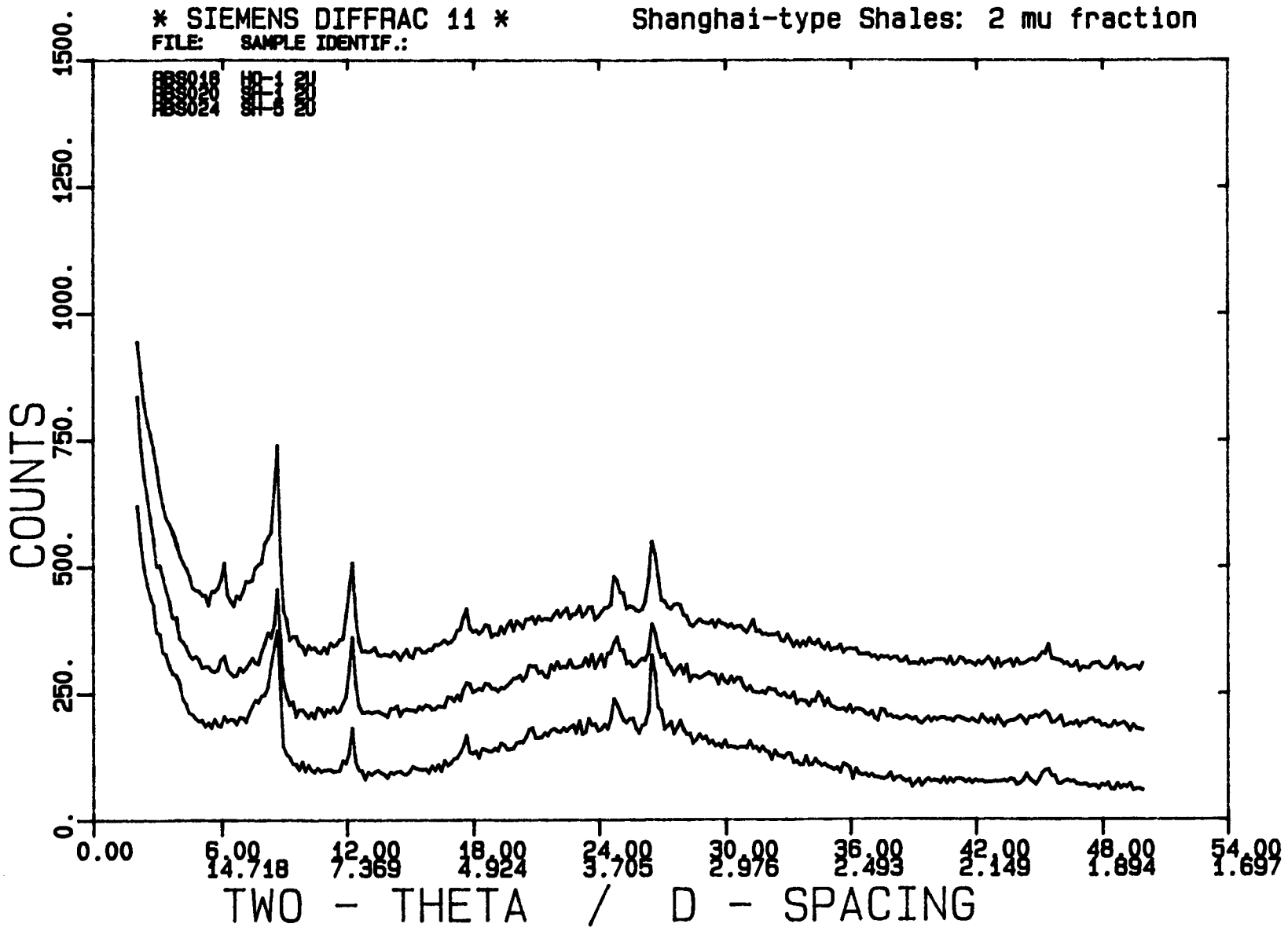
* SIEMENS DIFFRAC 11 *
Shanghai-type Shales: 2 mu fraction
FILE: SAMPLE IDENTIF.:
COUNTS
0.
250.
500.
750.
1000.
1250.
1500.
0.00
6.00
12.00
18.00
24.00
30.00
36.00
42.00
48.00
54.00
14.718
7.369
4.924
3.705
2.976
2.493
2.149
1.894
1.697
TWO - THETA / D - SPACING

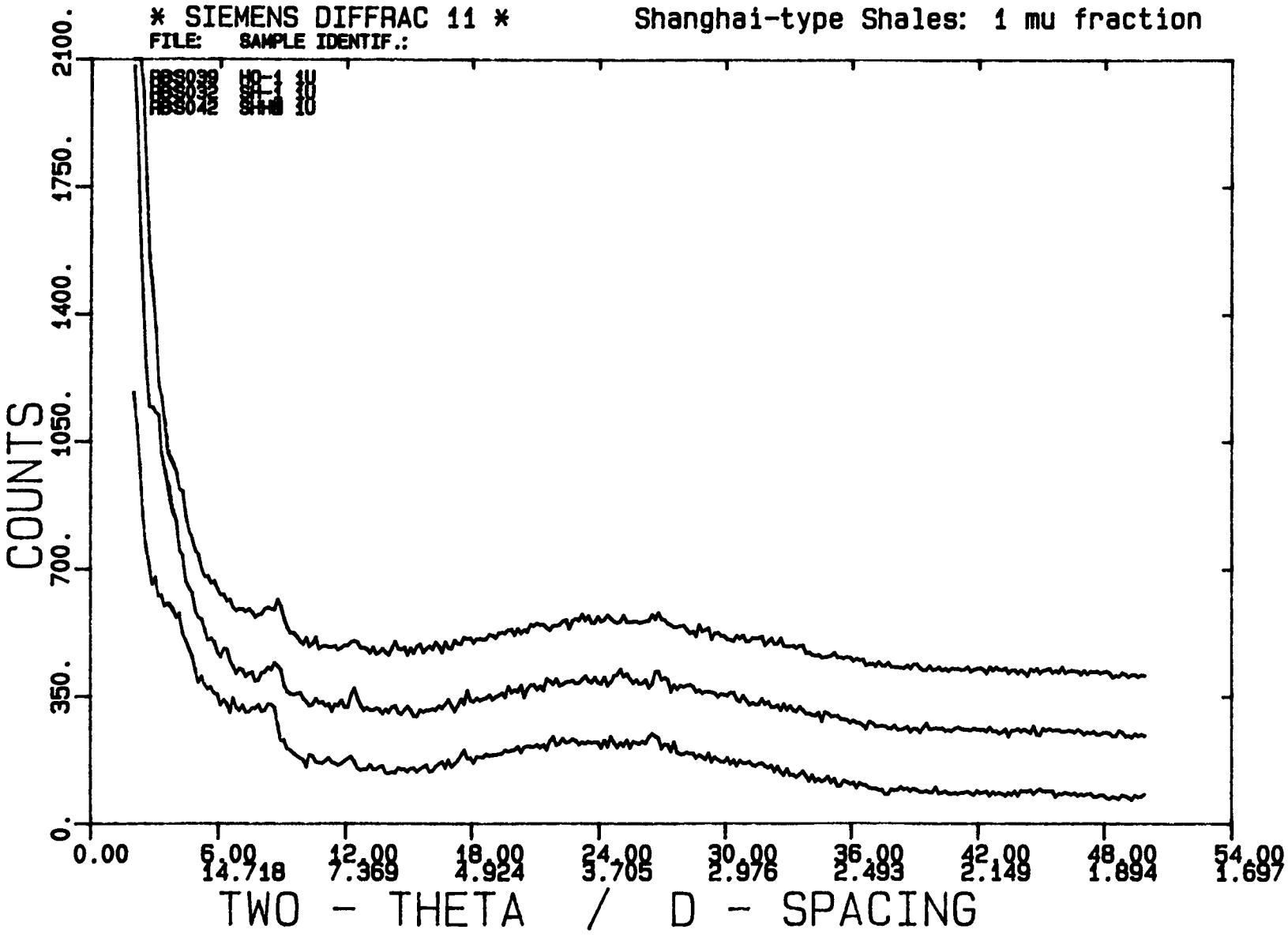
* SIEMENS DIFFRAC 11 *
Shanghai-type Shales: 1 mu fraction
FILE: SAMPLE IDENTIF.:
COUNTS
2100.
1750.
1400.
1050.
700.
350.
0.
0.00
6.00
12.00
18.00
24.00
30.00
36.00
42.00
48.00
54.00
14.718
7.369
4.924
3.705
2.976
2.493
2.149
1.894
1.697
TWO - THETA / D - SPACING

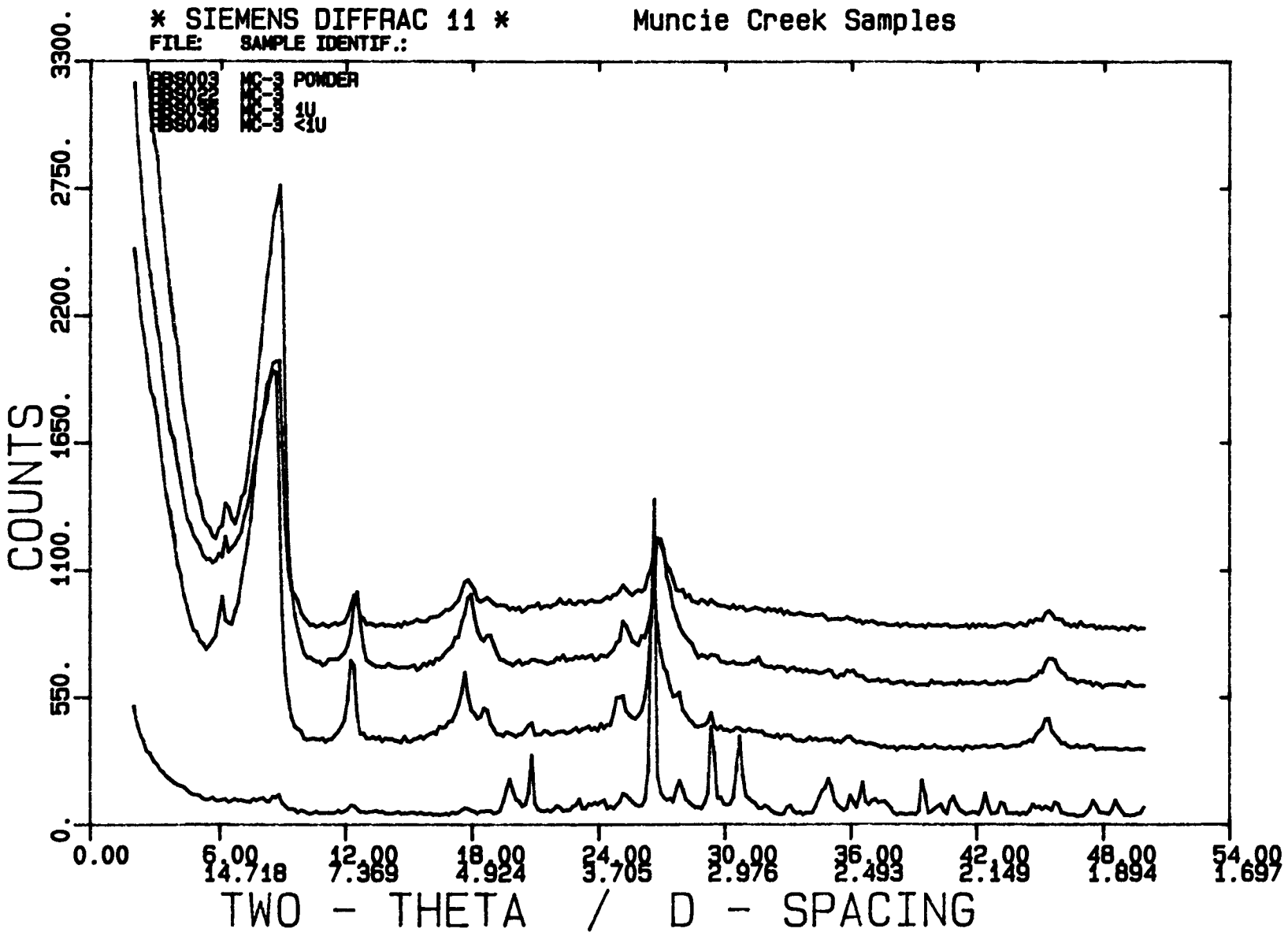
* SIEMENS DIFFRAC 11 *
Muncie Creek Samples
FILE: SAMPLE IDENTIF.:
MC-3 POWDER
MC-3 1U
MC-3 <1U
COUNTS
3300.
2750.
2200.
1650.
1100.
550.
0.
0.00
6.00
12.00
18.00
24.00
30.00
36.00
42.00
48.00
54.00
14.718
7.369
4.924
3.705
2.976
2.493
2.149
1.894
1.697
TWO - THETA / D - SPACING

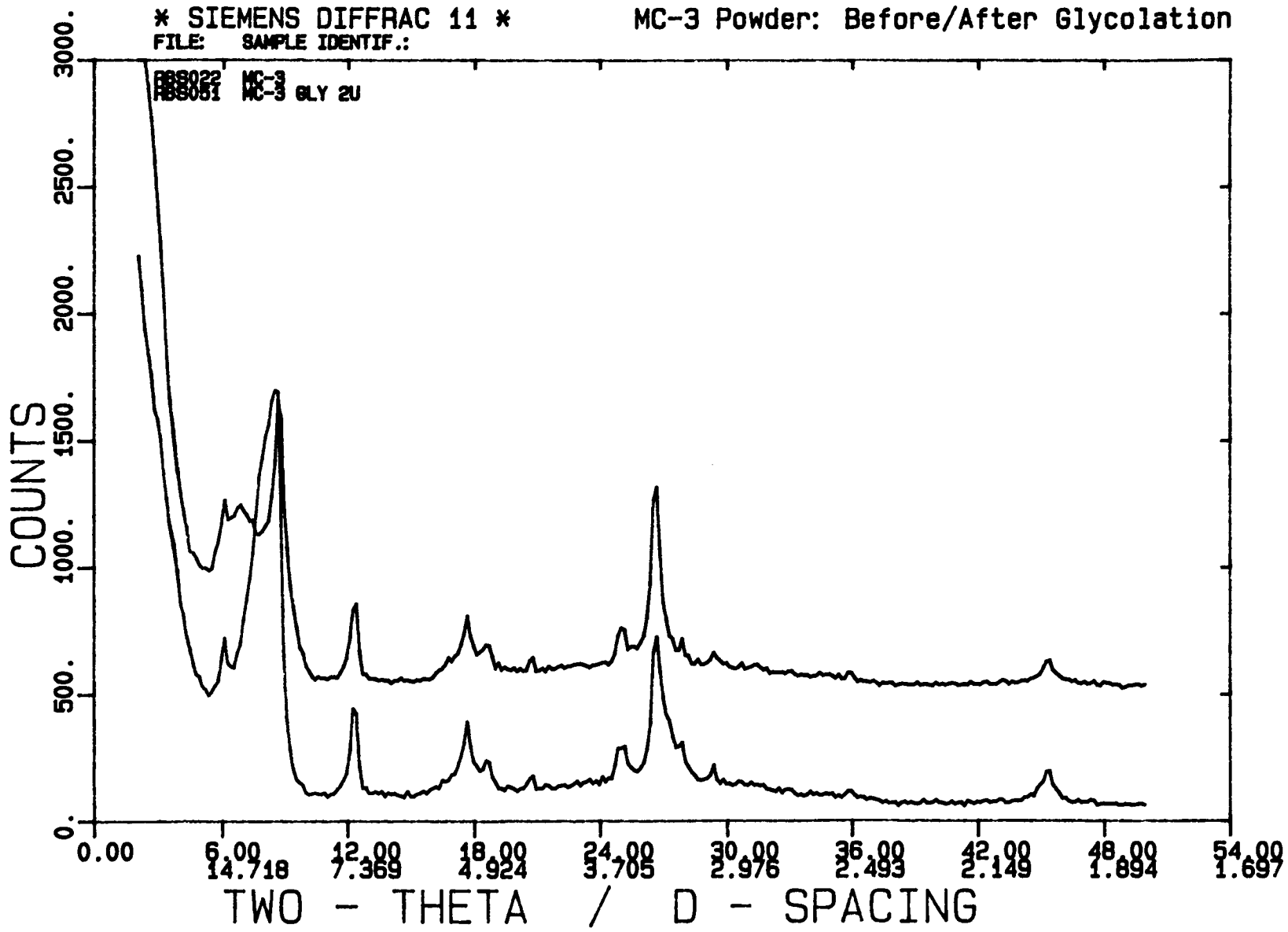
* SIEMENS DIFFRAC 11 *
MC-3 Powder: Before/After Glycolation
FILE: SAMPLE IDENTIF.:
RBS022 MC-3
RBS051 MC-3 GLY 2U
COUNTS
3000.
2500.
2000.
1500.
1000.
500.
0.
0.00
6.00
12.00
18.00
24.00
30.00
36.00
42.00
48.00
54.00
14.718
7.369
4.924
3.705
2.976
2.493
2.149
1.894
1.697
TWO - THETA / D - SPACING

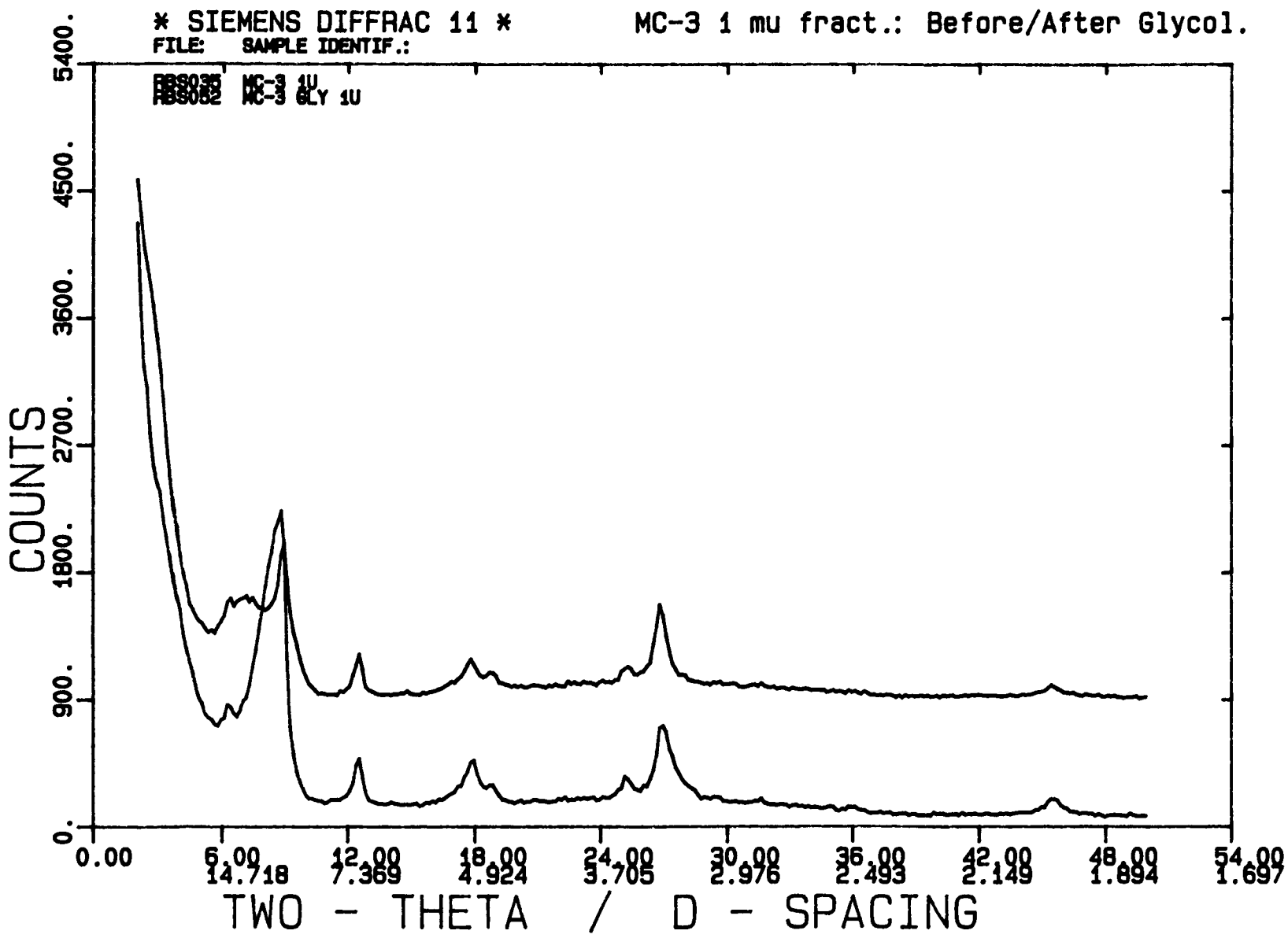
* SIEMENS DIFFRAC 11 *
MC-3 1 mu fract.: Before/After Glycol.
FILE: SAMPLE IDENTIF.:
RBS035 MC-3 1U
RBS052 MC-3 GLY 1U
COUNTS
5400.
4500.
3600.
2700.
1800.
900.
0.
0.00
6.00
14.718
12.00
7.369
18.00
4.924
24.00
3.705
30.00
2.976
36.00
2.493
42.00
2.149
48.00
1.894
54.00
1.697
TWO - THETA / D - SPACING

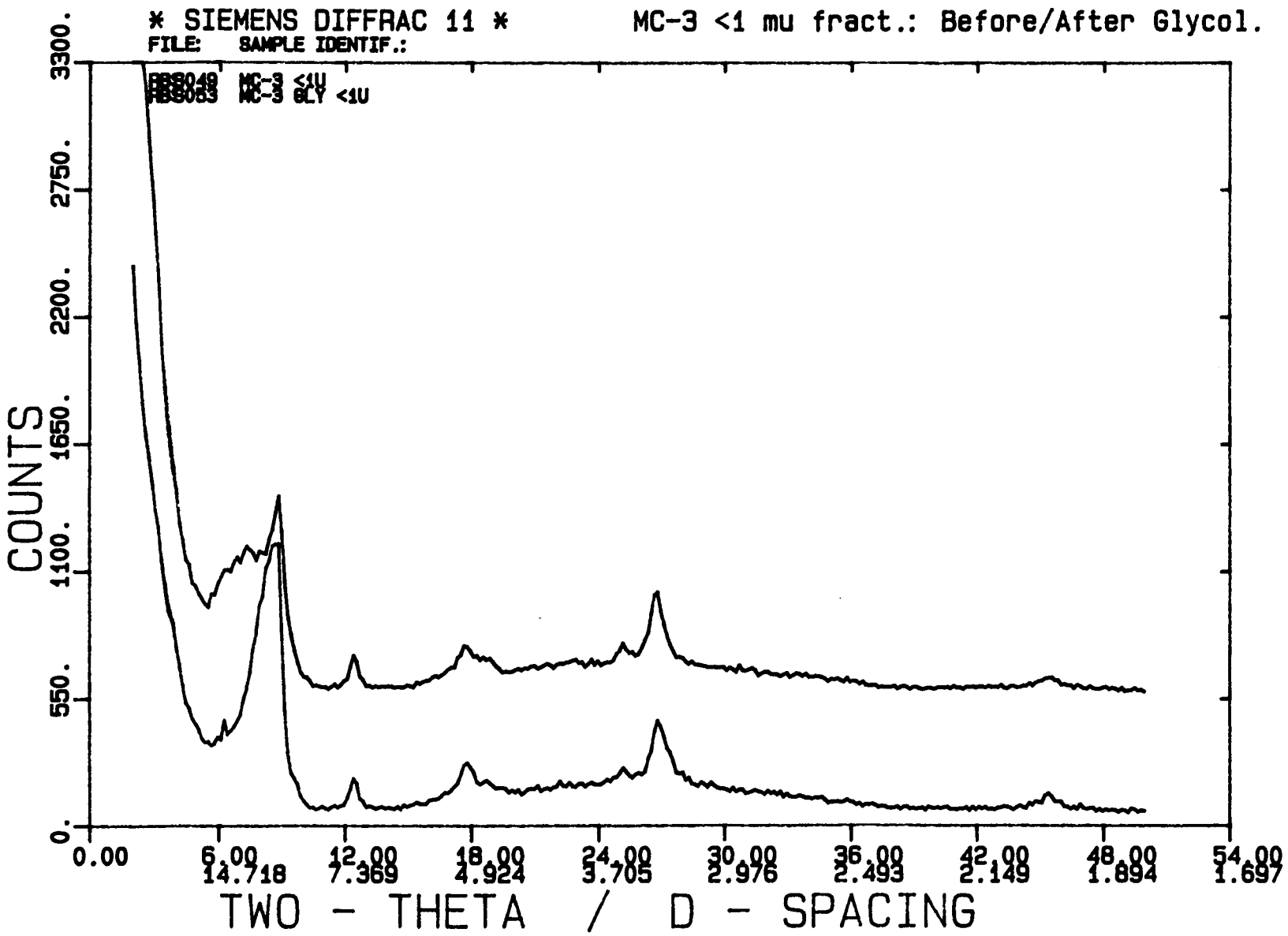
* SIEMENS DIFFRAC 11 *
MC-3 <1 mu fract.: Before/After Glycol.
FILE: SAMPLE IDENTIF.:
MC-3 <1U
MC-3 GLY <1U
COUNTS
3300.
2750.
2200.
1650.
1100.
550.
0.
0.00
6.00
12.00
18.00
24.00
30.00
36.00
42.00
48.00
54.00
14.718
7.369
4.924
3.705
2.976
2.493
2.149
1.894
1.697
TWO - THETA / D - SPACING

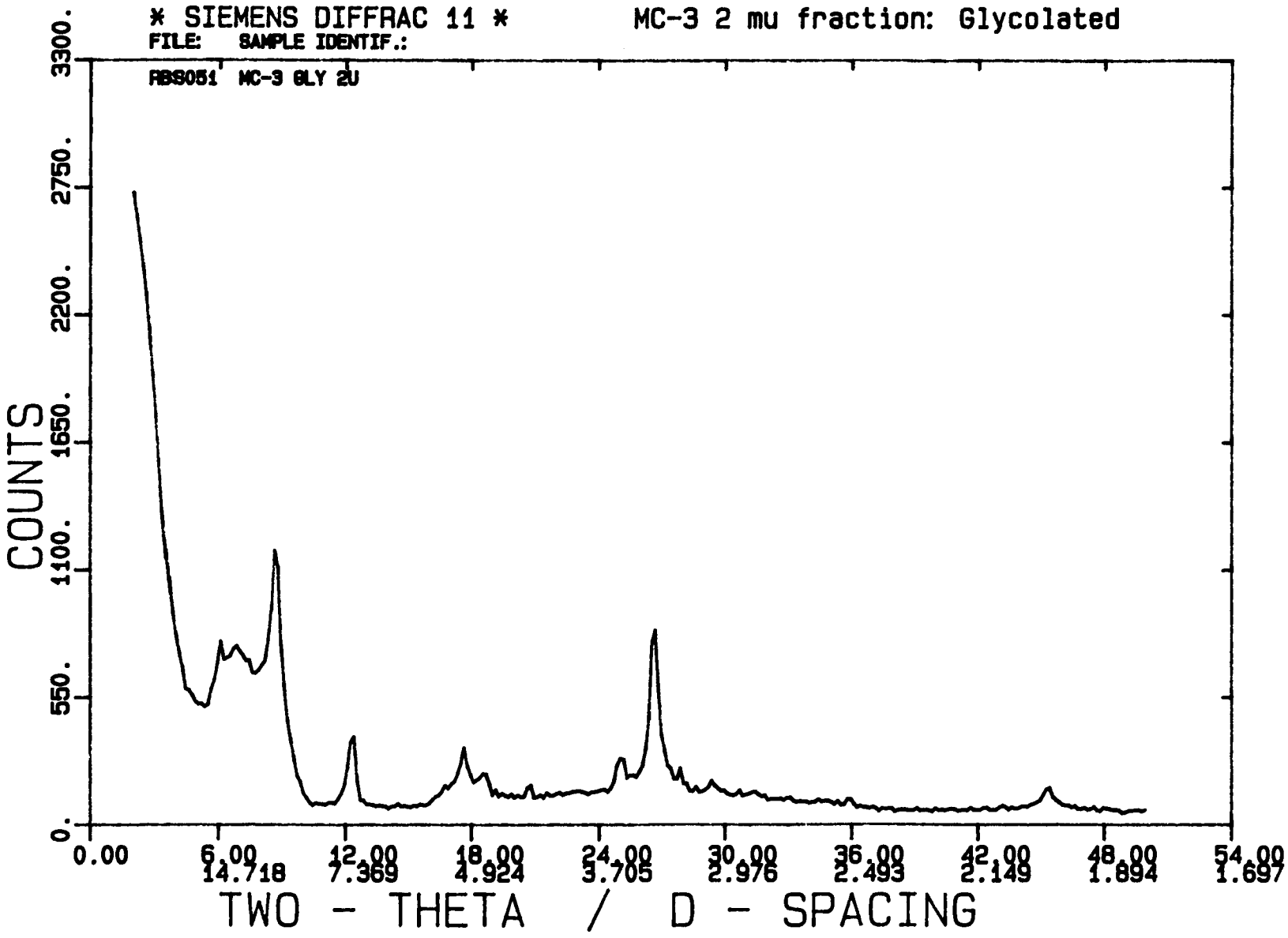
* SIEMENS DIFFRAC 11 *
MC-3 2 mu fraction: Glycolated
FILE: SAMPLE IDENTIF.:
RBS051 MC-3 GLY 2U
COUNTS
3300.
2750.
2200.
1650.
1100.
550.
0.
0.00
6.00
12.00
18.00
24.00
30.00
36.00
42.00
48.00
54.00
14.718
7.369
4.924
3.705
2.976
2.493
2.149
1.894
1.697
TWO - THETA / D - SPACING

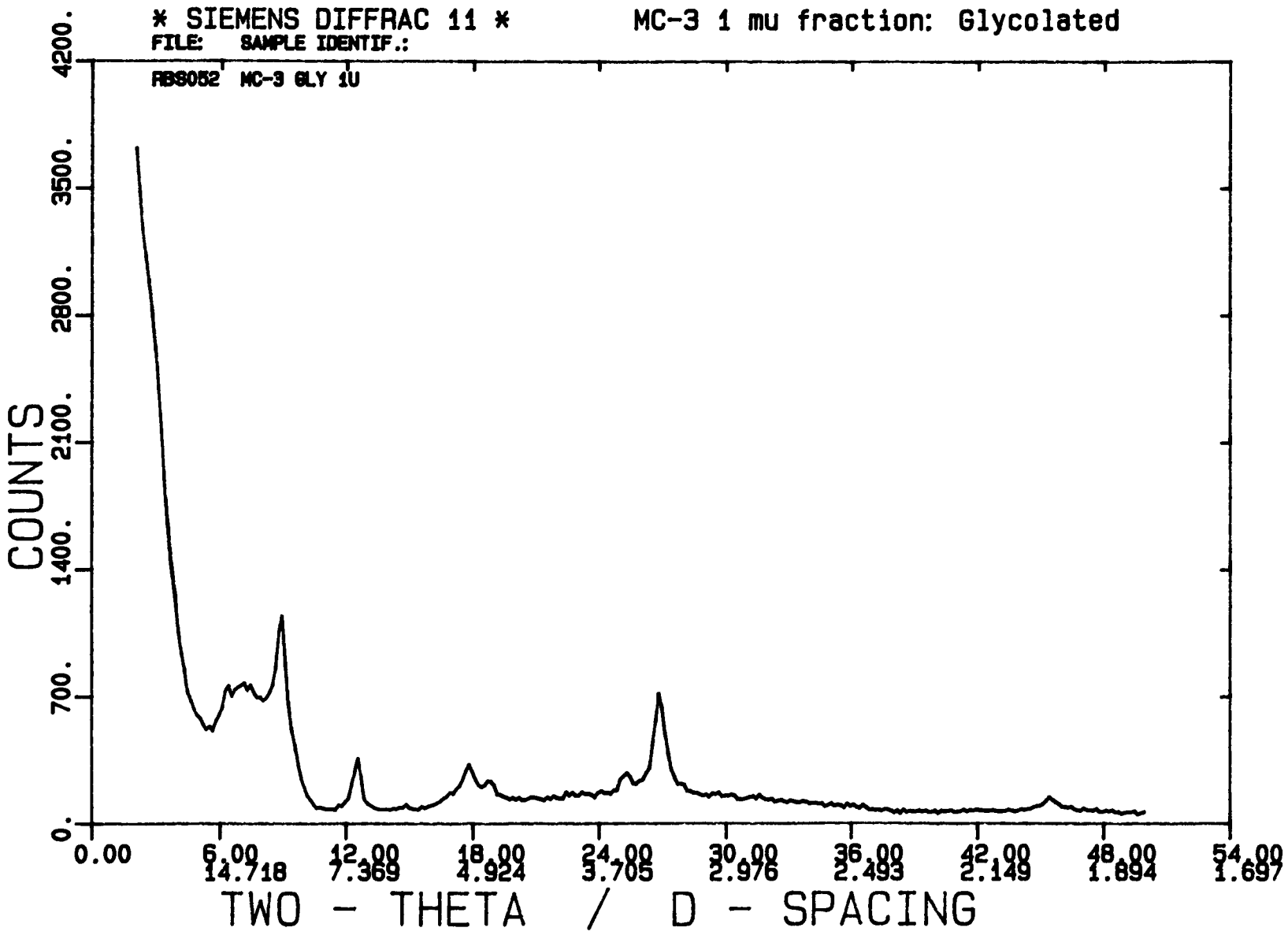
* SIEMENS DIFFRAC 11 *
MC-3 1 mu fraction: Glycolated
FILE: SAMPLE IDENTIF.:
RBS052 MC-3 GLY 1U
COUNTS
4200.
3500.
2800.
2100.
1400.
700.
0.
0.00
6.00
12.00
18.00
24.00
30.00
36.00
42.00
48.00
54.00
14.718
7.369
4.924
3.705
2.976
2.493
2.149
1.894
1.697
TWO - THETA / D - SPACING

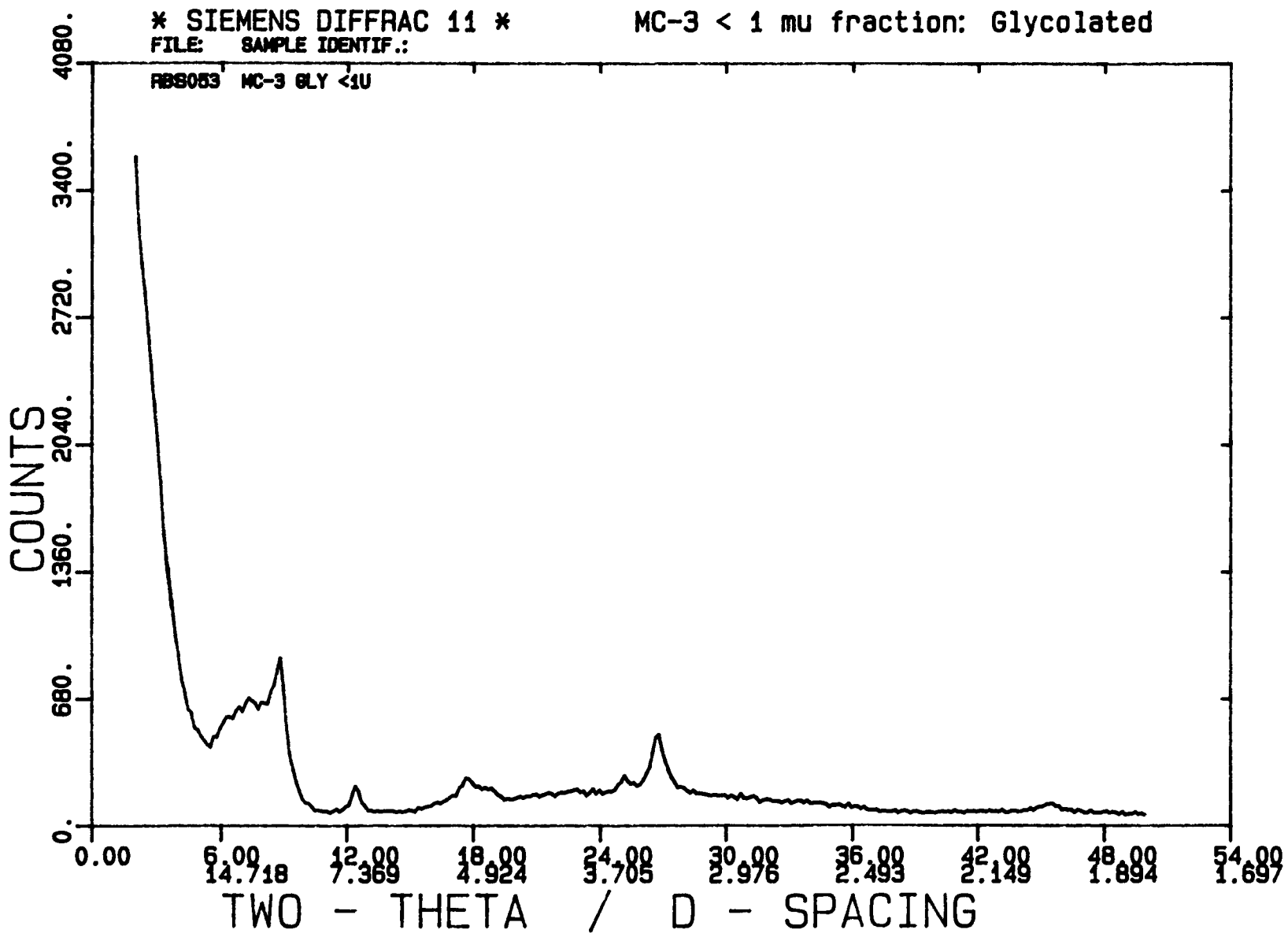
* SIEMENS DIFFRAC 11 *
MC-3 < 1 mu fraction: Glycolated
FILE: SAMPLE IDENTIF.:
RBS053 MC-3 GLY <1U
COUNTS
4080.
3400.
2720.
2040.
1360.
680.
0.
0.00
6.00
12.00
18.00
24.00
30.00
36.00
42.00
48.00
54.00
14.718
7.369
4.924
3.705
2.976
2.493
2.149
1.894
1.697
TWO - THETA / D - SPACING

Appendix M. Rock-Eval Data

Rock-Eval Data From Selected Samples						
SAMPLE	TOC	S1(ppm)	S2(ppm)	Tmax (°C)	S2/TOC	S1/S1+S2
HB1	10.31	1200.00	49500.00	419.00	0.48	0.02
QH1	22.72	3280.00	137000.00	415.00	0.60	0.02
SH2	5.59	490.00	10900.00	426.00	0.19	0.04
LB1	17.45	1540.00	70300.00	417.00	0.40	0.02
HBC1	19.43	1390.00	83700.00	419.00	0.43	0.02
QHC1	4.89	2060.00	18900.00	428.00	0.39	0.10
SHC1	0.66	250.00	520.00	528.00	0.08	0.32
MQB	14.95	1480.00	41700.00	417.00	0.28	0.03
MQD	36.85	4530.00	176000.00	415.00	0.48	0.03
MQSB1	36.20	5610.00	195000.00	418.00	0.54	0.03

Appendix N. Sulfur Isotope Data

Sulfur Isotope Data from Sulfides				
Stratigraphy	Avg. Value	Location	Samples	Lithology
Virgilian Series black shales			19	
Shanghai-type:				
Shanghai Creek Shale Member	+3.0	Forest City Basin	4	black shales
Holt Shale Member	–5.3	Forest City Basin	3	dark gray shale
Heebner-type:				
Larsh/Burroak Shale Member	–29.2	Forest City Basin	4	black shale
Queen Hill Shale Member	–36.5	Forest City Basin	3	black shale
Heebner Shale Member	–36.6	Forest City Basin	5	black shale
Missourian Series black shales			11	
Heebner-type:				
Eudora Shale Member	–41.8	Forest City Basin	2	dark gray shale
Muncie Creek Shale Member	–40.8	Forest City Basin	2	dark gray shale
Stark Shale Member	–26.6*	Illinois/F.C. Basin	3	black shale
Hushpuckney Shale Member	–27.7*	Forest City Basin	4	black shale
Desmoinesian black shales			31	
Heebner type:				
Unofficial "V" shale over Croweburg Coal Mbr. (Desmoinesian Heebner-type)	–14.5*	Western Interior Coal basin	10	black shale
Mecca-type:				
Anna Shale Member	–9.6*	Illinois Basin	1	gray shale
Mecca Quarry Shale Member	–10.2*	Illinois Basin	15	black shale
Logan Quarry Shale Member	–4.8	Illinois Basin	2	black shale
Holland Shale Member	–42.2	Illinois Basin	3	black shale
Desmoinesian gray shales	+14.1*	Illinois Basin	4	gray shale

*denotes values for individual grains of sulfide minerals from Coveney and Shaffer (1988).
data from Schultz and Coveney (in press)

Appendix O. Statistical Analyses Program

```
                    STATISTICS PROGRAM FOR SPSS/SAS
//PGELRBS JOB, 'GEOPARSAS',
// MSGCLASS=A.REGION=2048K,TIME=(0.20)
// EXEC SPSS
//SYSIN DD
//REC1 DD
//SASSY DD UNIT=SYSDA,VOL=SER=WRK151,DSN=&&GPAR,
// SPACE=(TRK,(1,2)),DISP=(NEW,PASS),
// DCB=(LRECL=100,RECFM=FB,BLKSIZE=6000)
//EXEC SAS
//SYSIN DD*
DATA LIST FILE=REC1
/1 ID 1-6, (A) LINE 1-80 (A)
DATA LIST FILE=TEMP1 FIXED RECORDS=5
RECODE  ID ('HB1','QH1','LB3','QH3','QHC3','QHC2','HBC6','HP3',
 'HP4','EU1','ST2','ST3','MC1'=1)/
('SH1','SH2','SHC3','SHC2'=2)/
(ELSE=3)/INTO GRP/
PROXIMITIES SORG TO U
 /MEASURE=CORR
 /VIEW=VARIABLE
 /MATRIX=OUT (*)
CLUSTER
 /MATRIX=IN(*)
 /PRINT=SCHEDULE
FACTOR VARIABLES=SORG TO U
 /EXTRACTION=PA1
 /ROTATION=VARIMAX
 /PRINT=ROTATION
 /SAVE=REG (ALL FAC)
 /PLOT=FAC1 WITH FAC2 FAC3
 /WRITE OUTFILE=SASSY TABLE
 /1 FAC1 TO FAC9 (9F8.4)
     DATA ROCKS;INFILE GPAR;
     INPUT (FAC1-FAC9) (9*8.4);
     PROC CLUSTER OUTTREE=XXX METHOD=WARD RMSSTD RSQ CCC PSEUDO;
SAS  VAR=FAC1-FAC4
     PROC TREE DATA=XXX;
     PROC PLOT DATA=XXX;
     PLOT CCC * NCL;
     //**
REGRESSION VARIABLES=SORG TO U GRP
 /STATISTICS=DEFAULTS
 /DEPENDENT=GRP
 /METHOD=STEPWISE
DISCRIMINANT GROUPS=GRP(1,3)/VARIABLES=SORG TO U
 /METHOD=WILKS
 /FUNCTIONS=1
 /PIN=0.01
 /STATISTICS=MEAN STDDEV TABLE COEFF RAW UNIVF
 /PLOT=COMBINED
CLUSTER SORG TO U
 /MEASURE=SEUCLID
 /METHOD=CENTROID
 /PRINT=SCHEDULE
```

```
 /PLOT=DENDROGRAM
//**
```

Appendix P. Sample Locations

OUTCROP NO.	LOCATION	COUNTY	SAMPLE NO.	LITHOLOGY
1	NW, 21,12S., 19E.	DOUGLAS	HB-1, HB-2	B, G
2	NWNW, 18, 12S., 18E.	DOUGLAS	QH-1	B
3	SESW, 15, 12S., 18E.	DOUGLAS	LB-1, LB-2	B, G
4	C 15, 11S., 16E.	SHAWNEE	HO-1	B
5	NW, 34, 9S., 18E.	JEFFERSON	LB-3	B
6	NW, 36, 11S., 17E.	DOUGLAS	QH-2	G
7	NW, 6, 18S., 16E.	OSAGE	QH-3	B
8	SWNW, 3, 19S., 15E.	COFFEY	LB-4	B
9	SESW, 11, 21S., 15E.	COFFEY	QH-4	B
10	NE, 5, 23S., 14E.	COFFEY	QH-5	G
11	SWSE, 24, 22S., 12E.	GREENWOOD	SH-1	B
12	NW, 4, 26S., 11E.	GREENWOOD	SH-2	DG
13	SWNE, 9, 30S., 10E.	ELK	SH-3	G
14	NESW, 8, 33S., 11E.	CHAUTAUQUA	QH-6	G
15	NWNW, 21, 33S., 11E.	CHAUTAUQUA	HB-3	DG
16	C 33, 33S., 11E.	CHAUTAUQUA	HB-4	G
17	NW, 7, 34S., 10E.	CHAUTAUQUA	SH-4	DG
18	KC, MO 31st Street	JACKSON	HP-1	B
19	Unity Village, KC, MO	JACKSON	HP-2, ST-1	B, B
20	Clinton Lake Spillway	DOUGLAS	HB-5	B
21	Farlinville Quarry North E/2, SW, 34, 20 S., 23 E.	LINN	ST-2	B
22	McAdam Quarry 1 mi. S. of Mound City	LINN	ST-3	B
23	Jacomo Park	JACKSON	HP-3	B
24	K-10 , 10 mi. E. of Eudor	DOUGLAS	MC-1	B
25	K-10 E. and Edgerton Rd	DOUGLAS	EU-1	B
26	KC, MO 63rd Street and Swope Park	JACKSON	HP-4	B
27	K-32 W and I-635	SHAWNEE	MC-2	B
28	Holliday Road NENW, 6, 12 N., 24 E.	JOHNSON	MC-3	B
29	K-52 Roadcut Mile 30		ST-4	B
30	Farwell Farm (NEB) NW, NW, NE, 23, 1 N., 12	PAWNEE	SH-5	B
31	I-435 E. KC, MO Exit 46	JACKSON	EU-2	B
32	K-69 Quarry N. of Inter.	JACKSON	LB-5	B
33	Barren Creek (IN) N/2, 33, 15 N., 8 W.	PARKE	HLD-1	B
34	Big Pond Creek (IN) 4, 15 N., 8 W.	PARKE	LOG-1	B
35	Mecca Quarry (IN) SE, 20, 15 N., 8 W.	PARKE	Velpen, Hosler	B except for C" samples

B= Black Shale
DG= Dark Gray Shale
G= Gray Shale

SHAWNEE GROUP CORES

CORE	OPERATOR	NO.	LEASE	LOCATION	COUNTY
1	SKELLY	1	BARTOSOVSKY	SESWSW, 9, 1S., 34W.	RAWLINS
2	MURFIN	2	ELVIN	SENWSE, 14, 3S., 27W.	DECATUR
3	TEO. GORE	1	DENNY	C NESW, 5, 5S., 34W.	RAWLINS
4	CONTIN.	406	ADELL UNIT	SESWSW, 2, 6S., 27W.	SHERIDAN
5	CONTINEN.	7	J.E. LEONARD	SWNWSE, 12, 6S., 27W.	SHERIDAN
6	TEXAS O&G	1	DOUGHERTY	NWSWSW, 23, 6S. 33W.	THOMAS
7	SHELL	10	KNIPP	NESESW, 14, 9S., 21W.	GRAHAM
8	SIN. PR.	1	GUY MERCER	C NENW, 28, 10S., 40W.	SHERMAN
9	TEXAS O&G	1	SMITH	NE C SW, 30, 11S., 36W.	LOGAN
10	SIN. PR.	1	WALLACE INV.	SESESE, 22, 11S., 39W.	WALLACE
11	SHELL	1	A. SMITH	C W2, 31, 13S., 14W.	RUSSELL
12	EMPIRE	1	SELLENS	NESWSW, 30, 15S., 13W.	RUSSELL
13	SHELL	1	MICHAELIS	NESENE, 31, 15S., 13W.	RUSSELL
14	SPRINGER	1	OESER SOUTH	SENWSW, 30, 16S., 11W.	BARTON
15	SHELL	3	PLOOG	C EL SW, 33, 18S., 9W.	RICE
16	BARNETT	1	WRIGHT	C S2 NW, 35, 19S., 8W.	RICE
17	ATLANTIC	1	DAGUE	C SWNW, 14, 20S., 33W.	SCOTT
18	ATLANTIC	1	MARK A	C SESE, 28, 20S., 33W.	SCOTT
19	SUPERIOR	684	H.L. TUCKER	SESWSE, 4, 29S., 42W.	STANTON
20	HUMMON	136	SMITH	C NWSW, 36, 31S., 11W.	BARBER
21	MESA	1119	SEACAT	W2E2NE, 19, 31S., 21W.	CLARK
22	HUMMON	1	HERBERT	C SWNW, 6, 32S., 10W.	BARBER
23	HUMMON	1	MCKEEVER	NWNENW, 7, 32S., 10W.	BARBER
24	HUMMON	3	RICKE ESTATES	C NWSE, 12, 32S., 11W.	BARBER
25	HUMMON	1	HRENCHER	C NENW, 13, 32S., 11W.	BARBER
26	COLORADO	110	DREYER	SESENW, 10, 32S., 43W.	MORTON
27	HUMMON	1	HARBAUGH	C NESE, 29, 33S., 11W.	BARBER
28	KRM	2	GIRK	C SWNW, 36, 33S., 20W.	COMANCHE
29	CITIES SERV.	2	GORE	C SESW, 4, 35S., 41W.	MORTON
30	USCOE	12	REDMOND DAM	NENENE, 11, 21S., 15E.	COFFEY

OTHER CORES

CORE	OPERATOR	NO.	LEASE	LOCATION	
31	TEXAS O&G	1	DOUGHERTY	NWSWSW, 23, 6S., 33W.	THOMAS
32	TEXAS O&G	1	SMITH	NE C SW, 30, 11S., 36 W.	LOGAN
33	SOHIO	14	C.C. OSWALD	SWNWSE, 8, 12S., 15W.	RUSSELL
34	SOHIO	23	O. WILCOX A	NWSENE, 8, 12S., 15W.	RUSSELL
35	SOHIO	24	O. WILCOX A	SENWNE, 8, 12S., 15W.	RUSSELL
36	SOHIO	25	O. WILCOX A	NENE, 8, 12S., 15W.	RUSSELL
37	SOHIO	25	O. WILCOX A	NENE, 8, 12S., 15W.	RUSSELL
38	SOHIO	31	O. WILCOX A	NENENE, 8, 12S., 15W.	RUSSELL
39	MCCULLOUCH	25	RUTHVEN I	C SE, 25, 12S., 15W.	RUSSELL
40	MCCULLOUCH	125	RUTHVEN	C SE, 25, 12S., 15W.	RUSSELL
41	SHELL	1	A. SMITH	C W2, 31, 13S., 14W.	RUSSELL
42	DEAN & CL.	1	HOKE	SWSWSW, 24, 14S., 13W.	RUSSELL
43	SKELLY	6	CARTER	SWNE, 33, 14S., 13W.	RUSSELL
44	SHELL	2	J.C. DUMLER	C SWNW, 24, 14S., 14W.	RUSSELL
45	EMPIRE	1	SELLENS	NESWSW, 30, 15S., 13W.	RUSSELL
46	ATLANTIC	1	MARK A	C SESE, 28, 20S., 33W.	SCOTT
47	SHELL	1	A.C. GORDON	C WLW2NE, 21, 21S., 10W.	RICE
48	SHELL	1	WELCH B	C SESE, 4, 24S., 4W.	RENO
49	PETRO-DYN.	1	GRAHAM	C SE, 21, 31S., 3W.	SUMNER
50	PETRO-DYN	1	CASSELMAN	C SESW, 4, 32S., 3W.	SUMNER
51	COLORADO	110	DREYER	SENW, 10, 32S., 43W.	MORTON

Appendix Q. Measured Sections and Core Descriptions

EXPLANATION

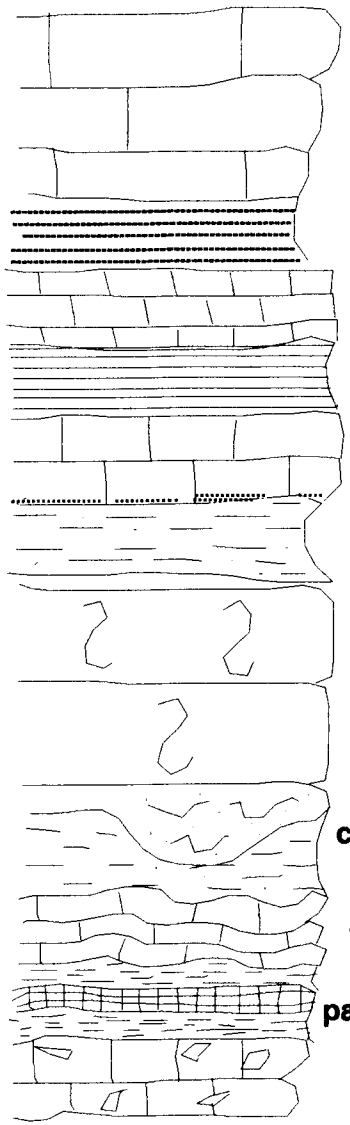

massive limestone

calcareous shale

slabby-bedded limestone

black shale

oolitic limestone

silty shale

algal mound complex

channel sandstone deposit

wavy-bedded limestone

paleosol in clay-rich shale

limestone with rip-ups

**** algal blades

algal wrap

Osagia

fusulinids

crinoids

mollusks

gastropods

fenestrate bryozoans

ramose bryozoans

br bryozoans

echinoid spines

Amblysiphonella

rugose corals

fist fistulipids

hash fossil hash zone

Syringopora

plant fragments

trilobites

high spirol gastropods

allochthonous coal

coal with underclay

XXXXXXXX
XXXXXXXX redbeds

black shale with phosphatic nodules

burrows, trails

concretions

▲ chert

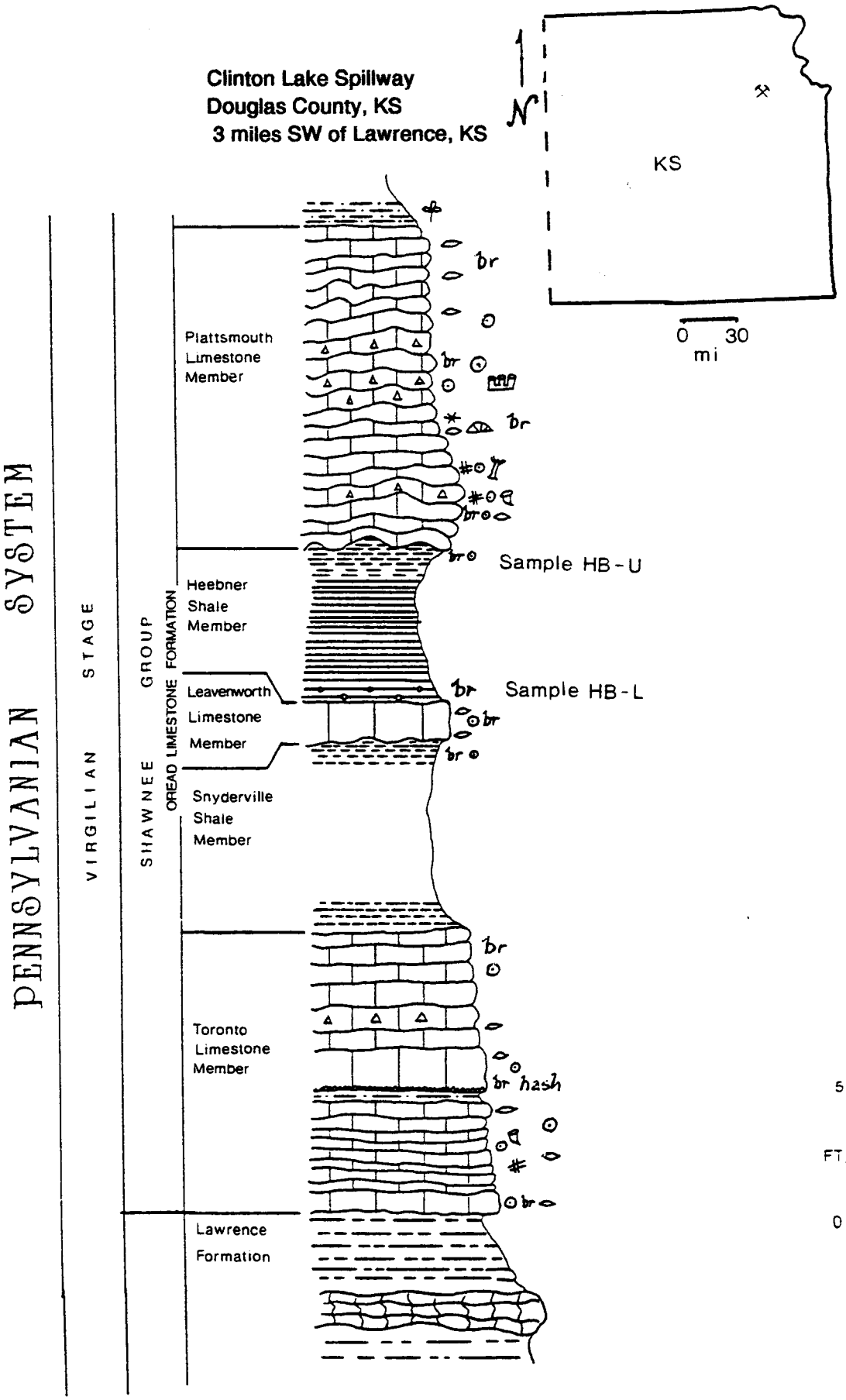
Clinton Lake Spillway
Douglas County, KS
3 miles SW of Lawrence, KS
N
KS
0 30
mi
PENNSYLVANIAN SYSTEM
VIRGILIAN STAGE
SHAWNEE GROUP
OREAD LIMESTONE FORMATION
Plattsmouth Limestone Member
Heebner Shale Member
Leavenworth Limestone Member
Snyderville Shale Member
Toronto Limestone Member
Lawrence Formation
Sample HB-U
Sample HB-L
br
hash
5
FT
0

Turnpike Section
NENW, sec. 21, T. 12 S., R. 19 E.
Douglas County, KS

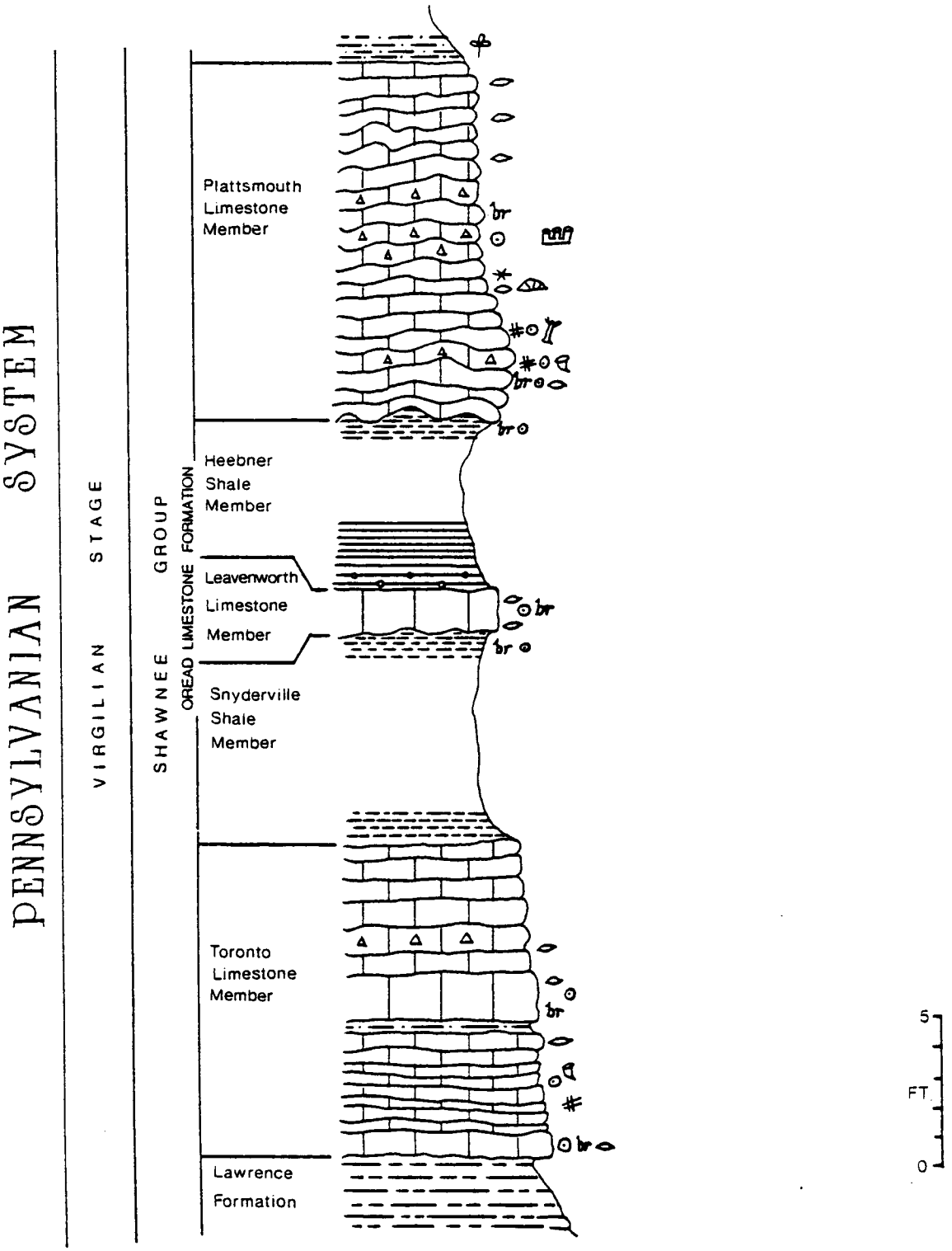

Turnpike Section
NWNW, sec. 18, T. 12 S., R. 18 E.
Douglas County, KS

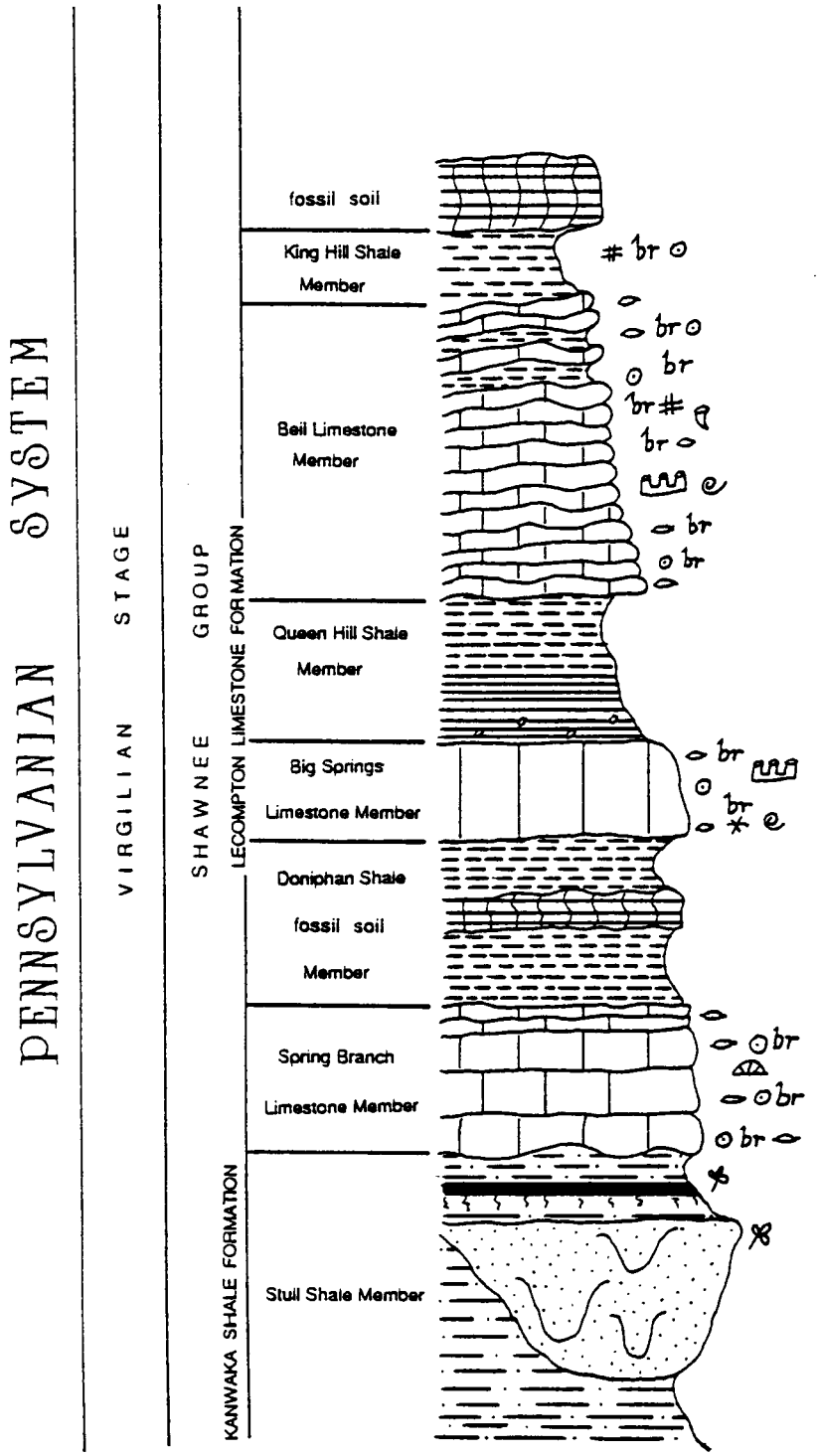

Turnpike Section
SESW, sec. 15, T. 12 S., R. 18 E.
Douglas County, KS

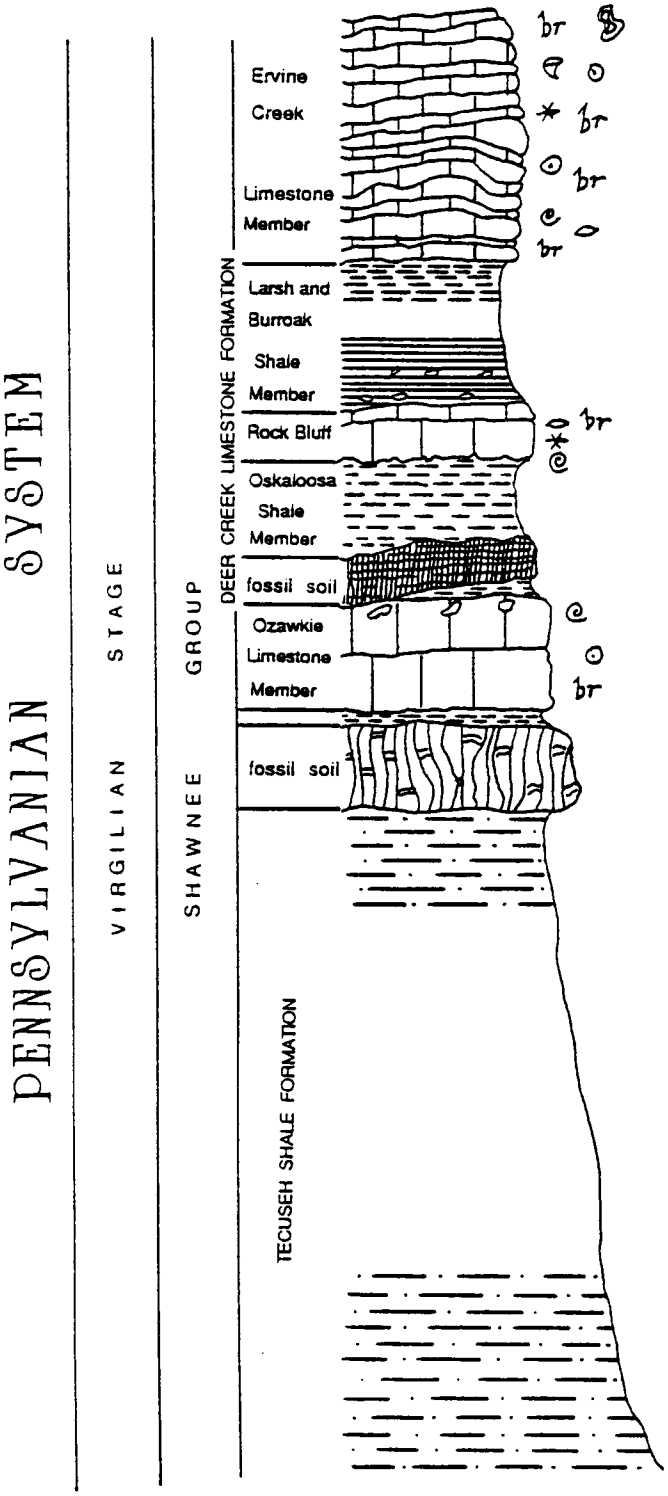

Calhoun Bluffs
c. sec. 15, T. 11 S., R. 16 E.
Shawnee County, KS

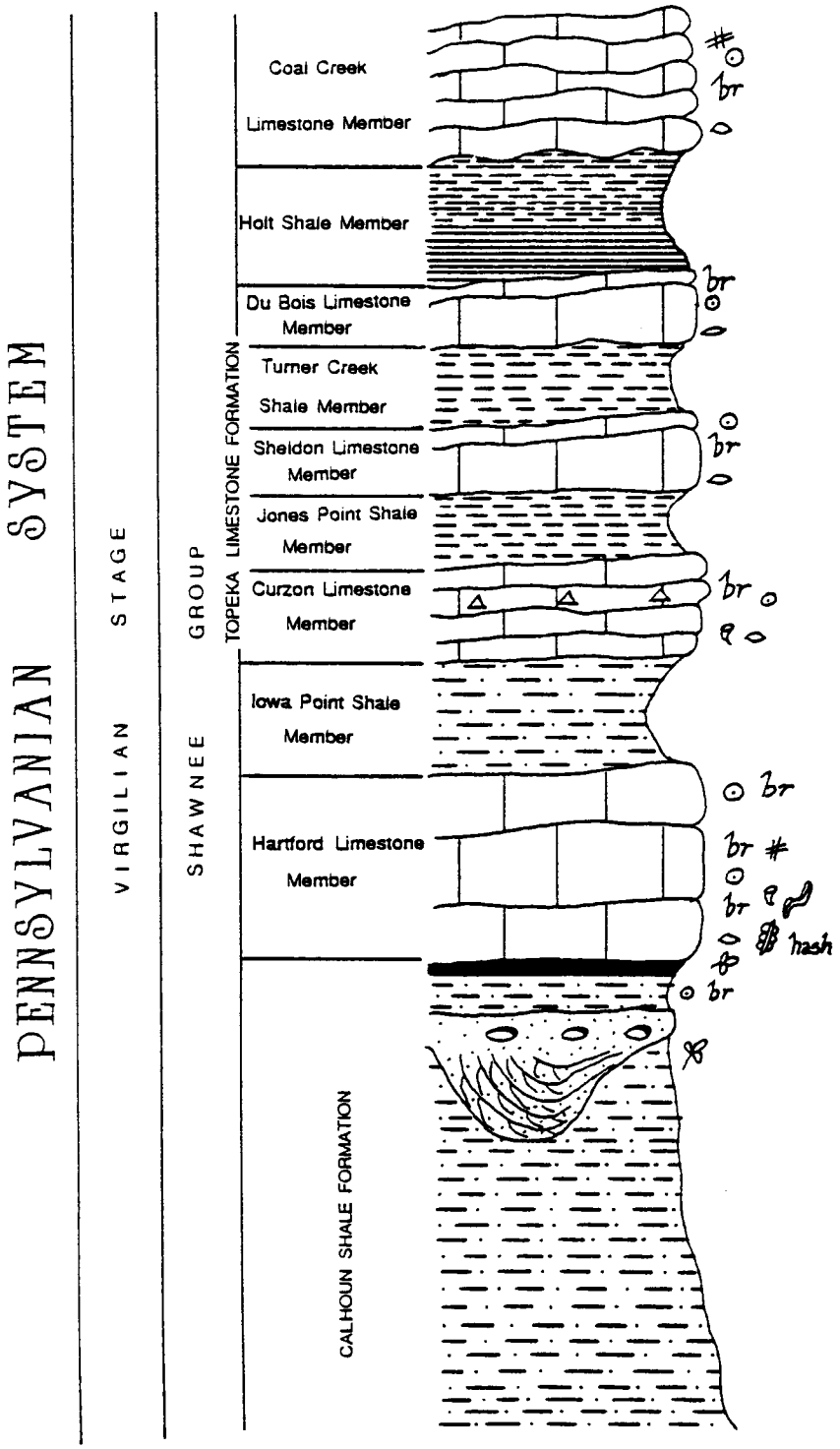

E. Ozawkie, K-92
NW, sec. 34, T. 9 S., R. 18 E.
Jefferson County, KS

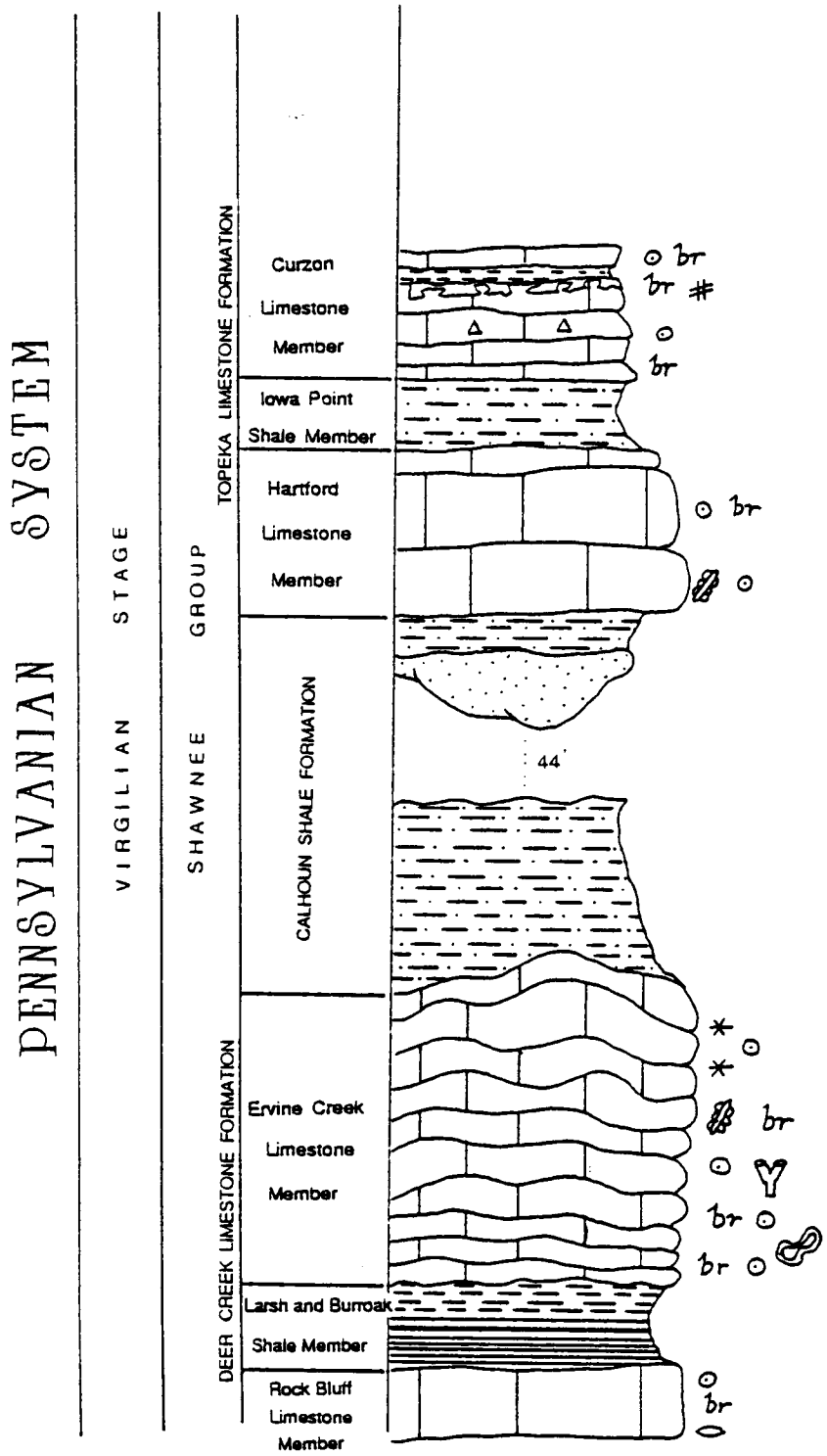

Grover's Station
NW, sec. 36, T. 11 S., R. 17 E.
Douglas County, KS

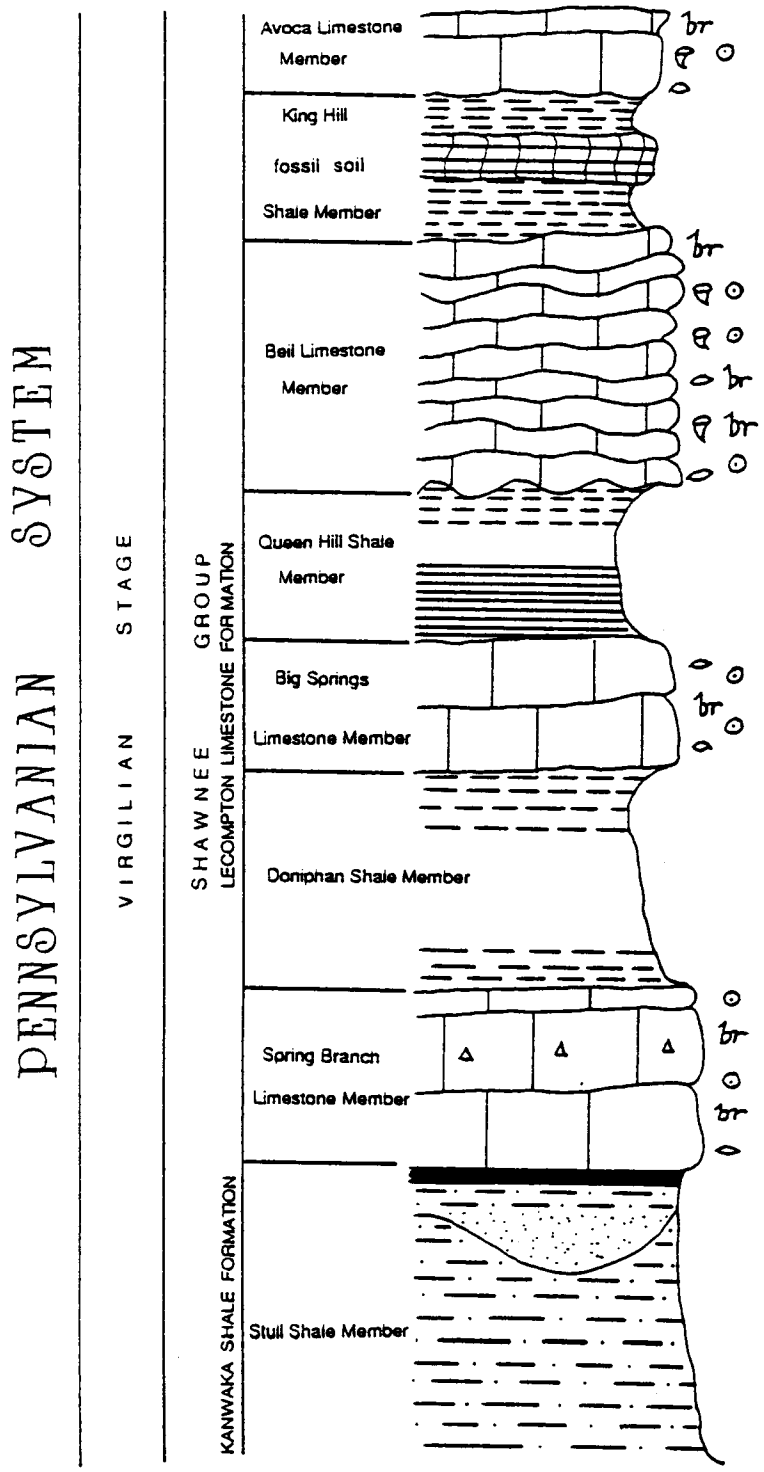

N. Bank of Marais des Cygnes
NW, sec. 6, T. 18 S., R. 16 E.
Osage County, KS

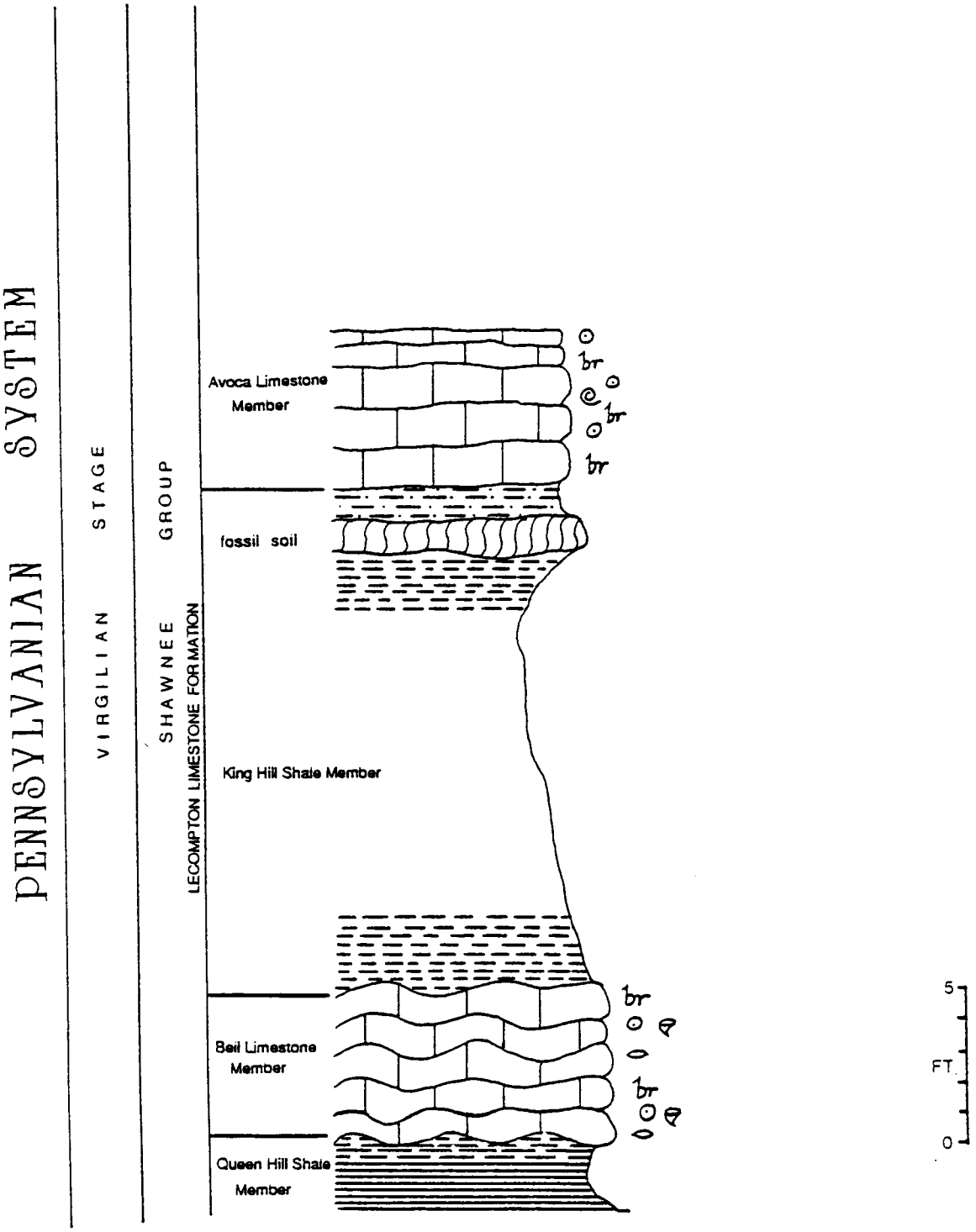

Frog Creek
SWNW, sec. 3, T. 19 S., R. 15 E.
Cóffey County, KS

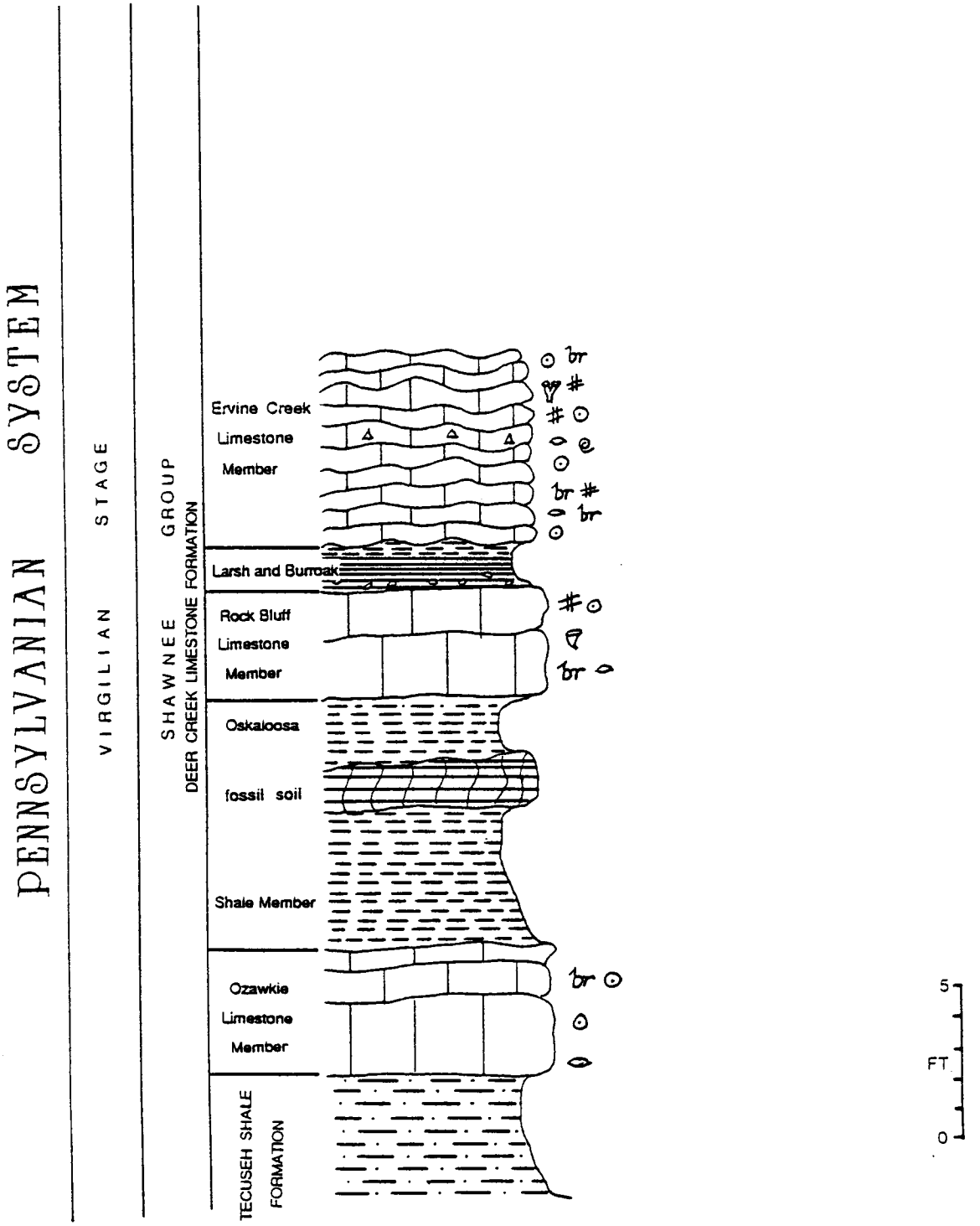

South Gridley
NE, sec. 5, T. 23 S., R. 14 E.
Coffey County, KS

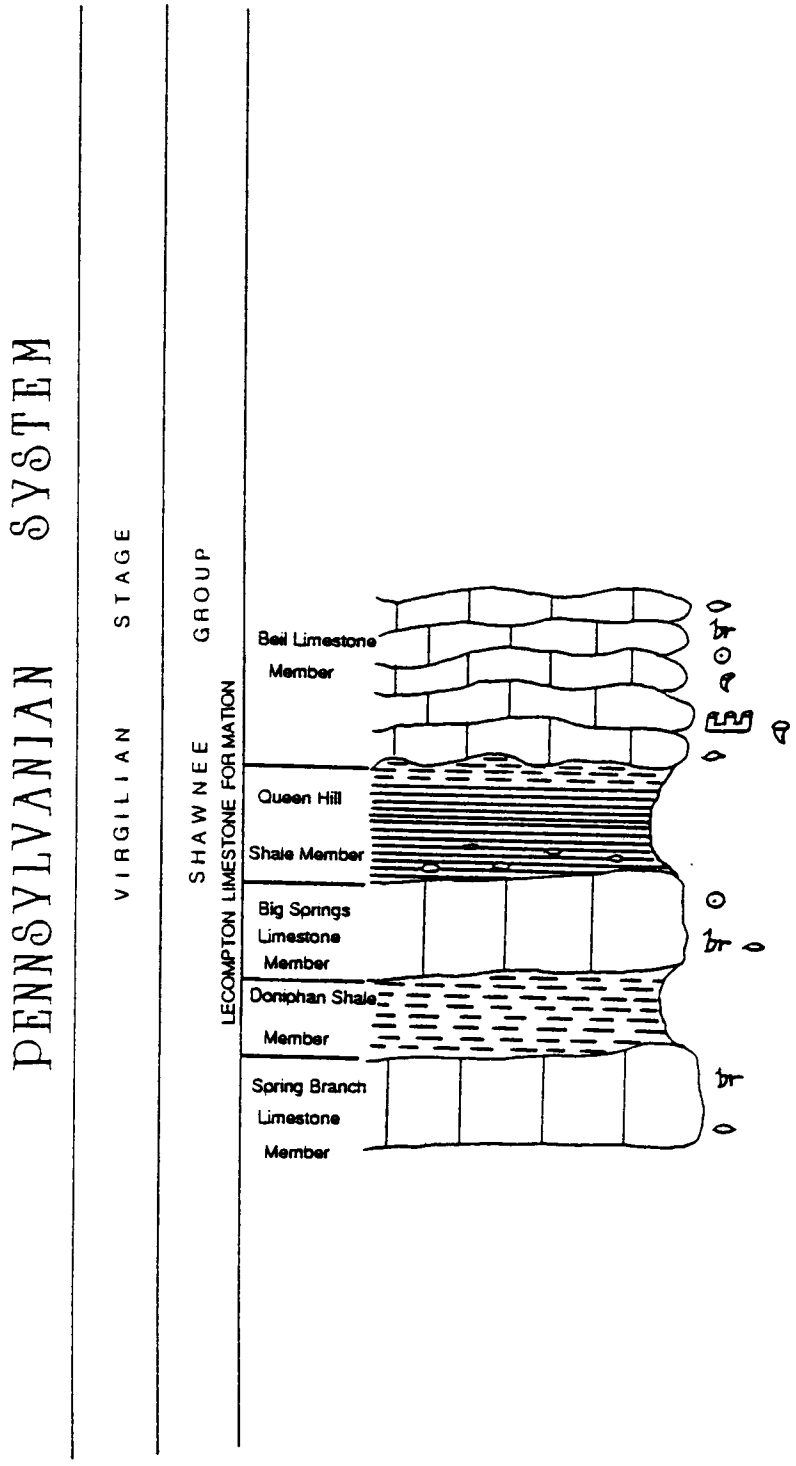

Lamont Section
SWSE, sec. 24, T. 22 S., R. 12 E.
Greenwood County, KS

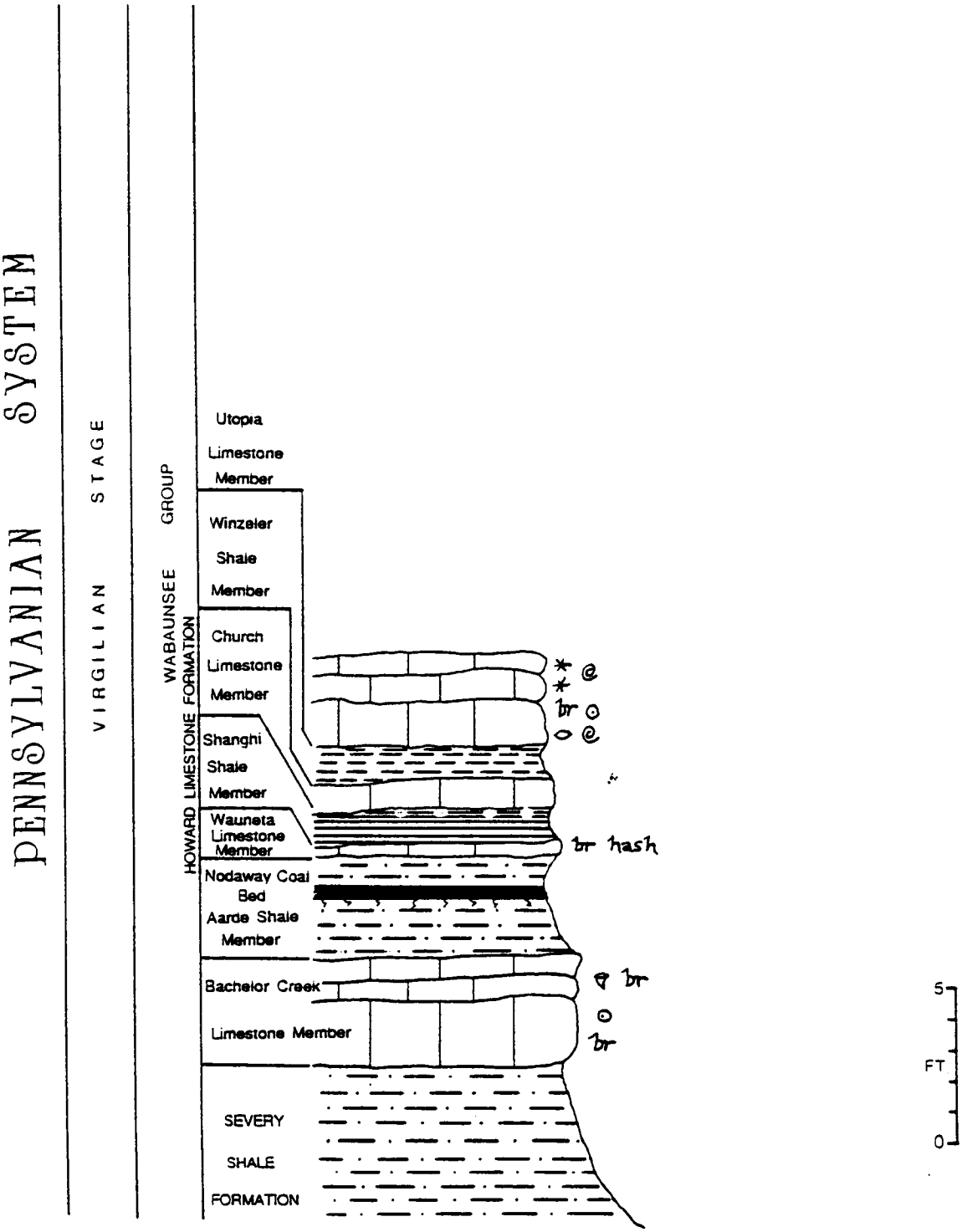

US–54
NW, sec. 4, T. 26 S., R. 11 E.
Greenwood County, KS

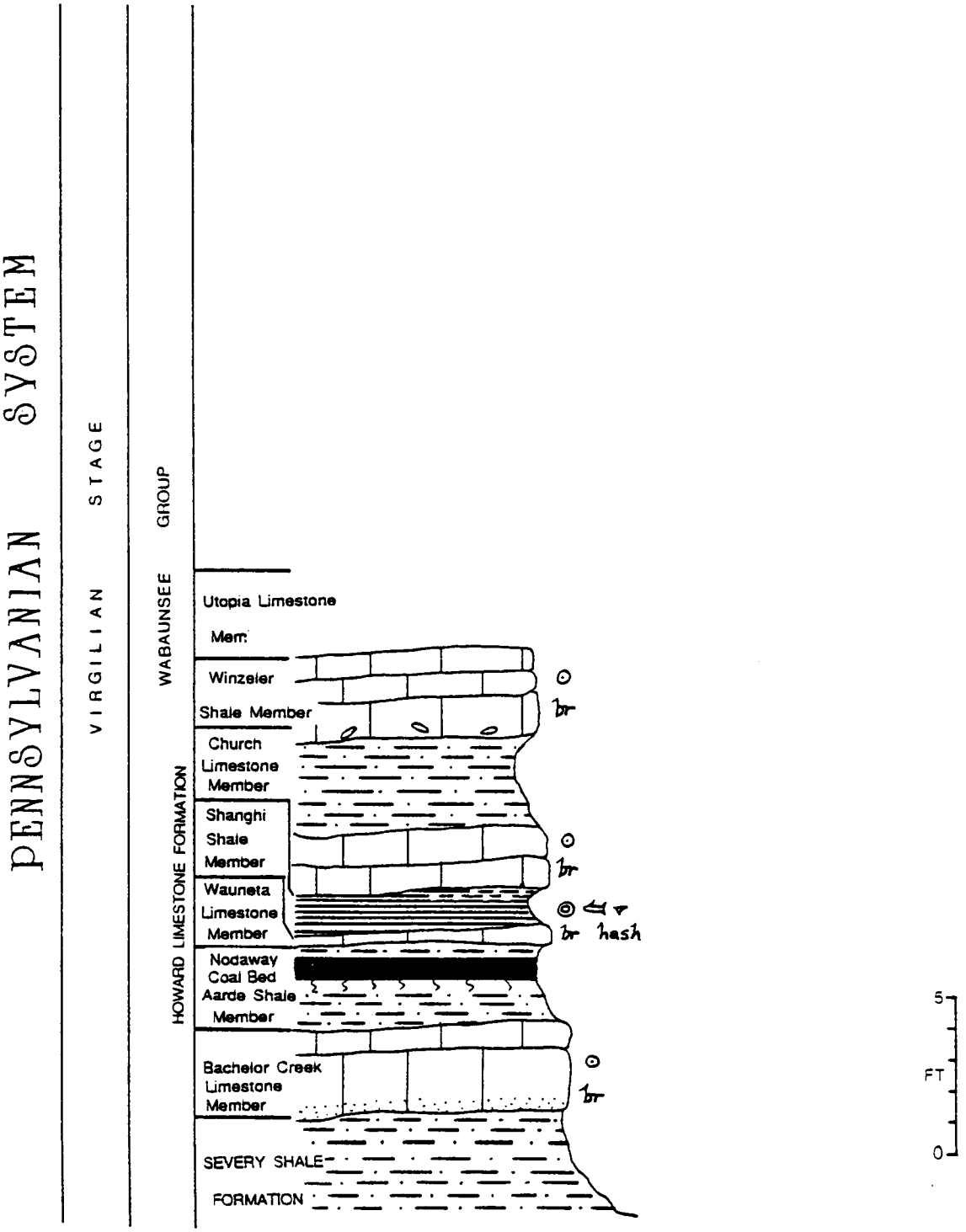

Elk River West of Howard, KS
SWNE, sec. 9, T. 30 S., R. 10 E.
Elk County, KS

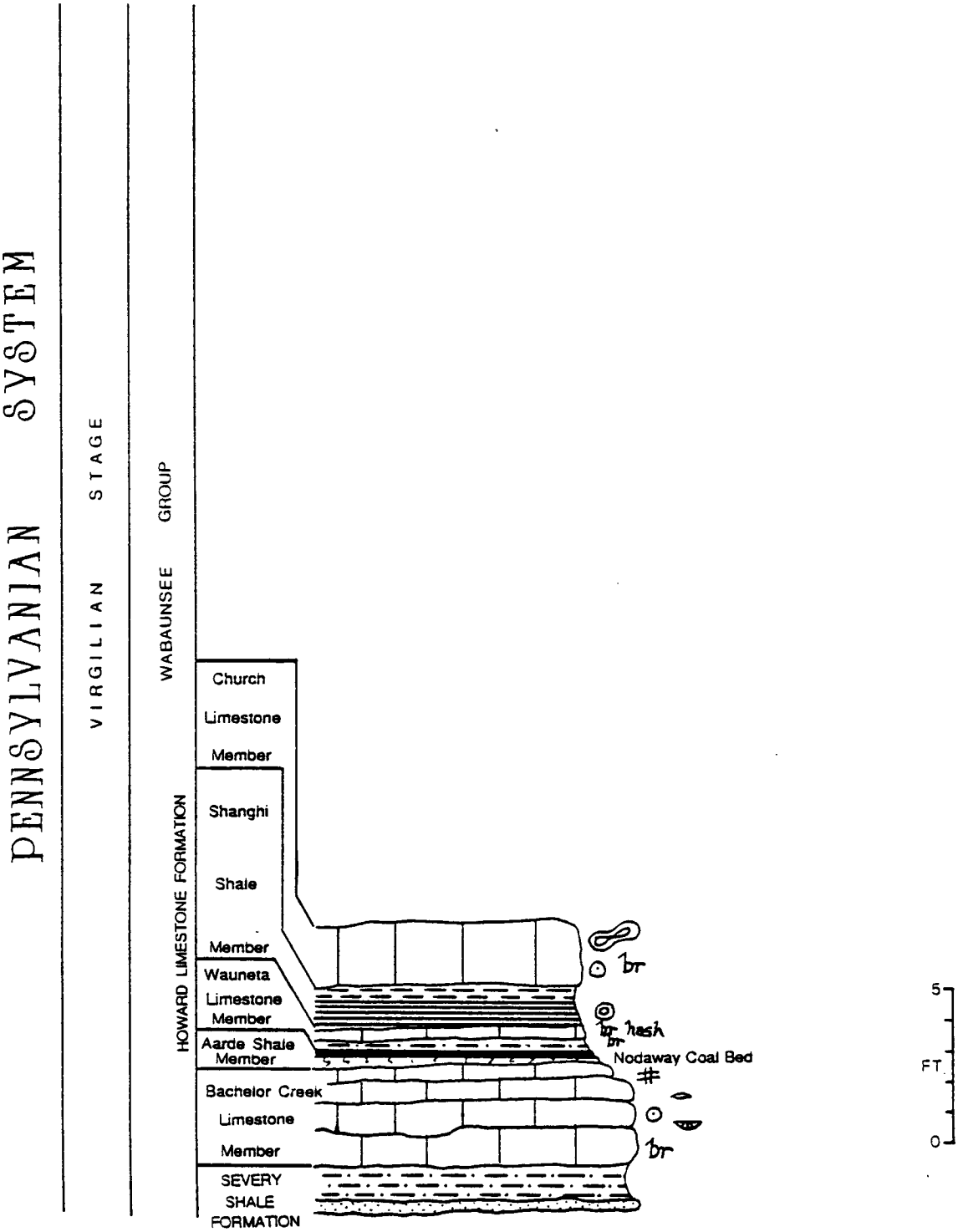

NW Sedan, KS, K–99
NESW, sec. 8, T. 33 S., R. 11 E.
Chautauqua County, KS

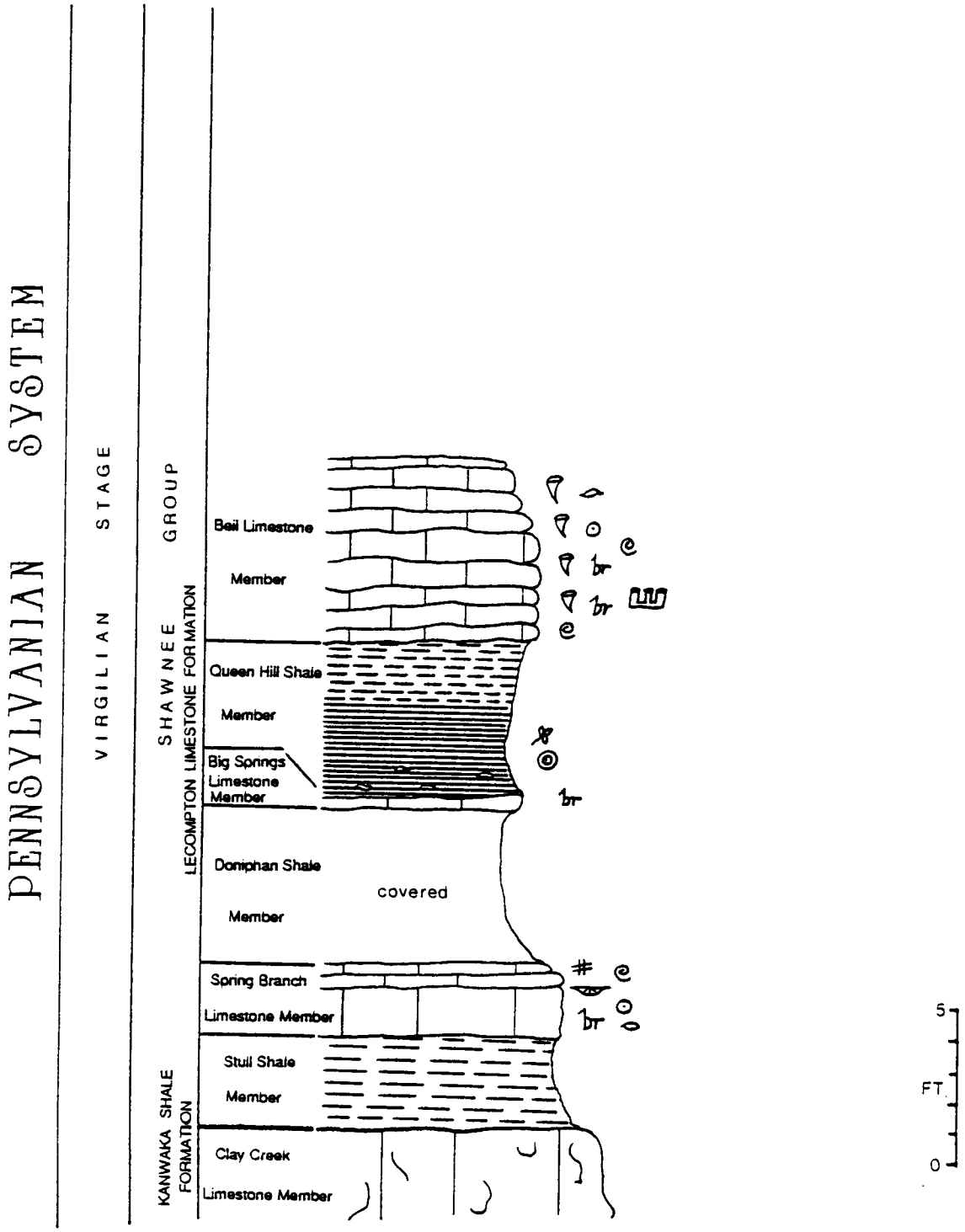

Sedan City Lake Spillway
NWNW, sec. 21, T. 33 S., R. 11 E.
Chautauqua County, KS

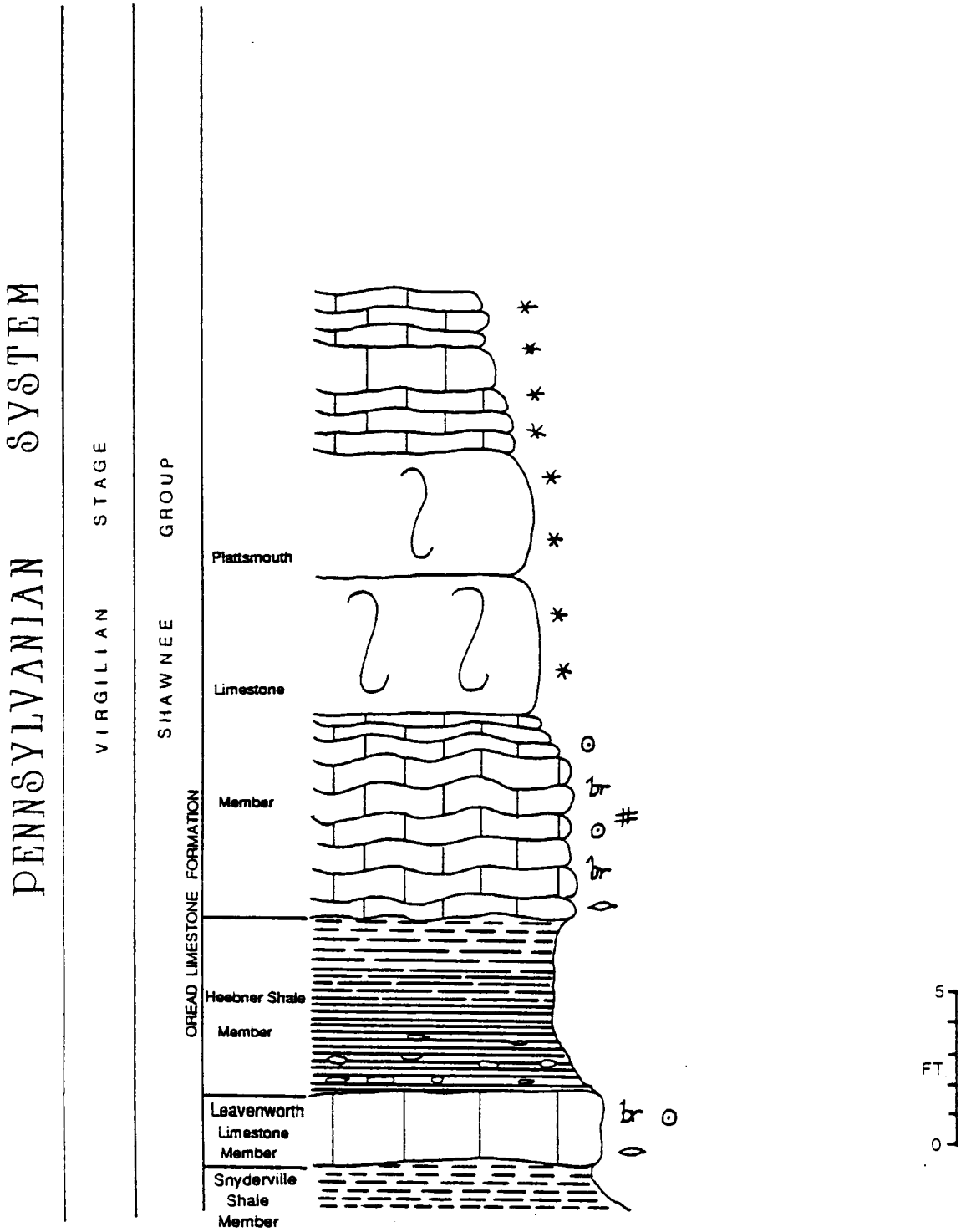

Wauneta Type Section, K–166
NW, sec. 7, T. 34 S., R. 10 E.
Chautauqua County, KS

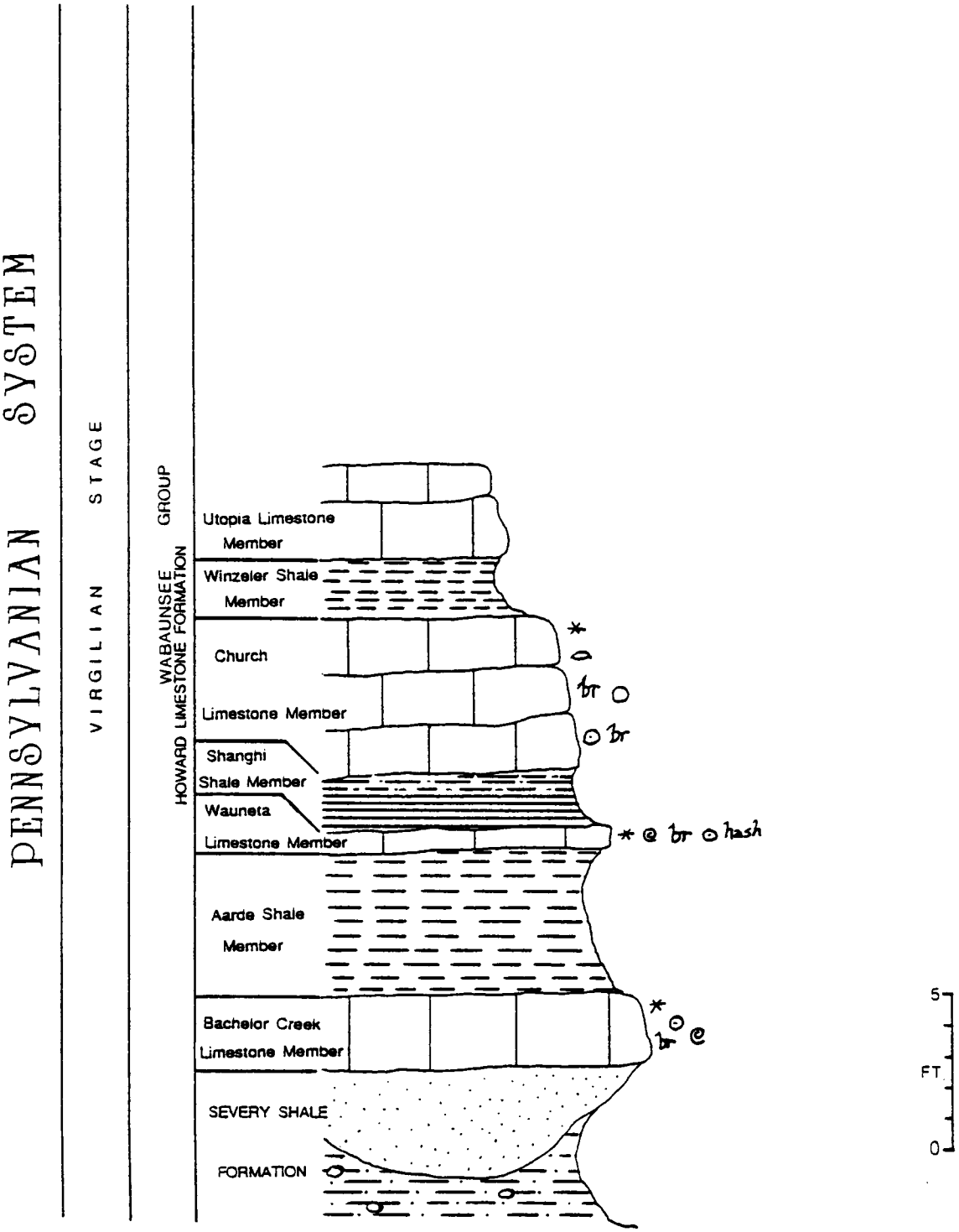

Conposite Section: Hilltop Quarry
NWNE, sec. 7, T. 23 S., R. 13 E.

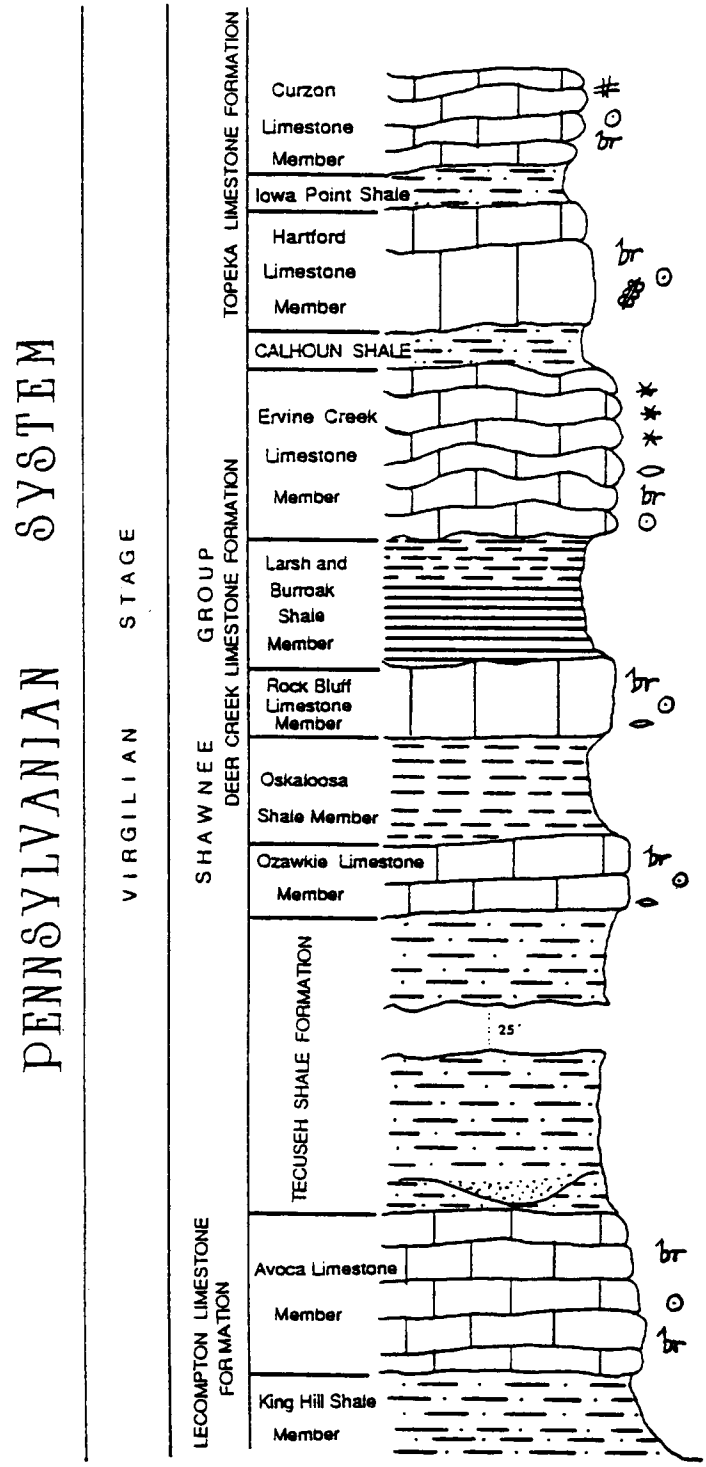

Severy Quarry
SWNW, sec. 11, T. 28 S., R. 11 E.
Greenwood County, KS

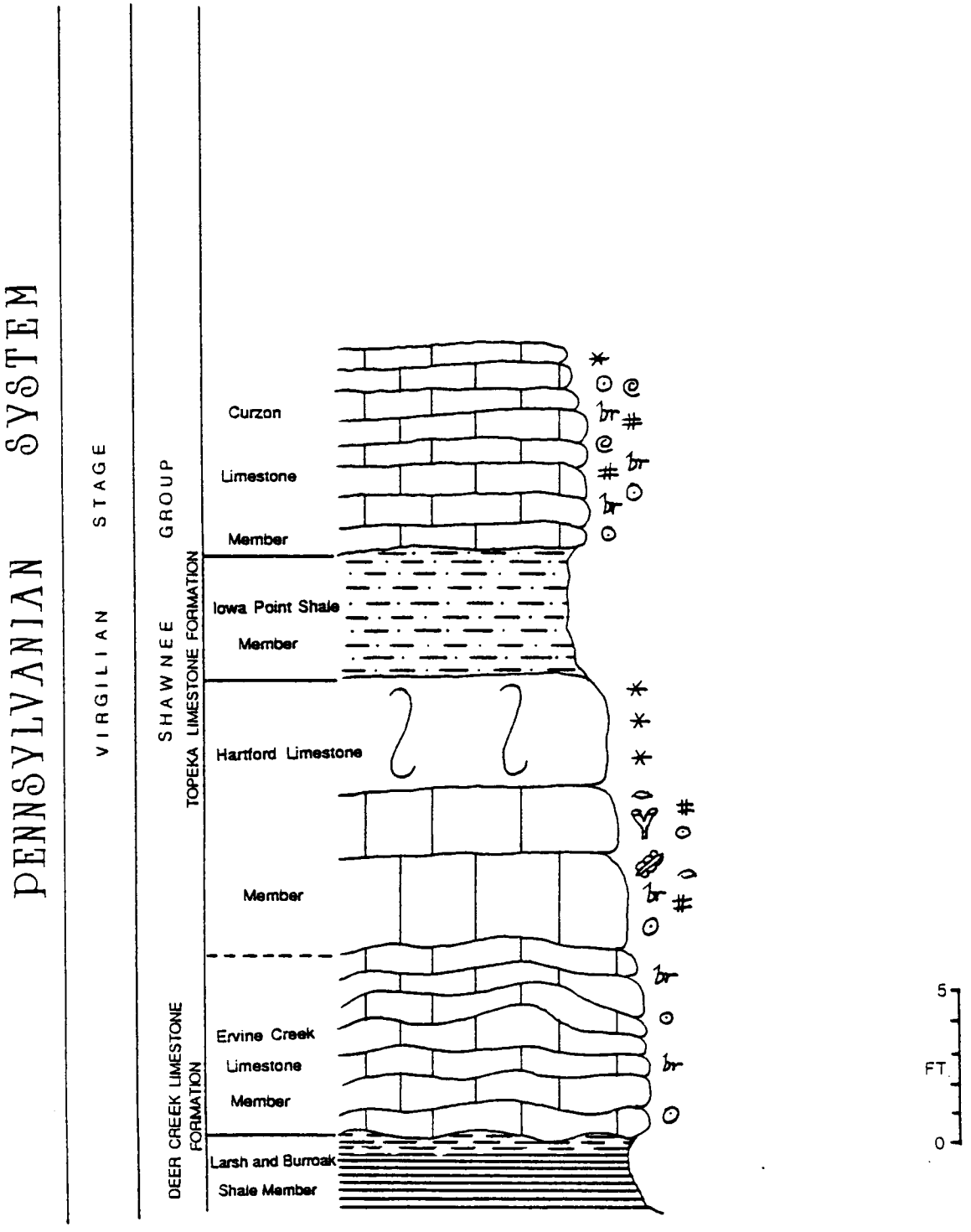

Long Creek, I–35
SENE, sec. 5, T. 19 S., R. 16 E.
Osage County, KS

PENNSYLVANIAN SYSTEM

VIRGILIAN STAGE

SHAWNEE GROUP

LECOMPTON LIMESTONE FORMATION

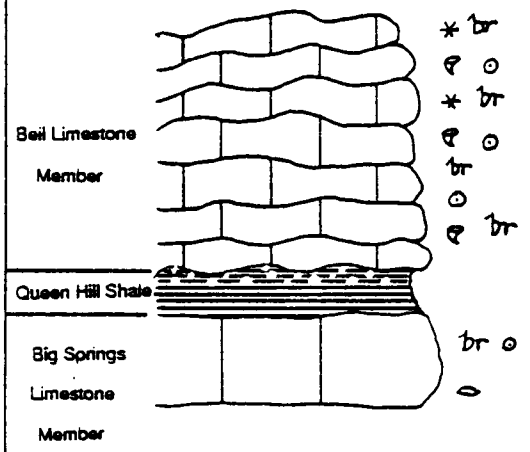

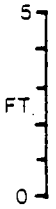

Dragoon Creek
SWNE, sec. 7, T. 16 S., R. 16 E.
Osage County, KS

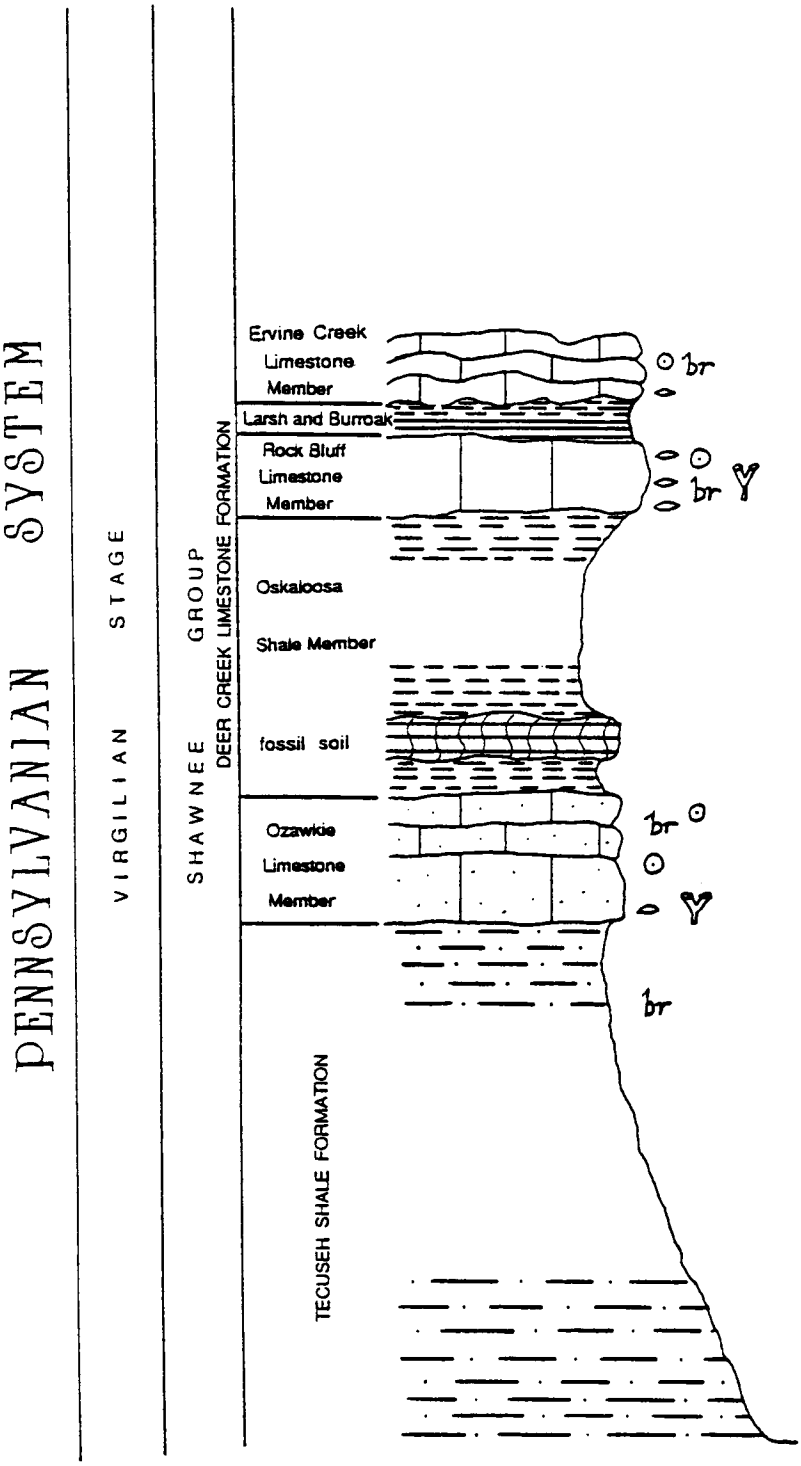

West Oskaloosa, K–92
NE, sec. 6, T. 10 S., R. 19 E.
Jefferson County, KS

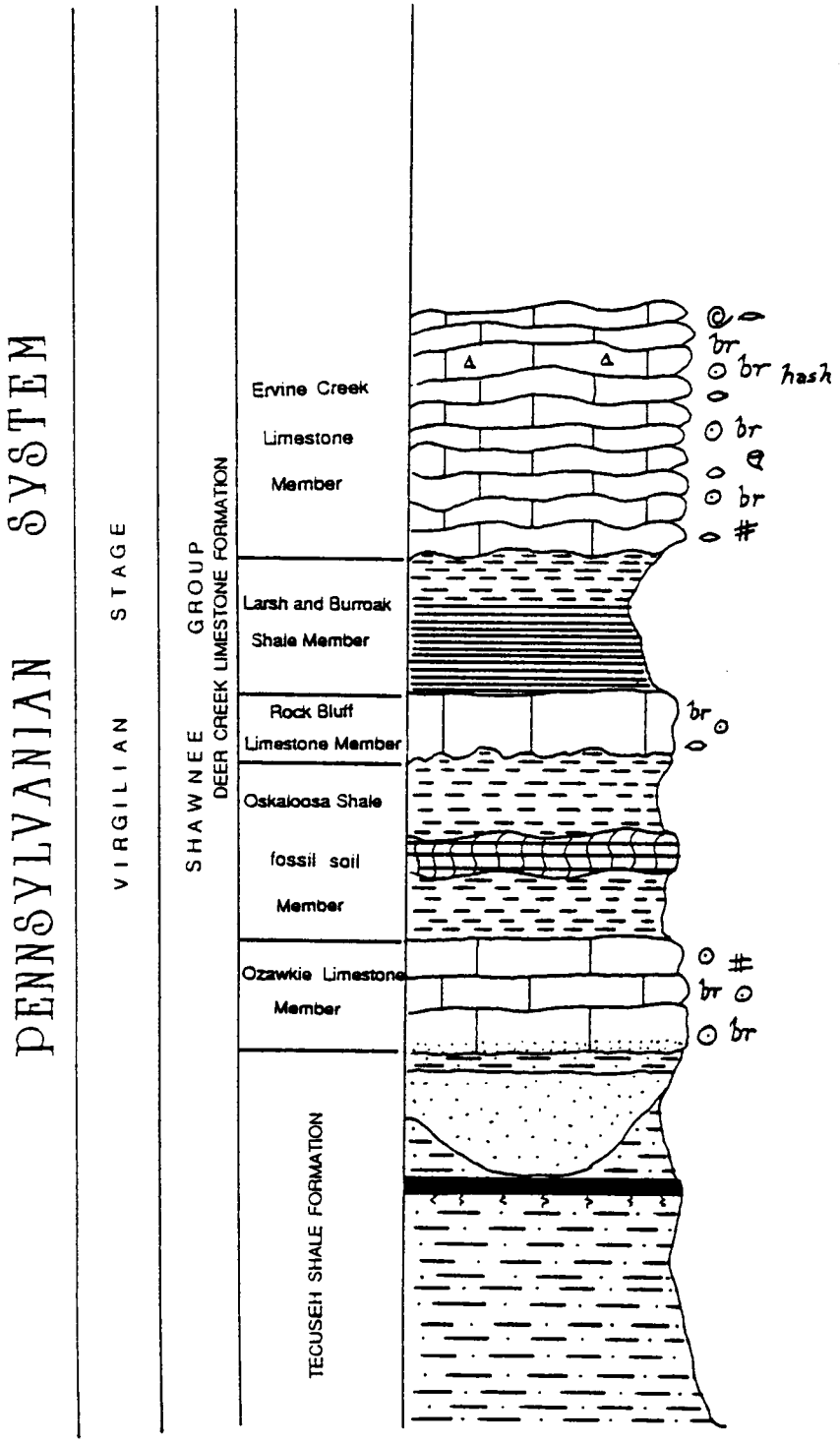

Composite Mecca Quarry Region
SWNE, sec. 29, T. 15 N., R. 8 W.
Parke County, IN

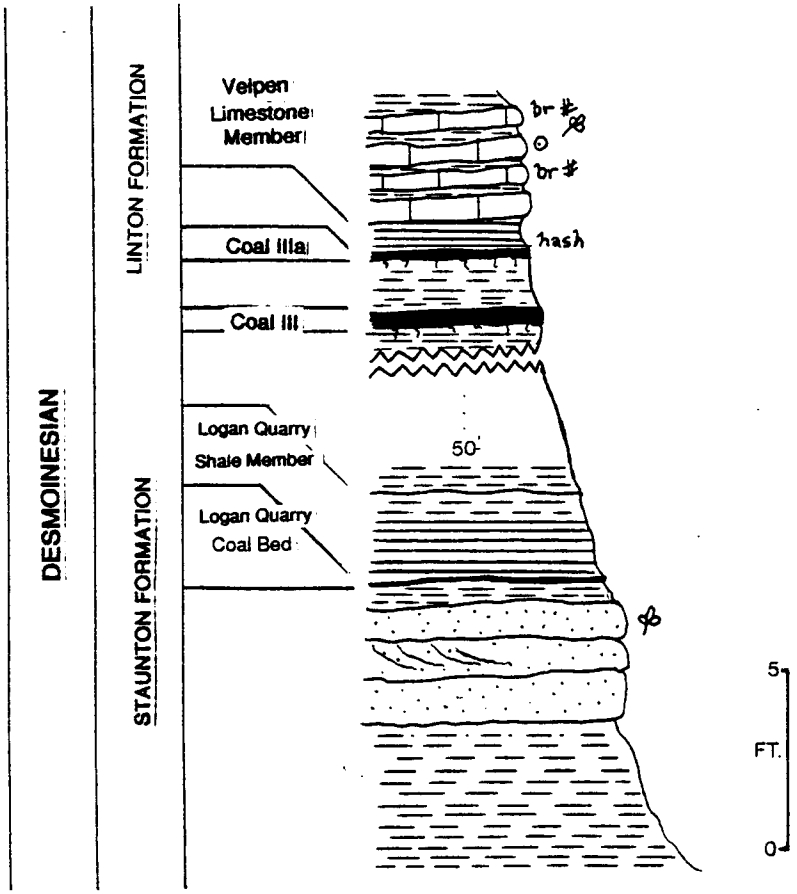

Big Pond Creek
NW, sec. 4, T. 15 N., R. 8 W.
Parke County, IN

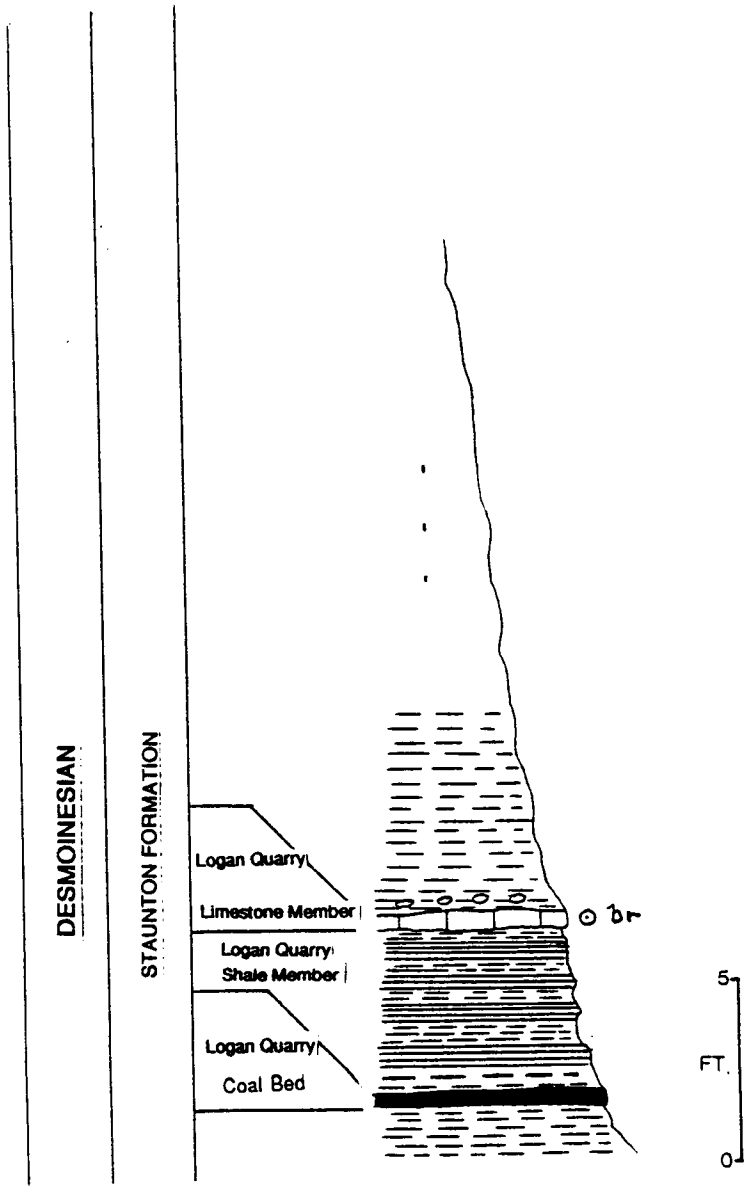

Raytown Section, I–435 and 350
SWSWNW, sec. 6, T. 48 N., R. 32 W.
Jackson County, MO

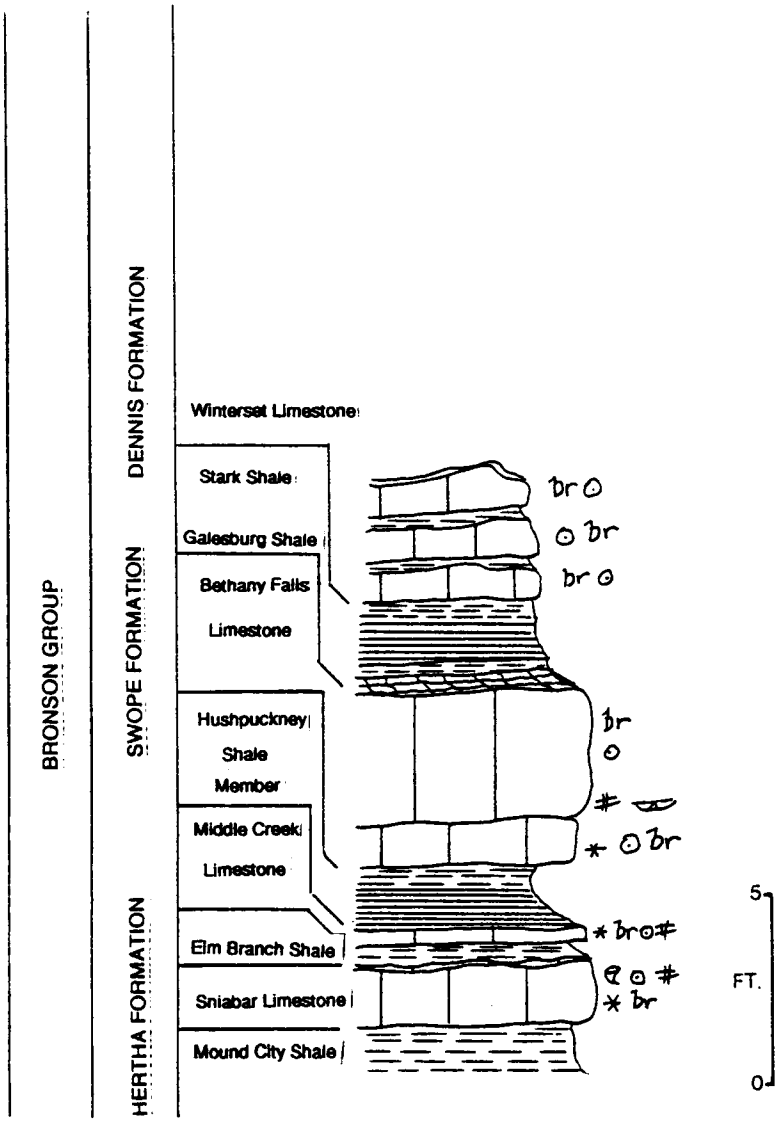

Farwell Farm Section
NWNWNE, sec. 23, T. 1 N., R. 12 E.
Pawnee County, NE

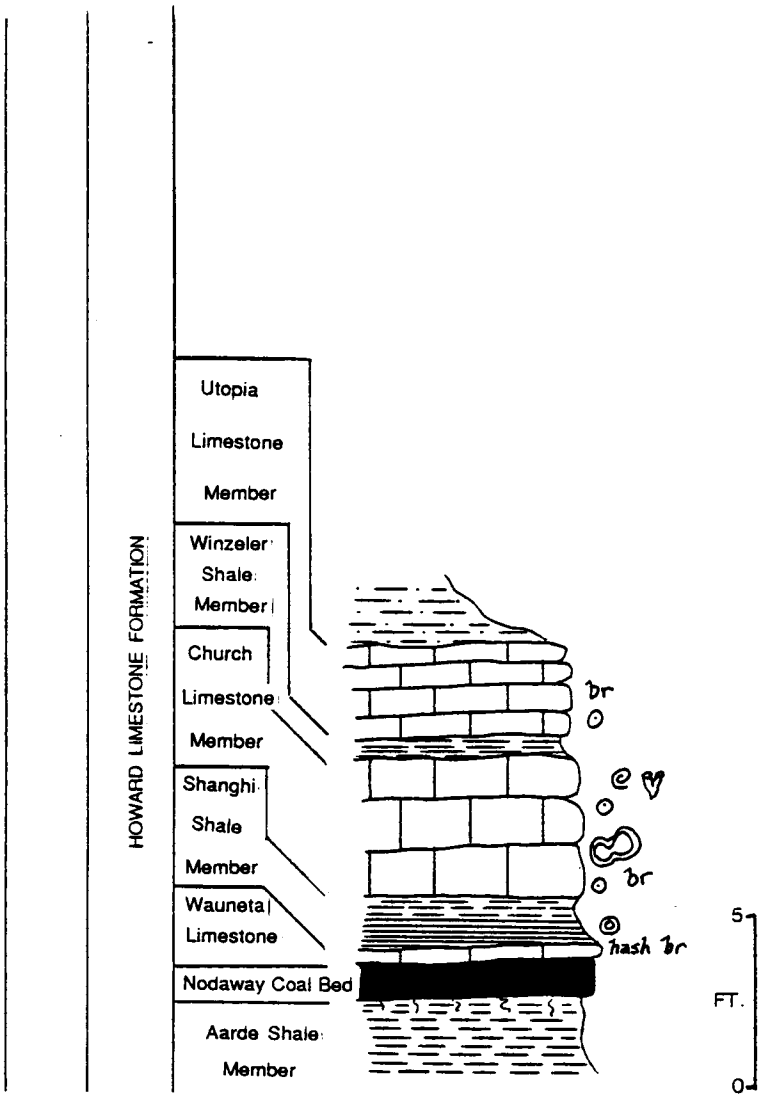

Barren Creek
N1/2, sec. 33, T. 15 N., R. 8 W.
Parke County, IN

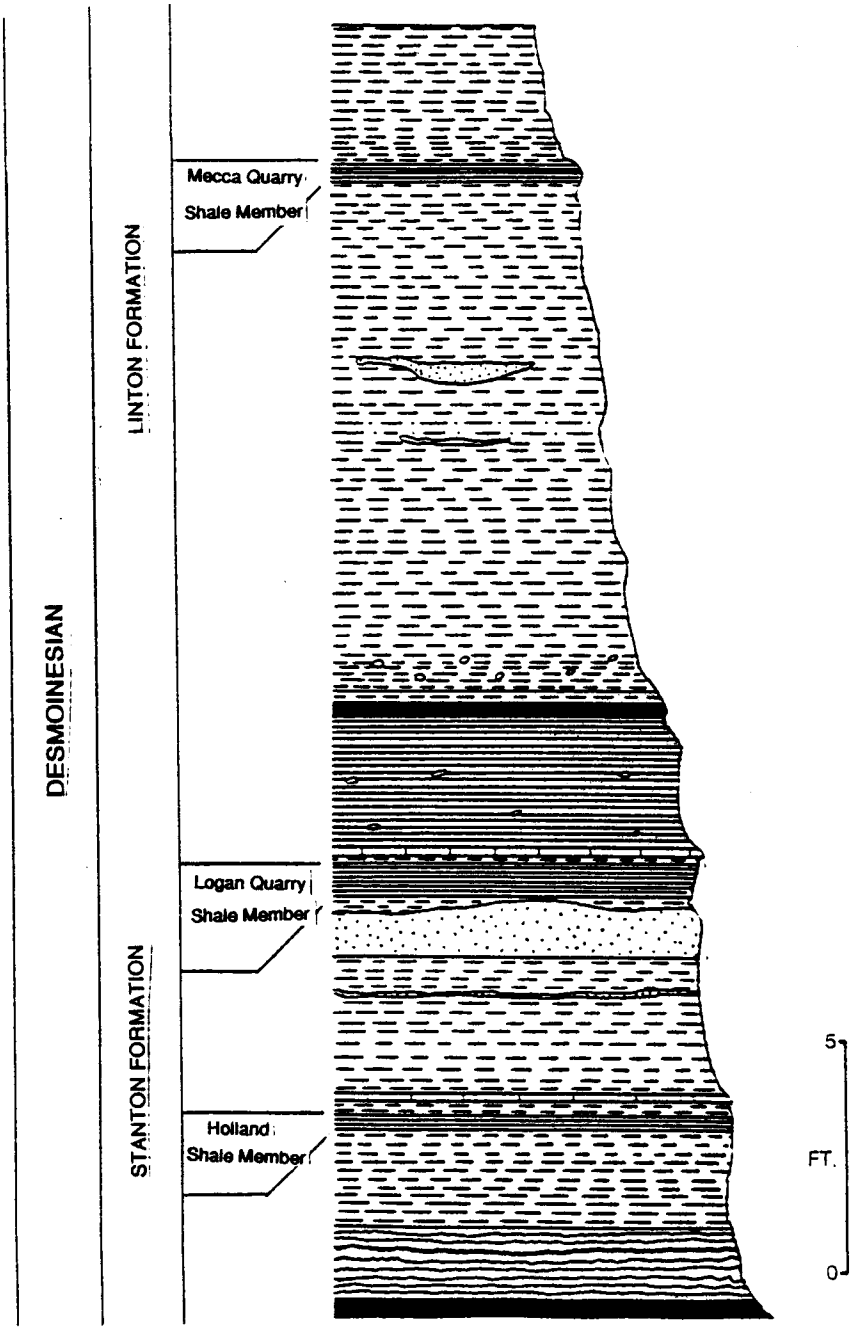

K–32 and I–635
Shawnee County, KS

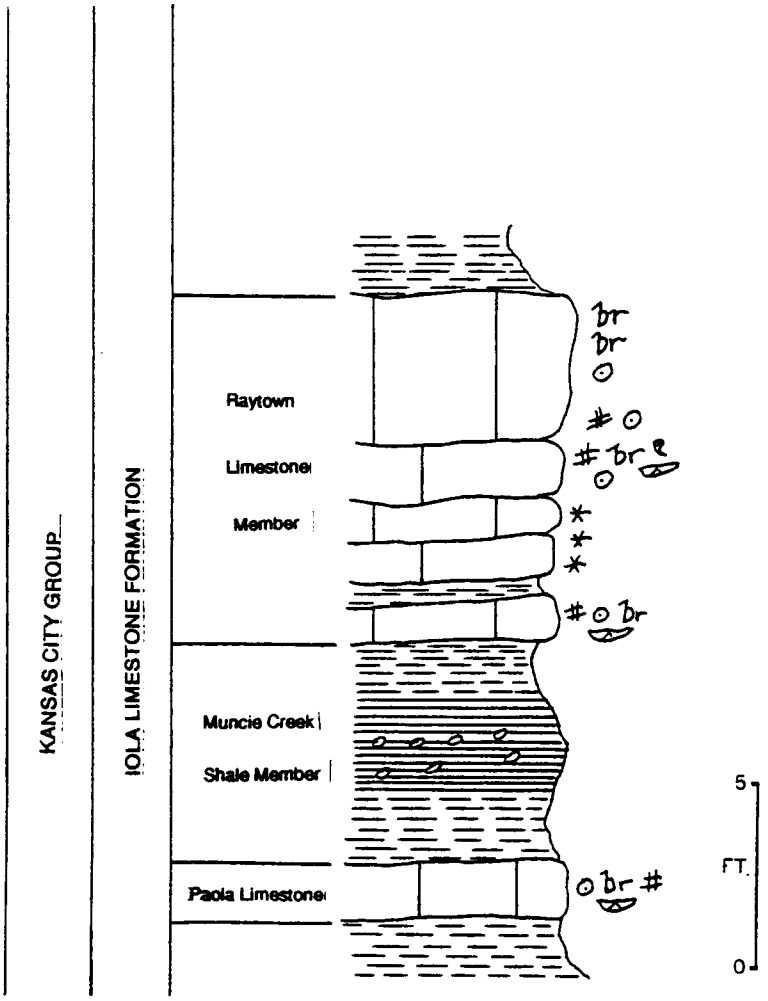

Holliday Road Section
NENW, sec. 7, T. 12 N., R. 24 E.
Johnson County, MO

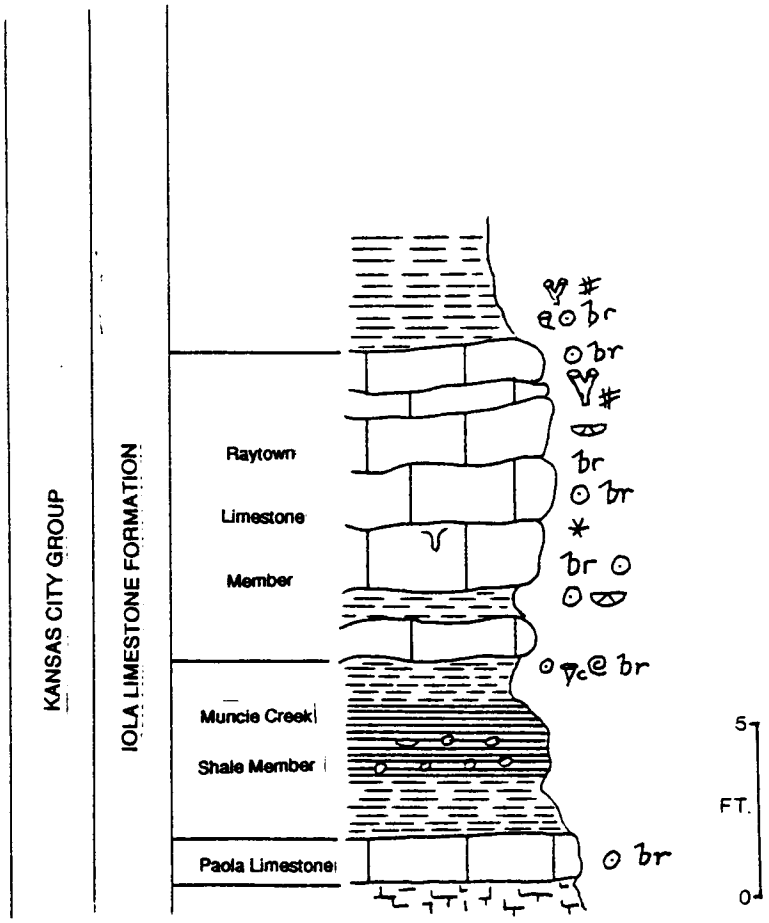

East Eudora
K–10 and Edgerton Road
Douglas County, KS

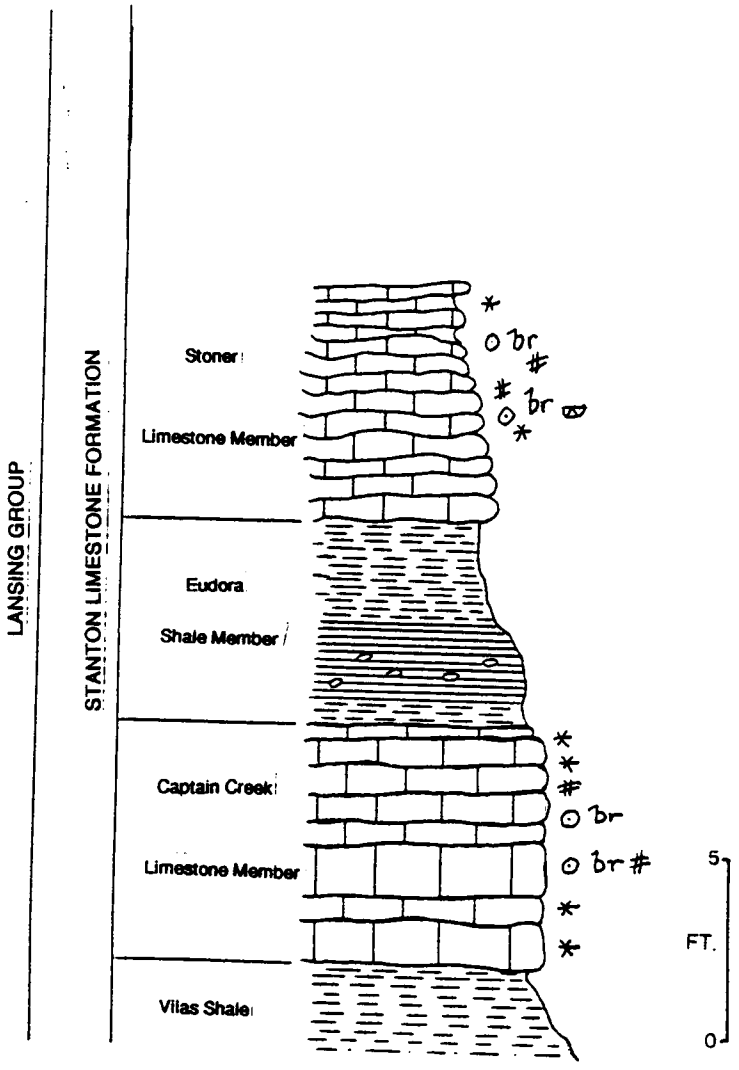

Unity Village
Kansas City, MO
Jackson County, MO

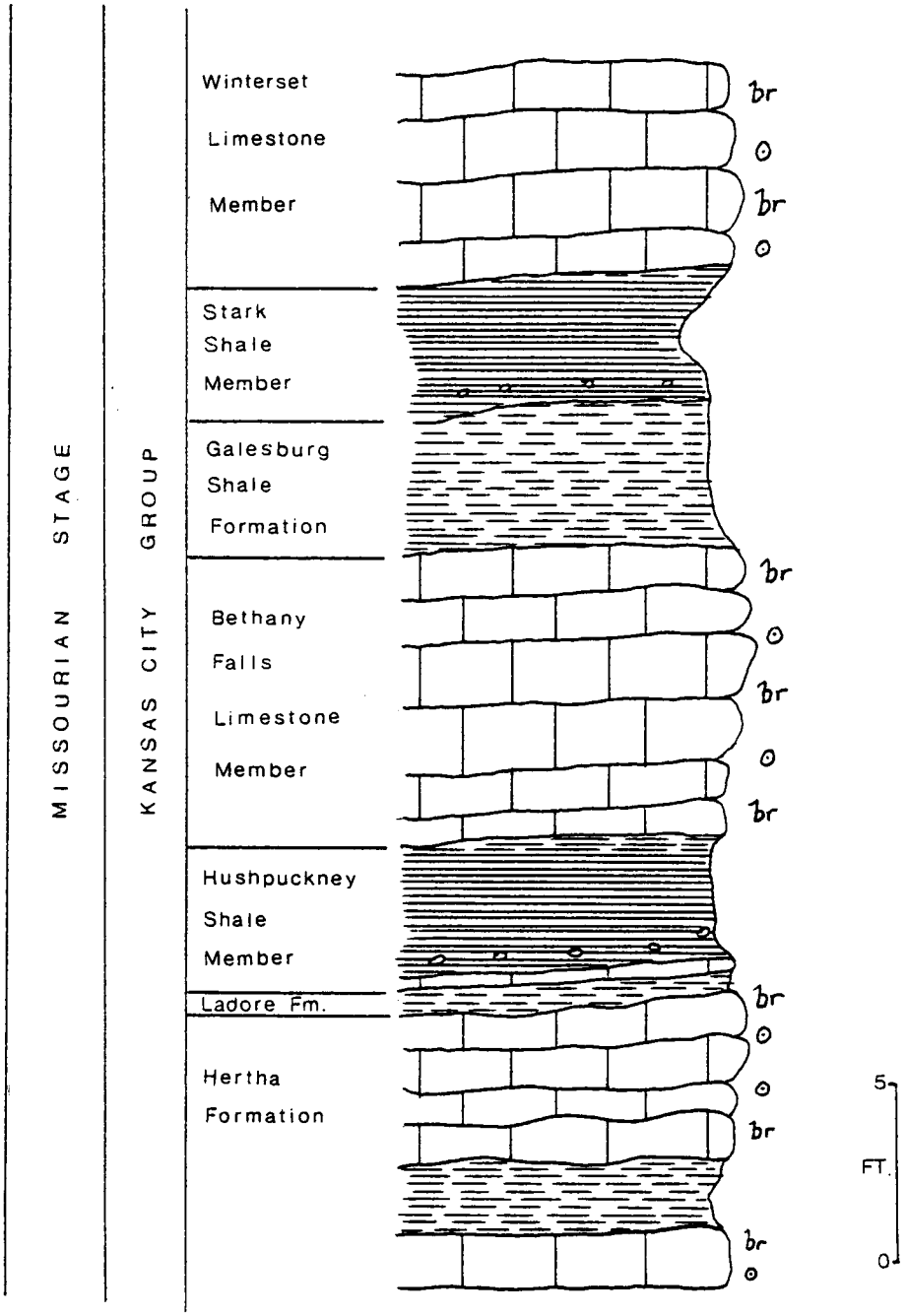

Skelly #1: Bartosovsky

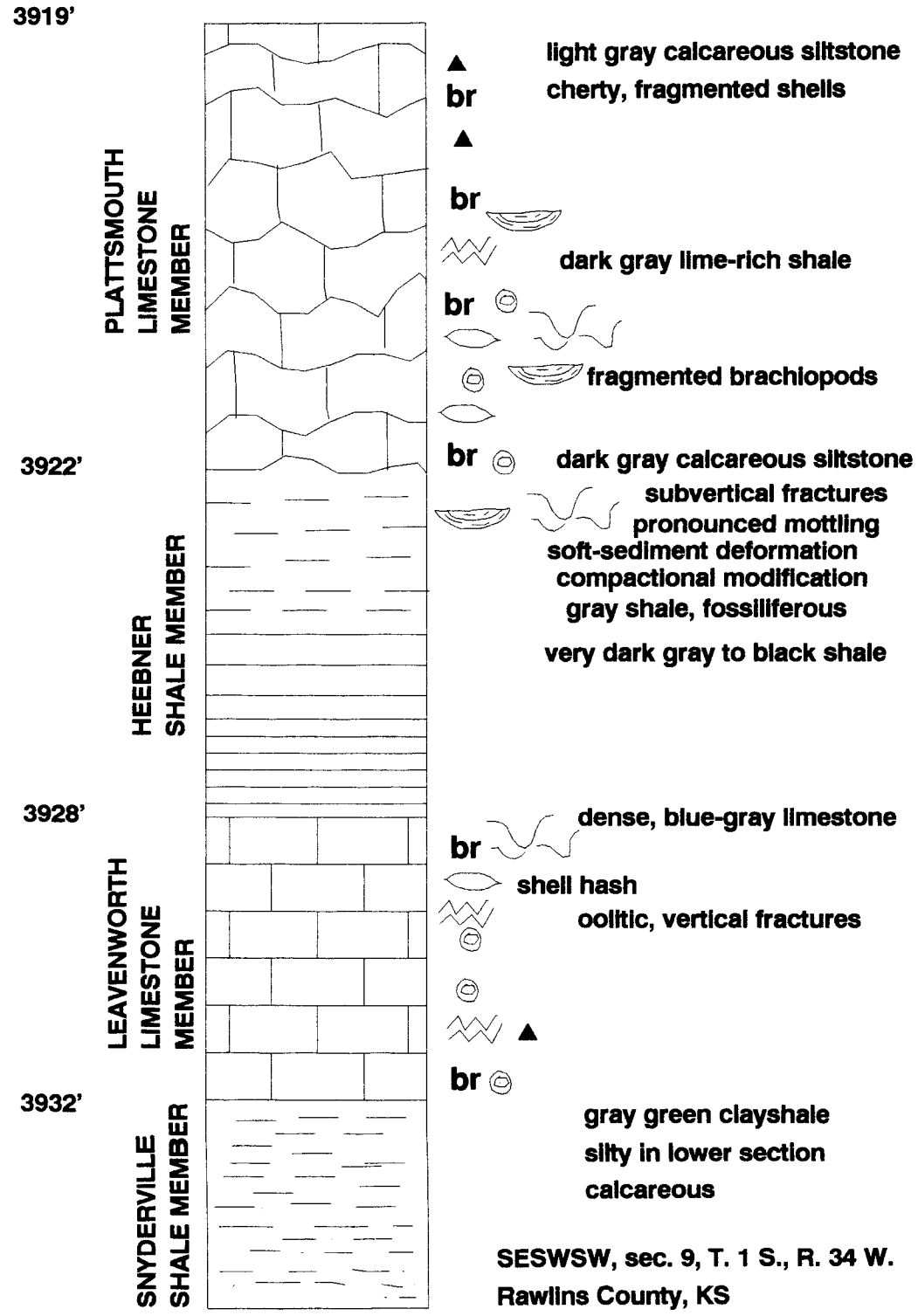

SESWSW, sec. 9, T. 1 S., R. 34 W.
Rawlins County, KS

Denny #1: Theodore Gore

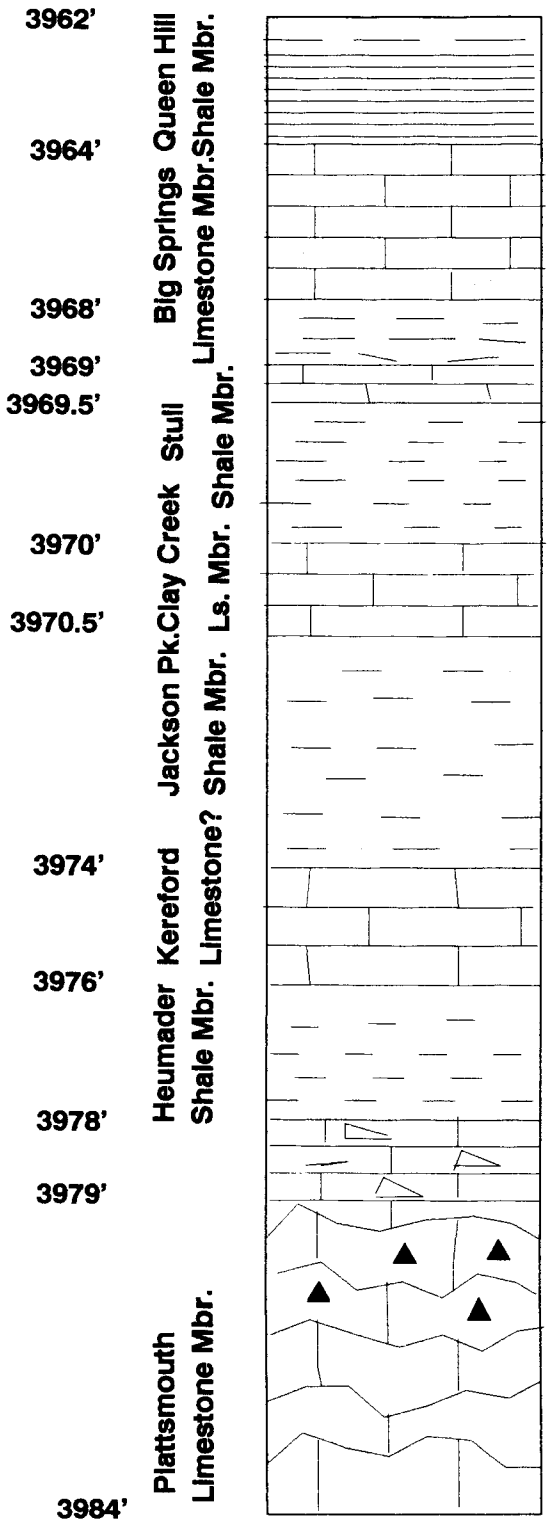

Black shale grades into dark gray
clay-rich, phosphatic at base

py Blue-gray ls., pyrite-rich
py lacks fauna, very dense, massive

sandy to silty at base

Doniphan Shale Mbr. blue-green, clay-rich shale

Spring Branch Limestone Mbr. creme ls., ferrugenous
lacks fauna

dark gray-green, waxy clayshale

chalky ls., lacks of fauna

blue-green silty shale

py pyrite framboids and clusters

homogenous gray limestone
algal fragments

gray-green clay-rich shale

red-orange, flat pebbly congl.
highly oxidized

creme crystalline ls.

cherty
wavy-bedded
br diverse fauna

C. NESW, sec. 5, T. 5 S., R. 34 W.
Rawlins County, KS

#1 Casselman: Petro Dynamics

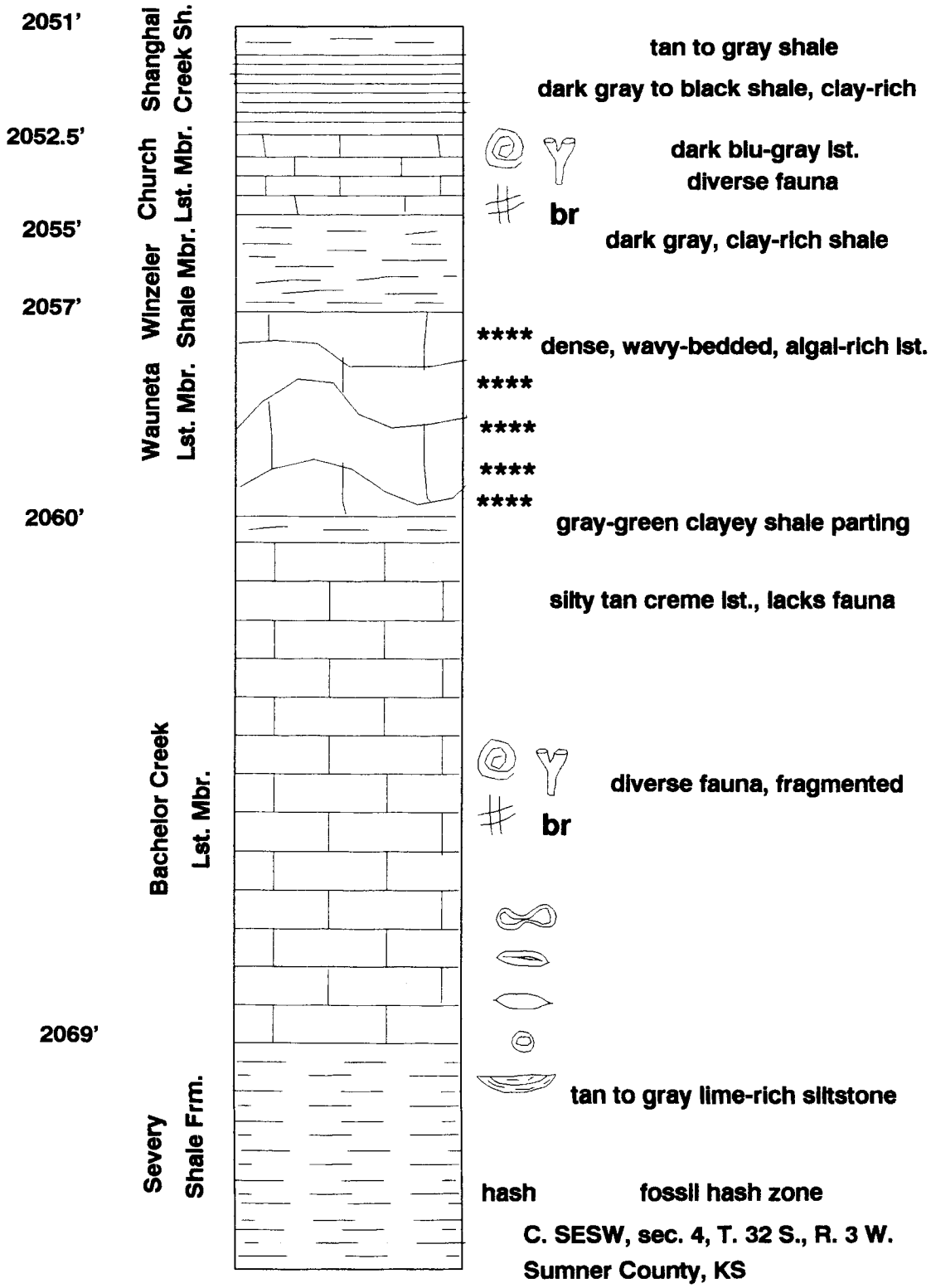

C. SESW, sec. 4, T. 32 S., R. 3 W.
Sumner County, KS

Branett #1: Wright

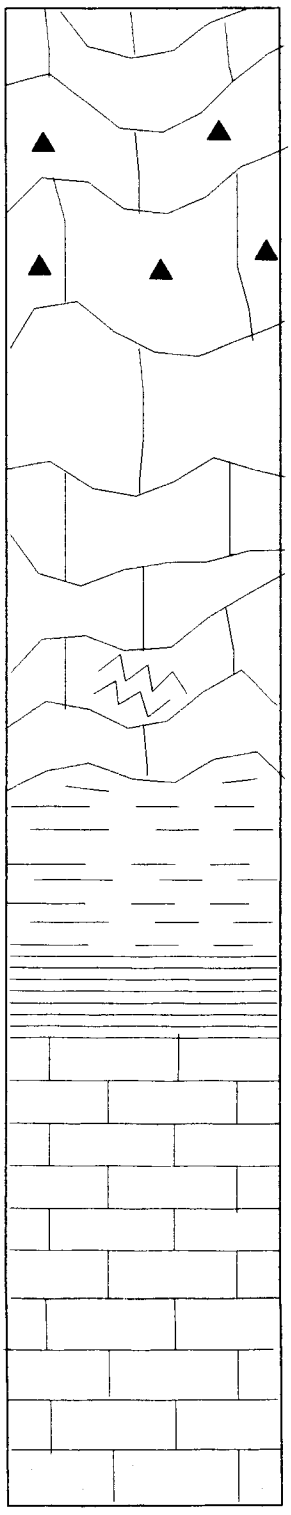

2586'

Bell Limestone Member

gray-tan gypsiferous lst.

wavy-bedded

cherty

wavy-bedded

algal wrap (Ottonosia)

wavy-bedded

sylolites, diverse fauna

br

hash

2599'

Queen Hill Shale Mbr.

tan to gray fossiliferous siltstone

dark gray to black, clay-rich shale
bioturbated near top of contact with hash

2602'

Big Springs Lst. Mbr.

dense, bluish gray lst.

lacks fauna

creme lst., massive

silty to sandy lst near base

2608'

C. S1/2 NW, sec. 35, T. 19 S., R. 8 W.
Rice County, KS